

## **General Disclaimer**

### **One or more of the Following Statements may affect this Document**

- This document has been reproduced from the best copy furnished by the organizational source. It is being released in the interest of making available as much information as possible.
- This document may contain data, which exceeds the sheet parameters. It was furnished in this condition by the organizational source and is the best copy available.
- This document may contain tone-on-tone or color graphs, charts and/or pictures, which have been reproduced in black and white.
- This document is paginated as submitted by the original source.
- Portions of this document are not fully legible due to the historical nature of some of the material. However, it is the best reproduction available from the original submission.

(NASA-CR-161378) SPACE VEHICLE ACOUSTICS  
PREDICTION IMPROVEMENT FOR PAYLOADS An  
~~Wyle Laboratories, Inc.~~ (Wyle  
Labs., Inc.) 203 p

~~SECRET~~  
Unclas

**WYLE LABORATORIES**  
SCIENTIFIC SERVICES AND SYSTEMS GROUP

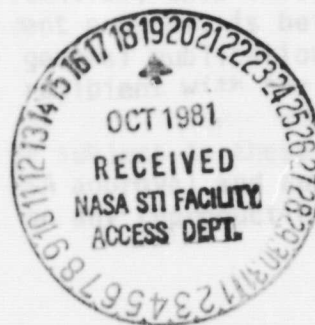


(NASA-CR-161378) SPACE VEHICLE ACOUSTICS  
PREDICTION IMPROVEMENT FOR PAYLOADS (Wyle  
Labs., Inc.) 203 p HC A10/MP A01 CSCI 20A

N81-32969

Unclas

G3/71 37455



research **REPORT**

WYLE LABORATORIES - RESEARCH STAFF  
RESEARCH REPORT WR 79-29

SPACE VEHICLE ACOUSTICS PREDICTION  
IMPROVEMENT FOR PAYLOADS

by

Robert E. Dandridge

for

NATIONAL AERONAUTICS AND SPACE ADMINISTRATION  
GEORGE C. MARSHALL SPACE FLIGHT CENTER  
Marshall Space Flight Center, Alabama 35812

October 1979

Work Performed Under Contract Number NAS8-33193

**WYLE LABORATORIES**

SCIENTIFIC SERVICES AND SYSTEMS GROUP  
P. O. BOX 1008 • HUNTSVILLE, ALABAMA 35807  
TWX (810) 726-2225 • TELEPHONE (205) 837-4411

COPY NO. \_\_\_\_\_

## FOREWORD

This report presents an analytic assessment of the modal analysis method for predicting the noise environment for space vehicle payloads in the low frequency regime. Two experimental cases are used to validate the analytical results, and recommendations are made to further improve the prediction model.

This report was prepared by Wyle Laboratories, Scientific Services and Systems Group, for the George C. Marshall Space Flight Center, National Aeronautics and Space Administration. The work was performed under contract NAS8-33193 entitled "Space Vehicle Acoustics Prediction Improvement for Payloads." Administration of this study was provided under the technical direction of the Systems Dynamics Laboratory with Mr. Stan Guest serving as the technical monitor.

The author would like to express his appreciation to Mr. Stan Guest for his guidance in identifying the main problem areas to be investigated, and to Dr. Ken Plotkin, of the Wyle Research Staff, for supplying much valuable information and assistance in this study.



## SUMMARY

The modal analysis method developed by Wyle [1] has been extensively modified for the prediction of space vehicle noise reduction in the payload enclosure, and this program has been adapted to the Marshall Space Flight Center IBM 360 computer. The predicted noise reduction levels for two test cases were compared with experimental results to determine the validity of the analytical model for predicting space vehicle payload noise environments in the 10 Hz to 250 Hz one-third octave-band regime. The prediction approach for the two test cases generally gave reasonable magnitudes and trends when compared with the measured noise reduction spectra. The discrepancies in the predictions could be corrected primarily by improved modeling of the vehicle structural walls and of the enclosed acoustic space to obtain a more accurate assessment of normal modes. Techniques for improving and expanding the noise prediction for a payload environment are also suggested.

# TABLE OF CONTENTS

	<u>Page</u>
FOREWORD	(ii)
SUMMARY	(iii)
LIST OF FIGURES	vi
LIST OF TABLES	vii
1.0 INTRODUCTION	1
2.0 LITERATURE SURVEY	4
2.1 CLASSICAL MODAL ANALYSIS . . . . .	4
2.2 ARCHITECTURAL ACOUSTIC ANALYSIS . . . . .	6
2.3 STATISTICAL ENERGY ANALYSIS . . . . .	6
2.4 FINITE ELEMENT ANALYSIS . . . . .	7
2.5 EMPIRICAL ANALYSIS AND/OR EXTRAPOLATION . . . . .	8
3.0 DISCUSSION OF THE MODAL ANALYSIS METHOD	9
4.0 COMPUTER PROGRAMS	17
4.1 STRUCTURE OF PROGRAM . . . . .	18
4.2 CALCULATION OF BANDWIDTH RESPONSE . . . . .	20
4.2.1 Acoustic Resonance in a Band . . . . .	22
4.2.2 Resonant Structural Transmission in a Band . . . . .	23
5.0 TEST CASES FOR ANALYTICAL PREDICTION MODEL	26
5.1 ACOUSTIC TESTS ON ORBITER OV-101 . . . . .	26
5.1.1 Test Configuration . . . . .	26
5.1.2 Microphone Locations . . . . .	26
5.1.3 Exterior Noise Source Levels . . . . .	30
5.1.4 External Noise Field Description . . . . .	30
5.1.5 Determining the Measured Payload Bay Noise Reduction . . . . .	34
5.1.6 Spatial Variability of the Measured Noise Reduction . . . . .	38
5.2 INPUTS FOR THE ANALYTICAL MODEL PREDICTION . . . . .	38
5.2.1 Absorption of OV-101 Payload Bay . . . . .	38
5.2.2 Structure of the Orbiter . . . . .	42
5.2.3 Payload Bay Doors . . . . .	42
5.2.4 Payload Door Resonant Frequencies . . . . .	49
5.2.5 Structural Damping . . . . .	54
5.2.6 Payload Bay Resonant Frequencies . . . . .	54
5.2.7 Acoustic Losses . . . . .	54
5.3 PREDICTION OF PAYLOAD BAY NOISE REDUCTION . . . . .	58
5.3.1 Comparison Between Measured and Predicted Noise Reduction for Empty Payload Bay . . . . .	61
5.3.2 Damping Effects on the Payload Bay Noise Reduction . . . . .	64
5.3.3 Spatial Variability of the Predicted Noise Reduction . . . . .	66
5.4 ACOUSTIC ENVIRONMENT FOR A PAYLOAD CONFIGURATION FROM MODEL TESTS	66
5.4.1 Payload Configuration . . . . .	68
5.4.2 Measured Data for the Delta-D Payload Effects . . . . .	68

## TABLE OF CONTENTS (CONCLUDED)

	<u>Page</u>
5.5 INPUTS FOR THE ANALYTICAL MODEL OF THE PAYLOAD EFFECTS. . . . .	68
5.5.1 Payload Delta-D Configuration. . . . .	72
5.5.2 Structure of the Orbiter . . . . .	72
5.5.3 Payload Bay Door Resonant Frequencies and Structural Damp- ing Factor . . . . .	72
5.5.4 Payload Bay Resonant Frequencies with Payload Present. . .	72
5.5.5 Acoustic Damping of OV-101 Payload Bay with Payload Present. . . . .	72
5.6 PREDICTION OF THE NOISE REDUCTION OF PAYLOAD BAY WITH A PAYLOAD PRESENT . . . . .	74
5.6.1 Comparison between Empty Payload Bay and a Payload Configuration. . . . .	74
5.6.2 Comparison of Measured and Predicted Payload Effects on Empty Bay Noise Levels . . . . .	78
5.6.3 Spatial Variability of the Payload Noise Effects . . . . .	78
 6.0 CONCLUSIONS	 80
 7.0 RECOMMENDATIONS	 82
 REFERENCES	 84
 APPENDIX A - Computer Program Description	

# LIST OF FIGURES

	<u>Page</u>
3-1. Dimensions and Coordinates of Concentric Cylindrical Cavity . . .	9
3-2. Experimental Noise Levels on Orbiter Door at 018, . . . . .	11
3-3. Microphone Locations on Upper and Side Surfaces of 6.4% Model . .	12
3-4. Typical Circumferential and Radial Acoustic Wave Patterns and the Corresponding Circumferential Structural Wave Patterns. . . .	13
3-5. Geometry and Coordinates of Shell and Panel . . . . .	14
3-6. Cylindrical Shell Mode Examples . . . . .	15
4-1. Flowchart of Main Program PURTON. . . . .	19
4-2. Flowchart of Main Program ACOBAN. . . . .	24
4-3. Flowchart of Main Program STRBAN. . . . .	25
5-1. Position of F-104 Aircraft for OV-101 Acoustic Tests. . . . .	27
5-2. Microphone Locations Inside OV-101 Payload Bay. . . . .	28
5-3. Microphone Locations Outside OV-101 Payload Bay . . . . .	29
5-4. Test Measurements of Exterior Noise Levels on Orbiter . . . . .	31
5-5. Test Measurements of Exterior and Interior Noise Levels on Orbiter . . . . .	35
5-6. Measured Noise Reduction Levels for Empty Payload Bay . . . . .	39
5-7. Variability of Measured Payload Bay Acoustic Levels for OV-101 Tests 1 and 2 . . . . .	40
5-8. Payload Bay Reverberation Time. . . . .	41
5-9. Space Shuttle Configuration . . . . .	43
5-10. Cross Section of Space Shuttle Cargo Bay Showing Typical Truss Frame . . . . .	44
5-11. Structural Configuration of Cargo Bay Doors Showing Skins, Hinge Line Torque Box and Circumferential Frames. . . . .	45
5-12. Circumferential $q = 3$ Mode Shape for Homogeneous and Hinged Doors	49
5-13. 4-Door - Fuselage Model Modes - Frequency = 8.17 cps. . . . .	52
5-14. 4-Door - Fuselage Model Modes - Frequency = 9.65 cps. . . . .	53
5-15. Deformed Parallelepiped . . . . .	56
5-16. Predicted Noise Reduction for Empty Payload Bay . . . . .	60
5-17. Comparison of Measured and Predicted Noise Reduction for Empty Payload Bay . . . . .	62
5-18. Predicted Empty Payload Bay Noise Reduction Relative to Measured Noise Reduction . . . . .	63
5-19. Effects of Structural Damping on the Payload Bay Noise Reduction.	65

## LIST OF FIGURES (CONCLUDED)

		<u>Page</u>
5-20.	Predicted Noise Reduction at One Point in Empty Payload Bay . . .	67
5-21.	Diagram of the Delta-D Payload Model. . . . .	69
5-22.	Effect of Delta-D Payload on Subvolume Space-Averaged Sound Pressure Levels . . . . .	70
5-23.	Predicted Noise Reduction for Payload Configuration Delta-D . . .	75
5-24.	Predicted Noise Reduction for Empty Payload Bay and Payload Delta-D . . . . .	76
5-25.	Predicted Change in Empty Bay Noise Levels with Addition of Payload Configuration Delta-D. . . . .	77
5-26.	Spatial Variation of Empty Bay Interior Sound Pressure Level Measurements. . . . .	79

## LIST OF TABLES

5-1.	One-Third Octave-Band Sound Pressure Levels on Door, Test 2 . . .	32
5-2.	One-Third Octave-Band Sound Pressure Levels on Door, Test 3 . . .	33
5-3.	One-Third Octave-Band Sound Pressure Levels Inside Payload Bay, Test 2. . . . .	36
5-4.	One-Third Octave-Band Sound Pressure Levels Inside Payload Bay, Test 3. . . . .	37
5-5.	Summary of Orbiter 001 Payload Bay Door Weights . . . . .	46
5-6.	Properties of Payload Bay Door Materials. . . . .	47
5-7.	Structural Properties of Payload Bay Doors. . . . .	48
5-8.	Structural Modal Frequencies and Indices for Payload Bay Door Model through 50 Hz Band . . . . .	50
5-9.	Comparison Between Door Resonant Frequencies from Finite Element Model and Present Model Symmetric Modes . . . . .	51
5-10.	Resonant Frequencies for Door Panels Between Frames . . . . .	51
5-11.	Acoustic Modal Frequencies, Empty Payload Bay, Through 100 Hz Band. . . . .	55
5-12.	Comparison Between Some Acoustic Modes from the Present Model and a Perturbated Rectangular Parallelepiped Model. . . . .	56
5-13.	Acoustic Modal Frequencies for Payload Configuration "Delta-D" through the 100 Hz Band . . . . .	73

## 1.0 INTRODUCTION

The use of orbiting and interplanetary space vehicles to place various payloads into space has been growing, and this growth will increase sharply when the Space Shuttle becomes operational. Payload utilization will greatly increase because of the relatively low launch cost that will be available with the Space Shuttle and because of the increasing space applications for scientific research, communications, energy, and for many other areas in which the application of the space environment may be beneficial to man.

In addition to an increased number of payload launches, there will also be an increase in payload complexity. These sophisticated payloads will also be sensitive to the acoustic environments to which they will be exposed. Therefore, it will be important in the payload design stage to consider the acoustic environment surrounding the payload. Also, the definition of these acoustic environments will be needed to allow an accurate assessment of the test limits for qualification testing of the payload and its components. From these considerations, it can be seen that an accurate prediction of the payload acoustic environment will be an important factor in the success of the payload missions.

The purpose of this program is to improve the technology base for defining the acoustic environments for space vehicle payloads. One goal of the study is to improve the acoustic environment prediction accuracy in the low frequency range where considerable acoustic energy is generated by the engines at liftoff. A computer program is also desired that will efficiently compute the space vehicle internal environments for any given external excitation and payload configuration. The program should also be flexible in order to incorporate state-of-the-art techniques in noise transmission analysis.

A review of the current prediction techniques for determining the interior acoustic environment of space vehicles has been performed, and the results are discussed in Section 2.0 - Literature Survey. The survey of the literature on this subject will provide a basis for choosing the best techniques available to improve the accuracy and efficiency of payload acoustic environment predictions. Since one of the goals in the study is to improve the internal noise predictions in the lower frequency regime, a classical modal analysis approach is taken.

An analytical model using the modal analysis techniques developed by Plotkin, Kasper, and Glenn [1] was selected as a logical starting point for this study. Earlier work done by Cockburn and Jolly [2] provided the basis for the more recent development by Plotkin et al. The computer programs [1] were utilized on the present contract to provide a computational tool for predicting noise reduction levels. Incorporation of state-of-the-art improvements to provide greater efficiency and accuracy for these computer programs was also applied.

The initial step in the modal analysis formulation is to express the interior sound field and structural displacement in terms of normal acoustic and vibrational modes. To facilitate the analysis, these modes are determined by approximating the actual structural geometry with a cylindrical shell with rigid end caps. Unique features incorporated into the model include the capability of treating independent shell panel segments of the structure, such as the Shuttle payload bay doors, and the capability of accounting for payload volume by the introduction of an internal concentric cylindrical payload. Application of boundary conditions requiring compatibility of the sound field with vibration of the structure at the bounding surface allows a determination of the acoustic energy coupled into the structure and ultimately radiated into the interior. The classical approach is theoretically an exact analysis from the physical standpoint. The degree of accuracy is dependent on the approximation involved in modeling the actual configurations in terms of simple geometric forms. Section 3.0 discusses the modal analysis approach in more detail.

A major practical limitation usually associated with modal analysis calculations is that calculation time and cost become very large as frequency increases due to the large number of modes involved. The computer program used for this study incorporates an innovative summation scheme, which minimizes computation time. The program is described in Section 4.0. The calculation begins with modes nearest a frequency of interest. Summation then proceeds through a sorted list of modes, with logic subroutines selecting the next modes to be included in the series. The modal summation thus considers the most important terms first, so that convergence is achieved with a minimum of wasted time due to calculation of unimportant modes.

Three versions of the computer program were prepared to calculate noise reduction (NR) at a single excitation frequency or averaged over an arbitrary bandwidth. The basic program computes the NR from a discrete excitation frequency input. This program is used when no structural or cavity resonances occur in the frequency band of interest. To obtain a band-averaged NR with this program, the response is calculated, at sufficient frequency intervals, and summed to arrive at a band averaged value of NR. The other two versions are bandwidth programs that analytically approximate an integration factor for each resonance within the band of interest. One version of the bandwidth program applies this method to acoustic resonances only, and the second version applies it to the structural resonances only. The total NR is then obtained by combining the two bandwidth NR calculations.

Section 5.0 describes a test on the Shuttle orbiter OV-101 at Edwards Air Force Base, where two F-104s were run-up to generate a simulated launch noise source. Predictions for this test case were made and compared to the measured test results. Also, a prediction case for the introduction of a payload configuration on the change of the empty payload bay NR levels is compared with a model test case.

The conclusions of the study are arrived at in Section 6.0. The accuracy of the noise reduction predictions is discussed. The applicability of the modal analysis method to the orbiter payload acoustic environment predictions is also reviewed.

Recommendations for improving the modal analysis approach used for this investigation are given in Section 7.0. Techniques for improved analytical modeling of the structure and payload bay configurations are suggested. Modifications for improving the generality and flexibility of the computer program are also given.

Appendix A gives a complete description of the computer program. It describes the three versions of the main program (PURTON, ACOBAN and STRBAN) and their subroutines. User instructions for the input parameters are given, and a computer program listing of a sample run is also shown.



## 2.0 LITERATURE SURVEY

Several methods that develop the noise transmission analysis for predicting the noise levels within an enclosure subjected to external acoustic excitation have been found in the literature. Generally, the method for computing space vehicle interior noise levels follows one of these approaches:

- Classical modal analysis
- Architectural acoustics
- Statistical energy analysis
- Finite element methods
- Empirical analysis and/or extrapolation.

Each of these approaches will be briefly discussed next while noting their respective references in the literature. Dowell [3] presents an extensive bibliography in the general area of vehicle interior noise prediction, which lists the available literature on each element of the problem.

### 2.1 CLASSICAL MODAL ANALYSIS

Classical modal analysis as applied to the sound field inside an enclosure, such as a Shuttle payload bay, involves modeling the response of the vehicle structure and interior sound field in terms of the structural and acoustic natural modes. To obtain tractable results, the geometry must be idealized so that the mode shapes are simple analytic functions. Application of boundary conditions requiring compatibility of the sound field with the vibration of the structure at the bounding surfaces allows a determination of the acoustic energy coupled into the structure and ultimately radiated into the interior. Apart from the approximations involved in modeling the actual configuration in terms of simpler geometric forms, the modal approach is mathematically an exact treatment. The damping factor for each mode is also critical to the accuracy of the structural and acoustic response. The modal analysis method is generally the most useful at low frequencies where the modal density is low. The applicable frequency range is where the ratio of the acoustic normal mode wavelength to its corresponding cavity dimension is from about one-third to three [4]. At higher frequencies, computer time increases greatly due to the increasing number of modes involved in the summation process.

Recent developments in modal methods of sound transmission analysis are developing along two lines. Taborrak [5] has recently advanced the variational formulation (see Cragges [6]) of the principles underlying structural-acoustic problems. The formulation is intended for use in finite element analysis of the combined structural-acoustic problem. The method is powerful and especially of value for the analysis of irregularly shaped cavities and of complicated structures. The principle limitation being the computer storage and calculation time required, which increases geometrically with the size and complexity of the problem.

The other line of development has been the extension of the method of Cockburn and Jolly [2]. Many authors have built on this model, which is based on Lagrange's equation for the structure and Green's theorem for the acoustic field [1, 7, 8]. A versatile formulation has emerged from the work of Dowell [9], Vaicaitis [10], Cragges [11], Wolf [12] and Petyt [13]. The model is based upon a knowledge of the uncoupled, "in vacuo" structural modes and the rigid wall acoustic modes of the cavity. Given these modes, the model allows for full coupling between the structural wall and the acoustic cavity. Due to the component mode synthesis methodology employed in this model, multiple connected cavities may be considered. Any exterior acoustic excitation is theoretically allowed, including random noise with a specific correlation function [14]. This case, however, has not yet been actually computer coded and run. The acoustic and structural modes can be determined by any method, including the finite element calculation, in that "(1) By judicious selection of components, the appropriate component modeling may already be known without further analysis or, at the least, much easier to determine than that of the overall system. (2) In the synthesis when components are combined only the essential aspects (modes) of each component need be retained. Hence, the representation of the component in the total system may be much simpler than its original representation when treated separately." [3]

Component mode synthesis means a component of the response system is most efficiently represented in terms of its own (natural) modes. In the context of the present problem, an obvious distinction can be drawn between structural (wall) and acoustic (cavity) components. Their uncoupled normal modes are easier to calculate separately and then combined to obtain the overall coupled behavior of the system.

## 2.2 ARCHITECTURAL ACOUSTIC ANALYSIS

This geometrical acoustic analysis method, commonly referred to as the architectural acoustic approach, is based on the idealized assumption that the sound field enclosed within an arbitrary volume can be represented as an assemblage of an infinite number of plane waves traveling in all possible directions. By integrating the acoustic intensity over the volume and performing an energy balance, a simple relation can be derived between the incident sound power, the total acoustic absorption, and the resulting uniformly distributed sound pressure field. Since the sound field in an enclosure approaches the diffuse field idealization at sufficiently high frequencies due to the presence of closely spaced and overlapping resonances, this simple acoustic relationship has been found useful for many applications. Since the assumption of which architectural acoustic is based requires that the sound pressure be uniform throughout the enclosed volume, the method ceases to be valid at low frequencies where individual acoustic resonances become prominent. It is, therefore, a suitable method only for the evaluation of interior noise levels at high frequencies where the ratio of normal mode acoustic wavelength to its corresponding cavity dimension is about one-third or less.[4]

## 2.3 STATISTICAL ENERGY ANALYSIS

Statistical energy analysis (SEA) is a technique, developed in the 1960s, that treats the interaction of coupled dynamic systems in terms of their collective modal properties. The technique is based upon the modeling of each dynamic system as a group of modes with the energy of the system within a given frequency range assumed to be uniformly distributed among the modes within that range. The time-averaged power flow between the coupled system is then determined as a function of a general coupling factor and the difference in time-averaged modal energies of the system. SEA has been used extensively to predict the response and noise reduction of complex structures excited by random pressure fields.[15-18] Many complex aerospace structures can be considered as being built up from elementary structural elements such as simply support beams, plates, etc. A typical example is a shroud and payload assembly. A study that shows the application of the SEA to predict the response of this type of assembly to a reverberant field is presented by Conticelli [19]. For more complex structures, a good estimate of the modal density can be obtained by adding the modal densities of the various elements composing the structure.

When a multimodal system is excited in a band of frequencies its modes can be divided into resonant and nonresonant frequencies within the band. The energy transmission between nonresonant frequencies and between resonant and nonresonant conditions cannot be predicted by the SEA. For energy transmission between resonant modes, however, a power balance equation is given by Conticelli and Cockburn [18]. Some recent work with the SEA method can be found in References 20 through 23.

The major advantages of this approach is that the computations are relatively simple, and fine details of the system are not required. The primary disadvantage of the technique is the inability of the formulation to account for the specific characteristics of the dynamic systems. Also, the damping value specified for each frequency band significantly affects the response of the systems. Empirical means are usually required to obtain coupling parameters between the groups of structural and acoustic modes, and it is also assumed that the resulting motions are statistically independent, with energy equally partitioned among all modes in a given group. These assumptions are not necessarily valid at low frequencies where rather distinct modal coupling exist. In general, the assumptions on which SEA is based are valid only at high modal densities, corresponding to the frequency ranges commonly used in the architectural acoustics approach.

## 2.4 FINITE ELEMENT ANALYSIS

Finite element analysis can be described as a systematic numerical technique by which a continuous system can be modeled as an assemblage of elementary elements, expressing the state of the system in terms of parametric values at the element connecting points. The structure and acoustic cavity must be well defined in order to obtain an accurate modeling of the system. From the standpoint of variational calculus, the approach requires expressing the element properties in terms of a functional relationship and finding a optimal solution for the total assemblage.

The computer implementation of this technique over the past ten years has reached a high level of sophistication, particularly in relation to structural analysis--as evidenced by the development of NASTRAN and other similar user-oriented computer programs. Finite acoustic elements have also been applied to the calculation of the acoustic field within ducts [24]. The generality of the basic finite

element technique makes it a logical approach to consider for application to the analysis of the acoustic field within an enclosure. Applications of this technique have already been used by Wolf and Nefske [25, 26], for example, to determine approximate acoustic resonant frequencies and mode shapes for an automobile body interior. Also, the major aircraft manufacturers have developed finite element programs to analyze the structural vibration of fuselages.

Finite element analysis of a structure coupled with an interior sound field constitutes a major task in the development of the necessary equations, and the computer storage and computation time required also involves a major computational task. The finite element method, however, has been used effectively in conjunction with the modal analysis method [6, 8, 25, 27] for obtaining the normal modes of the system components, as mentioned in component mode synthesis in Section 2.1 - Classical Modal Analysis.

## 2.5 EMPIRICAL ANALYSIS AND/OR EXTRAPOLATION

Because of the complexities inherent in the analytical methods, considerable efforts have been made to develop empirical techniques for the prediction of vibration response [28-31]. Initial developments concentrated upon the normalized response of Tital and Jupiter space vehicles [28] to predict the induced interior noise of the vehicles. Subsequent developments [30, 31] have been limited to Saturn V-type structures, and response information has been summarized in the form of data banks. The most significant disadvantage of these empirical approaches is the fact that response data are presented for limited types of structures, and little attempt has been made to review all the vibration data with a view to deriving a generalized response prediction curve.

### 3.0 DISCUSSION OF THE MODAL ANALYSIS METHOD

When sound waves are transmitted through the walls of a cavity all wave motion is standing wave motion, and the acoustic energy content of the cavity is determined by the nature of its walls. For cavities with a ratio of sound wavelength-to-cavity dimension between one-third and three, it will be most convenient to analyze the acoustic response in terms of normal modes of the enclosure. This ratio corresponds to a normal mode frequency range of about 6.2 to 233 Hz for the Space Shuttle orbiter payload bay cavity. The lowest longitudinal normal mode of the empty payload bay cavity is about 9.3 Hz, and the lowest circumferential mode and radial mode are 41 Hz and 85 Hz, respectively. These normal cavity modes were based on the payload bay geometry shown in Figure 3-1.

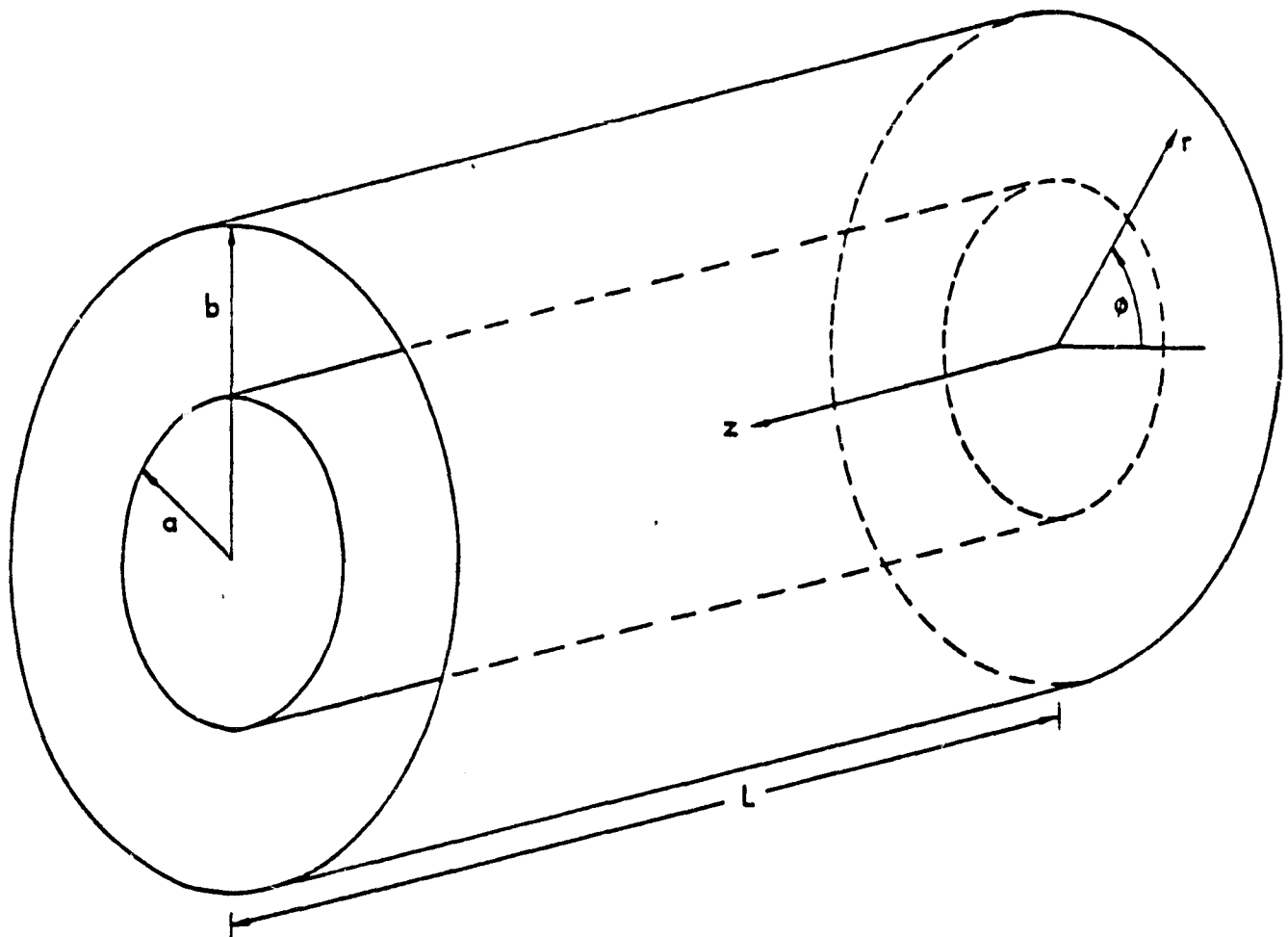


Figure 3-1. Dimensions and Coordinates of Concentric Cylindrical Cavity

Considerable external acoustic energy at these lower frequencies will be generated by the Space Shuttle engines, shown in Figure 3-2, from Reference 32, to excite the payload bay internal acoustic modes. The data in Figure 3-2 was measured at location 018 as shown in Figure 3-3. The payload bay doors will also have low frequency resonances that will couple with the external noise field to allow increased transmission of external noise into the payload bay cavity. For the case where the excitation frequency wavelength is much larger than the dimension of the cavity, the air in the enclosure can only exhibit stiffness reactance, expanding and contracting in phase, in response to the driving external pressure. This response is similar to a Helmholtz resonator condition. The introduction of payloads will also affect the lower order acoustic modes of the payload bay more than the higher order modes, because the acoustic wavelength will be smaller than the individual payload components in the higher frequency region. Therefore, the preceding factors indicate the usefulness of the normal mode analysis that allows a detailed description of the internal noise field surrounding the payload in a space vehicle.

The modal analysis approach has the advantage of permitting a detailed description of the enclosed sound field while providing a methodology for determining the interaction of the sound field with the vibrating structure. Although the modal approach is an exact analysis in the classical sense, its practical application requires that the structural shape and enclosed volume be modeled in terms of simple coordinate geometries. For application to space structures, the model is based on approximating the enclosed volume as a right circular cylinder, and the surrounding structure is consequently treated as a cylindrical shell. Apart from simplifying the overall shape of the structure, the model itself is sufficiently general to account for orthotropic structural properties as well as an arbitrary distribution of the shell surface into panels with different structural characteristics. An important feature of the model is the incorporation of a payload within the enclosed volume. In order to maintain a tractable mathematical solution, the payload geometry as shown in Figure 3-1 was taken as a circular cylinder positioned concentrically within the enclosing structure. Since the present analysis is intended for application in the low frequency range where the acoustic wavelengths will normally be large compared to individual payload components, it is not critical that full geometrical detail of the payload be

SEC NO. = 0109

318

TEST	P027-159	CAL. RANGE	995.85986	3.09997
MEAS. NO.	018	ENG. RANGE	170.00000	120.00000
LINK/CHAN	2-10	INTEGR TIME	0.19998	
SLICE TIME	9.0 - 7.0	OVERALL	190.73471	

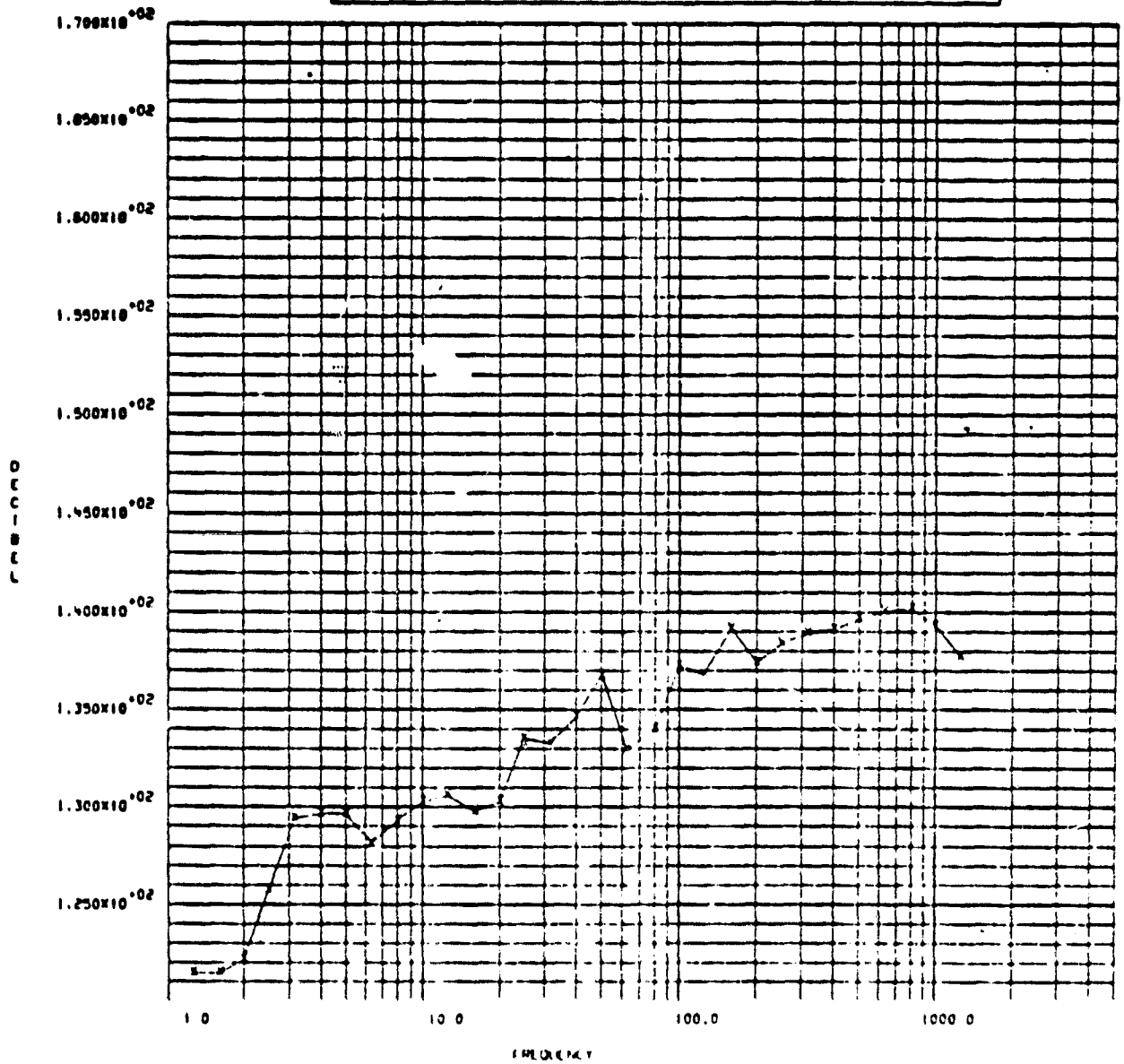


Figure 3-2. Experimental Noise Levels on Orbiter Door at 018.  
Taken from AMTF Test [32]



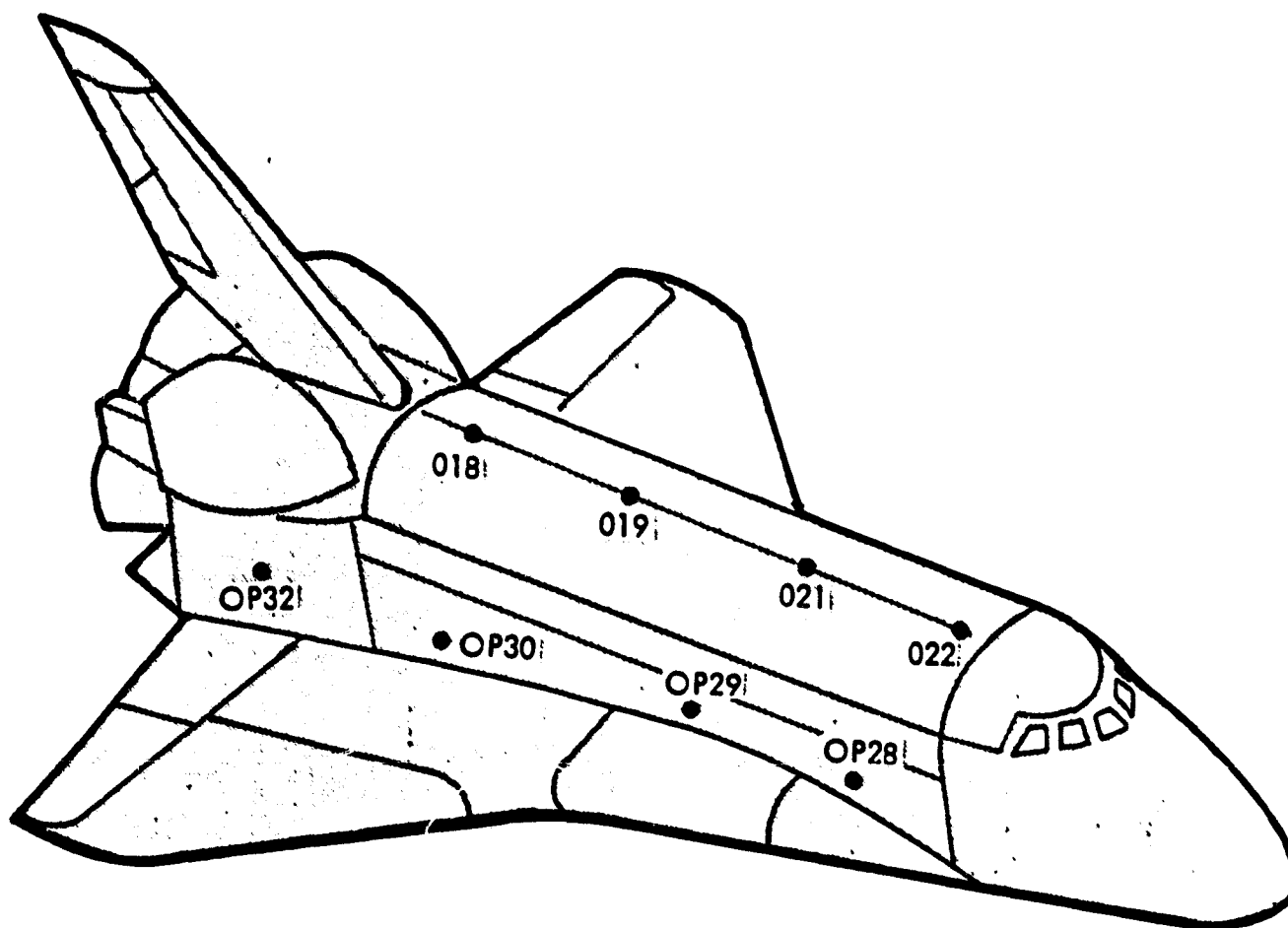


Figure 3-3. Microphone Locations on Upper and Side Surfaces of 6.4% Model [32]

included. The cylindrical model simulates the most important payload geometry factor -- the volume -- that can affect the enclosed noise field. The general treatment of the analysis is discussed in the following paragraphs.

The physical process involves the interior sound field exciting the shell, which in turn excites the interior cavity. The analytic development logically follows the inverse order, beginning with the interior sound field. Determining the interior noise field consists of finding a solution to the acoustic wave equation in terms of the normal acoustic modes of the containing volume, requiring the solution to satisfy appropriate boundary conditions at the structure wall surface [4]. Several acoustic mode shapes are shown in Figure 3-4 for typical circumferential and radial wave patterns. A corresponding circumferential structural wave pattern is also shown. The boundary conditions are that the acoustic particle velocity at the containing surface match the vibration velocity distribution

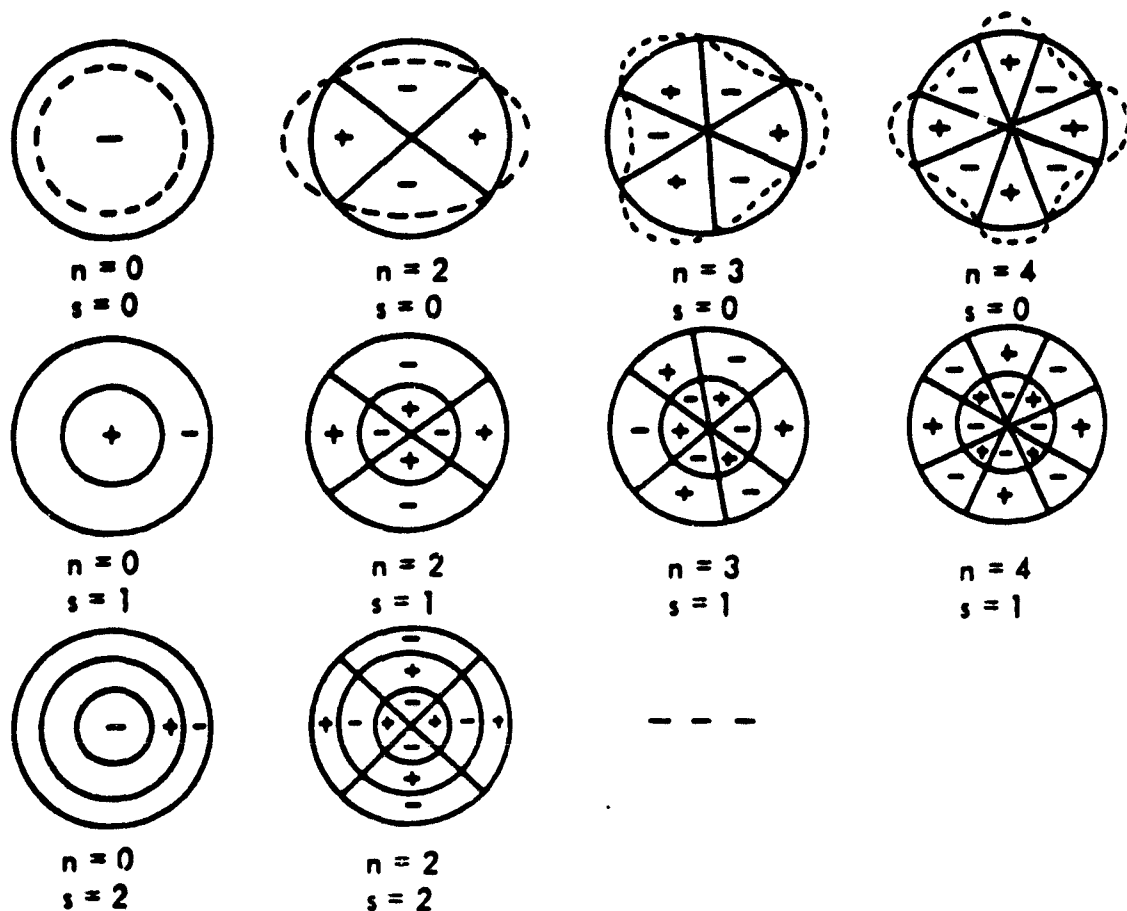


Figure 3-4. Typical Circumferential and Radial Acoustic Wave Patterns and the Corresponding Circumferential Structural Wave Patterns

of the structure. A Green's function is developed that relates the spatial distribution of the internal acoustic field to the vibrating structural surface. The acoustic response is derived for an arbitrary motion of the structure. In addition, for application to configurations containing a payload, it is required that acoustic boundary conditions be met along the surface of the payload. The payload is considered as a rigid solid that establishes the boundary condition of zero acoustic particle velocity along the surface. The effect of the boundary condition associated with the presence of the payload is to raise the resonant frequency of interior acoustic modes with radial components.

The vibration response of the space vehicle structure is then considered. The formulation begins with the equations of motion for the forced response of an orthotropic thin cylindrical shell. Solutions are developed for the response of the shell as a whole structure and for response of independent shell panel

segments. Figure 3-5 illustrates the geometry of the structural model. The vehicle structure is modeled as an orthotropic thin cylindrical shell using the Donnell-Mushtari shell equation found in Leissa [33]. Figure 3-6 illustrates several examples of cylindrical shell modes. The analysis is arranged so that individual panels bounded by shear diaphragm boundary conditions along circumferential and longitudinal coordinates could be permitted to respond while the remainder is held rigid. This permits separate transmission calculations for any panel location and for panels with significantly different properties. Coupling relations between normal shell modes and the internal noise field are developed, and then the response of the coupling of the shell to an arbitrary external pressure field is derived. A weak coupling assumption is made which states that

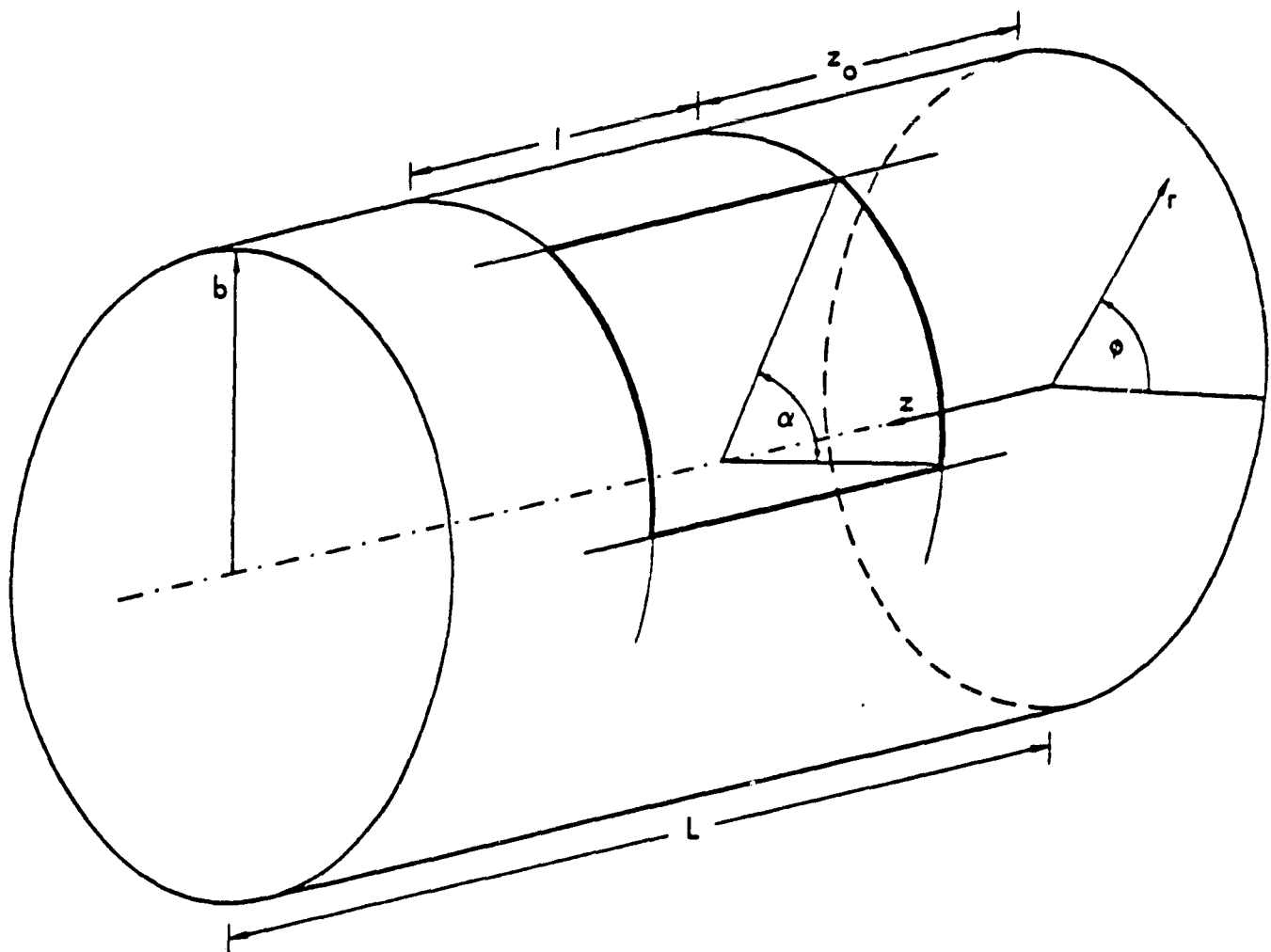
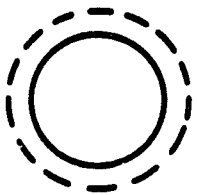


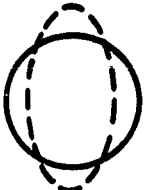

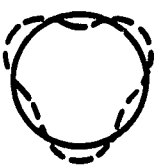

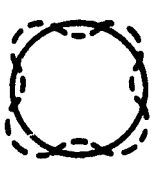
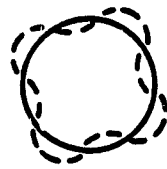

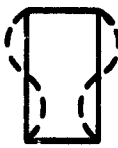

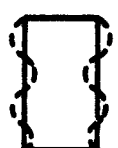


Figure 3-5. Geometry and Coordinates of Shell and Panel

$n^*$	Symmetric	Antisymmetric
0 (Bulge)		
1 Lateral Bending		
2		
3		
4		

a. Circumferential Modes

\*n = number of full circumferential waves.

$m^{**}$	Longit. Shape***
1	
2	
3	
4	

b. Longitudinal Bulge Modes

\*\*m = number of longitudinal half waves.

\*\*\*Motions shown occur at diametrically opposite points on plane of symmetry for circumferential modes in part a of this figure.

Figure 3-6. Cylindrical Shell Mode Examples (from Reference 44)

interaction between the structural and acoustic response will not change the structural modes calculated in a vacuum condition, and the interaction will not affect the rigid wall acoustic modes. Therefore, coupling between the structure and cavity can be calculated using the "in vacuo" structural response and rigid wall acoustic response of the cavity. The assumption of negligible structural damping coupling is also made due to the light damping occurring in the space vehicle structure [34].

The structural excitation by random acoustic fields is developed next. It is shown that the frequency-dependent coupling between the structure and a random exterior field is described in terms of the narrow-band spatial correlation function (also called the cross-power spectral density) of the exterior noise. Coupling relations are derived for excitation by jet noise and by a reverberant field.

The spatial correlation of the exterior noise field at a given frequency is particularly important in that it determines the manner in which structural modes are excited. For example, random noise fields are correlated over distances comparable to a wavelength. The net result is that the structural modes with wavelengths comparable to the area of in-phase excitation are strongly coupled to the noise field. At higher frequencies, the area over which the pressure field is correlated becomes smaller and the structural response is characterized by the local response of individual panels or panel groups rather than that of the entire shell. It is shown in Reference 1 that this behavior results in structural modes being statistically uncorrelated for noise excitation. This provides a valuable simplification since cross terms between modes, which are important for coherent excitation, may be neglected.

#### 4.0 COMPUTER PROGRAMS

The basic computer programs used in this study were developed by Wyle [1]. These programs have been modified to improve their efficiency, application, and accuracy to the problem of predicting payload environments. The programmed analytical model predictions were compared to test results as described in Section 5.0. This comparison was made to gain an idea of the model's accuracy and to determine feasible methods for improving the computer programs and the analytical model. Techniques for improving these noise prediction computer programs and the analytical model will be discussed in Section 7.0 - Recommendations, and a complete description of the programs is found in Appendix A. A general description of the computer program is given in this section.

The expressions derived in Reference 1 provide for the calculation of noise reduction at a single frequency, as a multiple summation over cavity acoustic modes and shell structural modes. The total expression for the ratio between interior and exterior pressure at a given frequency  $\omega$  may be written in summary as

$$\frac{\langle \overline{p_i^2} \rangle}{\langle \overline{p_o^2} \rangle} = \sum_{mn} \{ \left[ \sum_s Q_{ns}^2 (K_{ns} b) H_{mns}^2 \right] \left[ \sum_{pq} \tilde{H}_{pq}^2 \gamma_{mp}^2 \Gamma_{nq}^2 I_p I_q \right] \}, \quad (4-1)$$

where the terms in  $\{ \}$  and the summation variables are defined in Reference 1.

The amplification functions  $H^2$  and  $\tilde{H}^2$  are written in terms of modal resonant frequencies and associated constants as well as direct physical data (dimensions, material properties, etc). Calculation of noise reduction, therefore, consists of first computing these modal resonant quantities and then applying the following relationship to obtain the noise reduction in decibels:

$$NR = 10 \log_{10} \frac{\langle \overline{p_i^2} \rangle}{\langle \overline{p_o^2} \rangle}. \quad (4-2)$$

A set of computer programs has been developed that performs this calculation. The primary version of the program computes the noise reduction at a single frequency

as given by Equation 4-2. This program is described in detail in Section 4.1. Of practical interest is the noise reduction of broadband sound, described in terms of octave or one-third octave bands. While the puretone response could in principle be integrated numerically, this would require calculation of response at an enormous number of frequencies -- at least several around each resonance -- to be reliable. An exact analytic integration of the NR equation (4-2) was also not practical; therefore, two alternate "bandwidth" versions of the program were prepared, which make use of an approximate analytic frequency integration. These are described in Section 4.2. The computer program's computational details, input and output parameters, and a listing of a program run case are given in Appendix A.

#### 4.1 STRUCTURE OF PROGRAM

The greatest practical limitation to modal analysis techniques is that the number of modes grows geometrically as frequency increases. The number of terms to be included in the summation in turn grows geometrically with the number of modes. The highest frequency amenable to a modal calculation is limited by practical constraints of computer size and computation cost. For maximum practicality, a program must avoid computations that include modes not substantially contributing to the net response. Programs that deterministically compute all modes and functions within a specified range of indices have a domain of applicability that is seriously limited.

The computer program developed here was designed to avoid these limitations as much as possible. The main feature is that summation is performed in a selective manner, seeking the most important terms. The summation begins with the mode whose resonant frequency is closest to the excitation frequency. Successive terms are added by summing through an ordered list of frequencies. Summation continues until a convergence criterion is satisfied.

Figure 4-1 shows a flowchart of the program. This program is PURTON, which computes the response to a puretone. Overall, it is divided into two parts: calculation of modal frequencies, and the summation represented by Equation 4-1. To avoid repeated calculation of modal frequencies on successive runs for the same structure, all required output from the first part may be saved on a file. The option of computing or reading an existing file is separate for acoustic and structural modes.

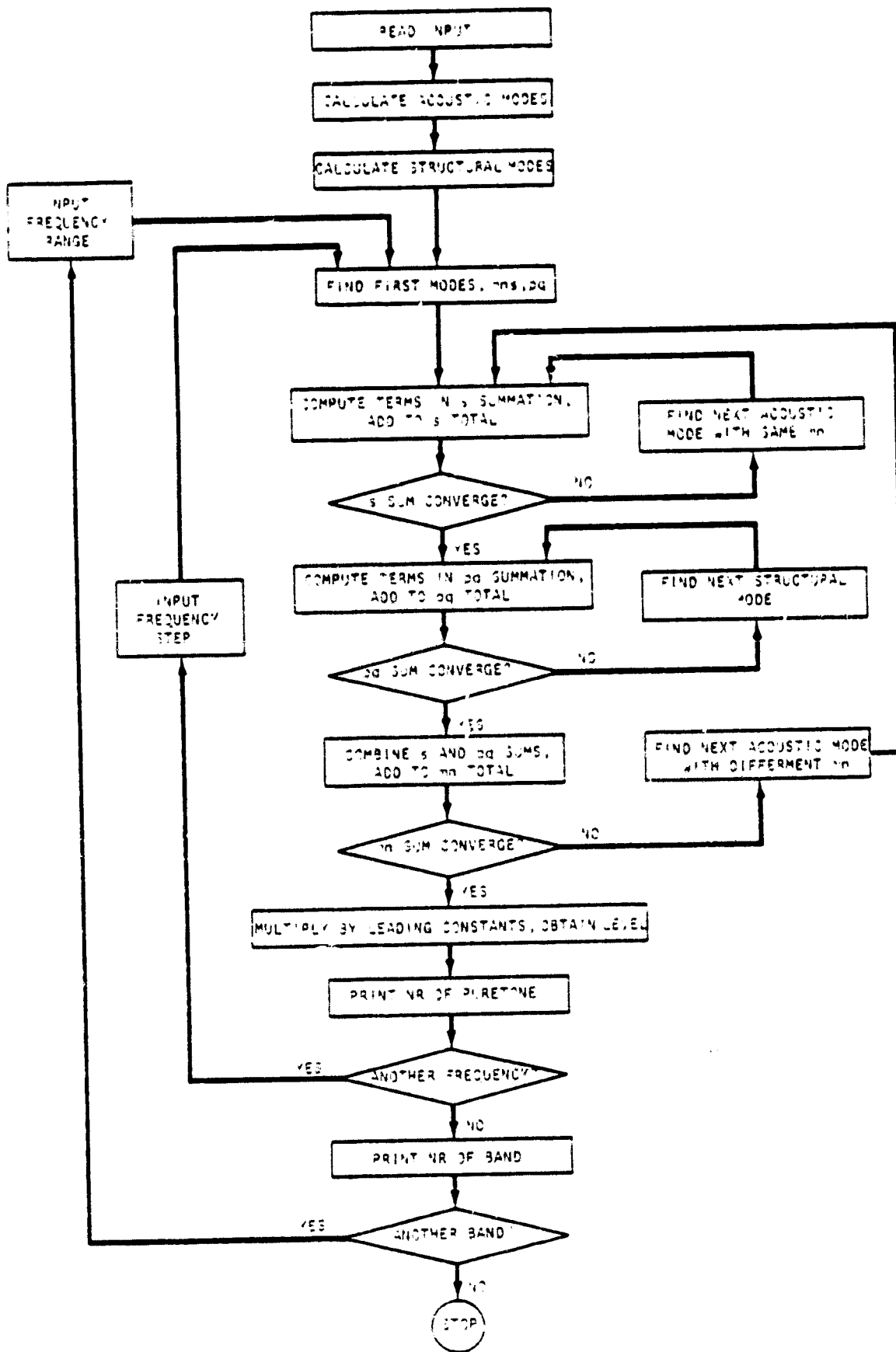


Figure 4-1. Flowchart of Main Program PURTON



The user specifies a range of modal indices for the first part of the program. The program modifies this in order to obtain a list of modes that is complete in frequency space. For example, if acoustic indices are specified from  $mns = 0,0,0$  to  $M,N,S$ , the list of computed modes would not be complete above  $\omega_{M,0,0}$ . Referring to Equation 6 from Reference 1, there are modes  $(m,0,0)$  with  $m > M$  such that the frequency is less than for modes with  $m \leq M$  and  $n,s > 0$ . To avoid skipped frequencies, the  $m$  loop is innermost, then  $n$ , then  $s$ , with the  $n$  and  $s$  loops terminated when  $\omega_{mns}$  exceeds  $\omega_{M,0,0}$ . In addition to providing a complete frequency list, this procedure minimizes the number of roots  $k_{ns}$  that must be obtained.

A similar procedure is followed when obtaining the structural frequencies. It is complicated slightly by the fact that  $\omega_{pq}$  is not monotonically increasing with  $q$  (as is  $\omega_{mns}$  with each of  $m, n, s$ ), and that there are three values of  $\omega_{pq}$  for each pair  $p, q$ . The basic principle is the same, however.

#### 4.2 CALCULATION OF BANDWIDTH RESPONSE

Equation 4-2 gives noise reduction at a single frequency; of practical interest is noise reduction averaged over a finite bandwidth. Numerical integration of the pure tone result would have been computationally very expensive. An exact analytic integration of a band is possible in principle, but in practice would be quite cumbersome. Each term in Equation 4-1 consists of the product of four linear oscillator terms of the form  $1/[(\omega^2 - \omega_0^2)^2 + \eta^2\omega^2]$ , together with polynomials in  $\omega$ . Integration could be accomplished by expansion in partial fractions of the sixteenth order denominator. Subsequent evaluation at limits corresponding to band edge frequencies would be unwieldy at best.

An approximate bandwidth result may be accomplished by noting that the strongest frequency dependence is due to the oscillator terms, and that only one at a time will be important if there is little modal overlap. Further, if the width of a resonance is small compared to the bandwidth of interest, then the integration may be taken over  $\pm\infty$  rather than just over a bandwidth. It is also assumed that the remainder of the expression is approximately constant over the width of the

resonant peak of interest, and may be evaluated at the resonant frequency. The linear oscillator term is thus replaced by

$$\int_{\text{band}} \frac{\omega^2 d\omega}{\left[ (\omega_0^2 - \omega^2)^2 - \eta^2 \omega^2 \right]} \approx \int_{-\infty}^{\infty} \frac{\omega^2 d\omega}{\left[ (\omega_0^2 - \omega^2)^2 - \eta^2 \omega^2 \right]} = \pi/\eta. \quad (4-3)$$

Applying this approximate integration to each resonance within the band of interest would give the complete resonant response. There would be a possibility of error, however, in that there could be duplication in case of overlapping modes. Also, nonresonant response would be neglected.

In order to avoid (or account for) these possible errors, two separate bandwidth programs were developed and used in conjunction with the puretone model. One version applied Equation 4-3 to acoustic resonances only, so that it considered a resonant acoustic field driven by nonresonant structural response. The other version applied Equation 4-3 to structural resonances only, so that it considered a nonresonant acoustic field driven by structural resonances. These two programs are described in the following subsections.

After modal frequencies are computed, the acoustic and structural frequencies are each sorted into lists in order of size. To retain identification of modal indices, arrays containing  $mns$  and  $pq$  are sorted in parallel to the frequencies. The structural constants  $C_{pq}$  are also sorted in parallel to the structural frequency list.

The summation of Equation 4-1, the second part of the program, begins with the acoustic mode with  $\omega_{mns}$  closest to the input frequency  $\omega$ . Summation first takes place over  $s$ . After the first term is computed, one term with higher frequency ("up" the list) and one with lower frequency ("down" the list) is computed. The summation over  $s$  continues, adding terms up and down the frequency list until convergence is obtained in both directions. The convergence criterion is that the ratio between the newest term and the running sum be less than some small amount. The next term added may be either up or down the list, depending on which of the last up and down terms was larger. Summation proceeds in the direction of the last largest term.

The summation over  $p, q$  is then performed in a similar manner, beginning with  $\omega_{pq}$  closest to the input frequency. The program does not place any distinction on which of the three  $\omega_{pq}$  is used, but does keep track so that modes are not inadvertently counted more than once.

The summations over  $s$  and over  $p, q$  together with the quantity denoted  $\{\}$  are then multiplied together and added to the cumulative summation. The  $m, n$  summation then advances up or down the acoustic frequency list to the next mode with different  $m, n$ .

The nature of the functions  $\gamma$ ,  $\Gamma$ , in the structure/cavity coupling term, and  $l$ , in the joint acceptance term, are such that many of these may be zero. Inclusion of a zero term would give a false indication of convergence. The program, therefore, tests for such zero terms, and if one is encountered, calculation advances to the next mode. To avoid errors due to rounding errors in floating point arithmetic, a zero condition is taken when the arguments of sine and cosine are terms within 0.01 radian of a zero condition.

The calculation of Equation 4-1 gives the spatially averaged noise reduction ratio. To obtain some indication of the spatial variation of the interior noise field, a parallel summing is performed where each acoustic modal coefficient is multiplied by the square of the mode shape, Equation 1 from Reference 1, evaluated at a point of interest. The program includes four such points, with location of the points specified by the user.

A third possible case is a nonresonant acoustic field driven by nonresonant structural response. This is a case readily handled by numerical integration of the pure tone program, since response in the absence of resonances would be smooth over a band.

#### 4.2.1 Acoustic Resonance in a Band

This bandwidth program, called ACOBAN, applies Equation 4-3 to  $H_{mns}^2$  in Equation 4-1. The summation over  $p, q$  proceeds exactly as in PURTON. The summations over  $m, n$  and  $s$  are combined into a single deterministic summation over all  $\omega_{mns}$  lying within the band specified by the user. The band is specified in terms of width (fraction of octave; for example, one octave, one-third octave, etc) and center

frequency. At each acoustic mode in the  $mns$  summation,  $\omega$  for use in other expressions is set equal to  $\omega_{mns}$ . Figure 4-2 shows the flowchart for this program.

#### 4.2.2 Resonant Structural Transmission in a Band

This bandwidth program, called STRBAN, applies Equation 4-3 to one resonator term in  $\tilde{H}_{pq}^2$  in Equation 4-1. The other two resonator terms, and the numerator, are treated as weak functions of  $\omega$  to be evaluated at the resonant  $\omega_{pq}$ . The order of summation is changed, with the  $m$ ,  $n$  and  $s$  summation performed first. These are done as in PURTON. The  $p,q$  summation is performed last, and is done as a deterministic sum over all resonant  $\omega_{pq}$  in the specified band. At each structural resonance in the band,  $\omega$  for use in the other terms is set equal to  $\omega_{pq}$ . Figure 4-3 shows the flowchart for this program.

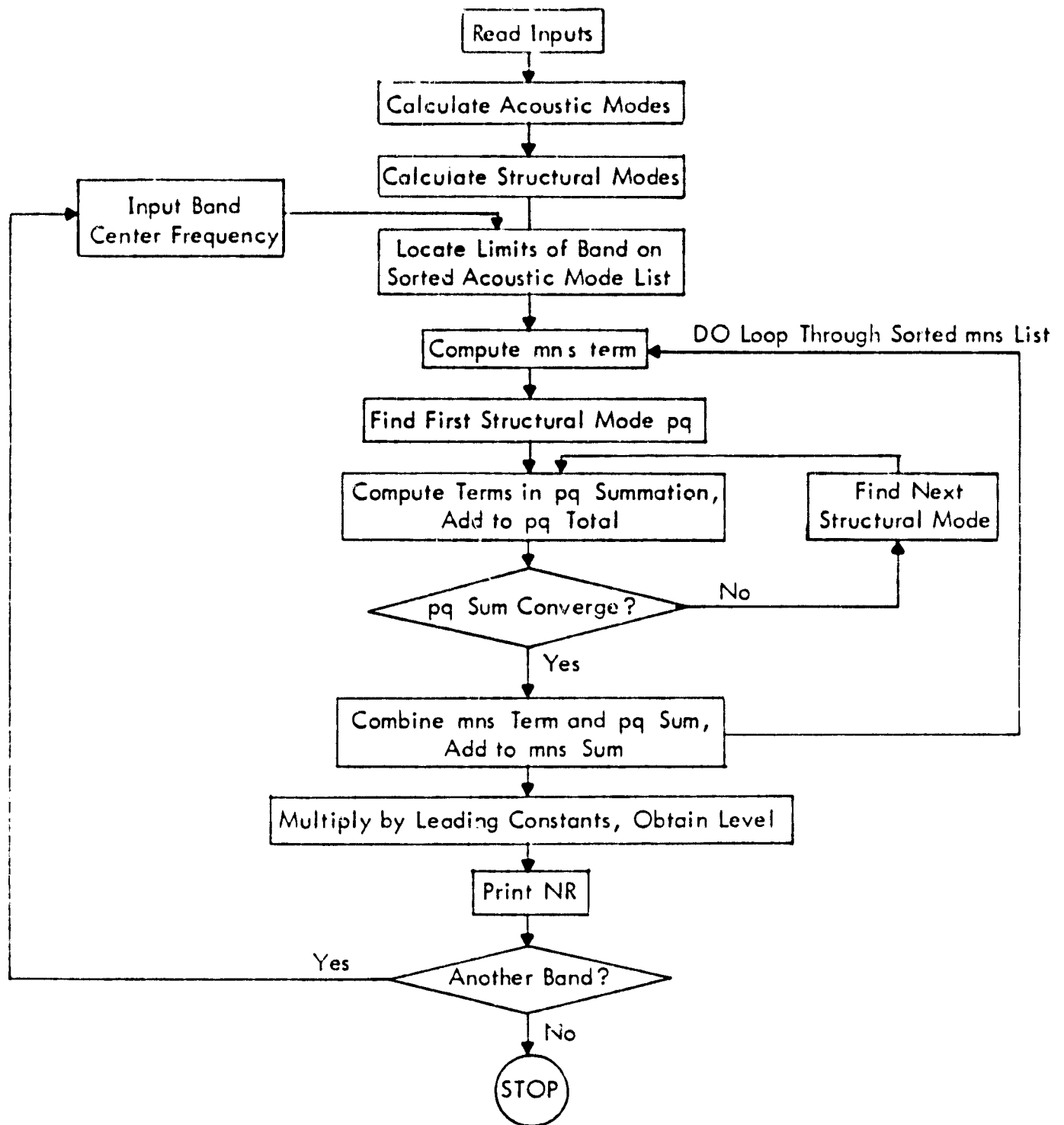


Figure 4-2. Flowchart of Main Program ACOBAN

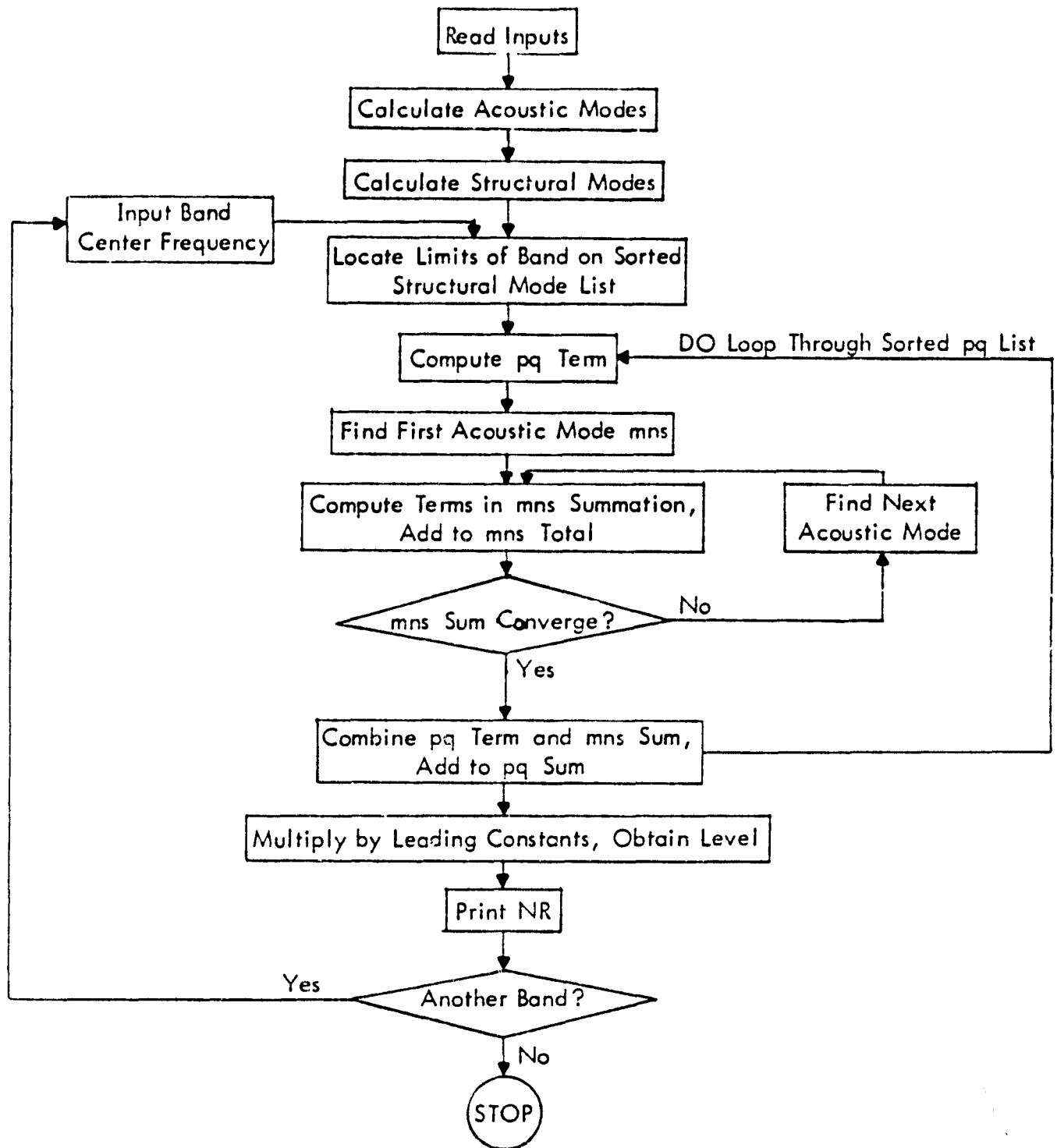


Figure 4-3. Flowchart of Main Program STRBAN

## 5.0 TEST CASES FOR ANALYTICAL PREDICTION MODEL

Test cases to be compared with the prediction methods were necessary to determine the validity of the analytical model, and to ascertain what improvements on the model might be necessary for better accuracy. Tests with the Space Shuttle orbiter with an empty payload bay [38] and Shuttle orbiter model tests with payload configurations [34] were used for these comparisons. Section 5.1 begins the information about the full scale acoustic test comparisons on the orbiter and Section 5.6 starts the discussion of the Shuttle model test comparisons with a payload configuration.

### 5.1 ACOUSTIC TESTS ON ORBITER OV-101

The acoustic tests were performed on the Space Shuttle Orbiter Vehicle (OV-101) at Edwards Air Force Base in California. Two F-104 jet aircrafts were used as the acoustic noise sources. This jet noise source provided a propagating excitation with spatial correlation characteristics similar to those expected during launch and with an intensity similar to the launch environment. Reference 38 gives the complete details and results of the tests, while the main test factors are summarized below.

#### 5.1.1 Test Configuration

Figure 5-1 illustrates the basic test configuration at Edwards AFB. The two F-104 jet aircraft were located aft of the orbiter to generate an acoustic field similar to that anticipated during launch. Two sets of tests were performed at the two aircraft distances of 100 feet and 250 feet. The 100-foot distance for tests 2 and 3 are of concern for this study. The two tests differed only due to the microphone locations for the test measurements of the payload bay interior noise levels, as discussed in the next section.

#### 5.1.2 Microphone Locations

The eight interior microphone locations for tests 2 and 3 are shown in Figure 5-2. The microphones in test 2, which were designated location A in Figure 5-2, were suspended on ropes that hung vertically down the payload bay centerline. In test 3 the microphones were pulled to the side, off the centerline, and into positions identified as location B, also shown in Figure 5-2. Exterior microphones were located on the orbiter surface as shown in Figure 5-3.

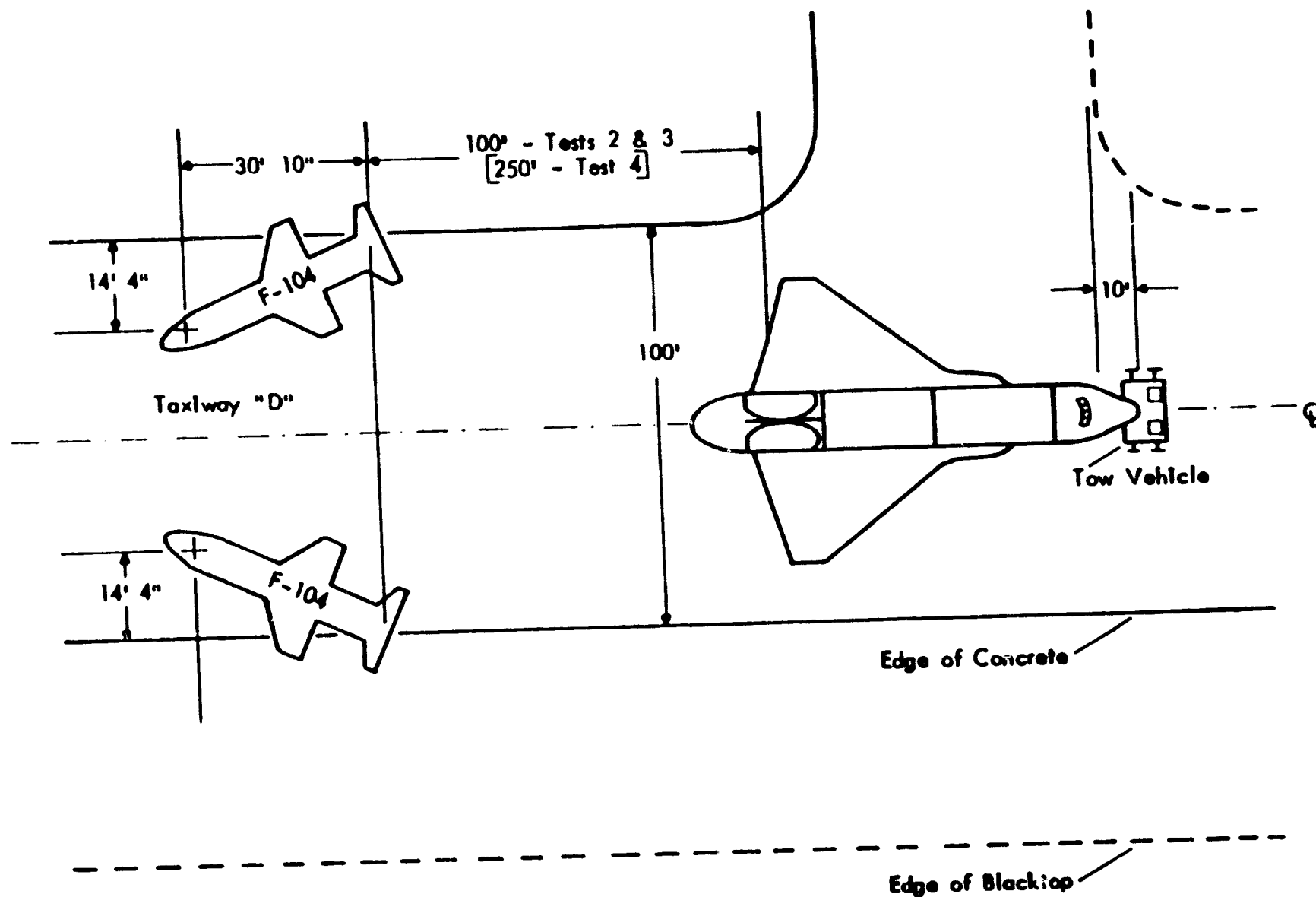
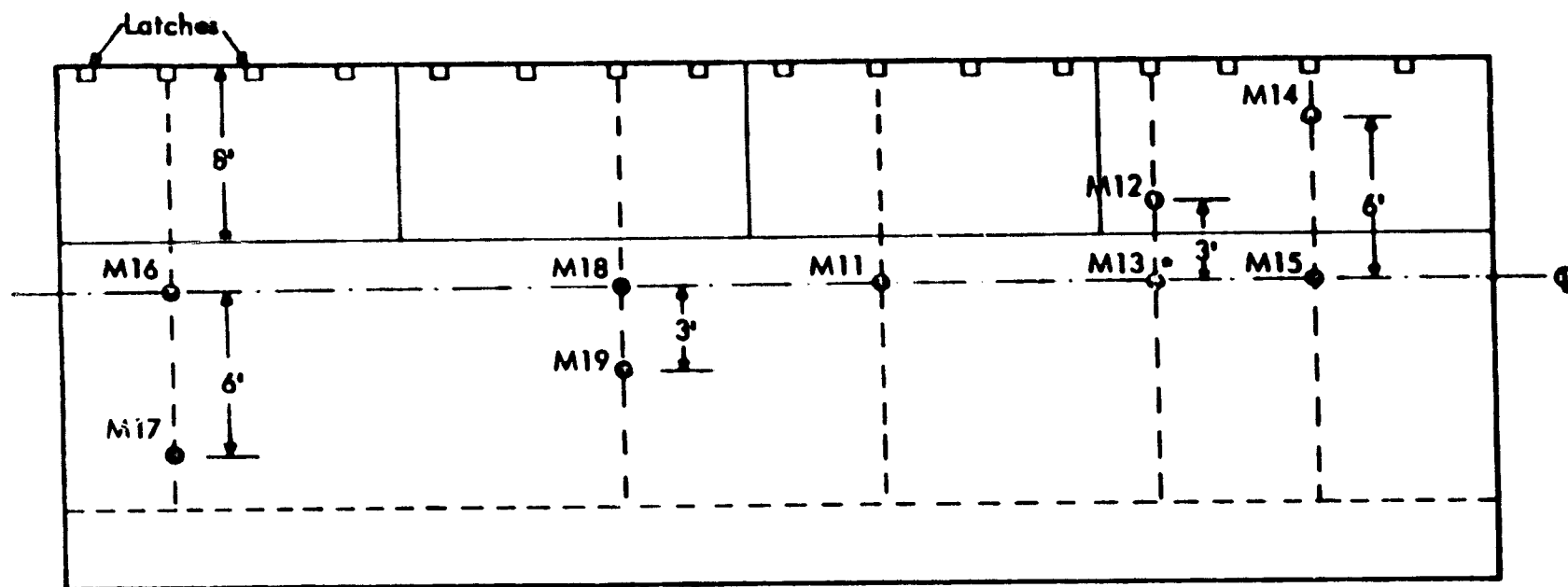


Figure 5-1. Position of F-104 Aircraft for OV-101 Acoustic Tests [38]





\*Malfunctioned

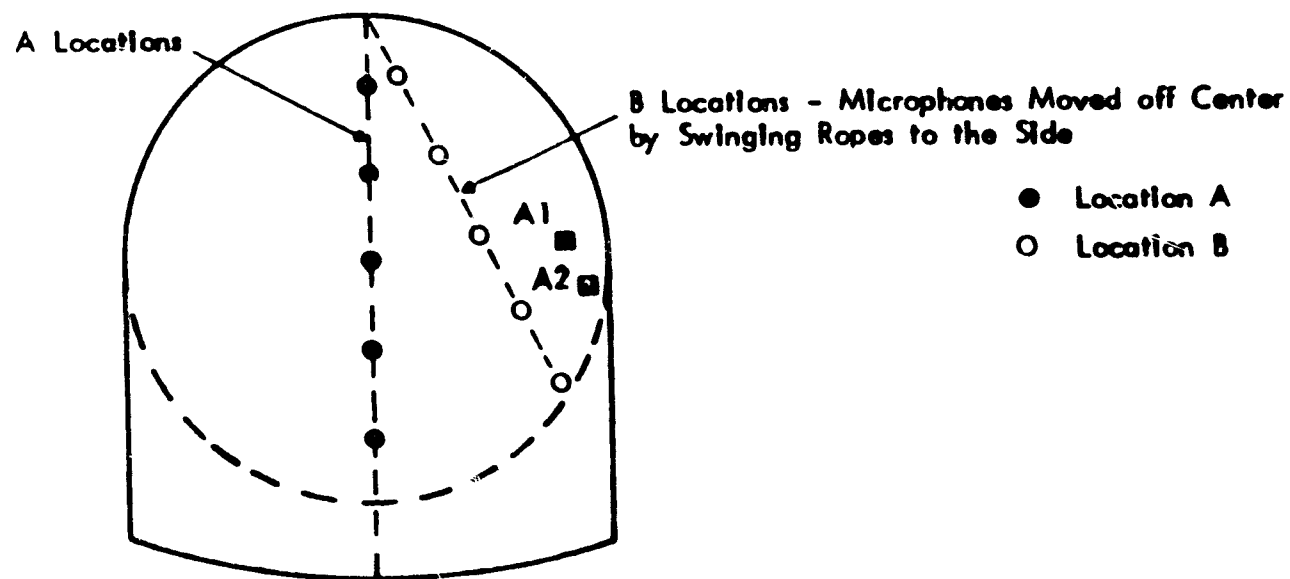


Figure 5-2. Microphone Locations Inside OV-101 Payload Bay [38]

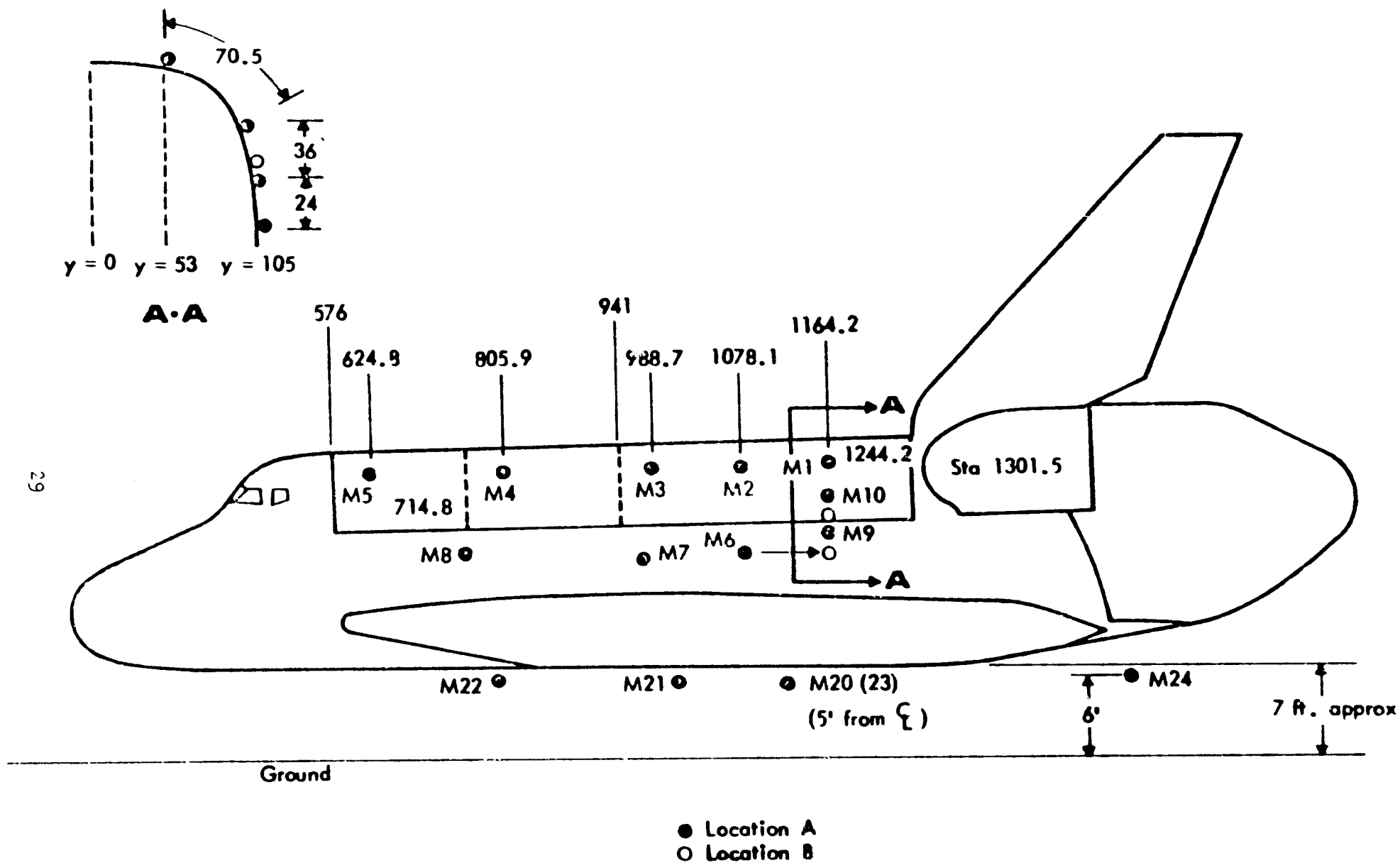


Figure 5-3. Microphone Locations Outside OV-101 Payload Bay [38]

### 5.1.3 Exterior Noise Source Levels

Since tests 2 and 3 were basically the same except for the location of the interior noise microphones, their exterior measurements were averaged to provide the forcing input on the structure. Noise transmission into the payload bay was primarily through the payload bay doors, especially in the low frequency range of excitation. Therefore, the test results for the doors alone will be used in the test and analytical comparison. The average exterior sound pressure levels (SPLs) measured on the doors are shown in Figure 5-4, along with a corrected door level. The corrected door levels were obtained because of a strong circumferential gradient at certain frequencies. Tables 5-1 and 5-2 list the measured one-third octave SPLs at each microphone location for test 2 and test 3, respectively.

### 5.1.4 External Noise Field Description

The correlation function for the convected excitation pressure field was represented by an exponentially decaying cosine function. For the longitudinal direction, it is given by

$$\rho_x(\xi, \omega) = \exp \left[ -\frac{k_x}{a_x} |\xi| \right] \cos(k_x \xi),$$

where  $k_x = \frac{\omega}{U_x}$ , wave number at frequency  $\omega$ ,  
 $U_x$  = phase (trace) velocity over surface of vehicle,  
 $a_x$  = correlation decay factor,  
 $\xi = x' - x$ , longitudinal distance between two points on surface of vehicle.

The circumferential correlation function is of the same form as the longitudinal function:

$$\rho_y(\zeta, \omega) = \exp \left[ -\frac{k_y}{a_y} |\zeta| \right] \cos(k_y \zeta),$$

where  $k_y$  = wave number at frequency  $\omega$ ,  
 $U_y$  = trace velocity in circumferential direction,  
 $a_y$  = correlation decay factor,  
 $\zeta = y' - y$ , transverse distance between two points.

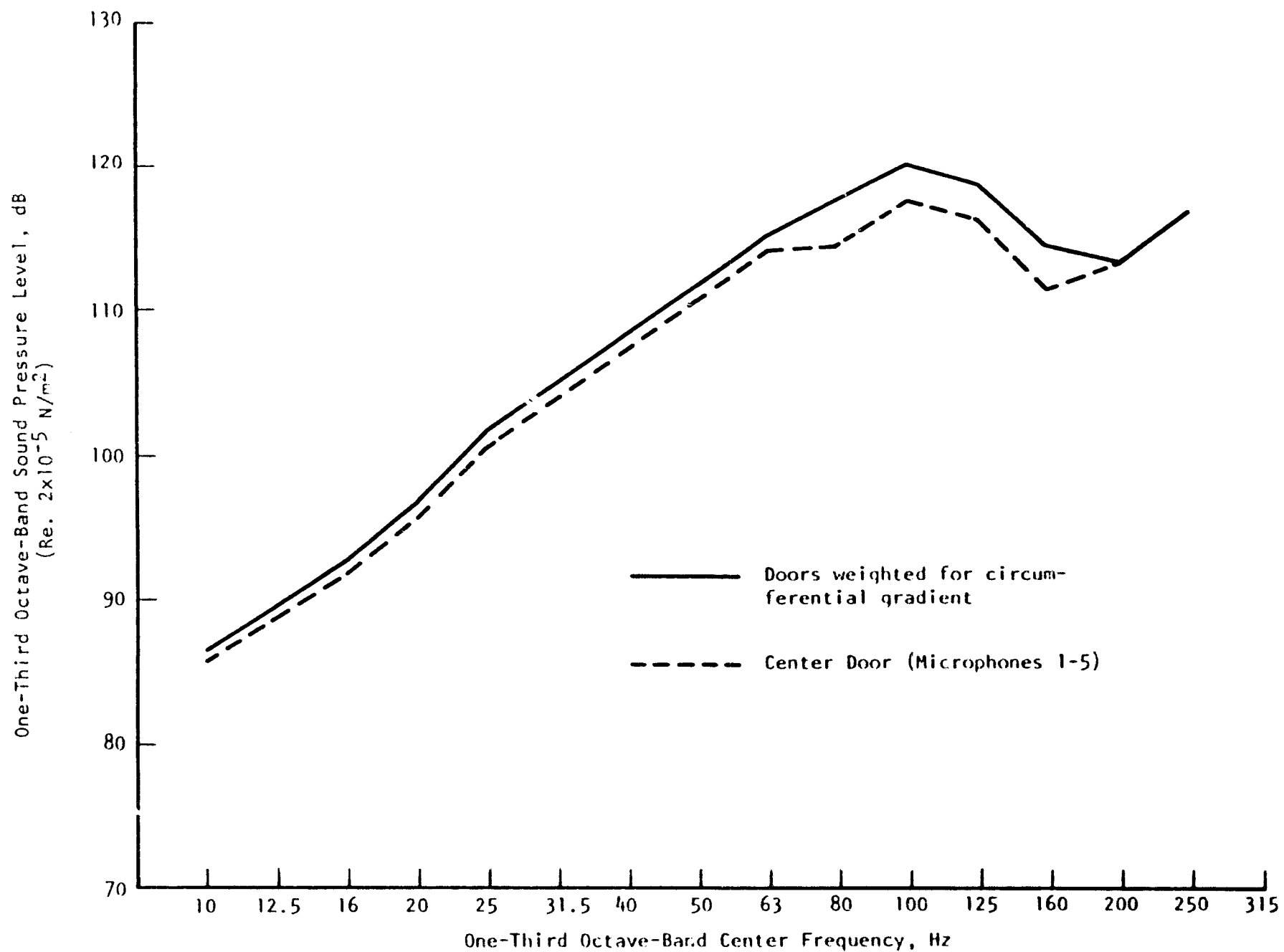


Figure 5-4. Test Measurements of Exterior Noise Levels on Orbiter

TABLE 5-1.  
ONE-THIRD OCTAVE-BAND SOUND PRESSURE LEVELS ON DOOR  
TEST 2 (NEAR SOURCE) 100 RPM [34]

FREQ>	10.0	12.6	15.8	20.0	25.1	31.6	39.8	50.1	63.1	79.4
TRANSDUCER										
M1	84.8	83.7	91.4	96.7	102.2	104.6	107.0	111.5	114.1	111.8
M2	84.8	87.8	90.6	95.5	100.8	104.0	107.3	110.3	113.5	113.3
M3	84.8	87.7	90.5	94.5	100.9	103.7	106.1	110.7	112.4	114.2
M4	83.5	88.6	91.2	95.0	100.2	104.3	107.9	111.8	113.4	112.9
M5	83.6	90.1	92.7	95.6	99.7	103.6	107.3	112.1	114.5	114.1
AVG	84.3	88.7	91.4	95.5	100.8	104.1	107.2	111.4	113.6	113.3
FREQ>	100.0	125.9	158.5	199.5	251.2	316.2	398.1	501.2	631.0	794.3
TRANSDUCER										
M1	114.0	113.0	108.8	113.3	117.1	118.6	122.3	117.6	115.3	117.7
M2	118.1	113.9	109.2	110.2	116.0	118.9	123.3	119.3	116.2	116.6
M3	117.4	115.0	110.0	113.0	113.5	117.3	123.6	120.4	116.9	117.4
M4	118.7	118.0	113.6	114.2	111.4	116.0	123.0	119.6	117.9	115.2
M5	115.8	115.2	111.6	112.7	113.0	113.6	119.9	119.1	118.1	114.5
AVG	117.1	114.8	111.0	113.1	114.7	117.3	122.6	119.3	117.0	116.4
FREQ>	1000.0	1258.9	1584.9	1995.3	2511.9	3162.0	3981.1	5011.9	6309.6	7943.3
TRANSDUCER										
M1	115.1	114.4	112.1	110.4	107.4	103.6	101.1	92.7	90.1	88.5
M2	118.2	114.9	113.5	112.8	110.3	107.4	105.5	103.4	98.3	95.8
M3	119.1	115.9	114.9	114.5	110.7	108.7	107.2	106.1	102.4	98.8
M4	118.3	118.0	115.5	114.0	112.6	110.5	107.9	107.2	102.4	99.4
M5	115.2	118.1	114.7	113.3	112.3	108.9	107.3	101.2	97.1	94.4
AVG	117.5	116.5	114.3	113.2	111.0	108.4	106.4	104.1	99.8	96.7

TABLE 5-2.

ONE-THIRD OCTAVE-BAND SOUND PRESSURE LEVELS ON DOOR  
TEST 3 (NEAR SOURCE) 1000 RPM [34]

FREQ>	10.0	12.6	15.8	20.0	25.1	31.6	39.8	50.1	63.1	79.4
TRANSDUCER										
M1	96.9	88.5	92.0	96.0	101.7	103.7	106.9	110.3	115.4	113.4
M2	96.1	87.3	90.9	95.0	100.7	103.2	107.3	109.8	114.4	115.4
M3	96.6	87.2	90.9	93.5	100.6	103.1	105.7	110.1	113.4	115.3
M4	96.0	88.1	91.0	94.2	100.5	103.8	107.9	110.5	114.4	114.6
M5	96.1	89.5	92.3	94.8	99.7	102.9	107.5	110.3	115.1	116.4
AVG	96.3	88.2	91.5	94.8	100.7	103.4	107.1	110.2	114.6	115.2
FREQ>	100.0	125.9	158.5	199.5	251.2	316.2	398.1	501.2	631.0	794.3
TRANSDUCER										
M1	112.8	115.1	110.1	115.2	121.0	120.2	121.5	116.6	115.5	118.7
M2	112.4	114.8	110.1	114.8	120.0	121.7	122.4	117.7	115.0	120.1
M3	112.5	118.6	111.8	112.3	118.5	120.9	122.2	116.9	116.2	120.0
M4	112.5	118.8	113.5	112.5	114.8	119.4	121.9	118.7	114.4	117.3
M5	117.0	119.2	113.5	111.0	112.1	115.8	119.4	118.0	114.7	117.9
AVG	118.1	117.4	112.1	113.5	118.3	120.0	121.6	117.7	115.2	118.9
FREQ>	1000.0	1258.9	1584.9	1995.3	2511.9	3162.3	3981.1	5011.9	6309.6	7943.3
TRANSDUCER										
M1	113.1	113.0	110.6	109.2	104.4	101.1	97.1	95.5	93.2	92.3
M2	114.4	115.2	113.5	112.3	108.3	105.2	102.8	99.8	96.1	94.3
M3	115.7	115.9	115.1	112.8	108.6	106.1	103.3	104.0	100.5	96.6
M4	116.7	115.4	113.2	112.8	110.2	107.1	103.7	101.3	95.8	94.8
M5	114.9	114.8	113.5	111.6	109.1	105.6	102.8	101.5	98.4	97.3
AVG	115.1	115.0	113.4	111.9	108.5	105.4	102.4	101.2	97.5	95.4

The correlation decay factors and trace velocities were determined experimentally from the test between microphone pairs, and their averaged values are given below for the payload bay doors:

$$k_x = kC_0/U_x = 0.92k,$$

where  $k = \omega/C_0$ , and  $C_0$  = speed of sound,

$$a_x = 34.4,$$

$$k_y = 0.26k,$$

$$a_y = 3.74.$$

From Reference 32, the AMTF values for the longitudinal factors are

$$k_x = 0.90k,$$

$$a_x = 31.0.$$

The values of  $a$  and  $k$  were assumed to be the same for tests 2 and 3.

#### 5.1.5 Determining the Measured Payload Bay Noise Reduction

The exterior sound pressure levels on the payload bay doors measured in tests 2 and 3 were averaged and weighted for circumferential gradient. These values are shown in Figure 5-4. Tables 5-1 and 5-2 also list the individual SPL for each microphone location and their average value at each one-third octave band.

Interior SPLs measured at location A (test 2) and location B (test 3) were space-averaged by the following equation to determine the payload interior noise levels:

$$\langle \text{SPL} \rangle = 10 \log_{10} \left[ 0.33(10)^{L_A/10} + 0.67(10)^{L_B/10} \right],$$

where  $\langle \text{SPL} \rangle$  = space averaged value of sound pressure level,

$L_A$  = the average SPL measured for microphones at location A in test 2,

$L_B$  = the average SPL measured for microphones at location B in test 3.

Figure 5-5 gives these space-averaged SPL results. Tables 5-3 and 5-4 give the SPL at each microphone location in the bay and also list the average one-third octave-band SPL. The SPLs at location B were weighted double those of location A

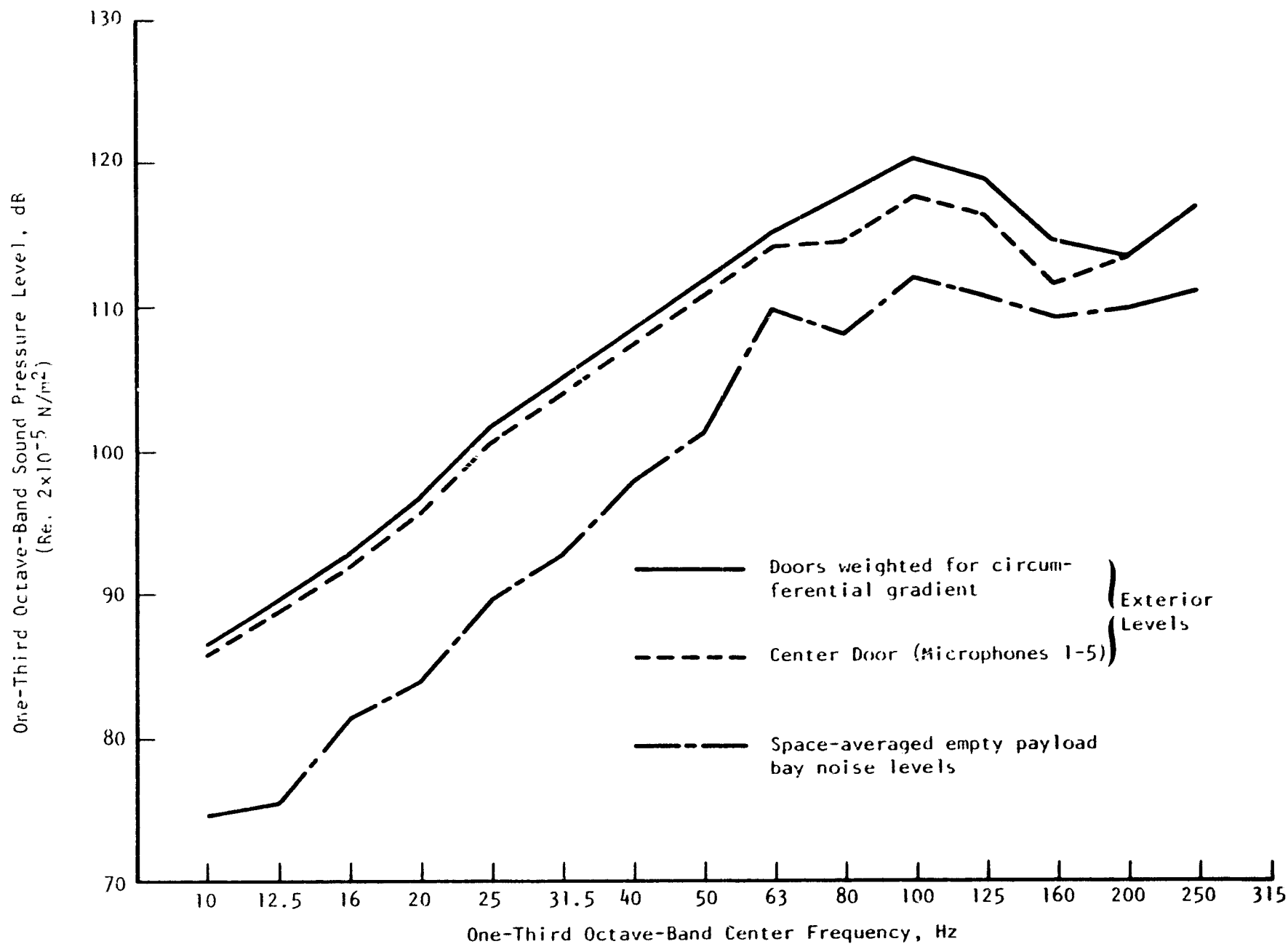


Figure 5-5. Test Measurements of Exterior and Interior Noise Levels on Orbiter



TABLE 5-3.

ONE-THIRD OCTAVE-BAND SOUND PRESSURE LEVELS INSIDE PAYLOAD BAY (ALONG CENTERLINE)

TEST 2 (NEAR SOURCE) 100% RPM [34]

FREQ>	10.0	12.6	15.8	20.0	25.1	31.6	39.8	50.1	63.1	79.4
TRANSDUCER										
H11	71.2	71.3	82.8	84.1	90.0	88.7	89.9	93.5	106.0	104.4
H12	74.0	73.3	75.0	76.4	87.2	86.2	90.3	89.8	101.2	104.0
H14	77.8	78.4	81.2	82.9	83.3	88.1	92.7	93.4	107.0	107.4
H15	74.6	73.9	82.0	84.7	86.0	81.1	91.7	92.9	103.9	106.3
H16	74.8	74.8	81.5	83.1	89.1	87.0	84.9	89.8	105.3	100.3
H17	77.1	77.5	82.4	84.5	89.0	92.7	92.5	92.0	109.5	107.0
H18	70.9	71.8	81.3	82.3	92.1	88.3	90.9	93.1	105.3	107.3
H19	72.3	74.4	83.0	84.0	92.9	85.9	93.0	94.7	107.0	107.6
AVG	74.7	75.1	81.0	83.3	89.7	88.2	90.7	93.6	106.2	106.1
FREQ>	100.0	125.9	158.5	199.5	251.2	316.2	398.1	501.2	631.0	794.3
TRANSDUCER										
H11	109.3	109.0	103.8	110.6	110.3	109.2	111.2	108.1	110.1	106.4
H12	107.8	108.7	107.3	112.1	110.6	109.0	113.2	109.5	107.8	106.6
H14	108.8	108.2	108.1	109.9	111.2	112.9	117.8	111.6	112.6	107.0
H15	110.9	106.2	110.9	109.0	110.7	110.3	113.5	109.2	111.3	106.8
H16	109.7	105.6	110.1	110.2	112.3	109.1	108.9	108.7	107.0	104.3
H17	114.3	111.2	109.7	113.1	113.7	116.0	106.4	108.9	106.2	105.9
H18	110.1	110.3	110.0	110.5	112.1	109.1	112.0	110.6	111.3	107.3
H19	110.3	109.1	108.7	112.0	112.1	109.0	112.6	110.8	110.8	107.0
AVG	110.7	108.9	109.3	111.1	111.8	110.1	112.2	109.0	110.3	106.5
FREQ>	1000.0	1258.9	1584.9	1995.3	2511.9	3162.3	3981.1	5011.9	6309.6	7943.3
TRANSDUCER										
H11	105.7	104.1	100.2	97.8	91.9	92.1	89.0	84.3	80.9	80.3
H12	105.3	102.3	101.0	96.0	95.3	91.2	87.9	83.0	81.2	79.9
H14	107.8	104.9	103.6	97.0	95.2	92.6	90.3	85.2	81.9	79.4
H15	107.2	104.8	103.0	97.7	95.1	92.9	90.0	85.6	83.7	79.0
H16	103.3	102.8	99.9	96.3	91.7	90.1	86.5	82.3	79.8	79.1
H17	104.8	102.6	101.0	96.6	92.1	89.7	87.6	82.2	80.2	80.7
H18	105.4	104.9	101.4	98.8	94.5	91.8	88.5	84.7	83.0	82.4
H19	105.4	105.4	101.7	99.0	94.6	92.2	88.7	85.4	81.2	80.7
AVG	105.8	104.1	101.9	97.6	94.2	91.7	88.7	84.3	81.8	80.5

TABLE 5-4.

ONE-THIRD OCTAVE-BAND SOUND PRESSURE LEVELS INSIDE PAYLOAD BAY (OFF TO SIDE)  
TEST 3 (NEAR SOURCE) 100% RPM [34]

FREQ	10.0	12.6	15.8	20.0	25.1	31.6	39.8	50.1	63.1	79.4
TRANSDUCER										
H11	71.5	71.8	83.4	85.0	89.0	95.1	95.6	101.3	105.7	103.2
H12	74.5	73.9	75.7	74.9	90.1	89.2	97.1	100.3	107.6	112.2
H14	75.9	76.3	79.7	83.3	81.6	88.3	94.4	94.6	105.8	108.0
H15	73.8	73.7	82.0	86.2	84.7	89.4	97.4	98.8	103.3	103.7
H16	73.4	76.2	81.8	84.0	88.6	95.7	100.5	102.4	110.8	106.6
H17	73.4	78.6	81.7	85.2	90.3	95.0	101.7	105.1	116.0	111.4
H18	71.7	73.2	81.9	83.5	91.0	94.0	99.7	104.3	107.7	102.0
H19	73.1	75.3	83.9	85.2	91.6	94.5	101.9	105.5	113.0	109.0
AVG	74.2	75.4	81.8	84.7	89.3	93.7	99.3	102.7	110.7	108.8
FREQ	100.0	125.9	158.5	199.5	251.2	316.2	398.1	501.2	631.0	794.3
TRANSDUCER										
H11	103.5	110.4	110.3	108.5	111.7	110.4	113.0	110.7	106.6	106.8
H12	112.3	112.4	102.1	102.4	106.5	111.1	113.5	112.7	107.4	106.4
H14	112.6	109.7	104.9	107.2	110.5	113.2	115.1	110.5	116.2	108.8
H15	108.0	110.0	108.4	111.9	110.3	110.7	113.2	111.2	103.3	107.7
H16	110.8	107.1	107.4	107.9	108.5	108.7	111.4	109.6	105.9	105.4
H17	110.2	112.9	111.7	111.3	112.6	109.3	110.4	110.7	110.7	105.3
H18	110.6	110.8	102.3	108.1	111.6	110.3	112.6	103.4	103.0	106.4
H19	114.3	112.1	107.8	107.9	109.0	111.1	113.0	111.4	107.7	106.8
AVG	111.5	110.8	105.9	109.2	110.1	110.9	113.0	110.8	108.5	106.8
FREQ	1000.0	1258.9	1584.9	1995.3	2511.9	3162.3	3981.1	5011.9	6309.6	7943.3
TRANSDUCER										
H11	106.6	104.4	101.1	97.7	94.4	91.5	88.0	83.7	81.7	80.1
H12	107.0	104.3	101.2	97.0	94.0	92.3	88.2	84.8	83.1	77.9
H14	107.2	104.4	102.4	97.5	95.3	93.0	89.5	85.1	82.4	79.8
H15	107.9	104.6	101.0	97.8	95.9	93.0	90.1	86.6	81.4	78.6
H16	105.1	101.8	100.5	96.5	93.0	89.9	87.3	82.0	80.0	80.7
H17	104.7	103.1	99.1	96.5	92.7	91.7	89.0	82.9	81.0	80.9
H18	106.7	103.7	100.4	98.7	94.6	92.9	88.7	84.4	82.5	83.1
H19	106.2	104.7	100.0	98.5	95.5	93.0	91.0	85.8	83.4	82.3
AVG	106.5	104.0	100.9	97.6	94.7	92.2	89.1	84.6	82.2	80.7

because of the payload bay symmetry. By the symmetry factor, the noise levels on the other side of the bay were assumed to have the same values as those at location B. This situation can be easily seen in Figure 5-2.

To determine the payload bay noise reduction (NR) from these one-third octave-band measured data, the space averaged interior noise levels were subtracted from the exterior door levels. Since the dominant noise transmission at these low frequencies is through the doors, little accuracy is lost on calculating the NR by considering only the transmission of the exterior noise through the doors. These noise reduction levels are plotted for each one-third octave band from 10 Hz to 250 Hz in Figure 5-6.

#### 5.1.6 Spatial Variability of the Measured Noise Reduction

The spatial variability of the empty payload bay measurements is shown in Figure 5-7. The scatter of the 16 measurements from tests 2 and 3 are given relative to the space-averaged level. The largest variation can be seen in the 40-Hz band, where the full range is about 20 dB. For bands below 100 Hz, the data scatter becomes more prevalent as the frequency decreases. Except for the 63 Hz band, all the measurements are less than 5 dB above the space-averaged value. But since 16 measurements is a relatively small sample within the entire payload bay space, there are undoubtedly some locations where the low frequency levels exceed the space averaged levels by more than 5 dB.

### 5.2 INPUTS FOR THE ANALYTICAL MODEL PREDICTIONS

The following section describes the data that were used to model the Shuttle Orbiter payload bay structure, the payload bay enclosure, and the payload geometry. These inputs for the analytical representation were used with the basic computer program developed by Wyle, which is described in Section 4.0.

#### 5.2.1 Absorption of OV-101 Payload Bay

The interior absorption of the payload bay was measured by exciting the bay with loudspeaker sources and determining the reverberation time. From the reverberation time, the volume loss factors in one-third octave bands were computed and the average wall absorption coefficients were estimated. Figure 5-8 shows the reverberation times used to compute the acoustic damping in the analytical model of the computer program.

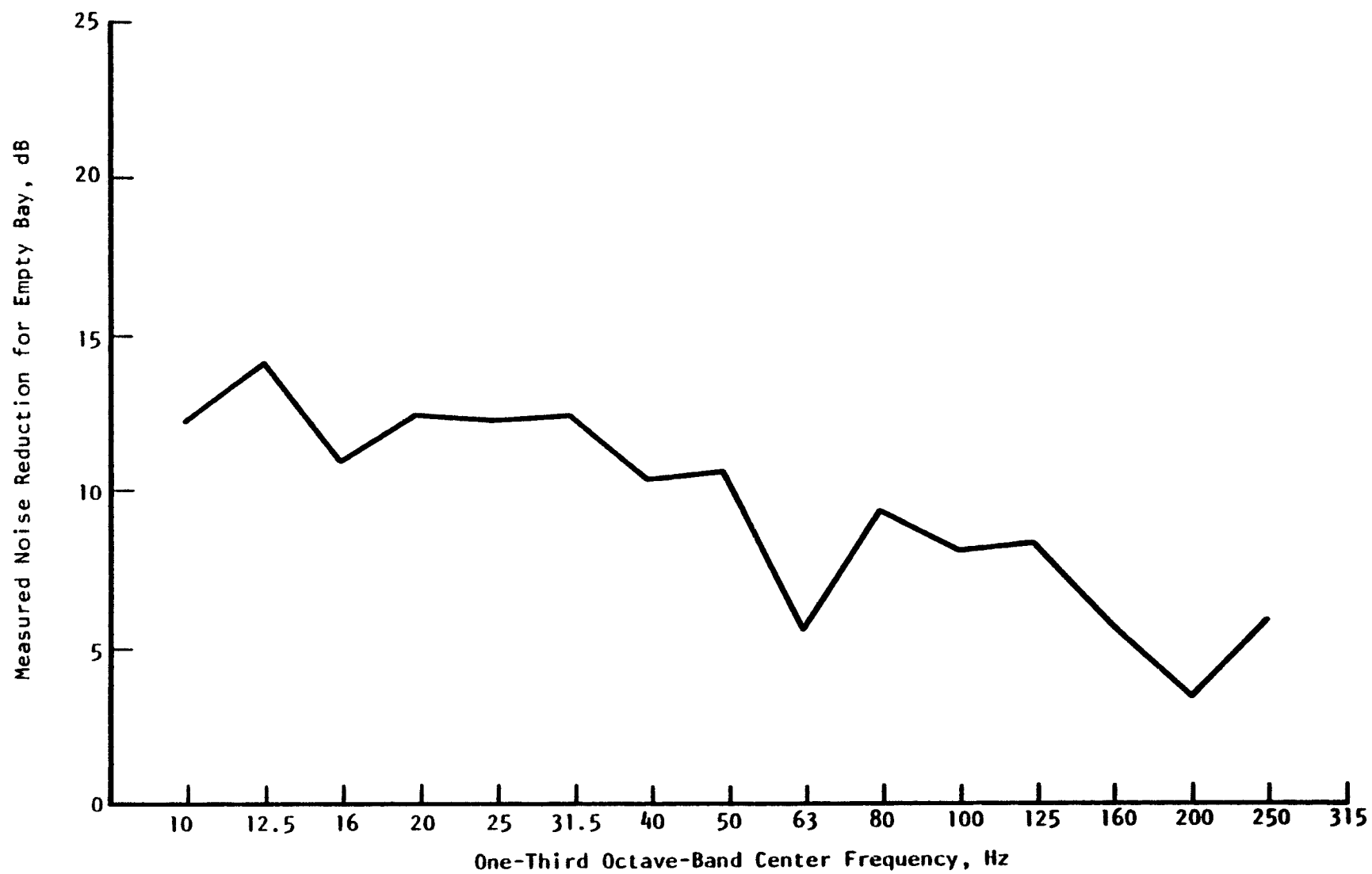


Figure 5-6. Measured Noise Reduction Levels for Empty Payload Bay

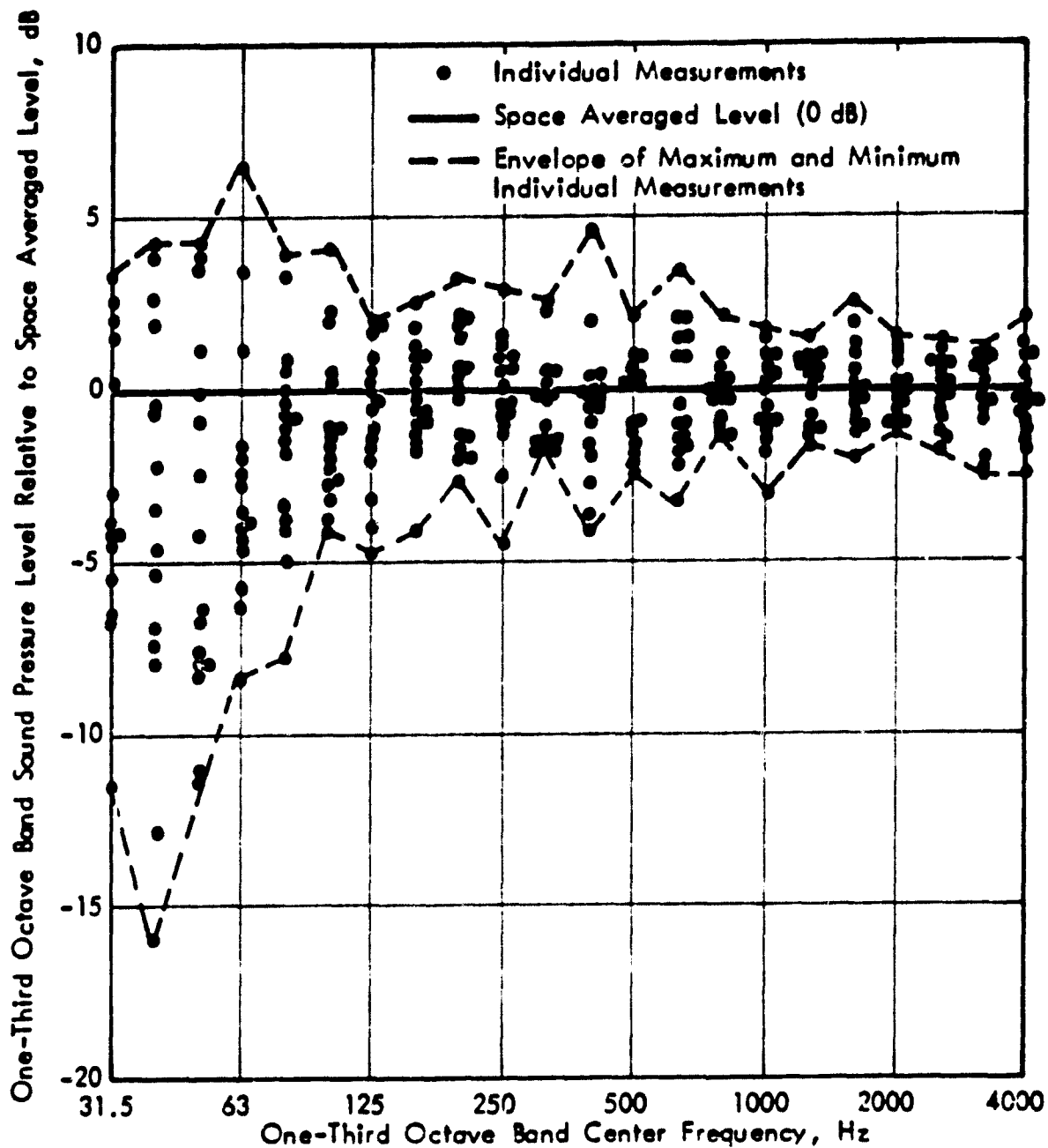


Figure 5-7. Variability of Measured Payload Bay Acoustic Levels for OV-101 Tests 1 and 2 [34]

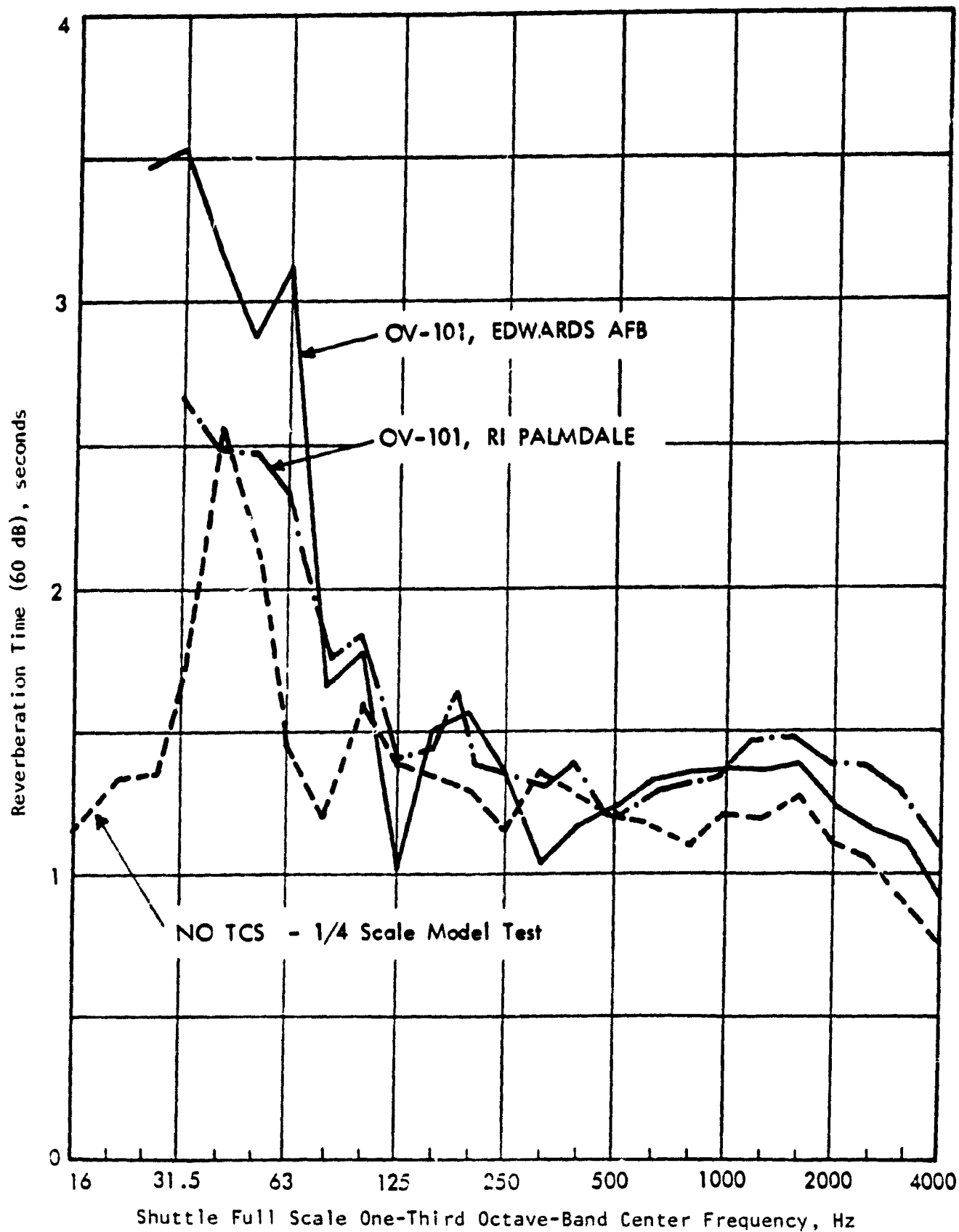


Figure 5-8. Payload Bay Reverberation Time

### 5.2.2 Structure of the Orbiter

Figure 5-9 shows a general view of the Space Shuttle orbiter. Figure 5-10 shows a typical cross section through the cargo bay that is approximately 60 feet long with a roughly circular usable cargo volume approximately 16 feet in diameter. The side walls and bottom are essentially flat, with truss frames (shown in Figure 5-10) at about 5-foot intervals. The doors, which have a roughly circular cross section, consist of five pairs that open in two pair of units as shown in Figure 5-11.

For the purposes of matching the orbiter structure to the cylindrical coordinate geometry of the analytic model, the payload bay structure is modeled in the following way:

- The structure is modeled as a cylinder, 16-foot diameter by 60-foot length, with rigid end walls.
- The doors are considered to comprise a 180-degree full length panel, joined to the fuselage by shear diaphragm boundary conditions.

Detailed structural and vibrational properties of the doors are discussed in Section 5.2.5.

### 5.2.3 Payload Bay Doors

The payload bay doors consist of five pairs, as noted above. Figure 5-11 shows the structural arrangement of one of the four main door halves. The structure consists of the skin, end frames, seven intermediate frames, a torque box at the hinge line, and a center beam. The skin is a graphite-epoxy sandwich with nomex filler. The frames are graphite-epoxy with hat-section intermediate frames. The fifth pair of doors (rearmost) is about one-eighth the length of the others, and has no intermediate frames. Not shown in Figure 5-11 are various latches, skin doublers, hardware, etc. Table 5-5 lists all components of the doors together with their weights [39]. Table 5-6 summarizes the material properties of the skin and frame materials [40]. The five door pairs are joined into two unit pairs that open and close separately. The joining is done with shear pins. When closed, the doors are latched with a combination of shear pins and latches.

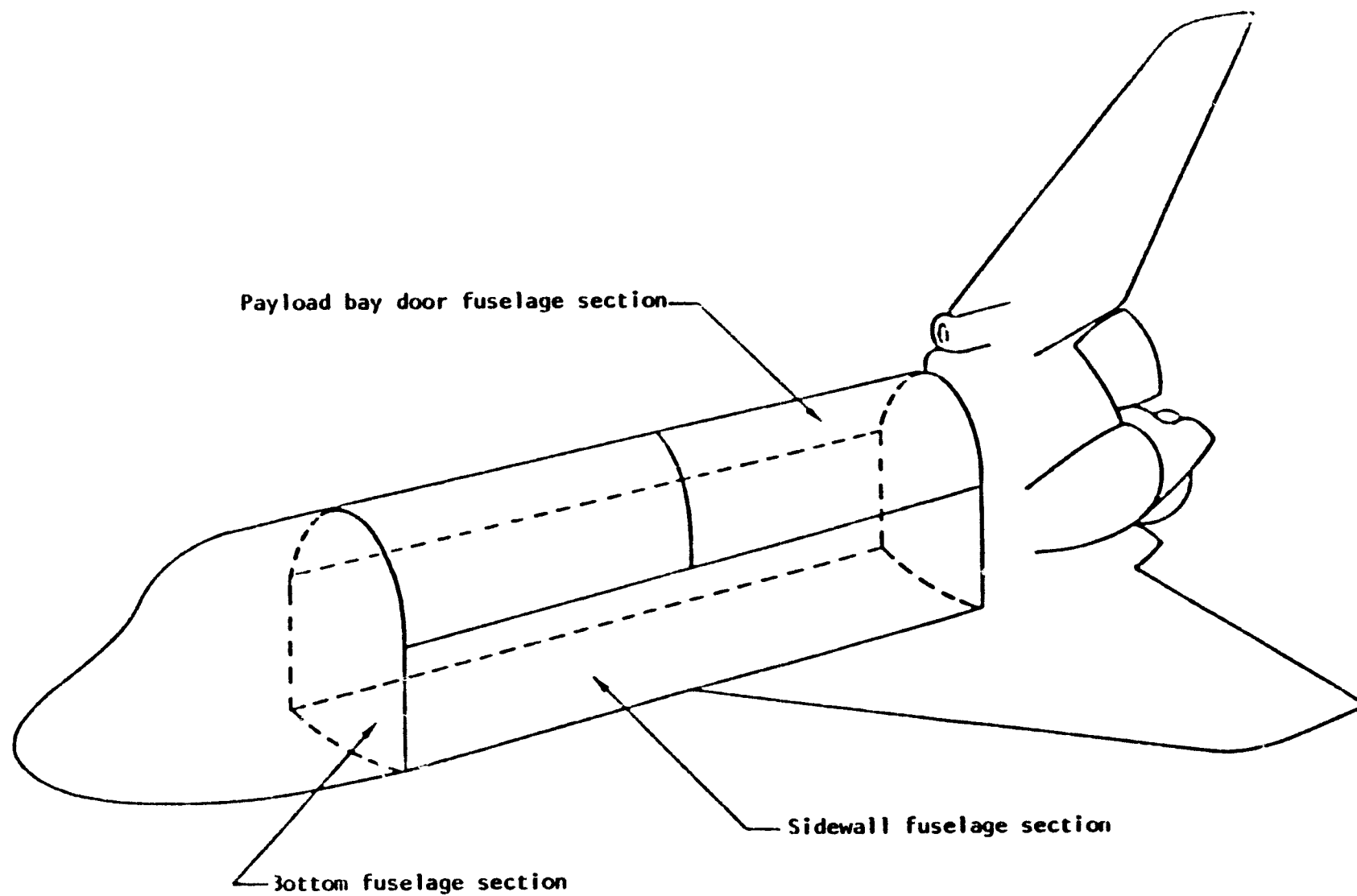


Figure 5-9. Space Shuttle Configuration



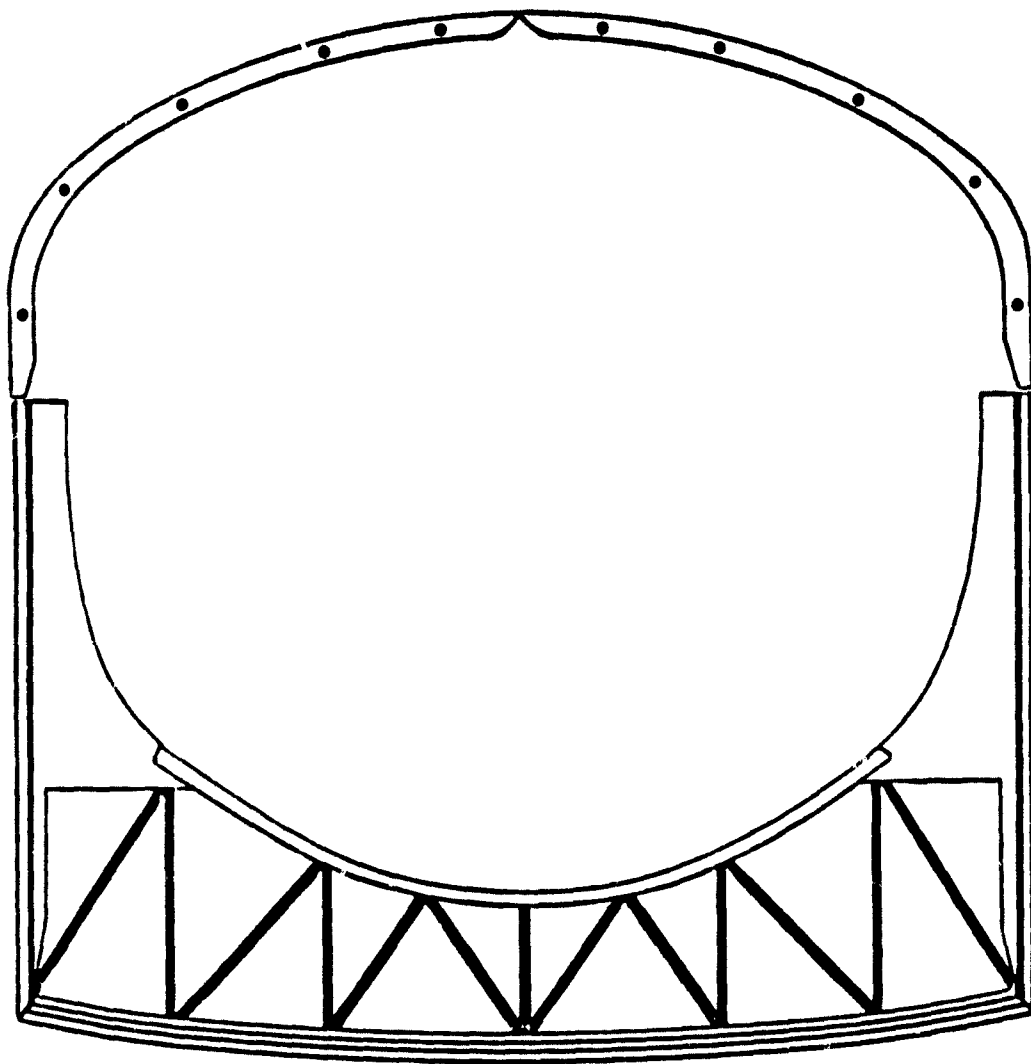


Figure 5-10. Cross Section of Space Shuttle Cargo Bay  
Showing Typical Truss Frame

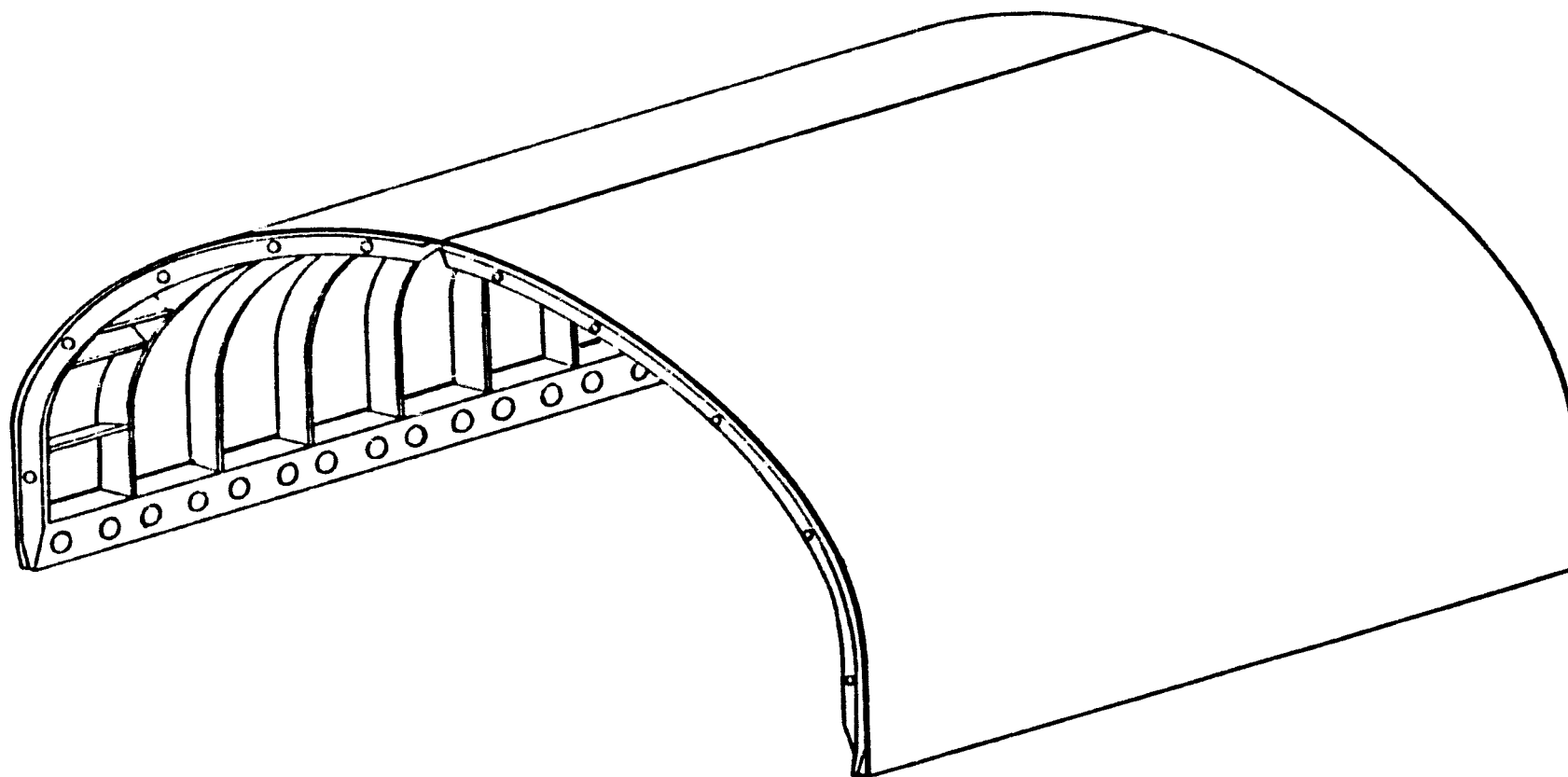


Figure 5-11. Structural Configuration of Cargo Bay Doors Showing Skins, Hinge Line Torque Box and Circumferential Frames

**TABLE 5-5.**  
**SUMMARY OF ORBITER 001 PAYLOAD BAY DOOR WEIGHTS**

<b>Component</b>		<b>Weight (lb.)</b>
<b>Forward Honeycomb Panel</b>	<b>Skin</b>	<b>373.1</b>
	<b>Core</b>	<b>87.1</b>
	<b>Bonding</b>	<b>100.2</b>
<b>Aft Honeycomb Panel</b>	<b>Skin</b>	<b>383.2</b>
	<b>Core</b>	<b>84.9</b>
	<b>Bonding</b>	<b>100.7</b>
<b>Intermediate Frames</b>		<b>549.5</b>
<b>Closeout Frames</b>		<b>260.0</b>
<b>Torque Boxes</b>		<b>134.6</b>
<b>Centerline Beams</b>		<b>106.4</b>
<b>Hingeline Closeouts</b>		<b>51.0</b>
<b>Latch Backup Structure</b>	<b>Right</b>	<b>75.8</b>
	<b>Left</b>	<b>72.8</b>
<b>Expansion Joints</b>		<b>202.9</b>
<b>Miscellaneous Hardware</b>		<b>99.1</b>
<b>Lightning Protection</b>		<b>90.9</b>
<b>Linkage and Hinges</b>		<b>58.0</b>
<b>Door Hinges on Door</b>		<b>195.4</b>
<b>Sealant</b>		<b>20.0</b>
<b>Seal Supports</b>		<b>116.4</b>
<b>Seals</b>		<b>293.0</b>

TABLE 5-6.  
PROPERTIES OF PAYLOAD BAY DOOR MATERIALS

<u>GR/E Skin</u>	
Thickness:	0.016" (each face sheet)
Young's Modulus:	$3.5 \times 10^6$ psi (90°)
	$12.8 \times 10^6$ psi (0°)
Density:	0.057 lb/in <sup>3</sup>
<u>Nomex Core</u>	
Thickness:	0.6"
Cell Size:	1/8 inch
Density:	0.3 lb/ft <sup>3</sup>

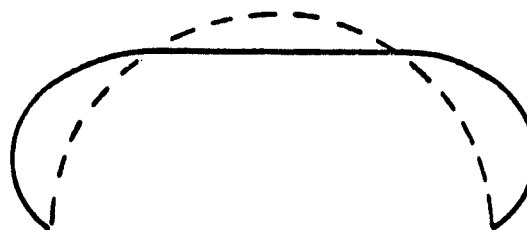
The door structure for the flight operational orbiter also includes two pairs of space radiators that open on a hinge line almost in common with the door hinges. When closed, the radiators are secured to the doors by a system of latches and ball joints. No strains from loads on the doors are transmitted to the radiators. The radiators were not installed on the OV-101 vehicle during these noise tests [38].

The structural properties of the doors as needed for the stiffnesses are summarized in Table 5-7. These were computed on the basis of the properties in Tables 5-5 and 5-6 and dimensions obtained from assembly drawings provided by NASA. Masses concentrated at the door/fuselage hinge line (torque boxes, hinge hardware, etc) were neglected in computing mass density because these are at a node.

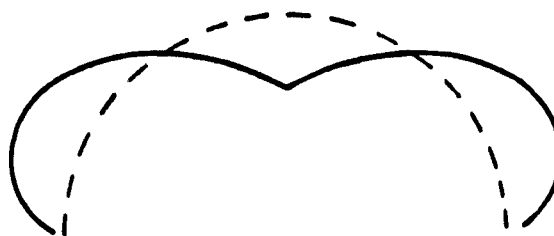
Representation of the doors as a single 180° panel is not entirely satisfactory because of the pin connections between halves at the top centerline. Figure 5-12a shows the cross-sectional mode shape for  $q = 3$  for the 180° homogeneous shell and the actual shape for the two-piece door with center hinge line is shown in Figure 5-12b. The true boundary conditions are not amenable to representation by an analytic expression as convenient to work with as Equation 30 from Reference 1. The main difference between Figures 5-12a and 5-12b is that b is considerably less stiff. The center hinge was, therefore, handled by reducing the

TABLE 5-7.  
STRUCTURAL PROPERTIES OF PAYLOAD BAY DOORS

QUANTITY	SYMBOL	WHOLE DOOR	PANEL BETWEEN FRAMES
Length	$l$	60 feet	1.5 feet
Radius	$b$	8 feet	8 feet
Circumferential Extent	$\alpha$	180°	90°
Stressed Skin Thickness (both layers)	$A_{S_s}/l$	0.00267 feet	0.00267 feet
Skin Filler Thickness	$t_F$	0.050 feet	0.050 feet
Shell Density	$\rho_s$	0.0989 slug/ft <sup>2</sup>	0.0128 slug/ft <sup>2</sup>
Longitudinal Young's Modulus	$E_{S_s}$	$1.843 \times 10^9$ lb/ft <sup>2</sup>	$1.843 \times 10^9$ lb/ft <sup>2</sup>
Circumferential Young's Modulus	$E_{S_\phi}$	$0.504 \times 10^9$ lb/ft <sup>2</sup>	$0.504 \times 10^9$ lb/ft <sup>2</sup>
Frame Young's Modulus	$E_F$	$1.843 \times 10^9$ lb/ft <sup>2</sup>	---
Frame Area	$A_F$	0.00986 ft <sup>2</sup>	---
Frame Moment of Inertia	$I_F$	$0.183 \times 10^{-3}$ ft <sup>4</sup>	---
Frame Spacing	$L_F$	1.58 feet	---
Frame-Skin Centroid Distance	$\bar{x}$	0.109 feet	---
Poisson's Ratio	$\nu$	0.3	0.3



a. Homogeneous Door Structure



b. Door Structure with Center Hinge

Figure 5-12. Circumferential  $q = 3$  Mode Shape for Homogeneous and Hinged Doors

circumferential bending stiffness to compensate. For a force directed downward at the center, the split semicircle (12b) will be displaced approximately 30 times as far as the whole semicircle (12a). This was determined by applying the calculation procedure in Section 80 of Reference 41 to both cases. A relaxation factor of 30 is probably too great for the doors, however, as the driving force will not be concentrated on the centerline. For purposes of calculating low frequency vibration of the doors, the circumferential bending stiffness was divided by a factor of 20.

#### 5.2.4 Payload Door Resonant Frequencies

Table 5-8 lists the payload bay door modal frequencies and indices through the 50 Hz one-third octave band. Table 5-9 shows the frequencies for eight of the first ten symmetric modes calculated from a finite element analysis of the door structure [42]. The finite element calculation is based on a structural description much closer to actual than the "relaxed" shell used here. The symmetric modes correspond to odd values of the circumferential modal index  $q$ . The first finite element frequency of 8.17 Hz corresponds well with the 1,3 mode of 9.3 Hz. The sequence of finite element frequencies increases in general with the

TABLE 5-8.

**STRUCTURAL MODAL FREQUENCIES AND INDICES  
FOR PAYLOAD BAY DOOR MODEL THROUGH 50 HZ BAND**

p, q	f	p, q	f
1, 2	7.5	4, 6	39.5
1, 3	9.3	4, 3	39.8
2, 3	14.9	5, 4	40.0
1, 4	16.0	5, 6	42.5
2, 4	17.6	3, 2	43.4
1, 1	17.7	6, 5	43.9
3, 4	22.4	6, 6	46.6
2, 2	23.1	1, 7	49.6
1, 5	25.1	2, 7	49.9
2, 5	25.8	2, 1	50.5
3, 3	26.0	3, 7	50.5
3, 5	27.6	6, 4	50.7
4, 4	30.2	4, 7	51.6
4, 5	31.3	7, 6	51.8
1, 6	36.4	7, 5	52.0
2, 6	36.7	5, 7	53.4
5, 5	36.9	5, 3	54.6
3, 6	37.7	6, 7	55.9

p = number of longitudinal half waves.

q = number of circumferential full waves.

TABLE 5-9.  
COMPARISON BETWEEN DOOR RESONANT FREQUENCIES FROM FINITE  
ELEMENT MODEL AND PRESENT MODEL SYMMETRIC MODES

PRESENT MODEL		FINITE ELEMENT MODEL
p, q	f	f
1, 3	9.3	8.17
2, 3	14.9	9.65
3, 3	26.0	10.85
4, 3	39.8	17.69
5, 3	54.6	20.04
6, 3	69.2	23.11
7, 3	50.5	26.07
8, 3	96.6	31.50

longitudinal modes p and with the odd q modes. The first and second symmetric modes are shown in Figures 5-13 and 5-14, respectively.

At high frequencies, when the wavelength is no longer large compared to the spacing between ring frames, the individual response of panels between frames must be considered. These are taken as independent panels, of circumferential extent 90 degrees and longitudinally between rings, with properties corresponding to the skin properties in Table 5-7 and supported by shear diaphragms. Table 5-10 lists the first few frequencies calculated for a typical skin panel between frames. The lowest frequency is over 400 Hz, so that these modes are of little importance for the present study.

TABLE 5-10.  
RESONANT FREQUENCIES FOR DOOR PANELS  
BETWEEN FRAMES

MODE p, q	FREQUENCY f
1, 1	421.1
1, 2	435.5
1, 3	458.9
1, 4	490.2
1, 5	528.7
1, 6	573.4
1, 7	623.7
1, 8	679.2
1, 9	739.8
1, 10	805.5



Figure 5-13. 4 Door - Fuselage Model Modes --  
Sym. TCL Constraints  
Frequency = 8.17 cps  
 $p, q = 1, 3$   
(from Reference 42)

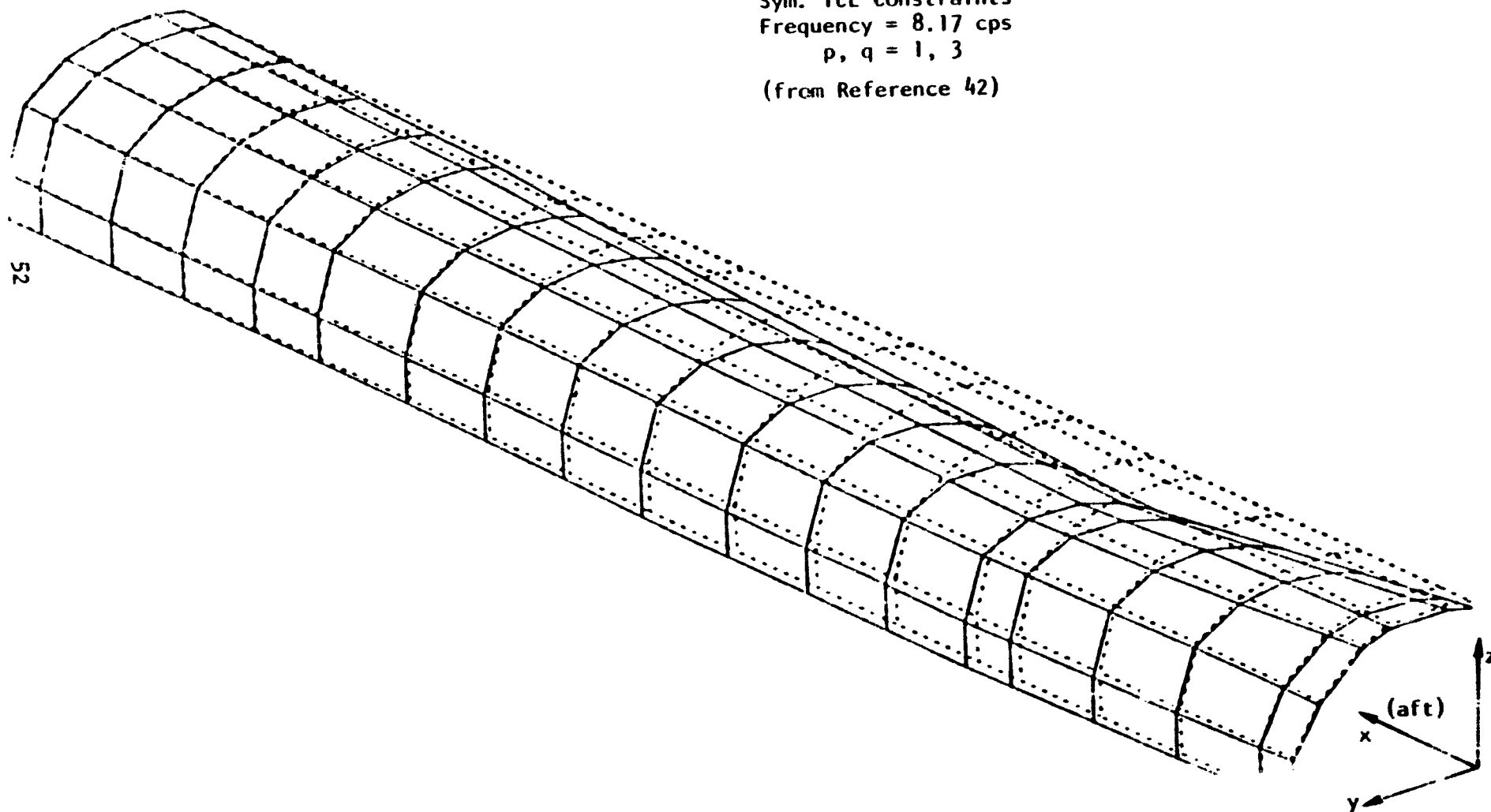
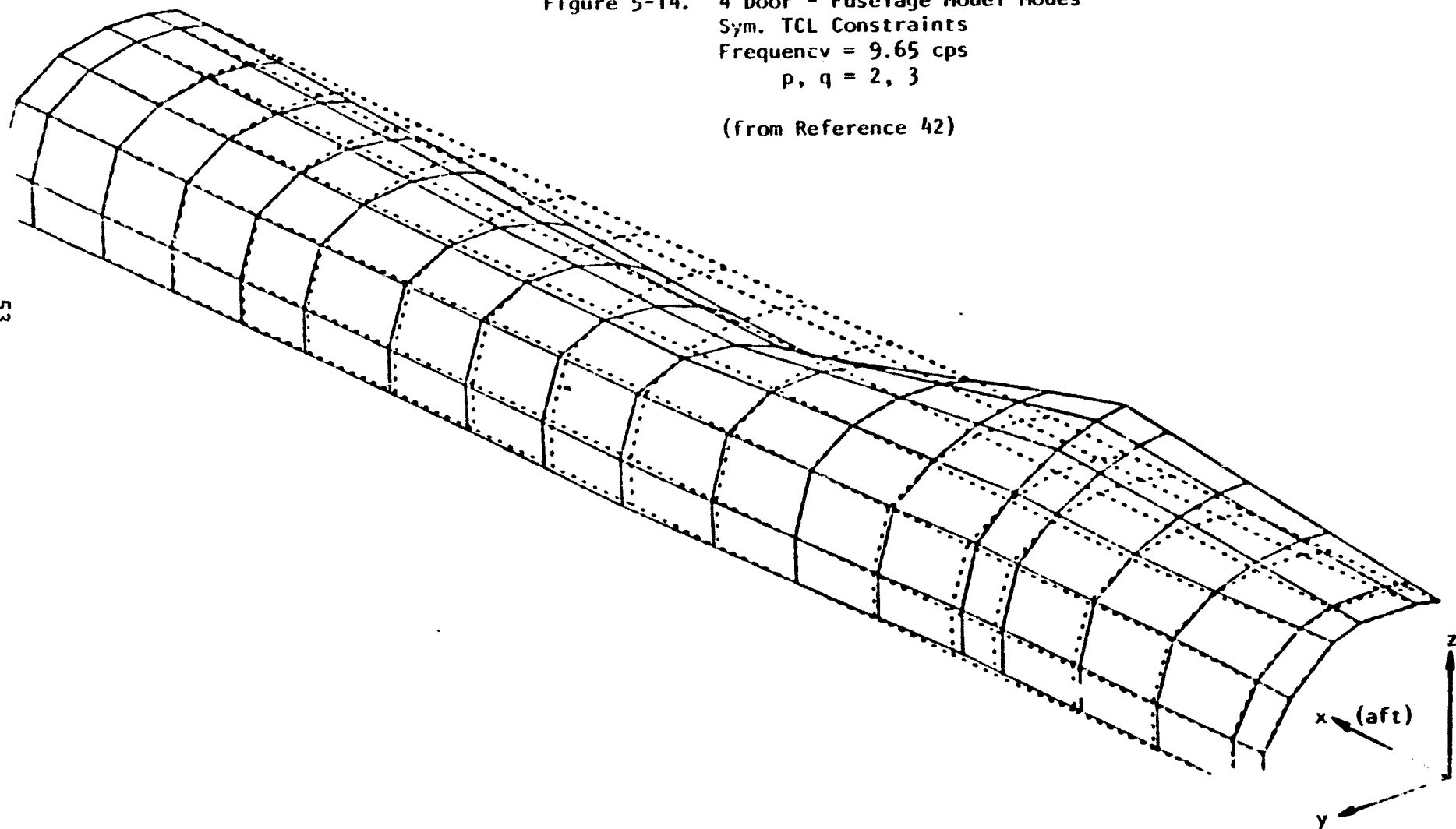


Figure 5-14. 4 Door - Fuselage Model Modes --  
Sym. TCL Constraints  
Frequency = 9.65 cps  
 $p, q = 2, 3$   
(from Reference 42)



### 5.2.5 Structural Damping

The structural damping values, in terms of the loss factor  $\Delta f/f$ , for the payload bay doors is taken from Reference 34 to be  $\eta = 2/f$ , where  $f$  is in hertz.

### 5.2.6 Payload Bay Resonant Frequencies

The interior of the payload bay was represented as a cylindrical cavity 16 feet in diameter and 60 feet long. Payloads were modeled as a concentric inner cylinder. For this test case comparison, the noise reduction was computed only for the empty bay case. Figure 3-1 describes the bay geometry.

Table 5-11 lists acoustic modal frequencies up to 112 Hz (this is through the 100 Hz one-third octave band) together with their modal indices. The first radial mode (i.e.,  $s \neq 0$ ) occurs in the 80 Hz band, so that (except for damping and volume effects) the empty bay calculation should give the same result as would calculations with payloads. Since low frequencies are the primary interest in the present study, there is little loss of generality in considering only the empty bay.

The payload bay normal acoustic modes were also calculated with the cavity idealized by a rectangular parallelepiped with one surface deformed to represent the payload bay doors. This is a perturbation technique used in Reference 34 to model the payload bay and the geometry. The dimensions of the analytical model are shown in Figure 5-15. Table 5-12 compares the normal modes from this computation with modes calculated using the right circular cylinder idealization.

### 5.2.7 Acoustic Losses

There are two ways in which acoustic energy can be lost from the payload bay:

- Absorption by hardware inside the bay. This includes the effect of payloads, of frame trusses, of structural textures, etc. At low frequencies, these may all act as porous materials.
- Transmission of sound out of the bay through the structure. This is the inverse process of transmission in.

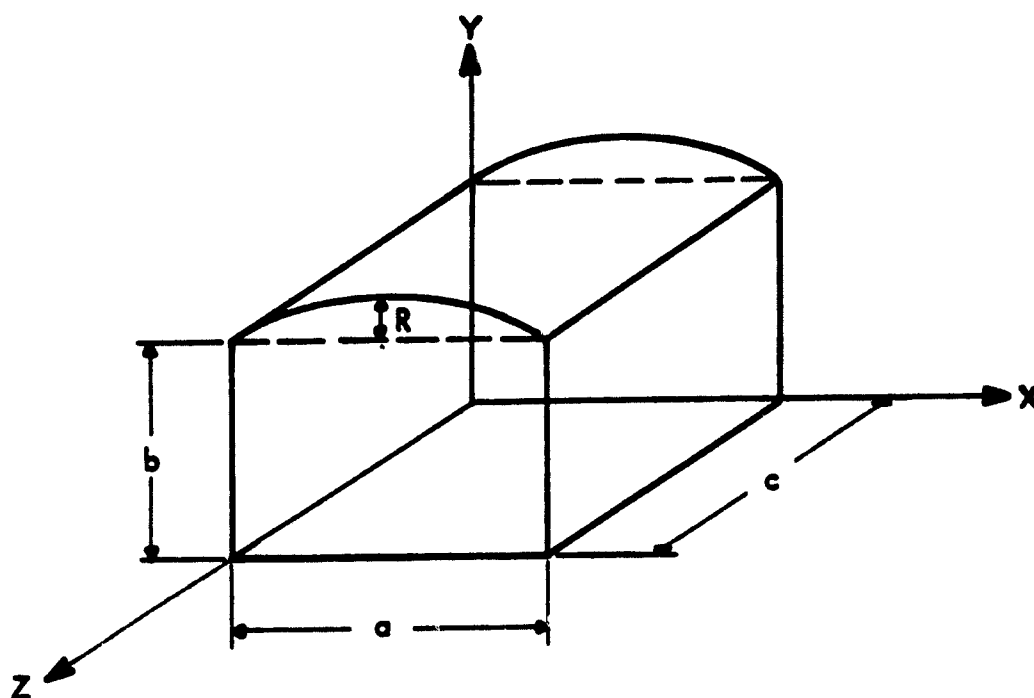
TABLE 5-11  
ACOUSTIC MODAL FREQUENCIES, EMPTY PAYLOAD BAY,  
THROUGH 100 HZ BAND

m, n, s	f	m, n, s	f	m, n, s	f
0, 0, 0	0	2, 2, 0	70.3	1, 3, 0	93.7
1, 0, 0	9.3	3, 2, 0	73.3	7, 2, 0	94.0
2, 0, 0	18.6	8, 0, 0	74.4	2, 3, 0	95.1
3, 0, 0	27.9	7, 1, 0	76.9	5, 0, 1	97.0
4, 0, 0	37.2	4, 2, 0	77.3	3, 3, 0	97.4
0, 1, 0	40.9	5, 2, 0	82.2	4, 3, 0	100.4
1, 1, 0	41.9	9, 0, 0	83.7	8, 2, 0	100.7
2, 1, 0	44.9	8, 1, 0	85.1	10, 1, 0	101.6
5, 0, 0	46.5	0, 0, 1	85.1	6, 0, 1	101.7
3, 1, 0	49.5	1, 0, 1	85.6	11, 0, 0	102.3
4, 1, 0	55.3	2, 0, 1	87.1	5, 3, 0	104.2
6, 0, 0	55.8	6, 2, 0	87.8	7, 0, 1	107.1
5, 1, 0	61.9	3, 0, 1	89.5	9, 2, 0	107.7
7, 0, 0	65.1	4, 0, 1	92.8	6, 3, 0	108.7
0, 2, 0	67.8	10, 0, 0	93.0	11, 1, 0	110.2
1, 2, 0	68.4	9, 1, 0	93.1	12, 0, 0	111.6
6, 1, 0	69.2	0, 3, 0	93.3		

m = number of longitudinal half waves.

n = number of circumferential full waves.

s = number of radial full waves.



$a = 17.50$  ft;  $b = 12.58$  ft;  $c = 60.42$  ft;  $R = 4.33$  ft

Figure 5-15. Deformed Parallelepiped (from Reference 34)

TABLE 5-12.

COMPARISON BETWEEN SOME ACOUSTIC MODES  
FROM THE PRESENT MODEL AND  
A PERTURBATED RECTANGULAR PARALLELEPIPED MODEL

PRESENT MODEL		PERTURBATED RECTANGULAR PARALLELEPIPED MODEL
m, n, s	f	f
0, 1, 0	40.8	27.07
1, 1, 0	41.9	28.60
2, 1, 0	44.9	32.77
3, 1, 0	49.5	38.73
4, 1, 0	55.3	45.80
5, 1, 0	61.9	53.53
0, 2, 0	67.8	61.50
1, 2, 0	68.4	62.19
6, 1, 0	69.2	61.67
2, 2, 0	70.3	64.22
3, 2, 0	73.3	67.46
7, 1, 0	76.9	70.09

The loss factor may be represented by the empty payload bay reverberation test [34] mentioned in Section 5.2.1 as

$$\eta = \frac{2.2}{f T_{60}}, \quad (1)$$

where  $f$  is in hertz and  $T_{60}$  is reverberation time from Figure 5-8.

The second factor, retransmission of sound, is explicitly neglected in the formulation of the coupling equations. It is assumed that the shell is driven by the exterior sound field alone. This is correct only if the interior sound pressure is small compared to exterior, that is, NR is large. If NR is small, the effect of interior pressure must be considered. This is equivalent to calculating the inverse problem.

Calculation of transmission from inside to out is just as complex as the outside to inside analysis treated thus far. An approximate allowance can be made, however, by noting that the process is essentially linear. The interior and exterior pressure are related by

$$(p_i)_v = A p_o \quad (2)$$

where  $( )_v$  denotes in vacuo shell response; that is, the effect of interior pressure is not considered. Counting interior pressure,

$$p_i = A \left[ p_o - (p_i)_v \right]. \quad (3)$$

Equation 3 assumes the process is reversible. If only a single mode is considered, this is true. Since the present approximation has structural modes uncorrelated with each other, and acoustic modes are uncorrelated in the spatial average, this is a reasonable assumption. At low frequencies, there are few modes present, so that Equation 1 is reasonable from this viewpoint as well. At high frequencies, where there are many overlapping modes, an equation similar to 3 but in terms of intensity  $p^2$  rather than pressure would be more appropriate. This is the architectural acoustics regime, however, and is not of direct interest.

The computer programs includes this second factor as an adjustment to the noise reduction calculation. The NR was calculated initially in terms of  $(p_i)_v$ . Equations 2 and 3 were manipulated to relate this "true" interior pressure  $p_i$  as

$$p_i = \frac{(p_i)_v}{1 + (p_i)_v/p_o} \quad (4)$$

In terms of an adjustment to noise reduction,  $NR = -20 \log p_i/p_o$ ,

$$NR = (NR)_v + 20 \log_{10} \left[ 1 + 10^{-(NR)_v/20} \right] \quad (5)$$

The equivalent expression for the architectural acoustics case would have 10 in place of 20 in both cases.

### 5.3 PREDICTION OF PAYLOAD BAY NOISE REDUCTION

The inputs for analytically determining the orbiter empty payload bay noise reduction (NR) were submitted to the Wyle computer models for computation. All three versions of the computer program were required to calculate the total NR from the 10 Hz to 250 Hz one-third octave bands. The NR due to acoustic resonances was modeled by considering the nonresonant structural response of the doors driving resonant acoustic responses in the payload bay. The acoustic version of the program is called ACOBAN. When the NR was governed by the structural resonances occurring in the frequency band of interest, the response was considered to be a resonant structural response driving a nonresonant acoustic field. This program is called STRBAN. The noise reductions obtained by these programs were then added to obtain the total NR due to resonant acoustic and structural transmission by the following equation:

$$NR = -10 \log_{10} \left[ \frac{1}{10 \frac{NR_A}{10}} + \frac{1}{10 \frac{NR_S}{10}} \right],$$

where  $NR_A$  = resonant acoustic NR,

$NR_S$  = resonant structural NR.

If no resonance of the doors or payload bay cavity existed for a given octave band, then the PURTON version of the program was used to calculate the NR from the response of nonresonant structure driving a nonresonant condition in the payload bay cavity. The NR was computed at discrete frequencies in the desired one-third octave band and was then integrated by summing the individual NRs to obtain a total for the band.

The predicted one-third octave-band noise reduction levels are shown in Figure 5-16 for the empty payload bay case. At each one-third octave band, the values of space-averaged NR corresponding to the type of noise transmission are plotted. For example, the 10 Hz band from Figure 5-16 shows about the same noise transmission for both resonant structural and acoustic response. These two values of NR calculated by ACOBAN and STRBAN are combined to give the total one-third band level. At 10 Hz the puretone response integrated over the bandwidth by the PURTON program gives approximately the same result also.

A nonresonant condition is noted in the 12.5 Hz band since there are no structural door or payload bay resonances. This can be seen by Tables 5-8 and 5-11, respectively. Therefore, the PURTON version was used to compute the NR for single frequencies within the band and then integrated to obtain a one-third octave-band NR level.

In some frequency bands, it can be seen from Figure 5-16 that the noise transmission is dominated by either acoustic or structural resonances. For example, with the 20 Hz band, the NR is low because the noise transmission for the acoustic resonant case is very much greater than the structural resonant case due to strong acoustic responses created by the structural vibrations of the payload bay doors. This condition can be seen by looking at Tables 5-8 and 5-11. The 20 Hz band containing the 18.6 Hz acoustic longitudinal mode, where  $m = 2$ , can be excited by several matching structural modes with an equal wave number. These structural modes also have resonant frequencies close to the acoustic resonance. The 22.4 Hz door structural mode, on the other hand, with a longitudinal wave number  $p = 3$ , has only one close acoustic mode to couple with. That mode is at 27.9 Hz, which is in the 25 Hz band.



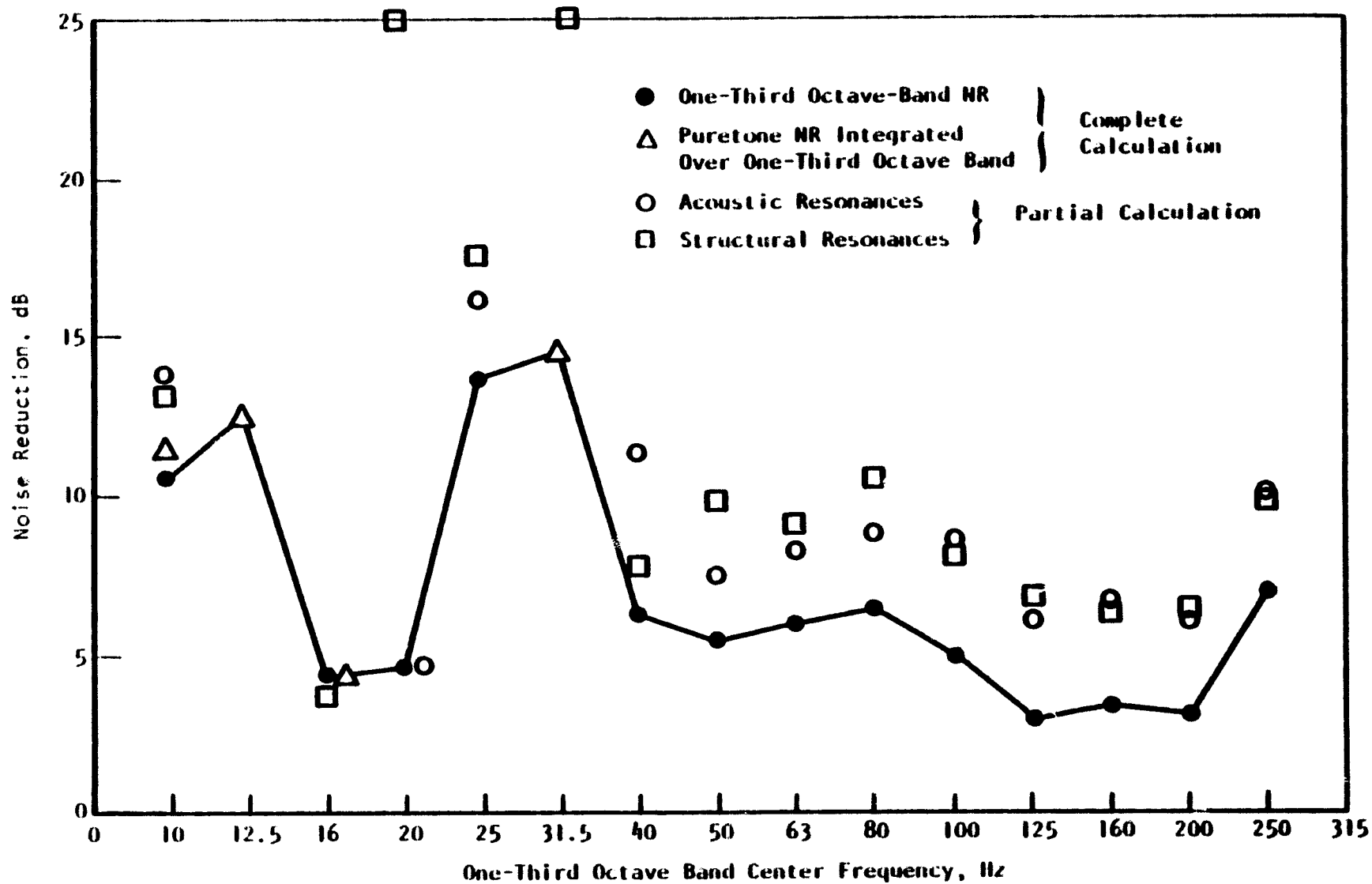


Figure 5-16. Predicted Noise Reduction for Empty Payload Bay

In the 16 Hz band in Figure 5-16, here is a case where the structural resonant response alone is responsible for the noise transmission because no payload bay acoustic modes exist. The 16 Hz door mode with a longitudinal wave number of one will couple well with the random external noise field because correlation lengths are typically comparable to acoustic wavelengths. Since the structural wavelength of the  $p = i$  mode is the length of the bay cavity (60 feet), and the 16 Hz acoustic excitation wavelength is about 70 feet, the payload bay door structural response is expected to be strong due to these comparable wavelengths. At the higher one-third octave bands in Figure 5-16, the noise transmission is about equally divided between the acoustic and structural resonant condition.

### 5.3.1 Comparison Between Measured and Predicted Noise Reduction for Empty Payload Bay

Figure 5-17 illustrates the NR curve from the measured data (Figure 5-6) plotted along with the NR predicted from the analytical model (Figure 5-16). The predicted NR curve seems to follow the measured NR trend, that of the NR decreasing with increased frequency in the 10 to 250 Hz range. Generally, the predicted NRs are fairly close to the measured levels, except at several one-third octave bands. In Figure 5-18, a plot to readily indicate the differences between the predicted and measured noise reduction levels is given. The predicted NR spectra is subtracted from the measured spectra to show these relative differences, and the 0 dB level is the measured NR used for this reference in Figure 5-17.

Approximately 87% of the predicted NR values are within 5 dB of the measured NRs, and approximately 60% are 3 dB or less from the measured levels. Bands of 10 and 12.5 Hz seem to have the best agreement with the test NRs. One important reason for this is that the door structural model modes closely match the more accurate finite element values as listed in Table 5-9. Also, the lower order longitudinal acoustic modes are easier to model at these frequencies, both in their mode shape and resonant frequency.

The worst discrepancy occurs in the 16 and 20 Hz one-third octave bands where the predicted NRs are about 6.5 and 7.5 dB less than the measured values, respectively. At 17.7 Hz, the payload bay door mode with  $p, q = 1, i$  (from Table 5-8) would be highly correlated to the random noise field, both longitudinally and circumferentially, for the reasons mentioned in Section 5.3. Therefore, this

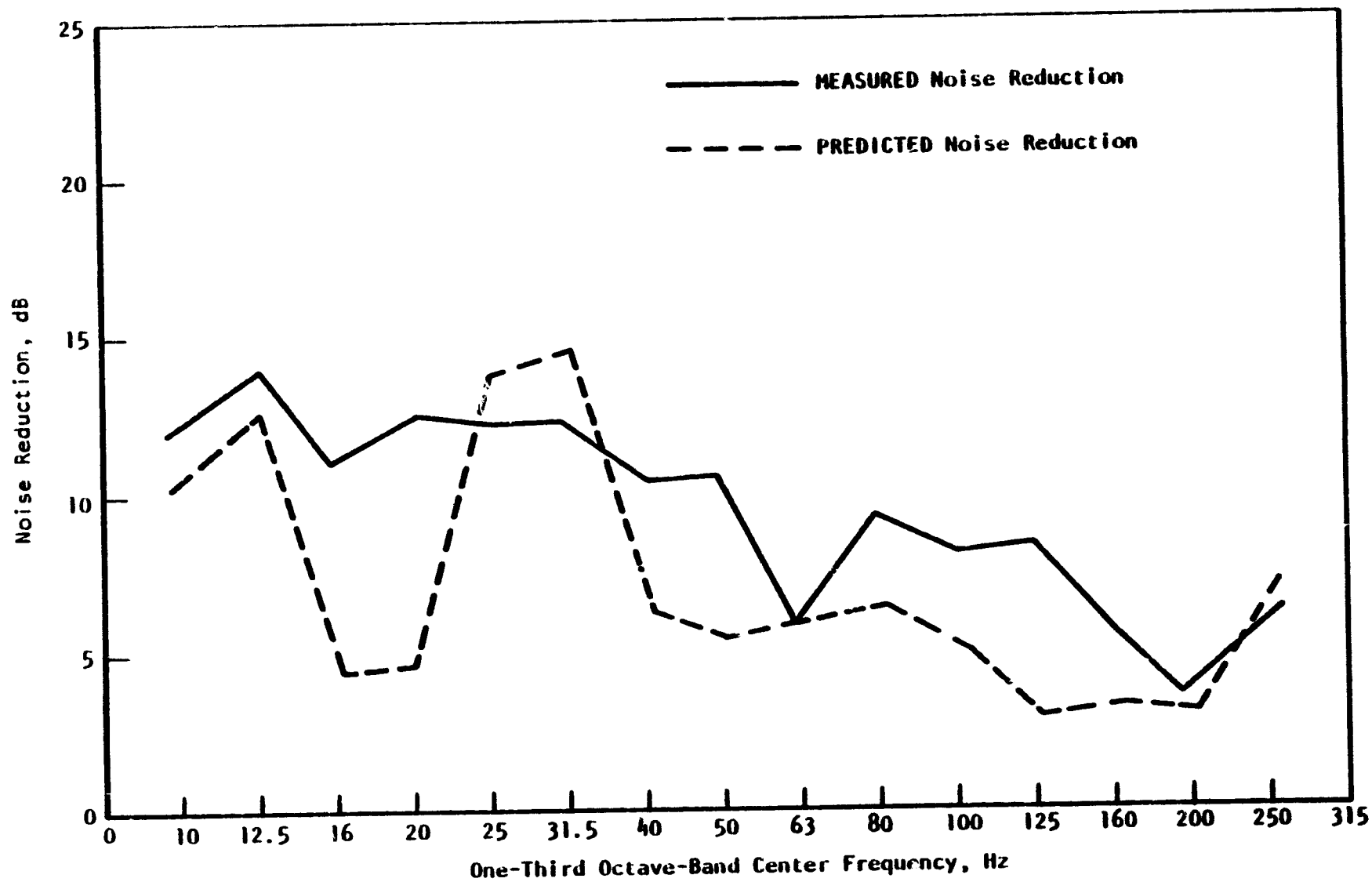


Figure 5-17. Comparison of Measured and Predicted Noise Reduction for Empty Payload Bay

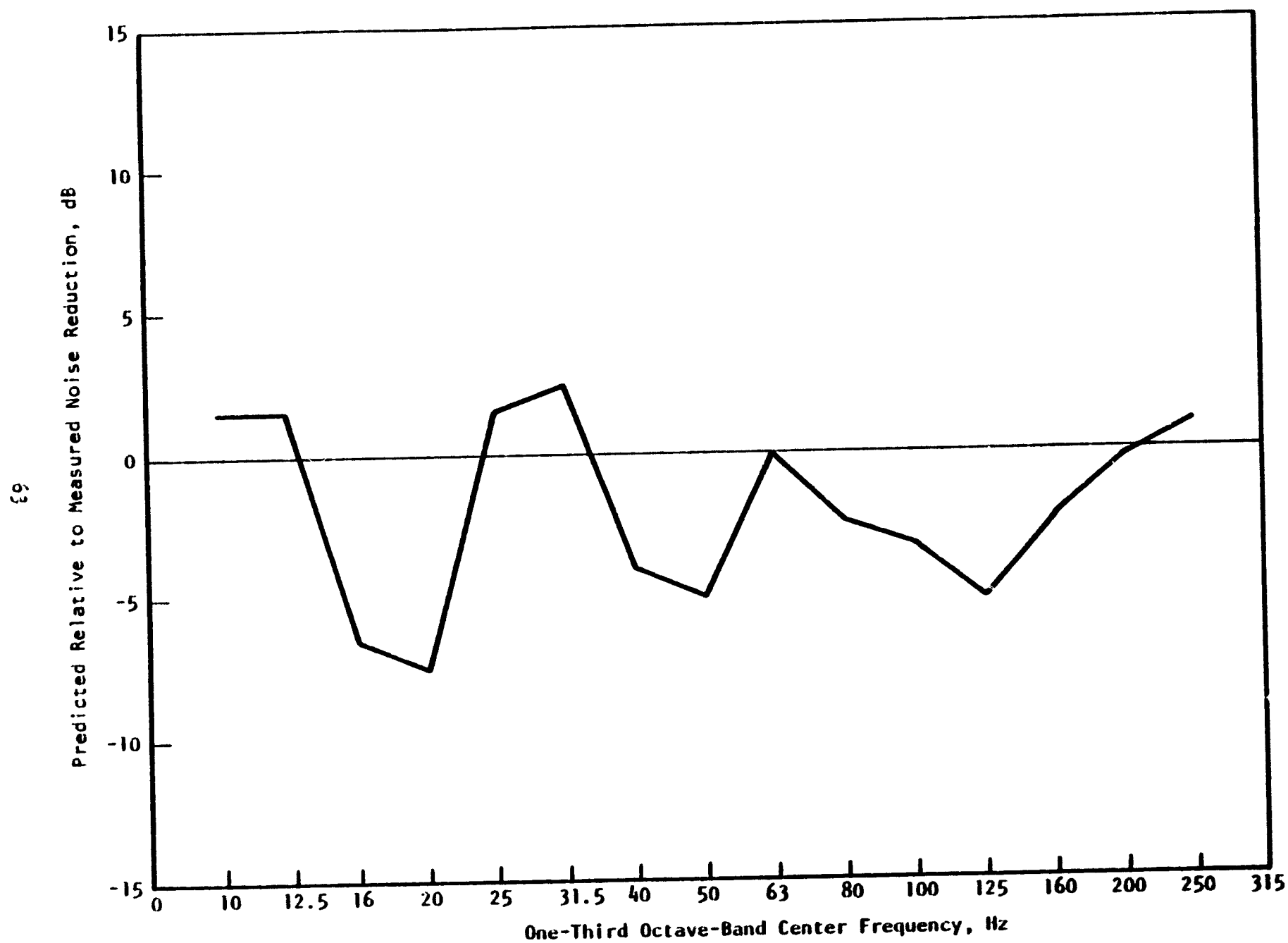


Figure 5-18. Predicted Empty Payload Bay Noise Reduction Relative to Measured Noise Reduction

predicted structural mode would couple easily with the external noise field and would transmit the noise more efficiently.

In the 20 Hz band, an acoustic resonance (18.6 Hz,  $m = 2$ ) in the payload bay can be excited by several structural modes having the same longitudinal wave number and having close resonant frequencies. These low order structural modes are also well coupled to the external noise field in this frequency range. Therefore, the dominant factor, in these frequency bands of more predicted noise transmission than the test results, seems to deal with the calculated door modes. The present model of the door modes does disagree somewhat with the higher finite element modes calculated in Table 5-9.

The acoustic modes are more easily modeled at lower frequencies, so more confidence can be placed in their accuracy. The modes for the present model of a cylinder were compared to the acoustic modes calculated for a perturbed rectangular parallelepiped model of the orbiter payload bay, as shown in Figure 5-15 and Table 5-12. The longitudinal modes were found to be the same for each model, and from Table 5-12 it can be seen that the resonant frequency of the  $n$  wave number modes for the present model are greater than the parallelepiped model modes in the lower frequency bands, but they become more closely matched as the frequency increases. The mode shapes will be slightly different for the  $n$  and  $m$  modes because of the different modal geometries representing the bay cross section. The  $m$  modes will have the same mode shape for each model.

Another factor that could significantly affect the prediction accuracy is the structural and acoustic damping factors. Possibly the damping values specified in the analytical model may not be entirely representative, which could easily lead to errors in the NR estimates.

### 5.3.2 Damping Effects on the Payload Bay Noise Reduction

The effect on the noise reduction of varying the structural damping factor can be seen in Figure 5-19. A smaller damping factor tends to reduce the noise reduction in the payload bay, and this same trend is also true for the acoustic damping factor effect on the noise reduction. Therefore, it can be observed that the damping value specified for the structural and acoustic normal modes is very important in an accurate modeling of the noise transmission problem.

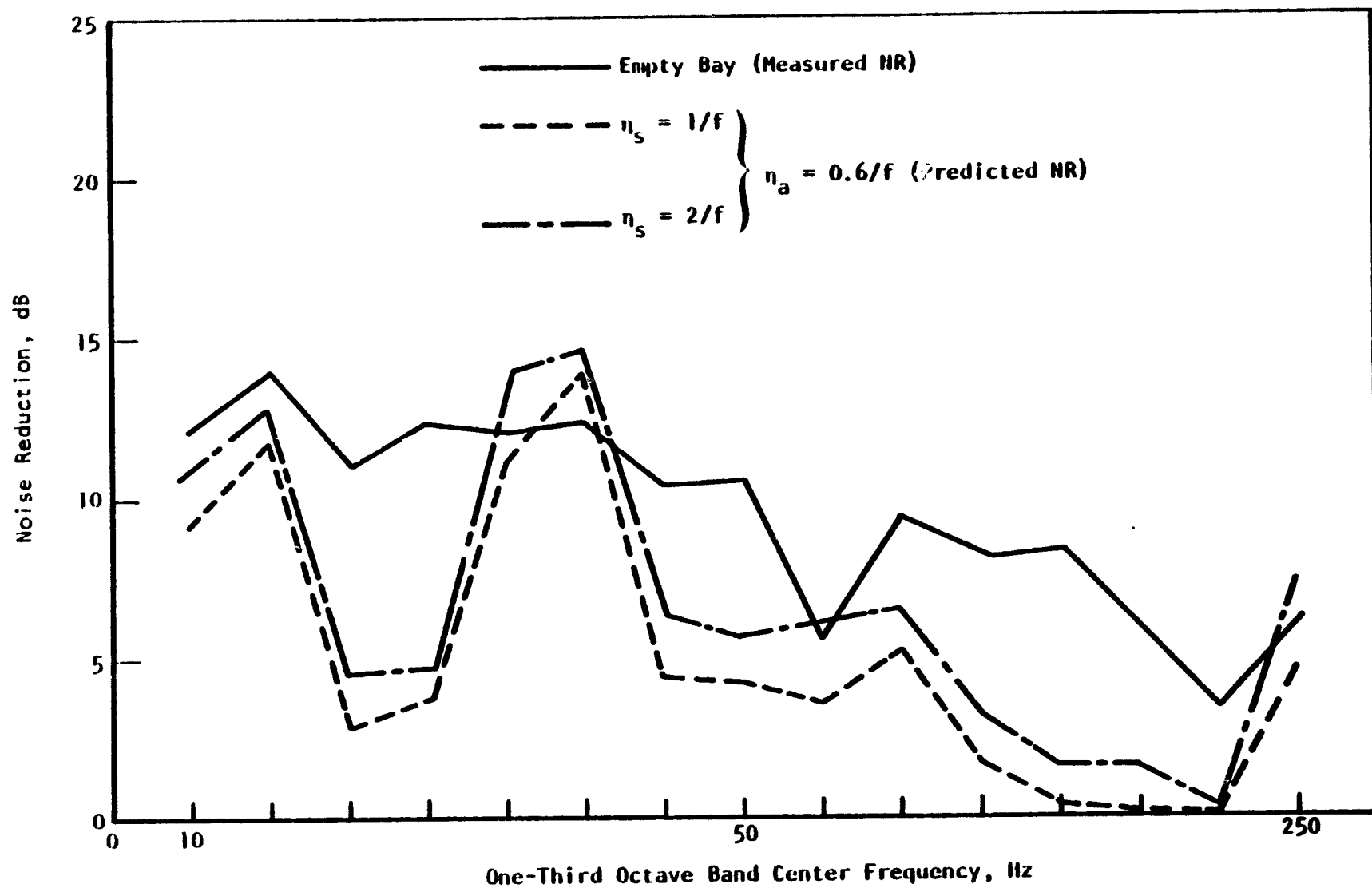


Figure 5-19. Effects of Structural Damping on the Payload Bay Noise Reduction

### 5.3.3 Spatial Variability of the Predicted Noise Reduction

To illustrate the spatial characteristics of the acoustic response in the payload bay, the calculated NR at one point in the bay is shown plotted in Figure 5-20. The point was taken on the centerline of the bay, 15 feet from the front of the enclosure. At this particular point, the NR varies greatly from the space-averaged value in most one-third octave bands. The NR at the point is generally larger than the average NR for the cavity. This trend can also be seen with the measured data in Figure 5-7, where the NR can vary greatly on the high side in the lower frequency bands. A node point is also noted at this location in the 20 Hz band due to a very high calculated NR. Also, the NR for some other locations can be expected to be much lower than the average value.

### 5.4 ACOUSTIC ENVIRONMENT FOR A PAYLOAD CONFIGURATION FROM MODEL TESTS

Acoustic tests were performed on the Rockwell International (RI) one-quarter scale flexible model of the Space Shuttle orbiter with model payload configurations [34]. A one-quarter scale model was constructed by RI for low frequency dynamic experiments related to problems such as flutter and "pogo," and was designed to represent the full scale dynamic characteristics of the orbiter. The dynamic characteristics associated with noise transmission may not be scaled with a high degree of accuracy with this model though, particularly for the payload bay doors. However, it is believed that the model is accurate enough to determine the changes in payload bay acoustic levels when payloads are introduced.

These tests involved the measurement of space-averaged sound pressure levels in the empty bay and when one of three payloads was present. The exterior noise field was generated by five loudspeakers located at the rear of the model, and the field had the properties of acoustic plane waves propagating in the forward direction. For the empty bay test, noise levels were measured at a total of 42 locations, and the data were reduced to a space-averaged one-third octave-band spectrum. When a payload was introduced in the bay, space-averaged spectra were obtained for each of the several subvolumes surrounding the payload. The differences between these spectra and that for the empty payload bay determined the effect of the payload on the bay noise levels.

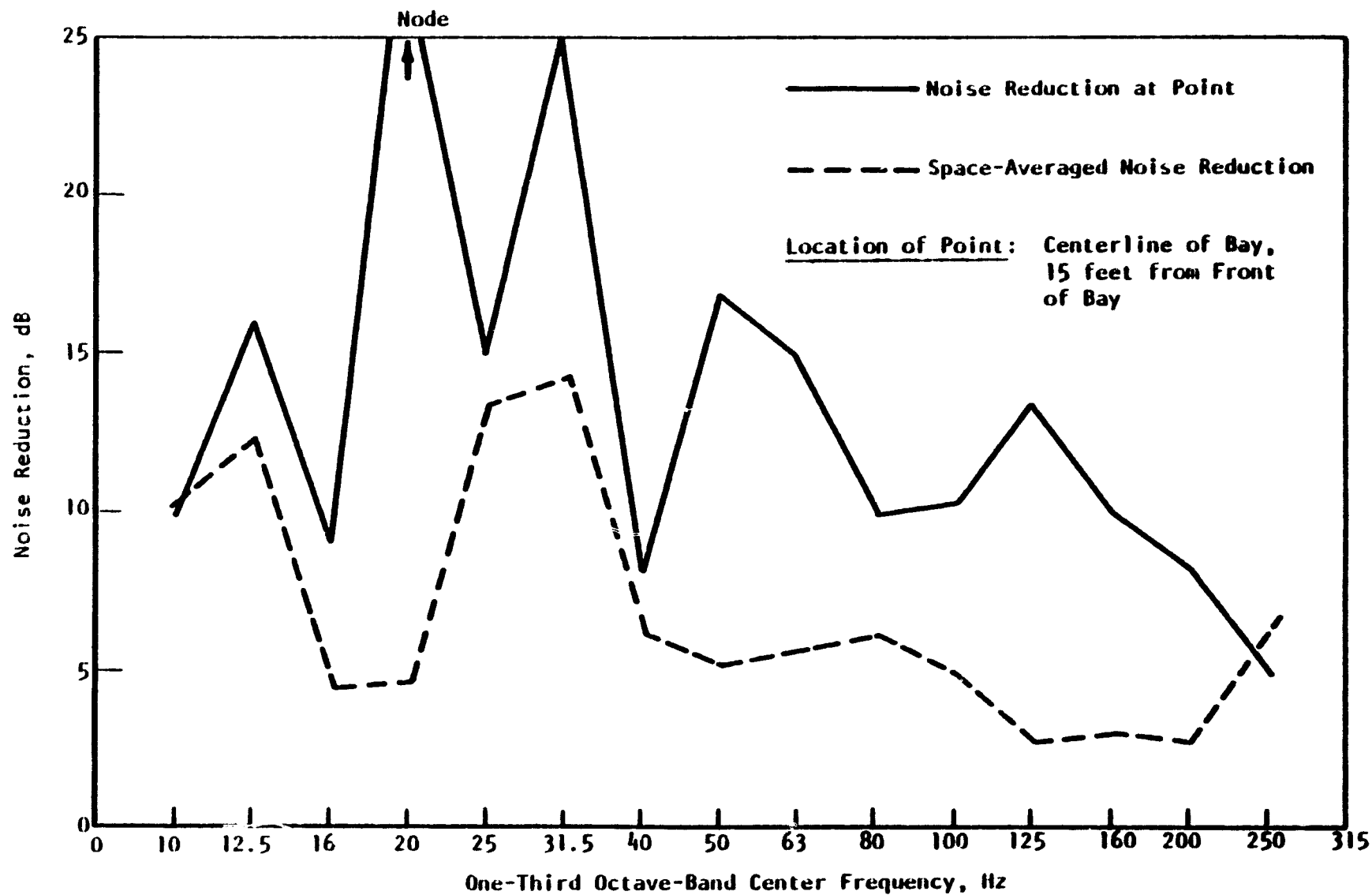


Figure 5-20. Predicted Noise Reduction at One Point in Empty Payload Bay



#### 5.4.1 Payload Configuration

The payload configuration, designated as "Delta-D," does not simulate any real payload, but was designed as a diagnostic payload because of its creation of interesting acoustic subvolumes within the payload bay. This payload configuration consists of a series of five cylinders of different diameters plus an aft pallet. Figure 5-21 illustrates a top and side view of the payload configuration. The large diameter cylinders are of considerable interest because they have a major impact on the payload bay acoustics [34, Vol. I] and constitute a challenging situation for any analytical model.

#### 5.4.2 Measured Data for the Delta-D Payload Effects

The space-average one-third octave-band levels for each of the seven subvolumes were subtracted from the average empty bay levels to obtain the relative effects of the payload introduction into the bay. These relative levels to the average empty bay levels are shown in Figure 5-22. From this data, it can be seen that large variations in levels occur in the low frequency range below the 31.5 Hz one-third octave band. The curves also show that empty bay levels are generally not affected significantly by the payload from the 31.5 Hz band to the 250 Hz band. The one exception is with the 95% diameter payload, where the levels above the payload are higher than the average empty bay levels.

### 5.5 INPUTS FOR THE ANALYTICAL MODEL OF THE PAYLOAD EFFECTS

The noise reduction results obtained with the computer program for the effects of a payload were based on the analytical model of the full scale orbiter OV-101 tested at Edwards AFB [34], as described in Section 5.1. The full scale data from the OV-101 test were used in the predictions because large differences were found to have occurred between the OV-101 and the one-quarter model noise reduction levels for an empty payload bay below the 63 Hz one-third octave-band region [34, Vol. V]. These differences demonstrated that the one-quarter scale orbiter model does not exactly represent the OV-101 acoustically. Therefore, no attempt was made to scale up the one-quarter model to predict the effects of the introduction of a payload on the empty bay noise levels. The predictions are compared to the model test data on a qualitative basis to obtain trends and relative magnitudes. The analytical inputs of one payload configuration are used in the computer programs described in Section 4.0 to obtain a space-averaged noise reduction spectrum for the entire space enclosing the payload.

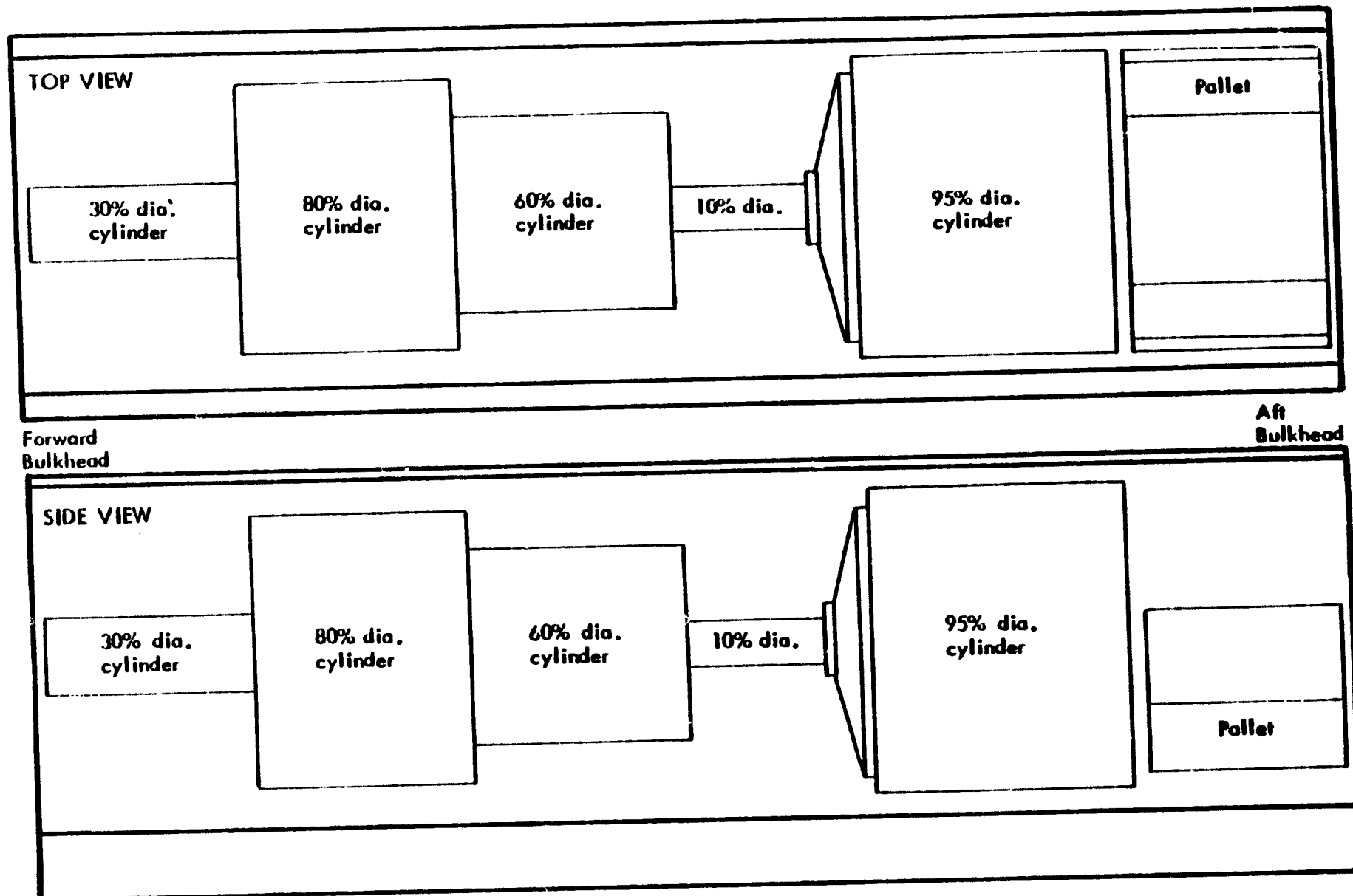


Figure 5-21. Diagram of the Delta-D Payload Model (from Reference 34)

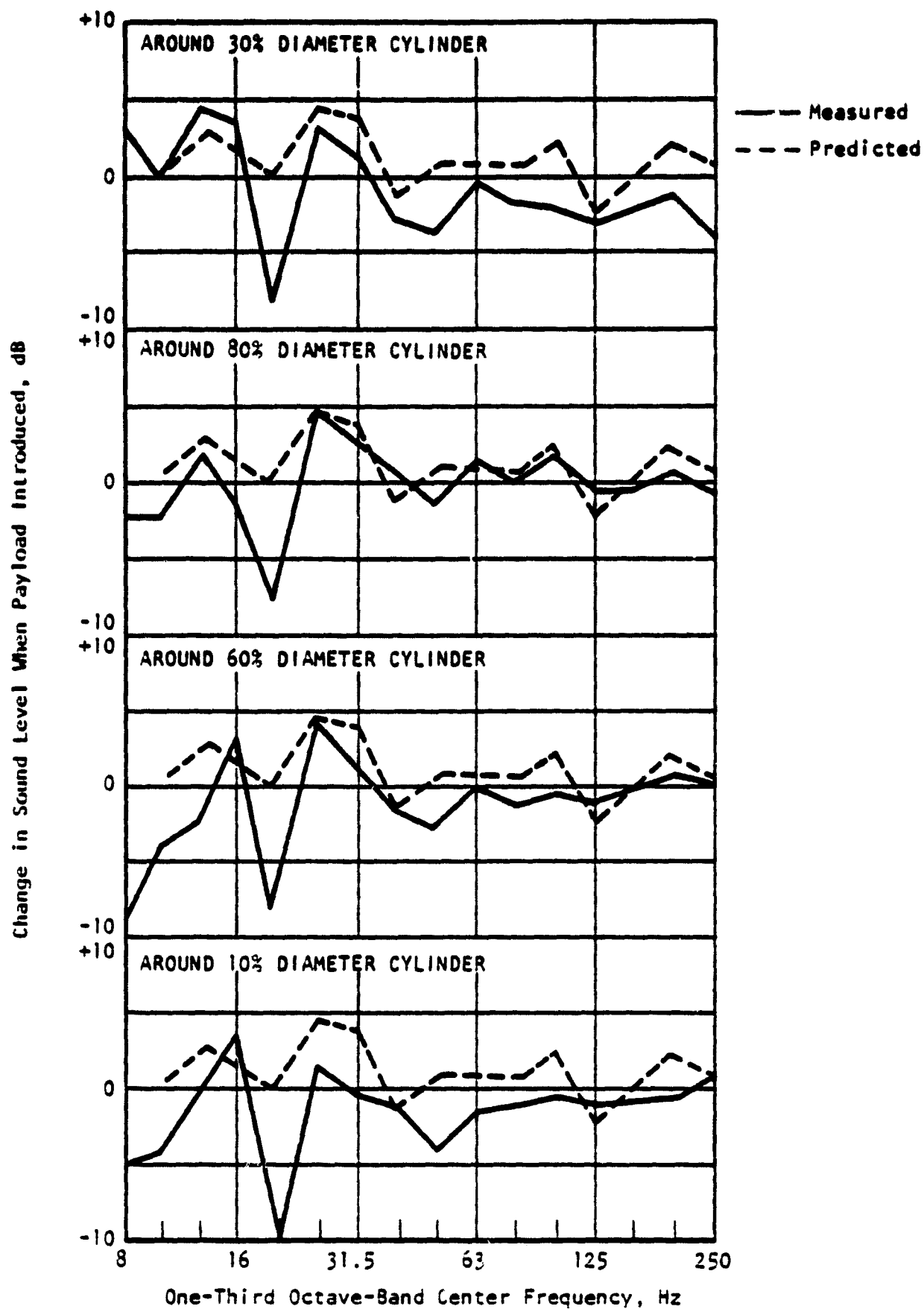


Figure 5-22. Effect of Delta-D Payload on Subvolume Space-Averaged Sound Pressure Levels

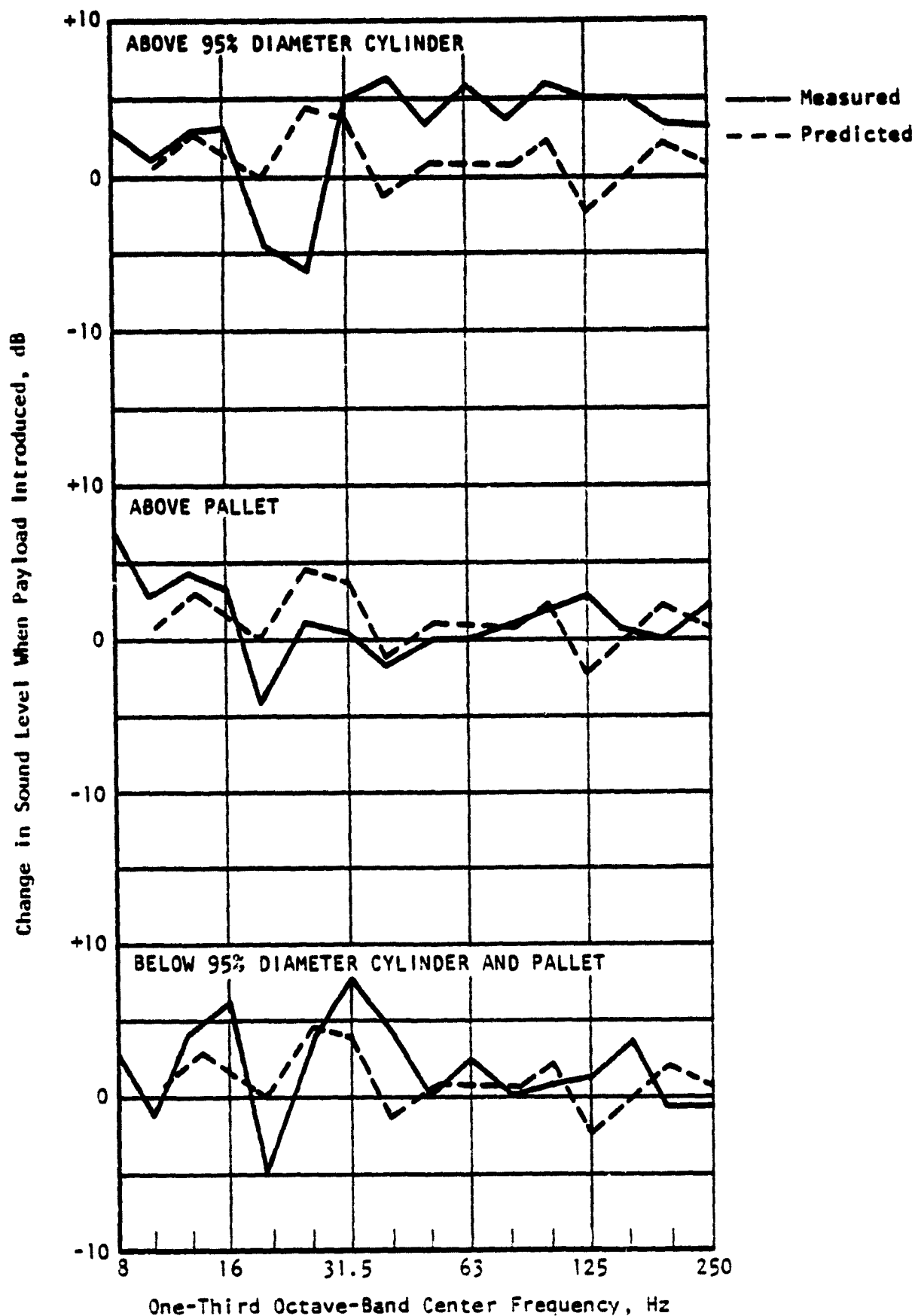


Figure 5-22. (Concluded)

#### 5.5.1 Payload Delta-D Configuration

This payload configuration, shown in Figure 5-21, was modeled by a single cylinder placed concentrically in the cylindrical model of the empty bay (Figure 3-1), with a volume equal to the total volume of the payload. This cylindrical payload simulation had a radius of 4.82 feet, and a payload bay length of 60 feet.

#### 5.5.2 Structure of the Orbiter

The orbiter structural properties are the same as described in Section 5.2.2 for the OV-101 used in the acoustic tests [38].

#### 5.5.3 Payload Bay Door Resonant Frequencies and Structural Damping Factor

The introduction of a payload configuration does not change the door modes or damping factor, so the value for these inputs are the same as given in Sections 5.2.4 and 5.2.5.

#### 5.5.4 Payload Bay Resonant Frequencies with Payload Present

For the introduction of the payload into the orbiter bay, Table 5-13 lists the bay modal frequencies and indices through the 100 Hz one-third octave band. On comparing the empty bay modes in Table 5-11 to the payload present modes, it is seen that the first three modes are the same. But the payload case brings the first circumferential mode ( $n=1$ ) of the empty bay (40.9 Hz) down to 28.0 Hz with the introduction of the payload. The payload also increases the first radial mode ( $s=1$ ) from 85.1 Hz of the empty bay to 177.8 Hz. Generally, the payload present case will not affect the empty bay longitudinal modes ( $m$ ), but it will lower the resonant frequencies of the circumferential modes ( $n$ ), and raise the resonant frequencies of the radial modes ( $s$ ).

#### 5.5.5 Acoustic Damping of OV-101 Payload Bay with Payload Present

The payload bay acoustic damping factors due to the payload being present was estimated to be greater than the empty bay values. The acoustic loss factor was based on 350 Sabins in Reference 43, and it is given by

$$\eta = \Delta f / f = 1.27 / f$$

where  $f$  is in Hz.

TABLE 5-13.

ACOUSTIC MODAL FREQUENCIES FOR PAYLOAD CONFIGURATION "DELTA-D",  
THROUGH THE 100 HZ BAND

m, n, s	f	m, n, s	f
0, 0, 0	0	8, 1, 0	79.5
1, 0, 0	9.3	0, 3, 0	83.2
2, 0, 0	18.6	9, 0, 0	83.7
3, 0, 0	27.9	1, 3, 0	83.7
0, 1, 0	28.0	2, 3, 0	85.3
1, 1, 0	29.5	7, 2, 0	85.7
2, 1, 0	33.6	3, 3, 0	87.8
4, 0, 0	37.2	9, 1, 0	88.3
3, 1, 0	39.5	4, 3, 0	91.2
5, 0, 0	46.5	8, 2, 0	93.0
4, 1, 0	46.5	10, 0, 0	93.0
5, 1, 0	54.3	5, 3, 0	95.3
0, 2, 0	55.8	10, 1, 0	97.1
6, 0, 0	55.8	6, 3, 0	100.2
1, 2, 0	56.5	9, 2, 0	100.6
2, 2, 0	58.8	11, 0, 0	102.3
3, 2, 0	62.4	7, 3, 0	105.7
6, 1, 0	62.4	11, 1, 0	106.1
7, 0, 0	65.1	10, 2, 0	108.4
4, 2, 0	67.0	0, 4, 0	110.2
7, 1, 0	70.9	1, 4, 0	110.6
5, 2, 0	72.6	12, 0, 0	111.6
8, 0, 0	74.4	8, 3, 0	111.6
6, 2, 0	78.9	2, 4, 0	111.8

## 5.6 PREDICTION OF THE NOISE REDUCTION OF PAYLOAD BAY WITH A PAYLOAD PRESENT

Figure 5-23 depicts the noise reduction (NR) calculations for the Delta-D payload configuration. As with the empty payload bay NR levels, several one-third octave bands have their noise transmission governed by either structural or acoustic resonances. Reasons for this situation are discussed in Section 5.3 for the empty bay NR results. Also, as the modal densities increase with increasing one-third octave band frequencies, the structural and acoustic resonant responses share about the same amount of the noise reduction.

### 5.6.1 Comparison between Empty Payload Bay and a Payload Configuration

In Figure 5-24, the NR curve from Figure 5-16 for the predicted empty bay NR levels is shown with the Delta-D payload configuration NR curve. The two curves seem to follow the same NR trend with frequency. The payload introduction causes the empty bay NR levels to decrease, which means, of course, that more noise transmission has occurred and the payload acoustic environment has increased noise levels over the empty bay levels.

Figure 5-25 shows the differences in NR between the two curves from Figure 5-24 more graphically. The difference between the empty bay NR and the payload present NR is equivalent to the change in the empty bay noise level when the payload is placed in the empty bay. The 0 dB level is the empty bay space-averaged noise level in Figure 5-25. As noted in this figure, the empty bay noise in the lower frequency bands (<40 Hz) seems to be affected more by the addition of the payload. The largest change is in the 25 and 31.5 Hz one-third octave bands. A possible reason for this condition is that the payload addition causes the empty bay circumferential acoustic modes in the 40 Hz band to be reduced in frequency where they now fall into the 25 and 31.5 Hz bands. This can be seen by comparing Tables 5-11 and 5-13. For the empty bay case, no acoustic modes exist in the 31.5 Hz band, but with the addition of a payload configuration, several acoustic modes are created in this one-third octave band. These acoustic modes are then excited by structural modes, resulting in transmission of more external noise into the bay cavity than with the empty bay situation.

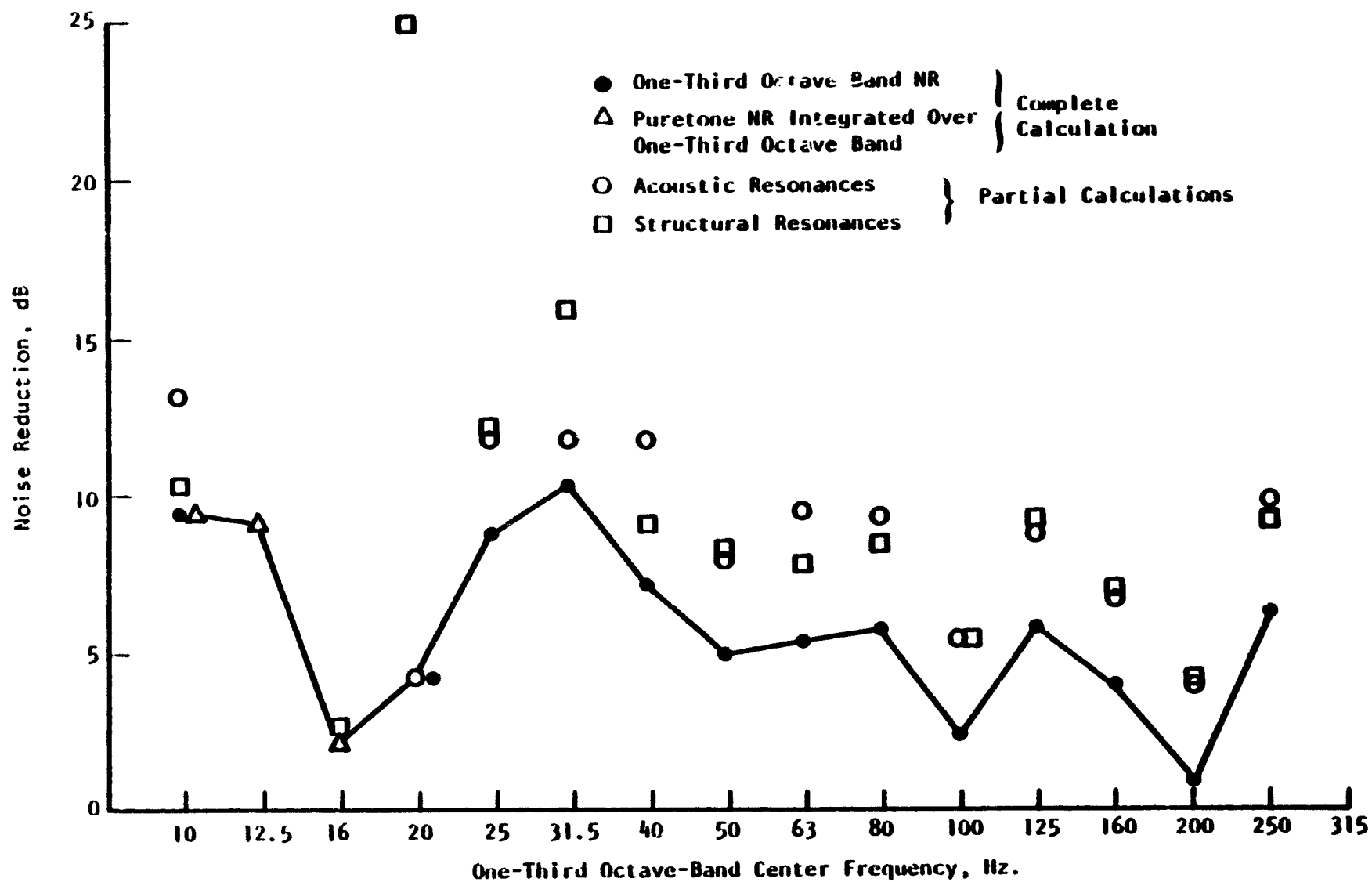


Figure 5-23. Predicted Noise Reduction for Payload Configuration Delta-D



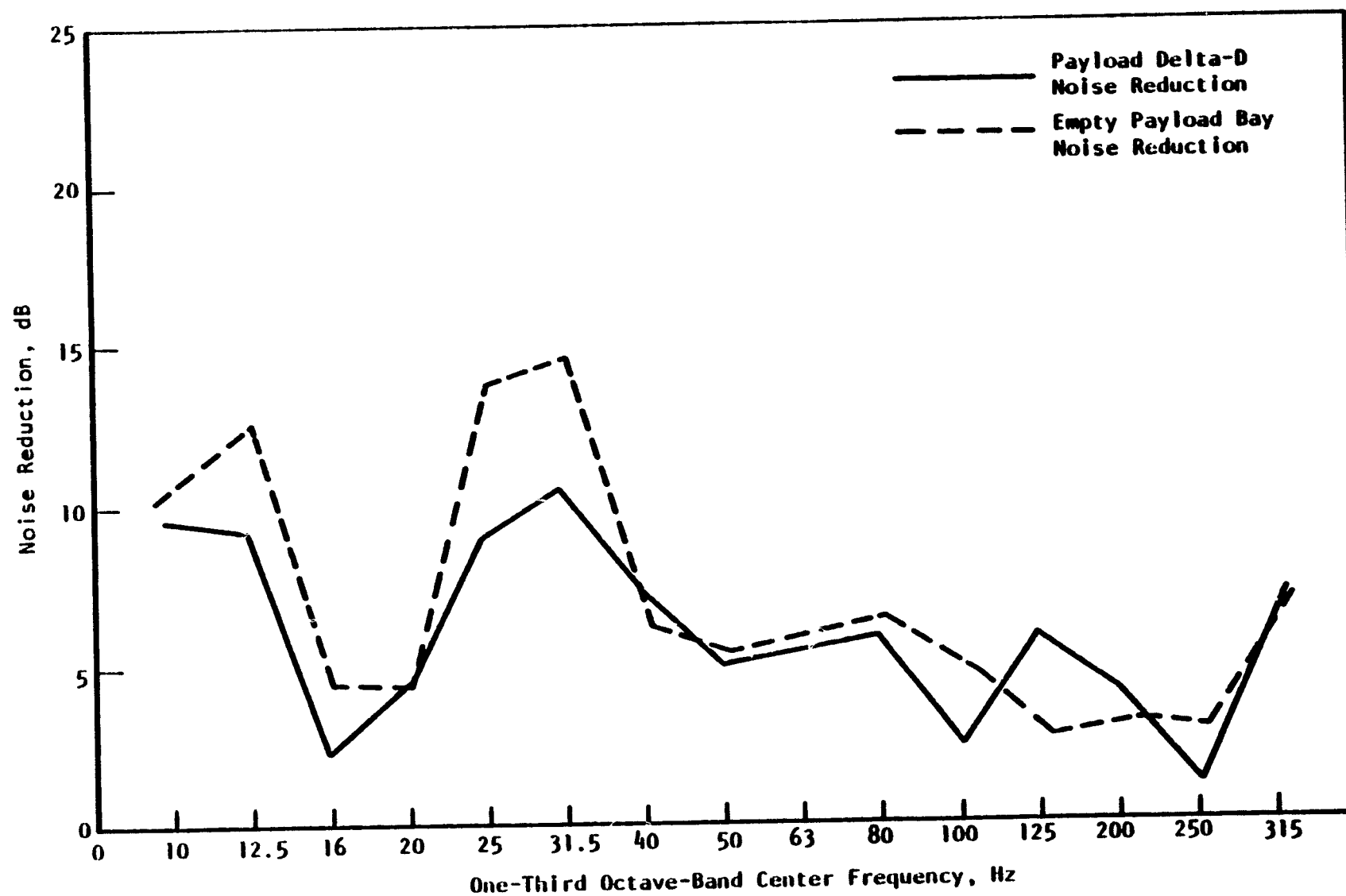


Figure 5-24. Predicted Noise Reduction for Empty Payload Bay and Payload Delta-D

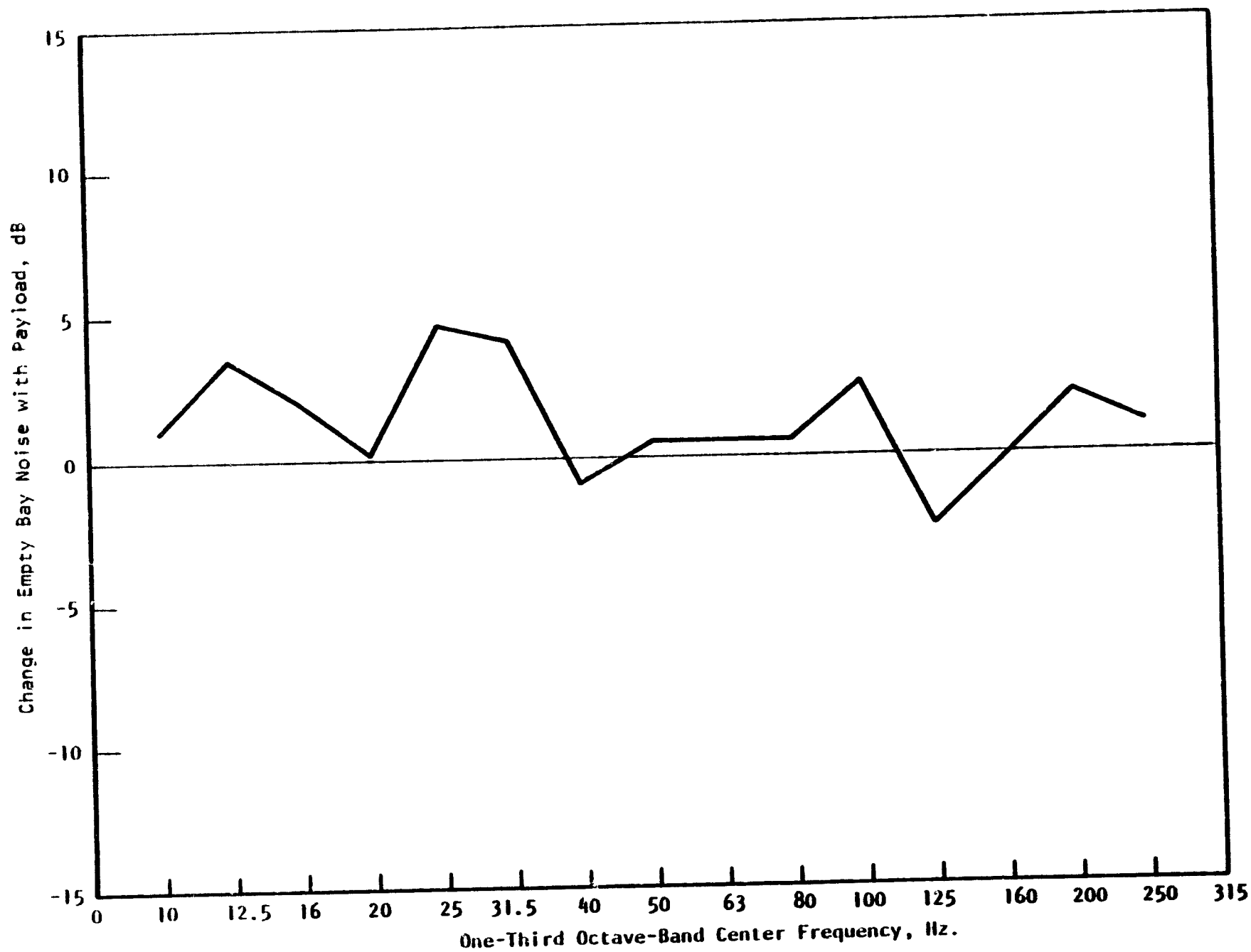


Figure 5-25. Predicted Change in Empty Bay Noise Levels with Addition of Payload Configuration Delta-D

### 5.6.2 Comparison of Measured and Predicted Payload Effects on Empty Bay Noise Levels

From the one-quarter scale orbiter model tests, changes in the empty payload noise levels due to the introduction of the payload configuration Delta-D are shown in Figure 5.22. Also on the same figure are the predicted values due to the payload effects. Only qualitative results should be gained from these comparisons, as explained earlier in Section 5.4.

The predicted changes seem to have about the same trends as do the measured data for most of the subvolumes surrounding each of the payload components. Even the magnitude of the changes in noise level is fairly similar for both the predicted and test cases with the 30-, 60- and 80-percent diameter cylinders. The most significant trend difference lies in the 20 Hz band with each subvolume. Although the model and the full scale OV-101 are not acoustically the same, the trend for the analytical model should probably be a little closer to the test model results at 20 Hz. In most subvolumes, the 20 Hz band for the model results is greatly affected by the payload introduction. It is likely that the normal acoustic modes of the empty bay were changed by the payload addition in such a way as to increase the noise reduction in the 20 Hz band. The measured changes above the large diameter cylinder of 95 percent show the most disagreement with the predicted results, as also noted in Section 5.4.1. Here, the measured changes are consistently higher above the 31.5 Hz band. The noise levels above the 95% cylinder, near the doors, are about 5 dB higher than the empty bay levels.

### 5.6.3 Spatial Variability of the Payload Noise Effects

As with the modal nature of the empty bay acoustic response, shown in Figure 5-26, the spatial variability is characteristic of the noise spectra for the subvolumes around the Delta-D payload components. The prediction method is also applicable for the payload present noise reduction computation, as demonstrated with the empty bay test case. The addition of the payload volume changes the acoustic normal modes of the empty bay. This in turn either couples or decouples their response with the structural modes, thereby changing the noise transmission characteristics relative to the empty bay levels.

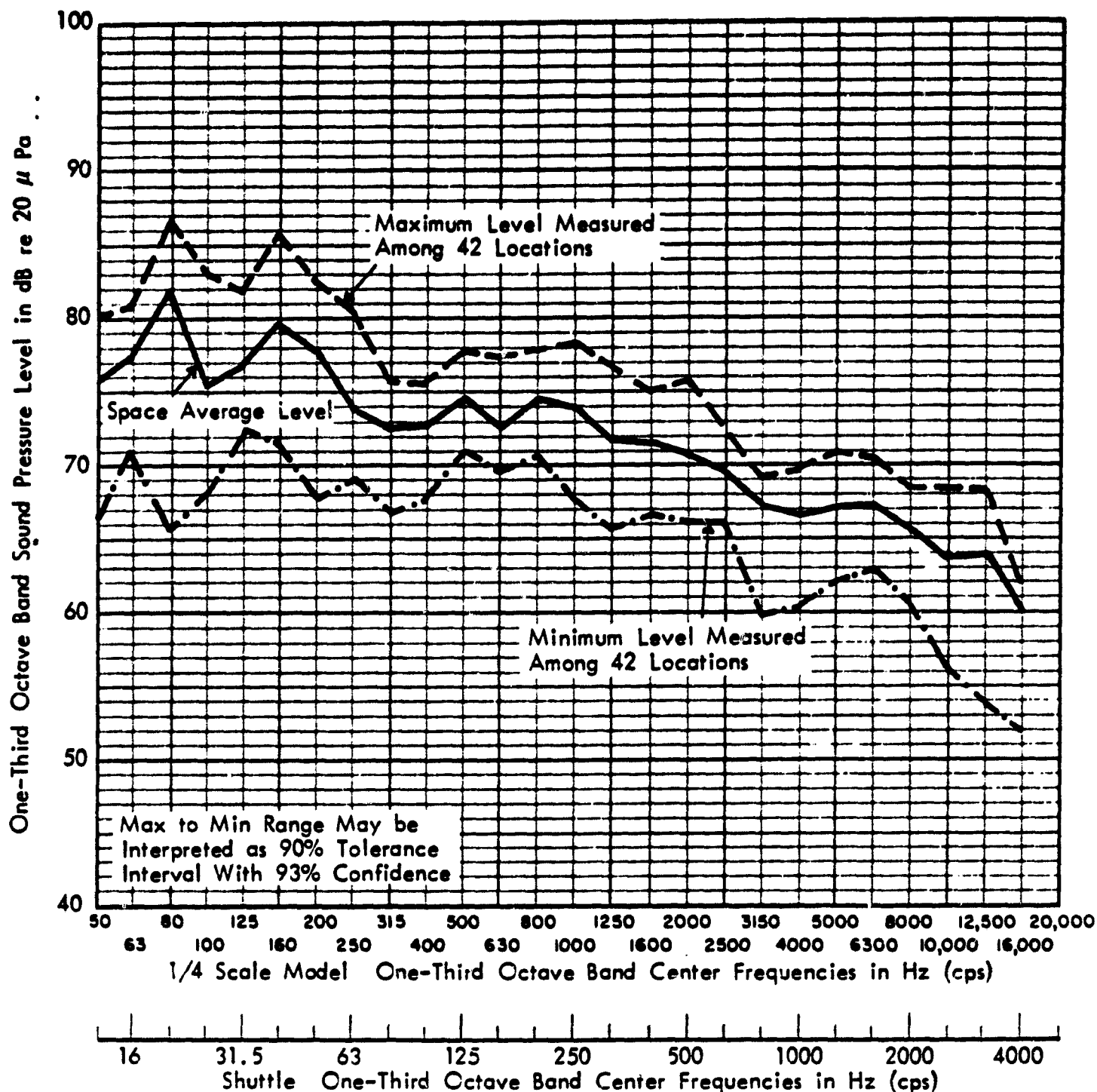


Figure 5-26. Spatial Variation of Empty Bay Interior Sound Pressure Level Measurements [34]

## 6.0 CONCLUSIONS

Results of the comparisons between the test cases and the predictions of the analytical models are summarized in this section to give an indication of the prediction method's applicability and accuracy for the estimation of a space vehicle's interior noise level.

The noise reduction (NR) predictions for the empty payload bay differ within  $\pm 5$  dB from the measured NR levels for 87% of the one-third octave bands in the 10 Hz to 250 Hz range. About 60% of the predicted NRs are within  $\pm 3$  dB of the measured levels. For most frequencies, the analytic calculations give over conservative NRs (lower NRs), as shown by Figures 5-17 and 5-18.

The greatest difference in the predicted and measured results is in the 16 and 20 Hz bands. Modeling of the payload bay door normal modes is believed to be in error for these frequency bands when compared to the finite element calculations. The questionable accuracy of the structural modes in the 100 and 125 Hz bands may also be responsible for more predicted noise transmission than measured.

Acoustic normal modes for the cylindrical model of the payload bay seem to agree fairly well with the modes calculated by a more representative payload bay shape of the rectangular parallelepiped with a curved upper surface to simulate the payload bay doors. The greatest disagreement in the model's modal characteristics occurs in the 25 Hz to 63 Hz bands. This may partially account for the discrepancy in the predictions at 40 Hz and 50 Hz one-third octave bands. The acoustic modes appear to be more closely modeled, with the exception possibly at 40 Hz and 50 Hz bands, than the door structural modes. This may be the primary reason for the discrepancies in the predictions in several of the one-third octave band mentioned above.

The modal nature of the low frequency response in the payload bay can be seen in the spatial variability characteristic of the measured noise levels. This spatial variability of the measured data for both the OV-101 acoustic tests and the model payload effects test can be seen in the experimental results. This spatial variability of the noise spectra can also be predicted by the programmed analytical model as shown in Figure 5-20. The ability to calculate the noise reduction at any given point in the payload acoustic environment may be important in

certain cases where the localized noise level may greatly exceed the space-averaged value. In terms of noise reduction, this means that the noise reduction may be lower than the average noise reduction for the space surrounding the payload.

The modal characteristics of spatial variability in the payload bay noise spectra at low frequencies makes the modal analysis method well suited to determine the noise reduction. This noise reduction is primarily dependent on individual structural and interior acoustic modal responses.

The simple modeling of the Delta-D payload configuration by a concentric cylinder with an equivalent volume gives reasonable predictions around most of the payload components. Similar magnitudes and trends for the payload effects are seen from the measured model data and the full scale predicted data, although the predicted payload NR for the 20 Hz band in every case is too high. This discrepancy could be attributed either to the math model or to the one-quarter scale model not being completely similar acoustically to the full scale OV-101. The worst payload sub-volume prediction is above the 95% diameter cylinder component of the payload configuration. Here, the trend in the predicted changes in noise level between the empty bay and with the payload introduction are lower.

The noise reduction prediction model is shown to give reasonable results for most frequencies and payload subvolumes for the two test cases given in the study. The main discrepancies could probably be eliminated by better modeling of the structural normal modes and, of lesser importance, by a more detailed representation of the payload acoustic cavity to obtain more accurate acoustic normal modes.

## 7.0 RECOMMENDATIONS

A modal analysis approach has been improved to predict the noise reduction in a space vehicle with payloads. Generally, reasonable results were obtained for most of the one-third octave bands of 10 to 250 Hz. Several additional improvements could be made in the area of modeling the structure and acoustic enclosure to obtain more accurate normal modes. Also the computer programs could be improved for more efficiency and flexibility. The following recommendations will be investigated for their feasibility and incorporation into the work on NASA contract number NAS8-33379 to further improve techniques for predicting the acoustic environment of space vehicle payloads.

The principle of component mode synthesis could be used with finite element techniques for determining the structural/acoustic system natural modes. The finite element method could be used to define the structural modal response. This method is also the most accurate analytical method available. These normal mode properties could then be incorporated into the present computer program, or possibly a finite element program could be added as a subroutine to the main program to directly compute the structural modes. The Donnell-Mushtari equations for determining the structural normal modes for the present model could also be modified to obtain another shell theory that may yield more representative normal modes of the structure walls.

The predicted acoustic resonances with the present model seem to be reasonable for the payload bay with and without a payload configuration. An improved model of the payload enclosure may be found in the perturbation technique applied to a rectangular parallelepiped where individual wall surfaces may be deformed to simulate the cavity shape. Finite element methods could also be employed to determine the mode shapes and frequencies of the payload enclosure, especially for irregular volumes. The subvolumes surrounding individual payload components may be used to determine the natural modes for their respective cavities. Then these modes could be coupled to adjacent subvolume modes until an equivalent normal mode determination for the entire cavity was obtained. This more rigorous treatment of the payload cavity might be necessary for complicated payload configurations and for large diameter payload components.

The major computational improvement for the computer program would be to combine the three versions of the present program into one program with the logic to apply the proper version to the noise reduction calculations. Also, plotting routines that would present the noise reduction as a function of frequency could be incorporated. Also, by applying the calculated noise reduction to the measured or predicted external noise spectrum, a plot of the internal noise spectrum for the payload enclosure could be generated.

The statistical energy method could be used to expand the frequency range for the noise reduction prediction program. This method would be more efficient to use in the higher frequency region than the modal analysis method because the higher modal density of the responses are more uniform over a one-third octave band and the calculations are more simplified.



## REFERENCES

1. Plotkin, K. J., P. K. Kasper and P. K. Glenn. "Prediction of Low Frequency Sound Transmission Through Aerospace Structures, With Application to the Space Shuttle," Wyle Research Report WR 78-5, February 1978.
2. Cockburn, J. A., and A. C. Jolly. "Structural-Acoustic Response, Noise Transmission Losses and Interior Noise Levels of an Aircraft Fuselage Excited by Random Pressure Fields," Technical Report AFFDL-TR-68-2 by Wyle Laboratories for the Air Force Dynamics Laboratory, January 1968.
3. Dowell, E. H. "Master Plan for Prediction of Vehicle Interior Noise," Princeton University, AIAA 5th Aeroacoustics Conference, Seattle, Wash., March 12-14, 1979.
4. Morse, P. H., and K. U. Ingard. Theoretical Acoustics, McGraw-Hill, Inc., 1968.
5. Tabarrok, B. "Dual Formulations for Acousto-structural Vibrations," Int. J. Num. Meth. Engng., 13, 197-201, 1978.
6. Craggs, A. "Sound Transmission between Enclosures--A Study Using Plate and Acoustic Finite Elements., Acoustica, 35, 89-98, 1976.
7. McDonald, R. Vaicaitis, and M. K. Myers. "Noise Transmission through Plates into an Enclosure, NASA TP 1173, 1978.
8. Wolf, J. A., Jr. "Modal Synthesis for Combined Structural-Acoustic Systems," AIAA J., 15, 743-745, 1976.
9. Dowell, E. H., G. F. Gorman and D. A. Smith. "Acoustoelasticity: General Theory, Acoustic Natural Modes and Forced Response to Sinusoidal Excitation, Including Comparisons with Experiment," J. Sound Vib., 52, 519-542, 1977.
10. Vaicaitis, R. "Noise Transmission by Viscoelastic Sandwich Panels," NASA TN D-8516, 1977.
11. Craggs, A. "An Acoustic Finite Element Approach for Studying Boundary Flexibility and Sound Transmission Between Irregular Enclosures," J. Sound Vib, 30, 343-357, 1973.
12. Wolf, J. A., Jr. "Three-Dimensional Acoustic Natural Modes and Frequencies," General Motors Res. Lab., Res. Memo. 15-86, 1976.
13. Petyt, M., and S. P. Lim. "Finite Element Analysis of the Noise Inside a Mechanically Excited Cylinder," Int. J. Num. Meth. Engng., 13, 109-122, 1978.
14. Dowell, E. H., and C. F. Chao. "Sound Transmission Analysis for Determining Interior Sound Levels," Quarterly Progress Reports, 1978.

15. Manning, J. E., et al. "Transmission of Sound and Vibration to a Shroud-Enclosed Spacecraft," BBN Report 1431, October 1966.
16. Smith, P. N., and R. H. Lyon. "Sound and Structural Vibration, NASA CR-160, March 1965.
17. Maidanik, G. "Response of Ribbed Panels to Reverberant Acoustic Fields," JASA, 34, 1962.
18. Conticelli, V. M., and J. A. Cockburn. "Vibration Response and Noise Reduction of Cylindrical Structures Exposed to Acoustic Environments - A Theoretical and Experimental Investigation," Wyle Laboratories Research Staff Report WR 72-1, January 1972.
19. Conticelli, V. M. "Study of Vibratory Response of a Payload Subjected to a High Frequency Acoustic Field," Wyle Laboratories Research Staff Report WR 69-9, May 1969.
20. Price, A. J., and M. J. Crocker. "Sound Transmission Through Double Panels Using Statistical Energy Analysis," J. Acoust. Soc. Am., 47, 683-693, 1970.
21. Wilby, J. F., and T. D. Scharton. "Acoustic Transmission Through a Fuselage Sidewall.," NASA CR-132602, 1970.
22. Wilby, J. F. "An Approach to the Prediction of Airplane Interior Noise," AIAA 3rd Aeroacoustics Conference, AIAA Paper 76-548, 1976.
23. Pope, L. D., and J. F. Wilby. "Band-Limited Power Flow into Enclosures," J. Acoust. Soc. Am., 62, 906-911, 1977.
24. Abrahamson, L. "A Finite Element Model of Sound Propagation in a Nonuniform Circular Duct Containing Compressible Flow," AIAA Paper 77-1301, Oct. 1977.
25. Wolf, J. A., Jr., and D. J. Nefske. "Vibration Analysis of Structural-Acoustic Systems Using Finite Elements," General Motors Research Lab. GMR-2281R, 1976.
26. Wolf, J. A., Jr., and D. J. Nefske. "NASTRAN Modeling and Analysis of Rigid and Flexible Walled Acoustic Cavities," General Motors Research Lab. GMR-1921R, 1977.
27. Jacobs, L. D., D. R. Lagerquist, and F. L. Gloyna. "Response of Complex Structures to Turbulent Boundary Layers," J. Aircraft, 7, 210-219, 1970.
28. Franken, P. A. "Sound Induced Vibrations of Cylindrical Vehicles," JASA, 34, 4, 453-454, April 1962.
29. Barnoski, R. L., et al. "Summary of Random Vibration Prediction Procedures," NASA CR-1302, April 1969.

30. Crane, K. L. "A Vibroacoustic Transfer Function Manual," Brown Engineering Report, 1969.
31. Bandgren, H. J., and W. C. Smith. "Development and Application of Vibro-acoustic Structural Data Banks in Predicting Vibration Design and Test Criteria for Rocket Vehicle Structures," NASA TN-D-7159, February 1973.
32. Guest, S. H., and J. H. Jones. "Space Shuttle Noise Suppression Concepts for the Eastern Test Range," Proc. 13th Space Congress, Cocoa Beach, Fla, April 7-9, 1976.
33. Leissa, A. W. "Vibration of Shells," NASA Report SP-288, 1973.
34. Piersol, A. G., L. D. Pope, P. E. Rentz, and J. F. Wilby. "Space Shuttle Payload Bay Acoustic Prediction Study," Bolt Beranek and Newman, Inc., Report 3286, 28 December 1976. Volume I, "Problem Definition and Experiments"; Volume II, "Analytical Model"; Volume III, "Manual for Simplified Prediction Procedure"; Volume IV, "Computer Users Manual"; Volume V, "Verification of Analytical Model and Overview of Study."
35. Abramowitz, M., and I. Stegun. Handbook of Mathematical Functions with Formulas, Graphs, and Mathematical Tables, National Bureau of Standards, Applied Mathematics Series 55, November 1964.
36. Gradshteyn, I. S., and I. W. Ryzhik. Tables of Integrals Series and Products, Academic Press, 1965.
37. McMahon, J. "On the Roots of the Bessel and Certain Related Functions," Annals of Mathematics, 9, p. 23, 1894.
38. Piersol, A. G., and P. E. Rentz. "Prediction of Space Shuttle Orbiter Payload Bay Launch Acoustic Levels Based Upon OV101 Acoustic Tests," BBN Report 3424, April 1977.
39. Chirby, A., Rockwell International. Private communication, February 14, 1977.
40. Bolt, Beranek and Newman, Inc. Memorandum 1013-07, February 17, 1976.
41. Timoshenko, S. Strength of Materials, 3rd edition, Vol. I, Van Nostrand, 1955.
42. LTV Aerospace Corp., Vought Systems Div. Subcontractor engineering memo 75-483109-V5, October 15, 1975.
43. Tierney, H. B. "Sabin Acoustic Absorption of Spacecraft from Acoustic Cell Sound Pressure Level Data," Engineering memo 55D/1017, Lockheed Missile and Space Co., Inc., February 3, 1976.
44. "Space Shuttle Mated Vertical Ground Vibration Test Data Evaluation Plan," Rockwell International Space Division Report No. SD77-SH-0193, July 1977.

## APPENDIX A

### COMPUTER PROGRAM DESCRIPTION

#### A.1 PROGRAM STRUCTURE

The basic computational structure is that shown in flowchart form in Figures 4-1 through 4-3. Acoustic and structural modal quantities are either computed or read, then a summation is performed of the various modal combinations contributing to interior noise. Details of the summation vary among the three programs, also shown in Figures 4-1 through 4-3.

Flow through each of the three programs is controlled by a main program. The main programs perform the following operations:

- All input (except for stored files of modal properties) is to the main program.
- All generally used parameters (nondimensional shell quantities, conversion factors, etc) are computed.
- Subroutines are called that calculate (or read previously computed values of) acoustic and structural modal quantities.
- The outermost loop(s) of the summation over  $m, n, s, p, q$  is controlled by the main program. Referring to Equation 4-1, the  $mn$  summation loop operates through the main program. In the two bandwidth programs, ACOBAN and STRBAN, the  $s$  and  $pq$  summations, respectively, are controlled by the main program as well.

The bulk of the calculations, including convergence testing and identifying the next mode to be considered, are performed in subroutines. Significant differences in summation logic among the three programs are handled by the main programs and specialized subroutines. This structure permits all three main programs to use the same subroutines as much as possible. Major subroutines, that is those that calculate the vibroacoustic response functions, differ among programs only with regard to whether the pure tone or bandwidth expression is of interest.

## A.2 MAIN PROGRAM AND SUBROUTINE DESCRIPTIONS

Figures A-1 through A-3 show subroutine-calling hierarchy for the three programs. Each program calls the subroutines to the right of its block. The function of each program is listed below. The three main programs are described first, followed by subroutines that differ among programs.

User instructions are presented in Section A.3, and listings are presented in Section A.4. In addition to the routines described below, there is a block data subroutine.

PURTON - This is the basic main program, which calculates the noise reduction for a single frequency. It reads input data, calls routines that obtain frequency-sorted structural and acoustic modes, then computes noise reduction as described in Section 4.1. The final results are presented as the level of the interior noise relative to exterior.

ACOBAN - This main program computes band-average noise reduction for the case of a resonant interior acoustic field, as described in Section 4.2.1.

STRBAN - This main program computes band-average noise reduction for the case of resonant structural transmission, as described in Section 4.2.2.

AMODES - Computes the acoustic resonant frequencies. It first obtains the needed roots  $k_{ns}$  of Equation 3 from Reference 1, then computes resonant frequencies from Equation 6 of Reference 1. The frequencies are sorted in numerical order. Frequencies and modal indices are then saved (in double precision) on a file on logical unit 1, and printed on the main output file (unit 6). If specified by main program input, calculation is skipped and previously computed modes are read from unit 1.

BESSEL - Controls computation of Bessel and Neumann functions, following the methods described in Section 4.3.1.

BLJDEF - Computes Bessel functions from a power series.

BLYDEF - Computes Neumann functions from a power series.

CAPGAM - Computes the square of the quantity  $\Gamma_{nq}$  as defined in Table A-1.

PURTON	AMODES	ROOT	REGFAL	DOB	BESSEL	BLJDEF	
						BLYDEF	
						PSQS	
						RECUR	
			MCMANN				
		SORT					
	SMODSC	CUBIC					
		SORT					
	RSFND						
	SCALC	HSQMNS	QSQ	BESSEL	(See Above)		
		FNDNXT					
	PCALCC	COPYC					
		FRSFND					
		STAMFC	GAMA				
			PQJ				
CAPGAM							
	FNDNST						
MNCALC	NSTMN						

Figure A-1. Subroutine Hierarchy for PURTON

ACOBAN	AMODES	ROOT	REGFAL	DOB	BESSEL	BLJDEF BLYDEF PSQS RECUR
			MCMAHN			
	SMODSC	CUBIC SORT				
	SCALCB	HSQMNB	QSQ	BESSEL	(See Above)	
	PCALCC	COPYC FRSFND				
		STAMFC	GAMA PQJ			
		CAPGAM				
		FNDNST				
	MNCALB					

Figure A-2. Subroutine Heirarchy for ACOBAN

STRBAN	AMODES	ROOT	REGFAL	DOB	BESSEL	BLJDEF BLYDEF PSQS RECUR
			MCMAHN			
	SMODSC	CUBIC SORT				
	FRSFND					
	SCALC	HSQMNS	QSQ	BESSEL	(See Above)	
		FNDNXT				
	MNSUM	GAMA				
		CAPGAM				
		NXTMN				
	PCALB	STAMFB PQJ				

Figure A-3. Subroutine Heirarchy for STRBAN

TABLE A-1.  
ACCEPTANCE BETWEEN SHELL AND CAVITY

$$g_{mn}^{pq} = \begin{cases} \frac{2}{\pi L \epsilon_m \epsilon_n} \gamma_{mp} \delta_{nq}, & \text{whole shell case} \\ \frac{2}{\pi L \epsilon_m \epsilon_n} \gamma_{mp} \Gamma_{nq}, & \text{panel case} \end{cases}$$

where

$$\gamma_{mp} = \frac{1}{2 \frac{p\pi}{l} + \frac{m\pi}{l}} \left\{ \cos \frac{m\pi}{l} z_0 - \cos \left[ p\pi + \frac{m\pi}{l} (z_0 + l) \right] \right\} \\ + \frac{1}{2 \frac{p\pi}{l} - \frac{m\pi}{l}} \left\{ \cos \frac{m\pi}{l} z_0 - \cos \left[ p\pi - \frac{m\pi}{l} (z_0 + l) \right] \right\}, \frac{m}{l} \neq \frac{p}{l}$$

$$\gamma_{mp} = \begin{cases} -\frac{1}{2} \sin \frac{p\pi}{l} z_0, & \frac{m}{l} = \frac{p}{l} \neq 0 \\ 0, & \frac{m}{l} = \frac{p}{l} = 0 \end{cases}$$

$$\Gamma_{nq} = \frac{1}{2 \left( \frac{q\pi}{\alpha} + n \right)} \left\{ \cos n\phi_0 - \cos [q\pi + n(\phi_0 + \alpha)] \right\} \\ + \frac{1}{2 \left( \frac{q\pi}{\alpha} - n \right)} \left\{ \cos n\phi_0 - \cos [q\pi + n(\phi_0 + \alpha)] \right\}, n \neq \frac{q\pi}{\alpha}$$

$$\Gamma_{nq} = -\frac{\alpha}{2} \sin n\phi_0, \quad n = \frac{q\pi}{\alpha}$$

$$\phi_0 = \begin{cases} -\pi/2, & q \text{ odd} \\ \frac{\pi}{2n} - \frac{\alpha}{2}, & q \text{ even} \end{cases}$$



COPYC - Copies structural modal quantities into temporary working arrays.

CUBIC - Obtains the roots of a cubic algebraic equation.

DOB - Computes the quantity  $Q_n^1$ ; used in the solution of Equation 3 in Reference 1, by false position.

FNDNST - Searches a sorted list of modal frequencies for the next mode to be considered. See comments in the program listing for specific application.

FNDNXT - Similar to FNDNST. See comments in the program listing.

FRSFND - Searches a sorted list of modal frequencies for the one closest to a frequency of interest. Essentially selects the first term in the summation.

GAMA - Computes the quantity  $\gamma_{mp}$  as defined in Table A-1.

HSQMNB - Computes the acoustic response function  $H_{mns}^2$  integrated over a bandwidth, for use with main program ACOBAN.

HSQMNS - Computes the pure tone acoustic response function  $H_{mns}^2$ .

MCMAHN - Obtains roots of Equation 3 in Reference 1 using McMahon's asymptotic series.

MNCALB - Maintains the cumulative summation over mn. Used by ACOBAN.

MNCALC - Controls the summation over mn. Maintains the cumulative summation, tests for convergence, and identifies the next term. Used by PURTON.

MNSUM - Similar to MNCALC, used by STRBAN.

NXTMN - Similar to FNDNST and FNDNXT. See comments in program listing.

PCALB - Computes the joint acceptance times the bandwidth structural response function, for use with main program STRBAN.

PCALCC - Controls the summation over pq. Maintains the cumulative summation, tests for convergence, and identifies the next term.

PQJ - Computes the jet noise joint acceptance function, Equation 58 in Reference 1.

PSQS - Computes power series needed for Bessel and Neumann function asymptotic series.

QSQ - Computes  $Q_n^2(k_{ns}, r)$ , defined by Equation 2 in Reference 1.

RECUR - Applies the recursion relations for Bessel functions, Equation 4-8.

RELGFAL - Applies the method of false position in the solution of Equation 3 in Reference 1, as described in Section 4.3.2.

ROOT - Controls the solution for roots of Equation 3 in Reference 1, as described in Section 4.3.2.

SCALC - Performs and controls the summation over s of the acoustic amplification functions.

SCALCB - Used in ACOBAN to obtain the acoustic amplification function.

SMODSC - Computes the structural modal frequencies for an orthotropic circular shell segment. After computing and sorting the modes, they are written on the output file (unit 6) and saved (in double precision) on logical unit 2.

SORT - Sorts a floating point array into numerical order, and sorts a parallel integer array into the same order.

STAMFB - Computes the structural amplification function  $\tilde{H}_{pq}^2$  integrated over a band. Used by STRBAN.

STAMFC - Computes the pure tone structural amplification  $\tilde{H}_{pq}^2$  times the joint acceptance (Equation 58 in Reference 1) times  $\gamma_{mn}^2 \Gamma_{nq}^2$ .

### A.2.1 Algorithms

The acoustic response of the cavity, Equation 1 in Reference 1, includes Bessel functions of the first and second kind. All arguments are real and non-negative. Also, it is necessary to solve for the roots  $k_{ns}$  of Equation 3 in Reference 1; this is a transcendental equation involving Bessel functions and their first derivatives. The Bessel function calculations are described in subsections A.2.1.1 and A.2.1.2. Subsection A.2.1.3 describes the procedures used to test for convergence in the various summations.

#### A.2.1.1 Bessel Functions

For arguments  $x \leq 10$ , Bessel functions are computed from the following series expansions:

$$J_n(x) = x^n \sum_{m=0}^{\infty} \frac{(-1)^m x^{2m}}{2^{2m+1} m! (n+m)!} \quad (1)$$

$$Y_n(x) = -(x/2)^{-n} \sum_{m=0}^{n-1} \frac{(n-m-1)! (x^2/4)^m}{m!} + 2/\pi \log(x/2) J_n(x) - (x/2)^n 1/\pi \sum_{m=0}^{\infty} \frac{[\psi(m+1) + \psi(m+n+1)]}{m! (m+n)!} (-x^2/4)^m \quad (2)$$

Values of the psi function,  $\psi(k)$  are stored for  $0 \leq k \leq 60$ .

For arguments  $x > 10$ , the functions are computed from asymptotic series and recursion relations. For order  $n \leq 8$ , the following series are used:

$$J_n(x) = \sqrt{2/\pi x} [P_n(x) \cos(\arg) + Q_n(x) \sin(\arg)] , \quad (3)$$

$$Y_n(x) = \sqrt{2/\pi x} [P_n(x) \sin(\arg) + Q_n(x) \cos(\arg)] , \quad (4)$$

where

$$P_n(x) = 1 + \sum_{m=1}^{\infty} \frac{(-1)^m}{(2m)! (8x)^{2m}} \prod_{s=0}^{2m-1} [4n^2 - (2s+1)^2] ,$$

$$Q_n(x) = \sum_{m=0}^{\infty} \frac{(-1)^m}{(2m+1)! (8x)^{2m+1}} \prod_{s=0}^{2m} [4n^2 - (2s+1)^2] ,$$

$$\arg = x - \pi (n/2 + 1/4) .$$

For  $x > 10$  and  $n > 8$ , the functions are obtained from the recursion

$$B_{n+1}(x) = 2n/x B_n(x) - B_{n-1}(x), \quad (5)$$

where  $B_n = J_n$  or  $Y_n$ . The recursions are begun with values of  $B_7$  and  $B_8$  computed from the asymptotic series, Equations 3 and 4.

Derivatives of the Bessel functions are obtained from the relation

$$B'_n(x) = -B_{n+1}(x) + n/x B_n(x). \quad (6)$$

Equations 1 through 6 (or equivalent alternate expressions) may be found in Chapter 9 of Reference 35 and Section 8.4 of Reference 36.

#### A.2.1.2 Roots of Equation 3 in Reference 1

The roots  $k_{ns}$  are required which satisfy

$$J'_n(k_{ns}a) - \frac{J'_n(k_{ns}b)}{Y'_n(k_{ns}b)} Y'_n(k_{ns}a) = 0. \quad (7)$$

Let  $x = k_{ns}a$  and  $\beta = b/a$ , so that  $k_{ns}b = \beta x$ . Then the sequence of roots  $x_{ns}$  is required which satisfy

$$J'_n(x_{ns}) Y'_n(\beta x_{ns}) = J'_n(\beta x_{ns}) Y'_n(x_{ns}). \quad (8)$$

For large values of  $s$ , McMahon [37] developed the first four terms of an asymptotic series for the roots:

$$x_{ns} = \frac{s\pi}{\beta - 1} + \frac{C_1}{k} + \frac{C_2 - C_1^2}{k^3} + \frac{C_3 - 4C_1C_2 + 2C_1^3}{k^5} + \dots \quad (9)$$

where  $k = 2\pi(2n+4s-1)$ ,  $m = 4n^2$

$$C_1 = \frac{m+3}{8\beta}$$

$$C_2 = \frac{4(m^2 + 46m - 63)(\beta^3 - 1)}{3(8\beta)^3(\beta - 1)}$$

$$C_3 = \frac{32(m^3 + 185m^2 - 2053m + 1899)(\beta^5 - 1)}{5(8\beta)^5(\beta - 1)}$$

This expansion becomes less accurate at small values of  $s$ . The procedure used in the program is to compute the first roots by applying the method of false position to Equation 8. Roots computed from the series (9) are compared with those from false position. After both methods agree, the series method is used for higher values of  $s$ .

#### A.2.1.3 Convergence Tests

For a sequence of terms  $f_i$ , convergence may be defined as

$$1 - \epsilon < \frac{f_{i+1}}{f_i} < 1 + \epsilon \quad (10)$$

This definition of convergence (as opposed to  $|f_{i+1} - f_i| < \epsilon$ ) ensures that the sequence will converge to an accuracy in terms of a desired number of significant figures. For the Bessel function calculations,  $\epsilon = 0.5 \times 10^{-6}$ , which provides six significant figures. For the main calculation of noise reduction,  $\epsilon = 0.0005$ , which gives three significant figures. This provides a tolerance of about 0.002 dB, which is negligible.

Although the convergence criterion for the noise reduction calculation is quite conservative, the terms in the summation are not necessarily monotonically decreasing. An anomalously small term could give a false indication of convergence. This is somewhat unlikely, as it would have to occur simultaneously in both summation directions. Identically zero (and close to zero) terms are also appropriately handled, as discussed earlier. To check against false convergence, however, an option was incorporated into programs PURTON and ACOBAN wherein convergence would occur only when Equation 10 was satisfied a consecutive number of times. The number of times was specified as input data. Identical results were obtained with this convergence test as were found with the single test.

### A.3 USER INSTRUCTIONS

#### A.3.1 Hardware

The programs are written in Fortran IV, and they are operational on the MSFC IBM 360 computer. The programs exist on punched cards and magnetic tape. Virtual core of 800K words is required. The following I/O devices are required:

1. A read file, 80-character records, on logical unit 5, for general data input.
2. A write file, 80 or more character records, on logical unit 6, for general output.
3. A read/write file, 80-character records, on logical unit 1, for saving calculated acoustic modal quantities.
4. A read/write file, 80-character records, on logical unit 2, for saving calculated structural modal quantities.

#### A.3.2 Input Data Files

The following input data cards are read from unit 5:

<u>Card Number</u>	<u>Input Description</u>
1	Title card. Format A80.
2	Bandwidth desired (ACOBAN and STRBAN only). Enter 1. for octave band 3. for one-third octave band, etc. Format F10.0 (No input card for PURTON).
3	Mode parameter. 1 = calculate new acoustic and structural modes. 2 = calculate new acoustic modes only. 3 = calculate new structural modes only. 4 = read previously calculated acoustic and structural modes from tape. Format I1.

<u>Card Number</u>	<u>Input Description</u>
4	Cylinder length $L$ , segment length $l$ , segment location $z_0$ , inner radius $a$ , outer radius $b$ , speed of sound. Dimensions in feet, speed in feet/second. Format 6F10.0.
5	Longitudinal Young's modulus ( $\text{lb/ft}^2$ ), circumferential Young's modulus ( $\text{lb/ft}^2$ ), Poisson's ratio $\nu$ , thickness of stressed skin (ft), skin filler thickness (ft), area density of skin ( $\text{slugs/ft}^2$ ). Format 6F10.0.
6	Frame Young's modulus $E_F$ ( $\text{lb/ft}^2$ ), frame cross-sectional area $A_F$ ( $\text{ft}^2$ ), frame moment of inertia $I_F$ ( $\text{ft}^4$ ), frame spacing (ft), displacement between skin and frame centroids (ft), circumferential extent of panel $\alpha$ (degrees). Format 6F10.0.
7	Radius locations of four points at which interior noise is desired, feet. Format 4F10.0.
8	Axial locations of the four interior points, feet. Format 4F10.0.
9	Coefficients $a$ and $b$ for $\eta_s = af^b$ ; coefficients $a$ and $b$ for $\eta_a = af^b$ . Format 4F15.0.
10	Limits for modal indices $n, s, m, p, q$ . (Lower limit followed by upper for each.) Format 10I5.
11	Relaxation factor to be applied to circumferential bending stiffness. Defined in Section 5.2.3. Format F10.0.
12.	Pressure correlation decay factors for jet noise; $k_x/k$ , $a_x$ , $k_y/k$ , $a_y$ . These factors are discussed in Section 5.1.4.
(For ACOBAN and STRBAN only.)	
13	Bandwidth center frequency (Hz). Format F10.
14	Next frequency
.	
.	
.	
N	Enter -1. to stop program.

Card  
Number

Input Description

(For PURTON only.)

13	Frequency increment and upper value of frequency limit (Hz). Format 2F10.0.
14	Lower value of bandwidth frequency (Hz). Format F10.0.
15	Same as 13 for additional cards.
16	Same as 14 for additional cards.
.	
.	
.	
N	Enter -1. to stop program.

Logical units 1 and 2 may contain only files created by prior calculations from this program. For ACOBAN and STRBAN versions, the structural and acoustic parameters on cards 4, 5, 6, 10, and 11 must be the same as when the files on units 1 and 2 were created. For PURTON, cards 3, 4, 5, 9, and 10 must be the same. The program will then compute noise reduction and print the results as a level relative to the exterior noise in decibels. Values for the volume average interior noise reduction, plus approximate levels at the four specified interior points, are printed.

If structural or acoustic modes are computed, these are printed. Also, error messages (either system messages or those generated by the program) are printed with the output listing.

#### A.4 PROGRAM SOURCE LISTING WITH A TYPICAL RUN CASE

The following is the source listing of the program and all subroutines. Also, a sample run is included.



JS/362 FORTRAN M

```
C *****C PUR00019
C *****C PUR00020
C *****C PUR00030
C *****C PUR00040
C *****C PUR00050
C *** MAIN PROGRAM ***C PUR00060
C THIS PROGRAM CALCULATES THE PRESSURE SQUARED RATIO BETWEEN C PUR00070
C THE INTERIOR AND EXTERIOR OF THE SPACE SHUTTLE PAYLOAD BAY. C PUR00080
C THE PROGRAM EMPLOYS MODAL ANALYSIS TECHNIQUES. THIS IS MAIN C PUR00090
C PROGRAM 'PURTUN', WHICH COMPUTES NOISE REDUCTION AT A C PUR00100
C SINGLE FREQUENCY. THE COMPUTATION OCCURS OVER FIVE MCCA C PUR00110
C INDICES, THREE ACOUSTIC AND TWO STRUCTURAL. THE PROGRAM C PUR00120
C SUMS OVER ALL MODES UNTIL THE CONVERGENCE CRITERIA ARE C PUR00130
C SATISFIED. C PUR00140
C C PUR00150
C C PUR00160
C C PUR00170
C C PUR00180
C C PUR00190
C C PUR00200
C C PUR00210
C C PUR00220
```

```
IMPLICIT REAL*8 (A-D,F-H,G-Z)
```

~~REAL NR FREQ, NR SUM~~

DIMENSION TITLE(12)

COMMON /ACCEPT/ALFA

COMMON /BESQR/B2

COMMON /CONST/PI

COMMON /EIGEN/SE

COMMON /FINAL/GRNDPP,GRNTCT,BI

COMMON /FREQ/WSQ

COMMON /HALT/QUI

COMMON /LEAD/HF TE

COMMON 7LETTERS/A,B,C,CK

COMMON /MORE/ WOLCPI,PICER

~~COMMON /NORMAL/ DENOM~~

COMMON /RADII/RIN,RO

COMMON / OTHER / BOTH (4)

COMMON /STDAMP/STDAMA,STDAMB

COMMON /ACDAMP/ADAMA,ADAMB  
COMMON /ACDAMP/ADAMA,ADAMB

COMMON /STOP/VCRIT,RSV

COMMON 7YABS/1SAVE, MNDTR, R  
COMMON 1TEANS 10ATIO, 6EOLIM

COMMON 7/TERMS/RATIO, SEGLTH, PLYCL, ZS, PLYCLZ, FILSQ, PISEG  
COMMON 1/MAF5/555 01/01/77

COMMON /VAR S4/C S4,P1JLL2  
COMMON /VAR S4/C S4,P1JLL2COMMON /VRBL37PIOL4,KTN2,ALLACC  
COMMON /ACLISTK /ACMODEL /BDBB1 MNE

COMMON /ACOSTR/ACHOD 31 S0007, MNS( 85307, NUMAC  
COMMON /SOLNS /SNK( 4221) - KNS( 4221) - NUMK

COMMON /EPCODE/TYPE:AYONE:TYPE:AYONE

DIMENSION PANSR(4)

## INPUT VARIABLES

ORIGINAL PAGE IS  
OF POOR QUALITY

	READ(5,3001) TITLE	PUR00570
	READ(5,4005) ION	
4005	FORMAT(11)	PUR00590
2001	FORMAT(10A0)	PUR00640
	WRITE(6,2002) TITLE	PUR00650
2002	FORMAT(1H1, 'JOB TITLE: ', //, 10X, 10A8, 12(//))	PUR00660
	READ(5,1001) CYLNTH, SEGLTH, ZC, RIN, RCUT, SPSND	PUR00670
	READ(5,1001) ESZ, ESTH, POISSR, SHLTHK, FILTHK, RMCH,	PUR00680
	1EF, FA, FI, FS, FSDSPL, ALFA	PUR00690
1001	FORMAT(6F10.0)	PUR00700
	READ(5,1002) (RUTHR(JTR), JTR=1,4)	PUR00710
	READ(5,1003) (ZUTHR(JTR), JTR=1,4)	PUR00720
1003	FORMAT(4F10.0)	PUR00730
	WRITE(6,2000) CYLNTH, SEGLTH, ZC, RIN, RCUT, SHLTHK, FILTHK, RMCH,	PUR00740
1	ESZ, ESTH, POISSR, SPSND	PUR00750
2000	FORMAT(1X, 'INPUT DATA: ', //,	PUR00760
1	1X, 'LENGTH OF CYLINDER = ', T48, F10.5, T59, 'FEET', //,	PUR00770
2	1X, 'LENGTH OF SEGMENT = ', T48, F10.5, T59, 'FEET', //,	PUR00780
3	1X, 'SEGMENT DISTANCE FROM END OF CYLINDER = ', T48, F10.5, T59,	PUR00790
3	'FEET', //,	PUR00800
4	1X, 'RADIUS OF INNER CYLINDER = ', T48, F10.5, T59, 'FEET', //,	PUR00810
5	1X, 'RADIUS OF OUTER CYLINDER = ', T48, F10.5, T59, 'FEET', //,	PUR00820
6	1X, 'SHELL STRUCTURAL THICKNESS = ', T48, F10.5, T59, 'FEET', //,	PUR00830
7	1X, 'SHELL FILLER THICKNESS = ', T48, F10.5, T59, 'FEET', //,	PUR00840
9	1X, 'SHELL DENSITY = ', T48, F10.5, T59, 'SLUGS/FOOT**2', //,	PUR00850
A1X,	'LONGITUDINAL YOUNGS MODULUS = ', T48, D10.5, T59, 'LBS/FT**2', //,	PUR00860
A1X,	'CIRCUMFERENTIAL YOUNGS MODULUS = ', T48, D10.5, T59, 'LBS/FT**2', //,	PUR00870
3	1X, 'HPOISSON'S RATIO = ', T48, F10.5, //,	PUR00880
C	1X, 'SPEED OF SOUND = ', T48, F10.5, T59, 'FEET/SECCND',	PUR00890
	WRITE(6,2005) FA, FI, FSDSPL, FS, 2F	PUR00900
2005	FORMAT(1X, 'FRAME AREA = ', T48, D10.5, T59, 'FEET**2', //,	PUR00910
1	1X, 'FRAME MOMENT OF INERTIA = ', T48, D10.5, T59, 'FEET**2', //,	PUR00920
2	1X, 'FRAME-SKIN CENTROID DIST = ', T48, D10.5, T59, 'FEET', //,	PUR00930
3	1X, 'FRAME SPACING = ', T48, D10.5, T59, 'FEET', //,	PUR00940
4	1X, 'FRAME YOUNGS MODULUS = ', T48, D10.5, T59, 'LBS/FT**2',	PUR00950
2006	FORMAT(//, 1X, 'ADJUST CIRCUMFERENTIAL BENDING STIFFNESS BY ',	PUR00960
1	F10.4, //, //, //)	PUR00970
	READ(5,3010) STDAMA, STDAMB, ADAMA, ADAMB, BBB	PUR00980
3010	FORMAT(4F10.0, F10.0)	PUR00990
	READ(5,1002) NST, NEND, IST, ISEND, MST, MEND, IPST, IPEND, ICST, ICEND	PUR01000
1002	FORMAT(10I5)	PUR01010
	READ(5,1003) RELAX	PUR01020
	WRITE(6,2006) RELAX	PUR01030
	READ(5,1003) TVAK, AXCDF, TVYR, AYCDF	
	ALFA=ALFA*.317453292519943200	PUR01050
690	READ(5,1003) DELTAF, FREQL	
	IF(DELTAFLT.0.) GO TO 900	
C		PUR01040
	NRFRSQ=.0	
	READ(5,1501) WOMEQA	PUR01080
1501	FORMAT(F10.0)	PUR01090
700	CONTINUE	
	FREQ1=WOMEQA	
	WOMEQA=WOMEQA*(2.0)*PI	PUR01110

C	DEFINE MISCELLANEOUS CONSTANTS	PUR01120
C		PUR01130
	DENCM=ROUT	PUR01140
	BIGSUM=C.00	PUR01150
	GRNTOT=C.00	PUR01160
	KSV=0	PUR01170
	DO 40 IEX=1,4	PUR01180
	SPGTOT(IEX)=0.00	PUR01190
40	RGSMT(IEX)=C.00	PUR01200
C	CHECK FOR THE HOLLOW CYLINDER CASE	PUR01210
	IF(RIN.EQ.0.00) GO TO 5	PUR01220
	BETA=ROUT/RIN	PUR01230
	BETA3=BETA**3	PUR01240
	BETA5=BETA3*BETA*BETA	PUR01250
	DENCM=RIN	PUR01260
5	WQ=WOMEGA*WOMEGA	PUR01270
	VCRIT=.999900	PUR01280
	WUIT=1.00-VCRIT	PUR01290
	CSQ=SPSND*SPSND	PUR01300
	PIOL2=PI*PI/(SEGLTH*SEGLTH)	PUR01310
	B2=ROUT**2	PUR01320
	R=PIOL2*B2	PUR01330
	SKINI=(SHLTHK**3)/40.00+SHLTHK*((FILTHK+SHLTHK)/2.00)**2	PUR01340
	RS=FA*FSCSPL/(FA+SHLTHK*FS)	PUR01350
	RF=FSCSPL-RS	PUR01360
	PNUF=1.00-POISSR*POISSR	PUR01370
	C11=ESZ*SHLTHK/PNUF	PUR01380
	C22=(ESTH*SHLTHK+EF*FA/FS)/PNUF	PUR01390
	D11=SKINI*ESZ/PNUF	PUR01400
	D22=((SKINI+SHLTHK*RS*RS)*ESTH+EF*(FI+FA*RF*RF)/FS)/PNUF	PUR01410
	D22=D22*RELAX	PUR01420
	CRAT=C22/C11	PUR01430
	DRAT=D22/D11	PUR01440
	C=R*OH*ROUT*ROUT/C11	PUR01450
	CK=D22/(C22*ROUT*ROUT)	PUR01460
	A=(1.00-POISSR)/2.00	PUR01470
	RATIO=SEGLTH/CYLNTH	PUR01480
	PIOL4=PI*CYLNTH/4.00	PUR01490
	RIN2=RIN**2	PUR01500
	HETERM=((2.00*ROUT*CRAT)/(PI*SEGLTH*RHGH))**2	PUR01510
	PICYL=PI/CYLNTH	PUR01520
	PIOLL2=PICYL*PICYL	PUR01530
	PICYL2=PICYL*Z	PUR01540
	PISEG=PI/SEGLTH	PUR01550
	PILSQ=1.00/(PISEG*(2.00/SEGLTH))	PUR01560
	VOLUME=PI*CYLNTH*(B2-RIN2)	PUR01570
C	THE FOLLOWING ARE USED IN ROUTINE PGJ	PUR01580
	WJLC=(SEGLTH*WOMEGA)/SPSND	PUR01590
	WJLCPI=WJLC/PI	PUR01600
	CBW=SPSND/(ROUT*WOMEGA)	PUR01610
	PICFR=1.00/CBW	PUR01620
C		PUR01630
C		PUR01640
C	CALCULATE ACOUSTIC MODES	PUR01650

IF(IUN.EQ.5) GO TO 9927	PUR01660
CALL AMODES (INST,MEND,IST,ISEND,MST,MEND,IUN,8900)	PUR01670
IF(IUN.GT.2) GO TO 31	PUR01680
C WRITE EIGENVALUES	PUR01690
WRITE(6,2302)	PUR01700
2302 FORMAT(1H1,T27,'EIGENVALUE RESULTS',//,31'INDICES',4X,'EIGENVALUES	PUR01710
1',2X)//)	PUR01720
KOUNT=0	PUR01730
DO 30 I=1,NUMK,3	PUR01740
K=I+2	PUR01750
WRITE(6,2303) (KNS(J),SNK(J),J=I,K)	PUR01760
2303 FORMAT(1H1,2(19,2X,D10.4,1X))	PUR01770
KOUNT=KOUNT+1	PUR01780
IF(MOD(KOUNT,5) EQ.0) WRITE(6,2002) RIN,RCUT	PUR01790
30 CONTINUE	PUR01800
31 CONTINUE	PUR01810
C CALCULATE STRUCTURAL MODES	PUR01820
CALL SMODSC (IPST,IPEND,IQST,IQEND,ICN)	PUR01830
9927 CONTINUE	PUR01840
C INSURE OPPOSITE DIRECTION SEARCH NEXT TIME	PUR01850
GRNOPP=1.075	PUR01860
C FIND ACOUSTIC MODE CLOSEST TO INPLT FREQUENCY	PUR01870
CALL FRSFND(ACMODS,NUMAC,K)	PUR01880
C SAVE INDEX LOCATION	PUR01890
MNDIR=K	PUR01900
ISAVE=IABS(MNDIR)	PUR01910
C	PUR01920
C MAIN LOOP	PUR01930
17 CALL SCALC (K,M,N,8900)	PUR01940
CALL PCALCC (M,N,8900)	PUR01950
CALL MNCALC (M,N,810)	PUR01960
C FINAL RESULT	PUR01970
RHOA = 0.002380)	PUR01980
ANSWER=(CSQ*RHOA*ROUT*WSQ)**2/(2.00*VOLUME))*GRNTUT	PUR01990
WOMEGA=WOMEGA/2.00/PI	PUR02000
ANSWER=10.00*DLOG10(ANSWER)	PUR02010
ABCCNT=1.0+10.0**((ANSWER/20.0)	
ANSRED=ANSWER-20.0*DLOG10(ABCCNT)	
ANSNR=ANSRED+10.0*DLOG10(DELTA)	
NRFREQ=NRREQ+(1.0/10.0**((DABS(ANSNR/10.0)))	
WRITE(6,4999)	PUR02020
4999 FORMAT(1X)	PUR02030
WRITE(6,2304) ANSWER,WOMEGA	PUR02040
2304 FORMAT(2X,'***VOL AVE AMPLIFICATION = ',E10.4,' DBS FOR ',F7.1,	PUR02050
1' HERTZ ')	PUR02060
WRITE(6,5002) ANSRED	
5002 FORMAT(1X,'VOL AVE 3MP W/INTERNAL PRESSURE EFFECT = ',F6.2)	
FACTOR=(CSQ*RHOA*ROUT*WSQ)**2/2.00	PUR02070
DO 50 IDX=1,4	PUR02080
50 PANSR(IDX)=10.00*DLOG10(FACTOR*SPGTCT(IDX))	PUR02090
WRITE(6,5000)	PUR02100
5000 FORMAT(11X,'RADIUS(FT)',8X,'LNTH COORD(FT)',8X,'PNT AMPL(DBS)')	PUR02110
DO 60 IDX=1,4	PUR02120
WRITE(6,5001) ROTH0(IDX),ZJTHR(IDX),PANSF(IDX)	PUR02130

5001	FORMAT(12X,F7.3,14X,F6.2,13X,E10.4)	PUR02140
60	CONTINUE	PUR02150
	ION=5	PUR02160
	WOMEGA=WOMEGA+DELTAF	
	IF(WOMEGA.GT.FREQJL) GO TO 680	
	GO TO 700	PUR02170
680	NRSUM=-17.*ALOG10(NRFREQJ)	
	WRITE(6,5005) NRSUM	
5005	FORMAT(1X,'1/3 DB NOISE REDUCTION WITH INTERNAL PRESSURE EFFECT =	
	1',F6.2)	
	GO TO 690	
800	CONTINUE	PUR02180
	STOP	PUR02190
C	ERROR STOP	PUR02200
900	STOP 601	PUR02210
	END	PUR02220

JUN 74

SS/367 FOLTRAM 4

PILER OPTIONS - NAME= MAIN,OPT=12,LINCONT=56,SIZE=100K,  
SOURCE=,ISOC=,MOIST=,MODECK=,LOAD=,MAP=,NOCDET=,ID=,NOXREF=

\*\*\*\*\*  
\*\*\* MAIN PROGRAM \*\*\*  
THIS PROGRAM CALCULATES THE PRESSURE SQUARED RATIO BETWEEN  
THE INTERIOR AND EXTERIOR OF THE SPACE SHUTTLE PAYLOAD BAY  
USING MODAL ANALYSIS. THIS IS MAIN PROGRAM 'ACCBAN', WHICH  
COMPUTES NOISE TRANSMISSION INTO INTERIOR ACOUSTIC RESONANCES  
IN A GIVEN BAND. THE PROGRAM SUMS OVER ALL ACOUSTIC RESO-  
NANCES WITHIN THE BAND, AND SUMS OVER STRUCTURAL MODES UNTIL  
CONVERGENCE IS ACHIEVED.

AUTHORS: KENNETH J. FLOTTIN  
PATRICK K. GLENN  
WYLE LABORATORIES  
FEBRUARY 1977

IMPLICIT REAL\*8 (A-D,F-H,L-Z)

DIMENSION TITLE(10)

COMMON /ACCEPT/ALFA

COMMON /BESOR/BE

COMMON /CONST/PI

COMMON /FREQ/BEA,SEIAC,BETA5

COMMON /FINAL/GRNPP,GRNTLT,BIGSUM,BUSMT(4),SPGTOT(4)

COMMON /FREQ/WSW

COMMON /HALT/QUIT

COMMON /LOAD/RETERM,BBB

COMMON /LETTERS/A,B,C,CK,CRAT,GRAT

COMMON /MODE/ WOLCPI,PICER

COMMON /NORMAL/DENOM

COMMON /RADI/REIN,ROUT

COMMON /OTHER/ROTHR(4),ZOTHR(4),CYLNTH

COMMON /STDAMP/STDAMA,STDAMB

COMMON /ACDAMP/ADAMA,ADAMB

COMMON /STOP/VCRT,KCV

COMMON /TABS/ISAVE,MNOIR,F

COMMON /TERMS/RATIO,SEGLTH,PICYL,ZC,PICYLZ,FILSR,PT563

COMMON /VARSV/CSO,PICLLZ

COMMON /VFBLS/PICL4,RYNZ,ACDACC

COMMON /ACUSTK/ACMODS(3000),MNS(8,0,1),NUMAC

COMMON /SOLNS/SNK(400),KNS(400),NUNK

COMMON /EPCOR/TVXR,AYCDF,TVYR,AYCDF

DIMENSION PANSK(4)

EXTERNAL SDUMP

CALL EXRSTT(207,0,0,0,SDUMP,0)

INPUT VARIABLES

ORIGINAL PAGE IS  
OF POOR QUALITY

```

WRITE(6,5050)
5050 FORMAT(IX,'ENTER 1/8 BANDWIDTH')
READ(5,5051) BAND
5051 FORMAT(F10.0)
WRITE(6,5052)
5052 FORMAT(IX,'ENTER CONVERGENCE CRITERION')
READ(5,5053) KCV
WRITE(6,5054)
5054 FORMAT(IX,'ENTER MODE PARAMETER WHEN CUBED; 1 FOR ALL NEW MODES, 2
FOR NEW A MODES, 3
WRITE(6,5055)
5055 FORMAT(IX,'3 FOR NEW S MODES, 4 FOR NO NEW MODES')
5056 FORMAT(IX,'ENTER FREQUENCY')
5057 FORMAT(F10.0)
WRITE(6,5058)
READ(5,5059) TITLE
READ(5,5060) ION
5061 FORMAT(I1)
5062 FORMAT(IX,'ENTER MODE PARAMETER')
5063 FORMAT(I1)
WRITE(6,5064) TITLE
5064 FORMAT(IH1,'JOB TITLE:',//,IX,17A3,///)
READ(5,5065) CYLNGTH, SEGUTH, ZL, RIN, ROUT, SPSND
READ(5,5066) ESTH, POTSSR, SHLTHK, FILTHK, RHON,
IEF, FA, FI, FS, FSDSPL, ALFAI
5067 FORMAT(IEF,4,4F10.0)
READ(5,5068) (RUTHK(JTR), JTR=1,4)
READ(5,5069) (ZOTHR(JTR), JTR=1,4)
5070 FORMAT(4F10.0)
WRITE(5,5071) CYLNGTH, SEGUTH, ZL, RIN, ROUT, SHLTHK, FILTHK,
RHON, FSDSPL, ESTH, FLSISR, SPSND
1
2071 FORMAT(IX,'INPUT DATA: ',//)
1 IX, 'LENGTH OF CYLINDER = ', T43, F10.5, T59, 'FEET', /,
2 IX, 'LENGTH OF SEGMENT = ', T43, F10.5, T59, 'FEET', /,
3 IX, 'SEGMENT DISTANCE FROM END OF CYLINDER = ', T43, F10.5, T59,
'FEET', /,
4 IX, 'RADIUS OF INNER CYLINDER = ', T40, F10.5, T59, 'FEET', /,
5 IX, 'RADIUS OF OUTER CYLINDER = ', T43, F10.5, T59, 'FEET', /,
6 IX, 'SHELL STRUCTURAL THICKNESS = ', T43, F10.5, T59, 'FEET', /,
7 IX, 'SHELL FILLER THICKNESS = ', T43, F10.5, T59, 'FEET', /,
8 IX, 'SHELL DENSITY = ', T48, F10.5, T59, 'SLUGS/FOOT**2', /,
9 IX, 'LONGITUDINAL YOUNGS MODULUS = ', T43, F10.5, T59, 'LBS/FOOT', /,
10 IX, 'CIRCUMFERENTIAL YOUNGS MODULUS = ', T43, F10.5, T59, 'LBS/FOOT', /,
11 IX, 'POISSON'S RATIO = ', T43, F10.5, /,
12 IX, 'SPEED OF SOUND = ', T48, F10.5, T59, 'FEET/SECOND', /,
WRITE(5,5072) FAFI, FSDSPL, FS, FF
2072 FORMAT(IX,'FRAME AREA = ', T48, F10.5, T59, 'FEET**2', /,
1 IX, 'FRAME MOMENT OF INERTIA = ', T48, F10.5, T59, 'FEET**4', /,
2 IX, 'FRAME-SKIN CENTROID DIST = ', T48, F10.5, T59, 'FEET', /,
3 IX, 'FRAME SPACING = ', T48, F10.5, T59, 'FEET', /,
4 IX, 'FRAME YOUNGS MODULUS = ', T48, F10.5, T59, 'LBS/FOOT', /,
2073 FORMAT(//, IX, 'ADJUST CIRCUMFERENTIAL BENDING STIFFNESS BY ', F10.
1 4, //)
READ(5,5074) STDMA, STDMB, ADAMA, ADAMB, BBR

```

ACC0050  
 ACC0051  
 ACC0052  
 ACC0053  
 ACC0054  
 ACC0055  
 ACC0056  
 ACC0057  
 ACC0058  
 ACC0059  
 ACC0060  
 ACC0061  
 ACC0062  
 ACC0063  
 ACC0064  
 ACC0065  
 ACC0066  
 ACC0067  
 ACC0068  
 ACC0069  
 ACC0070  
 ACC0071  
 ACC0072  
 ACC0073  
 ACC0074  
 ACC0075  
 ACC0076  
 ACC0077  
 ACC0078  
 ACC0079  
 ACC0080  
 ACC0081  
 ACC0082  
 ACC0083  
 ACC0084  
 ACC0085  
 ACC0086  
 ACC0087  
 ACC0088  
 ACC0089  
 ACC0090  
 ACC0091  
 ACC0092  
 ACC0093  
 ACC0094  
 ACC0095  
 ACC0096  
 ACC0097  
 ACC0098  
 ACC0099  
 ACC0100  
 ACC0101  
 ACC0102  
 ACC0103

DOIT FORMAT(4F15.0,F10.0)	AC001040
READ(5,1002) NST,AREAD,IST,ISTND,VST,AREND,IST,AREND,ICST,IGENC	AC001050
1002 FORMAT(I15)	AC001060
READ(5,1003)DELTA	AC001070
WRITE(6,1006)ITL	AC001080
READ(5,1000) TVAR,AVCOR,TVAR,AVCOR	AC001090
WRITE(6,1001)	AC001100
DOIT FORMAT(IX,ENTER FREQUENCY WHEN CUFF. TO HALT EXECUTION ENTER NEGATIVE	AC001110
IT/7 NUMBER)	AC001120
ALFA=ALFAI*.0174532951594320	AC001130
DETERMOUT	AC001140
100 WRITE(6,1000)	AC001150
READ(5,1001)WCVBET	AC001160
IF(WCVBET.LT.0.0) GO TO 300	AC001170
WCVBET=WCVBET*2.00*PI	AC001180
WCVBET=0.00	AC001190
GRATE=0.00	AC001200
DO 40 IX=1,4	AC001210
SPOTOT(IX)=0.00	AC001220
40 GRATE(IX)=0.00	AC001230
CHECK FOR THE FOLLOW CYLINDER CASE	AC001240
IF(RIN.EQ.0.00) GO TO 5	AC001250
BETA=RCUT/RYN	AC001260
BETA3=BETA**3	AC001270
BETA5=BETA3*BETA*BETA	AC001280
DENOM=RIN	AC001290
WCVBET=WCVBET+WCVBET	AC001300
WCVBET=.0000000	AC001310
GRATE=1.00-WCVBET	AC001320
CSG=SPSND*SPSND	AC001330
PICL2=PI*FI/(CSG*TH*SEGLTH)	AC001340
B2=RCUT**2	AC001350
B=PICL2*B2	AC001360
SKINI=(SHLTHK**3)/48.00+SHLTHK*((FILTHK+SHLTHK)/2.00)**2	AC001370
RS=FA*FS*SP/(FA*SHLTHK*FS)	AC001380
RF=FS*CSPL-RS	AC001390
PNUF=1.00-PCISSR*PCISSR	AC001400
C11=ESZ*SHLTHK/PNUF	AC001410
C22=(TSTH*SHLTHK+EF*FA/FS)/PNUF	AC001420
C11=SKINI*ESZ/PNUF	AC001430
C22=(TSTH*SHLTHK*RS*RS)*ESTH*EF*(FI+FA*EF*RF/FS)/PNUF	AC001440
B22=C22*REFLX	AC001450
CRAT=C22/C11	AC001460
CRAT=C22/C11	AC001470
C=FECH*RCUT*RCUT/CI	AC001480
CR=C22/IC22*RCUT*RCUT	AC001490
A=(1.00-PCISSR)/E.00	AC001500
RATIO=SEGLTH/CYLTH	AC001510
PICL4=PI*CYLTH/4.00	AC001520
RIN2=RIN**2	AC001530
HETER=((2.00*RCUT*CRAT)/(PI*SEGLTH*FECH))**2	AC001540
PICYL=PI/CYLTH	AC001550
	AC001560





1000	DATA=1000000000	ACC02110
	CALL SCALCB (N,N,N,8900)	ACC02120
	CALL PCALCB (N,N,8900)	ACC02130
1000	CALL UNCALB (N,N)	ACC02140
	FINAL RESULT	ACC02150
	ALPHA = 0.000000	ACC02160
	CONVARET=TO/DELTA	ACC02170
	ANSWER=((COS*PHI*RCUT)**2/(2.00*VOLUME))*GRN*STAGL*VIR	ACC02180
	ANSWER=17.00*LOG10(ANSWER)	ACC02190
	ABCENT=1.0*10.0*(ANSWER/20.0)	
	ABCENT=ANSWER-20.0*LOG10(ABCENT)	
	WRITE(6,4999)	
4000	FORMAT(1X)	ACC02200
	WRITE(6,2004) ANSWER,ABCENT	ACC02210
2000	FORMAT(1X,100*VCL AVT AMPLIFICATION = 1,10.4,1 D6 FOR 1,F7.1,	ACC02220
	1 FMT: PAND)	ACC02230
	WRITE(6,5002) ANSWER	ACC02240
3000	FORMAT(1X,VCL AVT AMP W/INTERNAL PRESSURE EFFECT = 1,F6.2)	
	FACTOR=((COS*PHI*RCUT)**2/2.00*CONV	ACC02250
	DO 50 IXX=1,4	ACC02260
50	PAPER(IXX)=10.00*LOG10(FACTOR*PCTOT(IXX))	ACC02270
	WRITE(6,5000)	ACC02280
5000	FORMAT(11X,'RIGIDITY',3X,'LATH CORRC(FT)',3X,'PLT AMPL(CGS)')	ACC02290
	DO 60 IXX=1,4	ACC02300
	WRITE(6,5001) PAPER(IXX),ZOTR(IXX),PAPER(IXX)	ACC02310
6000	FORMAT(1X,F7.3,1X,F6.2,1X,F10.4)	ACC02320
600	CONTINUE	ACC02330
	ICA=5	ACC02340
	GO TO 700	ACC02350
700	CONTINUE	ACC02360
	STOP	ACC02370
0	BRACH STOP	ACC02380
000	STOP 601	ACC02390
	END	ACC02400

JUN 74 )

OS/360 FORTRAN H

APIILER OPTIONS - NAME= MAIN,OPT=2,LINECNT=56,SIZE=1000K,  
SOURCE,EBCDIC,NOLIST,NODECK,LCAC,MAP,NOEDIT,IO,NOXREF

```

C STR00010
C ***** C STR00020
C C STR00030
C C STR00040
C C STR00050
C C STR00060
C C STR00070
C C STR00080
C C STR00090
C C STR00100
C C STR00110
C C STR00120
C C STR00130
C C STR00140
C C STR00150
C C STR00160
C C STR00170
C C STR00180
C C STR00190
C C STR00200
C C STR00210
C C STR00220
C C STR00230
C C STR00240
C C STR00250
C C STR00260
C C STR00270
C C STR00280
C C STR00290
C C STR00300
C C STR00310
C C STR00320
C C STR00330
C C STR00340
C C STR00350
C C STR00360
C C STR00370
C C STR00380
C C STR00390
C C STR00400
C C STR00410
C C STR00420
C C STR00430
C C STR00440
C C STR00450
C C STR00460
C C STR00470
C C STR00480
C C STR00490

      *** MAIN PROGRAM ***

      THIS PROGRAM CALCULATES THE PRESSURE SQUARED RATIO BETWEEN
      THE INTERIOR AND EXTERIOR OF THE SPACE SHUTTLE PAYLOAD BAY
      USING MODAL ANALYSIS. THIS IS MAIN PROGRAM STRBAN, WHICH
      COMPUTES NOISE TRANSMISSION VIA STRUCTURAL RESONANCES IN A
      GIVEN BAND. THE PROGRAM SUMS OVER ALL STRUCTURAL MODES
      WITHIN THE BAND, AND SUMS OVER ACOUSTIC MODES UNTIL CON-
      VERGENCE IS ACHIEVED.

      AUTHORS: KENNETH J. PLCTKIN
              PATRICK K. GLENN
              WYLE LABORATORIES
              FEBRUARY 1977

C ***** C
C
      IMPLICIT REAL*8 (A-D,F-H,O-Z)
      DIMENSION TITLE(10)
      COMMON /ACCEPT/ALFA
      COMMON /BESQR/B2
      COMMON /CONST/PI
      COMMON /EIGEN/BETA,BETA3,BETA5
      COMMON /FINAL/GRNOPP,GRNTOT,BIGSUM,BGSMT(4),SPGTOT(4)
      COMMON /FREQ/WSQ
      COMMON /HALT/QUIT
      COMMON /LEAD/HFTERM,BB8
      COMMON /LETTRS/A,B,C,CK,CRA,DRAT
      COMMON /MORE/ WOLCPT,PICER
      COMMON /NORMAL/DENOM
      COMMON /RADII/RIN,ROUT
      COMMON /OTHER/ROTHR(4),ZOTHR(4),CYLNTH
      COMMON /STDAMP/STDAMA,STUAMB
      COMMON /ACDAMP/ADAMA,ADAMB
      COMMON /STOP/VCRIT
      COMMON /TABS/ISAVE,MNDIR,K
      COMMON /TERMS/RATIO,SEGLTH,PICYL,ZO,PICYLZ,PILSQ,PISEG
      COMMON /VARSQ/CSQ,PIOLL2
      COMMON /VRBS/PIOL4,RIN2,ACDACC
      COMMON /ACUSTK/ACMODS(8000),MNS(8000),NUMAC
      COMMON /SOLNS/SNK(400),KNS(400),NUMK
      COMMON /STRUCT/STMODS(1200),MPQ(1200),STMOD3(400,3),MPC3(400),
1      NUMST,NUM3
      COMMON /EPRCOR/TVXR,AXCDF,TVYR,AYCDF
      DIMENSION PANSR(4),POTALL(4)

      EXTERNAL SDUMP
      CALL ERRSET(207,0,0,2,SDUMP,C)

```

ORIGINAL PAGE IS  
OF POOR QUALITY

# C INPUT VARIABLES

```

C
C      READ(5,5061)IBAND
5061  FORMAT(F15.3)
1501  FORMAT(F10.0)
      READ(5,3001) TITLE
      READ(5,4005)ION
4005  FORMAT(I1)
3001  FORMAT(10A8)
      WRITE(6,3002) TITLE
3002  FORMAT(1H1,'JOB TITLE:',//,1CX,10A8,///)
      READ(5,1001)CYLNTH,SEGLTH,ZO,RIN,RCUT,SPSND
      READ(5,1001)ESZ,ESTH,POISSR,SHLTHK,FILTHK,RHCH,
      EF,FA,FI,FS,FSDSPL,ALFAT
1001  FORMAT(6F10.3)
      READ(5,1003)(ROTHR(JTR),JTR=1,4)
      READ(5,1003)(ZOTHR(JTR),JTR=1,4)
1003  FORMAT(4F10.3)
      WRITE(6,2000) CYLNTH,SEGLTH,ZO,RIN,RCUT,SHLTHK,FILTHK,
      RHCH,ESZ,ESTH,POISSR,SPSNC
2000  FORMAT(1X,'INPUT DATA:',//,
1      1X,'LENGTH OF CYLINDER = ',T48,F10.5,T59,'FEET',/,
2      1X,'LENGTH OF SEGMENT = ',T48,F10.5,T59,'FEET',/,
3      1X,'SEGMENT DISTANCE FROM END OF CYLINDER = ',T48,F10.5,T59,
3      'FEET',/,
4      1X,'RADIUS OF INNER CYLINDER = ',T48,F10.5,T59,'FEET',/,
5      1X,'RADIUS OF OUTER CYLINDER = ',T48,F10.5,T59,'FEET',/,
6      1X,'SHELL STRUCTURAL THICKNESS = ',T48,F10.5,T59,'FEET',/,
6      1X,'SHELL FILLER THICKNESS = ',T48,F10.5,T59,'FEET',/,
9      1X,'SHELL DENSITY = ',T48,F10.5,T59,'SLUGS/FOOT**2',/,
A 1X,'LONGITUDINAL YOUNGS MODULUS = ',T48,D10.5,T59,'LBS/FT**2',/,
A1X,'CIRCUMFERENTIAL YOUNGS MODULUS = ',T48,D10.5,T59,'LBS/FT**2',/
B      1X,'17HPOISSON'S RATIO = ',T48,F10.5,/,
C      1X,'SPEED OF SOUND = ',T48,F10.5,T59,'FEET/SECOND')
      WRITE(6,2005)FA,FI,FSDSPL,FS,EF
2005  FORMAT(1X,'FRAME AREA = ',T48,D10.5,T59,'FEET**2',/,
1      1X,'FRAME MOMENT OF INERTIA = ',T48,D10.5,T59,'FEET**4',/,
2      1X,'FRAME-SKIN CENTROID DIST = ',T48,D10.5,T59,'FEET',/,
3      1X,'FRAME SPACING = ',T48,D10.5,T59,'FEET',/,
4      1X,'FRAME YOUNGS MODULUS = ',T48,D10.5,T59,'LBS/FT**2')
2006  FORMAT(1X,'ADJUST CIRCUMFERENTIAL BENDING STIFFNESS BY ',F10.
1      4,////)
      READ(5,3010)STDAMA,STDAMB,ADAMA,ADAMB,BBB
3010  FORMAT(4F15.3,F10.3)
      READ(5,1002)NST,NEND,IST,ISEND,NST,MEND,IPST,IPEND,IGST,IGEND
1002  FORMAT(10I5)
      READ(5,1003)RELAX
      WRITE(6,2006)RELAX
      READ(5,1003)TVXR,AXCDF,TVYR,AYCDF

```

STRO0500  
 STRO0510  
 STRO0540  
 STRO0550  
 STRO0640  
 STRO0660  
 STRO0670  
 STRO0680  
 STRO0700  
 STRO0710  
 STRO0720  
 STRO0730  
 STRO0740  
 STRO0750  
 STRO0760  
 STRO0770  
 STRO0780  
 STRO0790  
 STRO0800  
 STRO0810  
 STRO0820  
 STRO0830  
 STRO0840  
 STRO0850  
 STRO0860  
 STRO0870  
 STRO0880  
 STRO0890  
 STRO0900  
 STRO0910  
 STRO0920  
 STRO0930  
 STRO0940  
 STRO0950  
 STRO0960  
 STRO0970  
 STRO0980  
 STRO0990  
 STRO1000  
 STRO1010  
 STRO1020  
 STRO1030  
 STRO1040  
 STRO1050  
 STRO1060  
 STRO1070  
 STRO1080  
 STRO1090  
  
 STRO1100  
 STRO1110  
 STRO1120  
 STRO1130  
 STRO1140

```

C
C      CONVERT TO RADIANS
C      DEFINE MISCELLANEOUS CONSTANTS
C      ALFA=ALFAT*.017453292519943200
C

```

```

DENOM=ROUT
755 CONTINUE
REAC(5,1501)WOMEGI
IF(WOMEGI.LE.3.0) GO TO 800
WOMEGA=WOMEGI*2.00*PI
TOTALL=0.00
DO 40 IDX=1,4
40 POTALL(IDX)=0.00
C CHECK FOR THE HOLLOW CYLINDER CASE
IF(RIN.EQ.0.00) GO TO 5
BETA=ROUT/RIN
BETA3=BETA**3
BETA5=BETA3*BETA*BETA
DENOM=RIN
5 WSQ=WOMEGA*WOMEGA
VCRIT=.9999500
QUIT=1.00-VCRIT
CSQ=SPSND*SPSND
PIOL2=PI*PI/(SEGLTH*SEGLTH)
B2=ROUT**2
B=PIOL2*B2
SKINI=(SHLTHK**3)/48.00+SHLTHK*((FILTHK+SHLTHK)/2.00)**2
RS=FA*FSDSPL/(FA+SHLTHK*FS)
RF=FSDSPL-RS
PNUF=1.00-POISSR*POISSR
C11=ESZ*SHLTHK/PNUF
C22=(ESTH*SHLTHK+EF*FA/FS)/PNUF
D11=SKINI*ESZ/PNUF
D22=((SKINI+SHLTHK*RS*RS)*ESTH+EF*(FI+FA*RF*RF)/FS)/PNUF
DZZ=D22*RELAX
CRAT=C22/C11
DRAT=D22/D11
C=RHOM*ROUT*ROUT/C11
CK=D22/(C22*ROUT*ROUT)
A=(1.00-POISSR)/2.00
RATIO=SEGLTH/CYLNTH
PIOL4=PI*CYLNTH/4.00
RIN2=RIN**2
HFTERM=((2.00)*ROUT*CRAT)/(PI*SEGLTH*RHOM)**2
PICYL=PI/CYLNTH
PIOLL2=PICYL*PICYL
PICYLZ=PICYL*Z0
PISEG=PI/SEGLTH
PILSQ=1.00/(PISEG*(2.00/SEGLTH))
VOLUME=PI*CYLNTH*(B2-RIN2)
C THE FOLLOWING ARE USED IN ROUTINE PGJ
WOLC=(SEGLTH*WOMEGA)/SPSND
WOLCPI=WOLC/PI
CBW=SPSND/(ROUT*WOMEGA)
PICER=1.00/CBW
C
C
C CALCULATE ACOUSTIC MODES
IF(ION.EQ.5) GO TO 9927

```

```

STR01150
STR01180
STR01190
STR01200
STR01210
STR01220
STR01230
STR01240
STR01250
STR01260
STR01270
STR01280
STR01290
STR01300
STR01310
STR01320
STR01330
STR01340
STR01350
STR01360
STR01370
STR01380
STR01390
STR01400
STR01410
STR01420
STR01430
STR01440
STR01450
STR01460
STR01470
STR01480
STR01490
STR01500
STR01510
STR01520
STR01530
STR01540
STR01550
STR01560
STR01570
STR01580
STR01590
STR01600
STR01610
STR01620
STR01630
STR01640
STR01650
STR01660
STR01670
STR01680
STR01690

```

CALL AMCOES (NST,NEND,IST,ISEND,PST,MEND,ION,&900)	STR01700
C WRITE EIGENVALUES	STR01710
IF(ION.NE.2.AND.ION.NE.1) GC TO 31	STR01720
WRITE(6,2002)	STR01730
2002 FORMAT(1H,127,'EIGENVALUE RESULTS',//,3('INDICES',4X,'EIGENVALUES',4X,1,2X)//)	STR01740
KOUNT=0	STR01750
DO 30 I=1,NUMK,3	STR01760
K=I+2	STR01770
WRITE(6,2002) (KNS(J),SNK(J),J=1,K)	STR01780
2003 FORMAT(1H,3(19,2X,D10.4,1X))	STR01790
KCUNT=KCUNT+1	STR01800
IF(MOD(KOUNT,50).EQ.0) WRITE(6,2002) RIN,RCUT	STR01810
30 CONTINUE	STR01820
31 CONTINUE	STR01830
C CALCULATE STRUCTURAL MODES	STR01840
CALL SMOESC (IPST,IPFND,IWST,IGEND,ICN)	STR01850
9927 CONTINUE	STR01860
C INSURE OPPOSITE DIRECTION SEARCH NEXT TIME	STR01870
BANFAC=2.07**((1.0075AND)	STR01880
WSQB=WSQ/BANFAC	STR01890
WSQT=WSQ*BANFAC	STR01900
WSQC=WSQ	STR01910
DELTAW=DSQRT(WSQT)-DSQRT(WSQB)	STR01920
C	STR01930
C MAIN LOOP	STR01940
KTOP=0	STR01950
DO 70 K=1,NUMST	STR01960
IF(STMODS(K).GE.WSQT) GO TO 70	STR01970
IF(KTOP.EQ.0) KTOP=K	STR01980
IF(STMODS(K).LT.WSQB) GO TO 80	STR01990
70 CONTINUE	STR02000
80 KBOT=K-1	STR02010
IF(KBOT.LT.KTOP.OR.KTOP.EQ.0) GO TO 700	STR02020
DO 90 KS=KTOP,KBOT	STR02030
WSK=STMODS(KS)	STR02040
IP=MOD(MPW(KS),1000)	STR02050
IC=MPW(KS)/1000	STR02060
GRNOPP=1.070	STR02070
GRNTOT=0.00	STR02080
BIGSUM=0.00	STR02090
DO 1 IDX=1,4	STR02100
SPGTOT(IDX)=0.00	STR02110
1 BGSMT(IDX)=0.00	STR02120
CALL FRSFND(ACMODS,NUMAC,K)	STR02130
MNDIR=K	STR02140
ISAVE=IABS(MNDIR)	STR02150
10 CALL SCALC(K,M,N,&900)	STR02160
CALL MNSUM(M,N,IP,IQ,&10)	STR02170
90 CALL PCALB(KS,IP,IQ,TOTALL,PCTALL)	STR02180
C FINAL RESULT	STR02190
RHOA = 0.002380	STR02200
DUMVAR=1.00/DELTAW	STR02210
ANSWER=((CSQ*RHOA*ROUT)**2/(2.00*VOLUME))*TCTALL*DUMVAR	STR02220
	STR02230

```

IF ANSWER.LE.3.00 GO TO 801
ANSWER=10.00*DCOG1CTANSWER
ABCONT=1.0+1.0**((ANSWER/20.0)
ANSRED=ANSWER-20.0*DCOG1C(ABCONT)
WRITE(6,4999)
4999 FORMAT(1X)
WRITE(6,2004) ANSWER,WOMEG1
2004 FORMAT(2X,'***VOL AVE AMPLIFICATION = ',E10.4,' CBS FOR ',F7.1,
1' HERTZ BAND')
WRITE(6,5002) ANSRED
5002 FORMAT(1X,'VOL AVE AMP W/INTERNAL PRESSURE EFFECT = ',F6.2)
FACTOR=(CSQ*RHOA*ROUT)**2/2.00*DUNVAR
DO 50 IDX=1,4
FACPCT=FACTOR*POTALL(IDX)
IF(FACPOT.LE.0.00)FACPOT=1.0-70
50 PANSR(IDX)=10.00*DCOG1C(FACPCT)
WRITE(6,5000)
5000 FORMAT(11X,'RADIUS(FT)',8X,'LNTH COORD(FT)',8X,'PNT AMPL(CBS)')
DO 60 IDX=1,4
WRITE(6,5001) ROTHX(IDX),ZDTHR(IDX),PANSR(IDX)
5001 FORMAT(12X,F7.3,14X,F6.2,15X,E10.4)
60 CONTINUE
ION=5
GO TO 700
801 WRITE(6,805) ANSWER
805 FORMAT(' ANSWER= ',D10.4)
ION=5
GO TO 700
800 CONTINUE
STOP
C ERROR STOP
900 STOP 601
END

```

STR02240  
STR02250

STR02260  
STR02270  
STR02280  
STR02290  
STR02300

STR02310  
STR02320  
STR02330  
STR02340  
STR02350  
STR02360  
STR02370  
STR02380  
STR02390  
STR02400  
STR02410  
STR02420  
STR02430  
STR02440  
STR02450  
STR02460  
STR02470  
STR02480  
STR02490  
STR02500  
STR02510  
STR02520

ORIGINAL PAGE IS  
OF GOOD QUALITY

JUN 74 1

05:363 FCRTAN H

PILER OPTIONS - NAME= MAIN,OPT=02,LINECNT=56,SIZE=000CK,  
 SOURCE,EBCDIC,NOLIST,NODECK,LCAD,MAP,NCEDIT,ID,NCXREF  
 SUBROUTINE ACOES (NST,NEND,IST,ISEND,MST,MEND,ICN,\*)

AM000010  
 AM000020  
 AM000030  
 AM000040  
 AM000050  
 AM000060  
 AM000070  
 AM000080  
 AM000090  
 AM000100  
 AM000110  
 AM000120  
 AM000130  
 AM000140  
 AM000150  
 AM000160  
 AM000170  
 AM000180  
 AM000190  
 AM000200  
 AM000210  
 AM000220  
 AM000230  
 AM000240  
 AM000250  
 AM000260  
 AM000270  
 AM000280  
 AM000290  
 AM000300  
 AM000310  
 AM000320  
 AM000330  
 AM000340  
 AM000350  
 AM000360  
 AM000370  
 AM000380  
 AM000390  
 AM000400  
 AM000410  
 AM000420  
 AM000430  
 AM000440  
 AM000450  
 AM000460  
 AM000470  
 AM000480  
 AM000490  
 AM000500  
 AM000510  
 AM000520

```

C *****
C
C   THIS SUBROUTINE CALCULATES THE ACOUSTIC MODAL FREQUENCIES.
C   EACH FREQUENCY CALCULATED HAS THREE ASSOCIATED INDICES, M,N,IS.
C   THE FREQUENCIES SQUARED ARE CALCULATED AND PLACED IN ARRAY
C   ACMODS. THE THREE INDICES ARE PACKED INTO ONE WORD AND STORED
C   IN ARRAY MNS WITH THE SAME SUBSCRIPT AS ACMODS. ALTHOUGH THE
C   INDICES ARE PACKED IN THE ORDER M,N,IS THE CALCULATIONS ARE
C   PERFORMED IN NESTED LOOPS WITH M CIRCULATING FASTEST FOLLOWED
C   BY IS AND N. THE INDICES ALL BEGIN AT ZERO.
C *****
C
C   IMPLICIT REAL*8 (A-D,F-H,C-Z)
C   DIMENSION BUF(3),IBUF(3)
C   COMMON /CONST/PI
C   COMMON /NORMAL/DENOM
C   COMMON /VAL/SQ/CSQ,PIOL2
C   COMMON /ACUSTK/ACMODS(8000),MNS(8000),NUMAC
C   COMMON /SOLNS/SNK(400),KNS(400),NUMK
C   GO TO (100,130,230,230),ICN
C
C   INITIALIZE THE INCREMENT TEST VARIABLE FOR ROUTINE REGAL.
C   THIS VALUE OF ZERO IS PASSED THROUGH RCOT TO REGAL FOR
C   USE THE FIRST TIME REGAL IS CALLED.
C   100 XNS=J.DC
C       CRITH=1.030
C       I=1
C       J=1
C
C   LOOP OVER THREE MODAL INDICES
C
C   NOTE THAT THE DEGENERATE CASE OF M=0,N=0,IS=0 WHICH PRODUCES
C   W2MNS=0 IS ELIMINATED THROUGH THE USE OF CRITH WHICH IS
C   ALWAYS GREATER THAN ZERO.
C   10 N=NST
C   11 IS=IST
C   FIND THE NS TH EIGENVALUE
C   12 CALL ROOT (N,IS,XNS,ESC)
C   NORMALIZE THE EIGENVALUE FOR CLR USE
C   XNSSQ=(XNS/DENOM)**2
C   M=MST
C
C   CALCULATE MODAL FREQUENCY SQUARED AND CHECK IF IT WILL BE OF
C   CONSEQUENCE
C   16 W2MNS=CSQ*(XNSSQ+M*M*PIOL2)
C   IF(W2MNS.GT.CRITH) GO TO 21
C
C   SAVE FREQUENCY SQUARED AND PACKED INDICES
C   ACMODS(I)=W2MNS
C   IWORD=N*1000+IS
C   MNS(I)=M*100000+IWORD
C   I=I+1

```



20 M=M+1	AM000530
IF(M.GT.MEND) GO TO 22	AM000540
GO TO 16	AM000550
C IF M=MST HERE THE NS TH EIGENVALUE WAS NOT USED AND	AM000560
C SHOULD NOT BE SAVED	AM000570
21 IF(M.EQ.MST) GO TO 26	AM000580
C SAVE EIGENVALUES AND PACKED INDICES	AM000590
22 IF((IS.EQ.IST).AND.(N.EQ.NST))CRITH=M2MNS	AM000600
SNK(J)=XNS	AM000610
KNS(J)=IWORD	AM000620
J=J+1	AM000630
GO TO 27	AM000640
C REDEFINE MAXIMUM IS VALUE. IF THE M LOOP HAS KICKED OUT CN	AM000650
C THE FIRST VALUE OF M THEN THE VALUE OF IS AT THAT POINT IS THE	AM000660
C MAXIMUM VALUE OF IS WE NEED TO LOOK AT IN FURTHER ITERATIONS.	AM000670
26 ISEND=IS	AM000680
27 IS=IS+1	AM000690
IF(IS.GT.ISEND) GO TO 30	AM000700
GO TO 12	AM000710
30 N=N+1	AM000720
IF(N.GT.NEND) GO TO 31	
GO TO 11	AM000740
C NUMBER OF ACOUSTIC MODAL FREQUENCIES AND EIGENVALUES	AM000750
31 NUMAC=I-1	AM000760
NUMK=J-1	AM000770
CALL SORTTACMODS,MNS,NUMAC	AM000780
WRITE(1,250)NST,NEND,IST,ISEND,MST,MEND,NUMAC,NUMK	AM000790
NRC1=NUMAC/5	AM000800
IF(NRC1*5.LT.NUMAC)NRC1=NRC1+1	AM000810
DO 60 JJJ=1,NRC1	AM000820
IND1=5*(JJJ-1)+1	AM000830
IND2=IND1+4	AM000840
IF(IND2.GT.NUMAC)IND2=NUMAC	AM000850
WRITE(1,250)(MNS(III),III=IND1,IND2)	AM000860
WRITE(1,350)(ACMODS(III),III=IND1,IND2)	AM000870
60 CONTINUE	AM000880
NRC1=NUMK/5	AM000890
IF(NRC1*5.LT.NUMK)NRC1=NRC1+1	AM000900
DO 61 JJJ=1,NRC1	AM000910
IND1=5*(JJJ-1)+1	AM000920
IND2=IND1+4	AM000930
IF(IND2.GT.NUMK)IND2=NUMK	AM000940
WRITE(1,250)(KNS(III),III=IND1,IND2)	AM000950
WRITE(1,350)(SNK(III),III=IND1,IND2)	AM000960
61 CONTINUE	AM000970
250 FORMAT(8I10)	AM000980
350 FORMAT(50I6,10)	AM000990
C WRITE STRUCTURAL MODE FREQUENCIES	AM001000
TWOPI=2.0*PI	AM001010
WRITE(6,2500)	AM001020
2500 FORMAT(1H1,T18,'ACOUSTIC MODAL FREQUENCIES AND INDICES'	AM001030
1 /,,/, 3('INDICES',3X,'FREQUENCIES',3X),,,)	AM001040
KOUNT=0	AM001050
DO 40 I=1,NUMAC,3	AM001060

```

      K=I+2
C      WRITE FREQUENCIES IN HERTZ
      L=1
      DO 35 J=1,K
        BUF(L)=DSQRT(ACMODS(J))/TWOP
        IBUF(L)=MNS(J)
      35 L=L+1
      WRITE(6,2301) (TBUF(J),BLF(J),J=1,3)
2001  FORMAT(1H,3(19,3X,F8.1,4X))
      KOUNT=KOUNT+1
      IF(MOD(KOUNT,5).EQ.0) WRITE(6,2000)
4)  CONTINUE
      RETURN
200  READ(1,255)INST,NEND,TST,ISEND,MST,MEND,NUMAC,NUMK
      NRC1=NUMAC/5
      IF(NRC1*5.LT.NUMAC)NRC1=NRC1+1
      DO 70 JJJ=1,NRC1
        IND1=5*(JJJ-1)+1
        IND2=IND1+4
        IF(IND2.GT.NUMAC)IND2=NUMAC
        REAC(1,250)(MNS(III),III=IND1,IND2)
        READ(1,350)(ACMODS(III),III=IND1,IND2)
70  CONTINUE
      NRC1=NUMK/5
      IF(NRC1*5.LT.NUMK)NRC1=NRC1+1
      DO 71 JJJ=1,NRC1
        IND1=5*(JJJ-1)+1
        IND2=IND1+4
        IF(IND2.GT.NUMK)IND2=NUMK
        REAC(1,250)(KNS(III),III=IND1,IND2)
        READ(1,350)(SNK(III),III=IND1,IND2)
71  CONTINUE
      RETURN
57  RETURN 1
      END

```

```

AM001070
AM001080
AM001090
AM001100
AM001110
AM001120
AM001130
AM001140
AM001150
AM001160
AM001170
AM001180
AM001190
AM001200
AM001210
AM001220
AM001230
AM001240
AM001250
AM001260
AM001270
AM001280
AM001290
AM001300
AM001310
AM001320
AM001330
AM001340
AM001350
AM001360
AM001370
AM001380
AM001390
AM001400
AM001410

```

JUN 74 )

05/360 FORTRAN H

PILER OPTIONS - NAME= MAIN,OPT=02,LINECT=56,SIZE=CCOCK,  
SOURCE,EBCDIC,NOLIST,NODECK,LCAD,MAP,NCEDIT,ID,NCXREF  
SUBROUTINE BESSEL (N,XX,BLJ,BLY)

```

C *****
C
C THIS ROUTINE DECIDES AND CONTROLS WHICH METHOD WILL BE USED TO
C CALCULATE THE BESSEL AND NEUMANN FUNCTIONS. THE SAME CRITERIA
C IS USED FOR BOTH. FOR ARGUMENTS GREATER THAN TEN, THE
C ASYMPTOTIC SERIES TECHNIQUE IS USED. THE ASYMPTOTIC SERIES IS
C FOLLOWED BY A RECURSION PROCEDURE IF THE ORDER SPECIFIED IS
C GREATER THAN EIGHT. FOR SMALLER ARGUMENTS THE ACTUAL SERIES
C DEFINITIONS OF THE FUNCTIONS ARE USED. THIS TECHNIQUE IS USED
C FOR ORDERS UP TO 55. ABOVE THAT THE VALUES FOR SMALL ARGUMENTS
C (LESS THAN 10) ARE DEFINED TO BE ZERO AND NEGATIVE INFINITY.
C THE RECURSION PROCEDURE MAY NOT WORK IF THE TECHNIQUE IS USED
C TO FIND A RESULT WHICH SHOULD BE LESS THAN 1.-10 IN ABSOLUTE
C VALUE DUE TO SUCCESSIVE ROUND-OFF ERRORS.
C *****
C
C IMPLICIT REAL*8 (A-D,F-H,O-Z)
C COMMON /CONST/PI
C COMMON /RADII/RIN,ROUT
C
C ASYMPTOTIC SERIES EXPRESSIONS
C BSLY(TOTP,TOTQ,ARG)=DSQRT(2.0C/(PI*XX))*(TCTP*DSIN(ARG)
1 +TOTQ*DCOS(ARG))
C BSLJ(TOTP,TOTQ,ARG)=DSQRT(2.0C/(PI*XX))*(TCTP*DCOS(ARG)
1 -TOTQ*DSIN(ARG))
C
C IF(XX.GT.10.00) GO TO 10
C IF(N.GT.55) GO TO 30
C USE ACTUAL SERIES DEFINITIONS
C CALL BLJDEF(N,XX,BLJ)
C NO NEED TO CALCULATE NEUMANN FUNCTIONS FOR HOLLOW CYLINDER CASE
C IF(RIN.EQ.0.00) RETURN
C CALL BLYDEF(N,XX,BLJ,BLY)
C RETURN
1) IF(N.GT.8) GO TO 20
C USE ASYMPTOTIC SERIES
C CALL PSQS(N,XX,TOTP,TOTQ,ARG)
C BLJ=BSLJ(TOTP,TOTQ,ARG)
C CHECK HOLLOW CYLINDER CASE
C IF(RIN.EQ.0.00) RETURN
C BLY=BSLY(TOTP,TOTQ,ARG)
C RETURN
C USE ASYMPTOTIC SERIES THEN RECURSION
2) CALL PSQS(8,XX,TOTP,TOTQ,ARG)
C BLJN=BSLJ(TOTP,TOTQ,ARG)
C CHECK HOLLOW CYLINDER CASE
C IF(RIN.EQ.0.00) GO TO 25
C BLYN=BSLY(TOTP,TOTQ,ARG)
C CALL PSQS(7,XX,TOTP,TOTQ,ARG)

```

BES00010  
 BES00020  
 BES00030  
 BES00040  
 BES00050  
 BES00060  
 BES00070  
 BES00080  
 BES00090  
 BES00100  
 BES00110  
 BES00120  
 BES00130  
 BES00140  
 BES00150  
 BES00160  
 BES00170  
 BES00180  
 BES00190  
 BES00200  
 BES00210  
 BES00220  
 BES00230  
 BES00240  
 BES00250  
 BES00260  
 BES00270  
 BES00280  
 BES00290  
 BES00300  
 BES00310  
 BES00320  
 BES00330  
 BES00340  
 BES00350  
 BES00360  
 BES00370  
 BES00380  
 BES00390  
 BES00400  
 BES00410  
 BES00420  
 BES00430  
 BES00440  
 BES00450  
 BES00460  
 BES00470  
 BES00480  
 BES00490  
 BES00500  
 BES00510  
 BES00520

BLJNM1=BSLJ(TOTP,TOTQ,ARG)  
BLYNM1=BSLY(TOTP,TOTQ,ARG)  
CALL RECUR(N,XX,BLJN,BLJNM1,BLJ)  
CALL RECUR(N,XX,BLYN,BLYNM1,BLY)  
RETURN

C HOLLOW CYLINDER CASE HERE  
25 CALL PSQS(7,XX,TOTP,TOTQ,ARG)  
BLJNM1=BSLJ(TOTP,TOTQ,ARG)  
CALL RECUR(N,XX,BLJN,BLJNM1,BLJ)  
RETURN  
30 BLJ=0.00  
BLY=-1.075  
RETURN  
END

BES00530  
BES00540  
BES00550  
BES00560  
BES00570  
BES00580  
BES00590  
BES00600  
BES00610  
BES00620  
BES00630  
BES00640  
BES00650  
BES00660

JUN 74 )

OS/360 FORTRAN H

DA

PILER OPTIONS - NAME= MAIN,OPT=02,LINECNT=56,SIZE=C000K,  
 SOURCE,EBCDIC,NOLIST,NODECK,LCAC,MAP,NCEDIT,IC,NCXREF  
 SUBROUTINE BLJDEF (N,X,BLJ)

C		C	BLJ00010
C	*****	C	BLJ00020
C		C	BLJ00030
C		C	BLJ00040
C	THIS ROUTINE CALCULATES THE BESSEL FUNCTION USING THE ACTUAL	C	BLJ00050
C	SERIES DEFINITION FOR ARGUMENTS LESS THAN OR EQUAL TO TEN.	C	BLJ00060
C		C	BLJ00070
C	*****	C	BLJ00080
C		C	BLJ00090
	IMPLICIT REAL*8 (A-D,F-H,C-Z)		BLJ00100
	COMMON /CONV/UP,DN		BLJ00110
	COMMON /FCTRL/FAC(57),PSI(60)		BLJ00120
C			BLJ00130
C	IF(X.EQ.0.00) GO TO 30		BLJ00140
C	WATCH LIMITS OF STORED FACTORIALS		BLJ00150
	Z=1.00		BLJ00170
	M=57-N		BLJ00160
	M=57-N		BLJ00160
	Z=1.00		BLJ00170
	ZZ=X*X		BLJ00180
	SUM=0.00		BLJ00190
	TOTAL=0.00		BLJ00200
	EJ=1.		BLJ00210
	DO 10 I=1,M		BLJ00220
	K=I-1		BLJ00230
	VAR=2.00**((2*K+N)		BLJ00240
	TOTAL=SUM+EJ*Z/FAC(I)/FAC(I+N)/VAR		BLJ00250
	IF(TOTAL.EQ.0.00) GO TO 5		BLJ00260
C	CHECK CONVERGENCE		BLJ00270
	VAL=SUM/TOTAL		BLJ00280
	IF(VAL.GT.DN.AND.VAL.LT.UP) GO TO 20		BLJ00290
5	EJ=-EJ		BLJ00300
	Z=Z*ZZ		BLJ00310
	SUM=TOTAL		BLJ00320
10	CONTINUE		BLJ00330
20	BLJ=X*N*TOTAL		BLJ00340
	RETURN		BLJ00350
30	IF(N.GT.0) GO TO 40		BLJ00360
	BLJ=1.00		BLJ00370
	RETURN		BLJ00380
40	BLJ=0.00		BLJ00390
	RETURN		BLJ00400
	END		BLJ00410

ORIGINAL PAGE IS  
 OF POOR QUALITY

JUN 74 1

05/269 FORTRAN H

DA

PILER OPTIONS - NAME= MAIN,OPT=C2,LINECNT=56,SIZE=3000K,  
 SOURCE,EBCDIC,NOLIST,NODECK,LCAC,MAP,NOEDIT,IO,NOXREF  
 SUBROUTINE BLYDEF (N,X,BLJ,BLY)

C		C	BLY00010
C	*****	C	BLY00020
C		C	BLY00030
C		C	BLY00040
C	THIS ROUTINE CALCULATES THE NEUMANN FUNCTION USING THE	C	BLY00050
C	ACTUAL SERIES DEFINITION FOR ARGUMENTS LESS THAN OR EQUAL TO 10	C	BLY00060
C		C	BLY00070
C	*****	C	BLY00080
C		C	BLY00090
	IMPLICIT REAL*8 (A-D,F-H,C-Z)		BLY00100
	COMMON /CONST/PI		BLY00110
	COMMON /CONV/UP,DN		BLY00120
	COMMON /FCTRL/FAC(57),PSI(60)		BLY00130
C			BLY00140
	IF(X.EQ.0.D0) GO TO 50		BLY00150
	TOTAL=0.D0		BLY00160
	CUM=0.D0		BLY00170
	SUM=0.D0		BLY00180
	Z=X*X/4.D0		BLY00190
	IF(N.EQ.0) GO TO 15		BLY00200
	ZZ=1.D0		BLY00210
	DO 10 I=1,N		BLY00220
	DIV=FAC(N-I+1)/FAC(I)		BLY00230
	CUM=CUM+DIV*ZZ		BLY00240
	ZZ=ZZ*Z		BLY00250
10	CONTINUE		BLY00260
15	ZZ=1.D0		BLY00270
	EJ=1.		BLY00280
	M=57-N		BLY00290
	DO 30 I=1,M		BLY00300
	DIV=ZZ/FAC(I)		BLY00310
	TOTAL=SUM+(PSI(I)+PSI(I+N))*EJ*DIV/FAC(I+N)		BLY00320
	IF(TOTAL.EQ.0.D0) GO TO 20		BLY00330
C	CHECK CONVERGENCE		BLY00340
	VAL=SUM/TOTAL		BLY00350
	IF(VAL.GT.DN.AND.VAL.LT.UP) GO TO 40		BLY00360
20	EJ=-EJ		BLY00370
	ZZ=ZZ*Z		BLY00380
	SUM=TOTAL		BLY00390
30	CONTINUE		BLY00400
40	DIV=((2.D0/X)**N)/PI		BLY00410
	BLY=(-DIV)*CUM+(2.D0/PI)*DLOG(X/2.D0)*BLJ-(((X/2.D0)**N)/PI)*TOTAL		BLY00420
	RETURN		BLY00430
50	BLY=-1.D75		BLY00440
	RETURN		BLY00450
60	BLY=1.D75		BLY00460
	RETURN		BLY00470
	END		BLY00480

JUN 74 )

OS/360 FORTRAN H

IMPIER OPTIONS - NAME= MAIN,OPT=02,LINECNT=56,SIZE=0000K,  
 SOURCE,EBCDIC,NOLIST,NODECK,LCAD,MAP,NOEDIT,IO,NCXREF  
 FUNCTION CAPGAM (N,IQ)

```

C
C*****C
C
C  ACCEPTANCE SQUARED IN THE CIRCUMFERENTIAL DIRECTION.
C  THIS SUBROUTINE COMPUTES THE STRUCTURAL TO ACOUSTIC
C*****C
C
  IMPLICIT REAL*8 (A-D,F-H,C-Z)
  COMMON /ACCEPT/ALFA
  COMMON/ CONST/PI
  BN = FLOAT(N)
  QPI = PI*FLOAT(IQ)
  QPIA = QPI/ALFA
  IF(DABS(BN-QPIA).GT.1.D-2) GO TO 10
  CAPGAM=ALFA/2.D0
  GO TO 20
10  TSTANG=QPI+ALFA*BN
  ANGUM=DMOD(TSTANG,PI*2.D0)
  IF(ANGUM.LT.1.D-2.OR.(PI*2.D0-ANGUM).LT.1.D-2)GO TO 30
  PHIJ=-ALFA/2.D0
  IF((IQ/2)*2.EQ.IQ.AND.N.NE.C)PHIO=PHIJ+PI/(BN*2.D0)
  IF(DABSDMOD(BN*PHIJ,PI)-PI/2.D0).LT.1.D-2)GO TO 30
  CAPGAM=(DCOS(BN*PHIO)-DCOS(QPI+BN*(PHIO+ALFA)))/(QPIA+BN)
  I  +DCOS(BN*PHIO)-DCOS(QPI-BN*(PHIO+ALFA)))/(QPIA-BN)
  CAPGAM=CAPGAM/2.D0
20  CAPGAM = CAPGAM**2
  RETURN
30  CAPGAM=1.D0
  RETURN
  END

```

CAP00010  
 CAP00020  
 CAP00030  
 CAP00040  
 CAP00060  
 CAP00050  
 CAP00070  
 CAP00080  
 CAP00090  
 CAP00100  
 CAP00110  
 CAP00120  
 CAP00130  
 CAP00140  
 CAP00150  
 CAP00160  
 CAP00170  
 CAP00180  
 CAP00190  
 CAP00200  
 CAP00210  
 CAP00220  
 CAP00230  
 CAP00240  
 CAP00250  
 CAP00260  
 CAP00270  
 CAP00280  
 CAP00290  
 CAP00300  
 CAP00310  
 CAP00320

JUN 74 )

05/360 FCRTRAN H

IMPIER OPTIONS - NAME= MAIN,OPT=02,LINECNT=56,SIZE=000CK,  
 SOURCE,EBCDIC,NOLIST,NODECK,LCAD,MAP,ACEDIT,ID,NCXREF  
 SUBROUTINE COPYC (N)

C		C	COP00010
C	*****	C	COP00020
C		C	CCP00030
C		C	COP00040
C	THIS SUBROUTINE COPIES STRUCTURAL MODES STMCDS AND INCICES	C	COP00050
C	MPQ INTO TEMPORARY ARRAYS FROM WHICH THEY ARE CROSSED OUT AS	C	COP00060
C	THEY ARE USED. THIS ROUTINE IS USED BY MAIN PROGRAMS 'PURTCN'	C	COP00070
C	AND 'ACCBAN'.	C	CCP00080
C		C	COP00090
C	*****	C	COP00100
C		C	COP00110
	IMPLICIT REAL*8 (A-D,F-H,C-Z)		COP00120
	COMMON /SAMPLE/TEMP(1200),LPQS(1200),NUMTMP		COP00130
	COMMON /STRUCT/STMODS(1200),MPQ(1200),STMOD3(400,3),MPQ3(400),		COP00140
1	NUMST,NUM3		CCP00150
C			COP00160
	DO 10 I=1,NUMST		COP00170
	TEMP(I)=STMODS(I)		COP00180
	LPQS(I)=MPQ(I)		COP00190
10	CONTINUE		COP00200
C	NUMBER OF ELEMENTS IN TEMP ARRAY		COP00210
	NUMTMP = NUMST		CCP00220
	RETURN		COP00230
	END		COP00240



JUN 74 )

GS/36J FORTRAN M

IMPIER OPTIONS - NAME= MAIN,OPT=02,LINECNT=56,SIZE=0000K,  
SOURCE,EBCDIC,NOLIST,NODECK,LCAD,MAP,NCEDIT,ID,NCXREF

```
SUBROUTINE CUBIC(X,P,Q,R,*)  
  IMPLICIT REAL*8(A-D,F-H,Q-Z)  
  DIMENSION X(3)  
  DATA PI/3.14159265358973900/  
  A=Q-P*P/3.00  
  B=(2.00)*P**3-9.00*P*Q+27.00*R)/27.00  
  IF((B**2/4.00+A**3/27.00).GT.0.00) GO TO 10  
  RTA3=DSQRT(-A/3.00)  
  PHI=DARCCOS(-B/(2.00*DSQRT(-A**3/27.00)))  
  X(1)=2.00*RTA3*DCOS(PHI/3.00)-P/3.00  
  X(2)=2.00*RTA3*DCOS(PHI/3.00+2.00*PI/3.00)-P/3.00  
  X(3)=2.00*RTA3*DCOS(PHI/3.00+4.00*PI/3.00)-P/3.00  
  RETURN  
10 WRITE(7,100)  
100 FORMAT(1X,'IMAGINARY ROOTS')  
  RETURN 1  
END
```

CUB00010  
CUB00020  
CUB00030  
CUB00040  
CUB00050  
CUB00060  
CUB00070  
CUB00080  
CUB00090  
CUB00100  
CUB00110  
CUB00120  
CUB00130  
CUB00140  
CUB00150  
CUB00160  
CUB00170



*	0.31135575853157400+01,	0.31570758461853050+01,	DAT00530
*	0.31987425128519720+01,	0.32387425128519720+01,	DAT00540
*	0.32772040513135100+01,	0.33142410883505470+01,	DAT00550
*	0.33495553740648330+01,	0.33844381326855220+01/	DAT00560
	DATA PSI2/0.341777146601885501,0.345002953053498401,		DAT00570
*	0.34812795305349840+01,	0.35115825608380150+01,	CAT00580
*	0.35409943255438970+01,	0.35695657541153250+01,	CAT00590
*	0.35973435318931030+01,	0.36243705589201300+01,	DAT00600
*	0.36506863483938140+01,	0.36763273740348400+01,	CAT00610
*	0.37013273740348400+01,	0.37257176179372780+01,	DAT00620
*	0.37495271417468020+01,	0.3772782955702500+01,	CAT00630
*	0.37955102284275630+01,	0.38177324506497850+01,	CAT00640
*	0.38394715810845680+01,	0.38607481768292480+01,	CAT00650
*	0.38815815101625820+01,	0.39019896734278880+01,	DAT00660
*	0.39219896734278870+01,	0.39415975165651420+01,	CAT00670
*	0.39608282857959110+01,	0.39796962103242130+01,	DAT00680
*	0.39982147288427320+01,	0.40163965470245500+01,	CAT00690
*	0.40342536898816930+01,	0.40517975495338150+01,	DAT00700
*	0.40650385288411600+01,	0.40859880813835330+01/	DAT00710
			CAT00720

END

ORIGINAL PAGE IS  
OF POOR QUALITY

JUN 74 )

OS/360 FORTRAN H

IMPIER OPTIONS - NAME= MAIN,OPT=02,LINECNT=56,SIZE=0000K,  
 SOURCE,EBCDIC,NOLIST,NCDECK,LCAD,MAP,NCEDIT,IO,NCXREF  
 FUNCTION DOB (N,RK)

```

C *****
C
C FUNCTION DOB EVALUATES THE EIGENVALUE EQUATION, WHICH IS THE
C EQUATION OF THE CROSS PRODUCT OF THE DERIVATIVES OF THE
C BESSEL AND NEUMANN FUNCTIONS. THE SIMPLE DERIVATIVE OF J(X) IS
C ALSO HANDLED FOR THE HOLLOW CYLINDER CASE.
C *****
C
C IMPLICIT REAL*8 (A-D,F-H,C-Z)
C COMMON /EIGEN/BETA,BETA3,BETA5
C COMMON /RADII/RIN,ROUT
C
C   AKN=N/RK
C   USE THE RECURSION RELATION TO FIND THE DERIVATIVES
C   CALL BESSEL (N,RK,AKJN,AKYN)
C   CALL BESSEL (N+1,RK,AKJNP1,AKYNP1)
C   CHECK FOR THE HOLLOW CYLINDER CASE
C   IF (RIN.EQ.0.D0) GO TO 1C
C   BK=RK*BETA
C   BKN=N/BK
C   CALL BESSEL (N,BK,BKJN,BKYN)
C   CALL BESSEL (N+1,BK,BKJNP1,BKYNP1)
C   EVALUATE EIGENVALUE EQUATION
C   DOB=(AKN*AKJN-AKJNP1)*(BKN*BKYN-BKYNP1)-(BKN*BKJN-BKJNP1)*
C   (AKN*AKYN-AKYNP1)
C   RETURN
1C DOB=AKN*AKJN-AKJNP1
C   RETURN
C   END

```

```

00800010
00800020
00800030
00800040
00800050
00800060
00800070
00800080
00800090
00800100
00800110
00800120
00800130
00800140
00800150
00800160
00800170
00800180
00800190
00800200
00800210
00800220
00800230
00800240
00800250
00800260
00800270
00800280
00800290
00800300
00800310
00800320

```

( JUN 74 )

OS/360 FORTRAN H

IMPIER OPTIONS - NAME= MAIN,OPT=02,LINECNT=56,SIZE=000CK,  
SOURCE,EBCDIC,NOLIST,NODECK,LCAD,PAP,ACEDIT,IC,NOXREF  
SUBROUTINE FNDNST (L,K,I,ISAVE,N,IA,NUM,\*,\*)

```
C *****
C
C THIS SUBROUTINE SEARCHES THE INPLT IA ARRAY FOR THE 'NEXT'
C REQUESTED VALUE. THIS NEXT VALUE MAY BE EITHER IN THE UPWARDS
C (DECREASING SUBSCRIPT) OR DOWNWARDS (INCREASING SUBSCRIPT)
C DIRECTION. THE INPUT IA ARRAY IS THE ARRAY OF INDICES FOR THE
C MODAL FREQUENCIES. THIS ROUTINE IS USED IN 'PCALCC', CALLED
C BY MAIN PROGRAMS 'PURTON' AND 'ACOBAN'.
C *****
C
C IMPLICIT REAL*8 (A-D,F-H,O-Z)
C DIMENSION IA(1)
C COMMON /ERRCR/LAST
C
C SAVE CURRENT INDEX
C LAST=I
C L*K LESS THAN ZERO MEANS PROCEED IN DOWNWARDS DIRECTION
C IF((L*K).LT.0) GO TO 30
C IF OPPOSITE DIRECTION, START AT INDEX LOCATION WE LAST USED
C IN THAT DIRECTION.
C IF(L.EQ.-1) I=ISAVE
C KK=I-1
C IF(KK.LT.1) GO TO 15
C SEARCH FOR MATCHING FIRST TWO (OR ONE) MODAL INDEX
C IN UPWARDS DIRECTION
C DO 10 II=1, KK
C J=KK-II+1
C IF(IA(J).NE.999999) GO TO 20
10 CONTINUE
15 CONTINUE
C IF(KK.LT.1.AND.L.EQ.-1) ISAVE=LAST
C RETURN 2
C IF OPPOSITE DIRECTION SAVE INDEX OF OTHER DIRECTION
20 IF(L.EQ.-1) ISAVE=LAST
C K=J
C I=J
C RETURN 1
C DOWNWARDS DIRECTION
30 JJ=I+1
C IF OPPOSITE DIRECTION START AT SAVED INDEX+1
C IF(L.EQ.-1) JJ=ISAVE+1
C IF(JJ.GT.NUM) GO TO 45
C DO 40 II=JJ, NUM
C IF(IA(II).NE.999999) GO TO 50
40 CONTINUE
45 CONTINUE
C IF(JJ.GT.NUM.AND.L.EQ.-1) ISAVE=LAST
C RETURN 2
50 IF(L.EQ.-1) ISAVE=LAST
```

FND00010  
FND00020  
FND00030  
FND00040  
FND00050  
FND00060  
FND00070  
FND00080  
FND00090  
FND00100  
FND00110  
FND00120  
FND00130  
FND00140  
FND00150  
FND00160  
FND00170  
FND00180  
FND00190  
FND00200  
FND00210  
FND00220  
FND00230  
FND00240  
FND00250  
FND00260  
FND00270  
FND00280  
FND00290  
FND00300  
FND00310  
FND00320  
FND00330  
FND00340  
FND00350  
FND00360  
FND00370  
FND00380  
FND00390  
FND00400  
FND00410  
FND00420  
FND00430  
FND00440  
FND00450  
FND00460  
FND00470  
FND00480  
FND00490  
FND00500  
FND00510  
FND00520

K=-11  
I=11  
RETURN 1  
END

FND00530  
FND00540  
FND00550  
FND00560

( JUN 74 )

05/360 FCRTAN H

IMPILER OPTIONS - NAME= MAIN,OPT=02,LINECNT=56,SIZE=C000K,  
SOURCE,EBCDIC,NOLIST,NODECK,LCAD,MAP,NCEDIT,IO,NCXREF  
SUBROUTINE FNDNXT (L,K,I,ISAVE,N,IA,NLM,\*,\*)

```
C *****
C
C THIS SUBROUTINE SEARCHES THE INPUT IA ARRAY FOR THE 'NEXT'
C REQUESTED VALUE. THIS NEXT VALUE MAY BE EITHER IN THE UPWARDS
C (DECREASING SUBSCRIPT) OR DOWNWARDS (INCREASING SUBSCRIPT)
C DIRECTION. THE INPUT IA ARRAY IS THE ARRAY OF INDICES FOR THE
C MODAL FREQUENCIES. THIS ROUTINE IS USED BY MAIN PROGRAMS
C 'FURTON' AND 'ACOBAN'.
C *****
C
C IMPLICIT REAL*8 (A-D,F-H,C-Z)
C DIMENSION IA(1)
C COMMON /ERROR/LAST
C
C SAVE CURRENT INDEX
C LAST=I
C L*K LESS THAN ZERO MEANS PROCEED IN DOWNWARDS DIRECTION
C IF((L*K).LT.0) GO TO 30
C IF OPPOSITE DIRECTION, START AT INDEX LOCATION WE LAST USED
C IN THAT DIRECTION.
C IF(L.EQ.-1) I=ISAVE
C KK=I-1
C IF(KK.LT.1) GO TO 15
C SEARCH FOR MATCHING FIRST TWO (OR ONE) MODAL INDEX
C IN UPWARDS DIRECTION
C DO 1) II=1, KK
C J=KK-II+1
C ITST=IA(J)/1000
C IF(ITST.EQ.N) GO TO 20
10 CONTINUE
15 CONTINUE
C IF(KK.LT.1.AND.L.EQ.-1) ISAVE=LAST
C RETURN 2
C IF OPPOSITE DIRECTION SAVE INDEX OF OTHER DIRECTION
2) IF(L.EQ.-1) ISAVE=LAST
C K=J
C I=J
C RETURN 1
C DOWNWARDS DIRECTION
3) JJ=I+1
C IF OPPOSITE DIRECTION START AT SAVED INDEX+1
C IF(L.EQ.-1) JJ=ISAVE+1
C IF(JJ.GT.NUM) GO TO 45
C DO 4) II=JJ, NUM
C ITST=IA(II)/1000
C IF(ITST.EQ.N) GO TO 50
40 CONTINUE
45 CONTINUE
C IF(JJ.GT.NUM.AND.L.EQ.-1) ISAVE=LAST
```

FND00010  
FND00020  
FND00030  
FND00040  
FND00050  
FND00060  
FND00070  
FND00080  
FND00090  
FND00100  
FND00110  
FND00120  
FND00130  
FND00140  
FND00150  
FND00160  
FND00170  
FND00180  
FND00190  
FND00200  
FND00210  
FND00220  
FND00230  
FND00240  
FND00250  
FND00260  
FND00270  
FND00280  
FND00290  
FND00300  
FND00310  
FND00320  
FND00330  
FND00340  
FND00350  
FND00360  
FND00370  
FND00380  
FND00390  
FND00400  
FND00410  
FND00420  
FND00430  
FND00440  
FND00450  
FND00460  
FND00470  
FND00480  
FND00490  
FND00500  
FND00510  
FND00520

ORIGINAL PAGE IS  
OF POOR QUALITY

RETURN 2  
50 IF(L.EQ.-1) ISAVE=LAST  
K=-11  
I=11  
RETURN 1  
END

FND00530  
FND00540  
FND00550  
FND00560  
FND00570  
FND00580

ORIGINAL PAGE IS  
OF POOR QUALITY



( JUN 74 )

OS/360 FCRTAN H

MPILER OPTIONS - NAME= MAIN,OPT=02,LINECNT=56,SIZE=0000K,  
 SOURCE,ESCDTC,NCLIST,NCOECK,LCAD,MAP,ACEDIT,IO,NOXREF  
 SUBROUTINE FRSFND (A,NSIZE,K)

C		C	FRS00010
C	*****	C	FRS00020
C		C	FRS00030
C		C	FRS00040
C	THIS ROUTINE IS USED TO FIND THE MODAL FREQUENCY IN THE INPUT	C	FRS00050
C	ARRAY WHICH IS NUMERICALLY CLOSEST TO THE EXTERIOR EXCITATION	C	FRS00060
C	FREQUENCY. THE VALUE RETURNED IS THE INDEX OF THE LOCATION	C	FRS00070
C	IN THE ASSOCIATED INDICIES ARRAY. THE RETURN VALUE IS GIVEN	C	FRS00080
C	A NEGATIVE SIGN IF THE NEXT CLOSEST VALUE IS IN THE UPWARDS	C	FRS00090
C	DIRECTION (DECREASING SUBSCRIPT) OR A POSITIVE SIGN IF THE	C	FRS00100
C	NEXT CLOSEST VALUE IS IN THE DOWNWARDS DIRECTION (INCREASING	C	FRS00110
C	SUBSCRIPT).	C	FRS00120
C	*****	C	FRS00130
C		C	FRS00140
C		C	FRS00150
C	IMPLICIT REAL*8 (A-D,F-H,C-Z)	C	FRS00160
C	DIMENSION A(1)	C	FRS00170
C	COMMON /FREQ/WSQ	C	FRS00180
C		C	FRS00190
C	NUM = CLOSEST EVEN NUMBER TO NSIZE	C	FRS00200
C	NUM=(NSIZE/2)*2	C	FRS00210
C	SEARCH TWO AT A TIME	C	FRS00220
C	DO 10 I=1,NUM,2	C	FRS00230
C	IF(A(I).GT.WSQ.AND.A(I+1).GT.WSQ) GO TO 10	C	FRS00240
C	IF THE CRITERIA IS SATISFIED THE FIRST TIME START	C	FRS00250
C	AT THE TOP OF THE ARRAY	C	FRS00260
C	IF(1.EQ.1) GO TO 70	C	FRS00270
C	FIND DISTANCE TO FREQUENCY (I)	C	FRS00280
C	TST1=DABS(WSQ-A(I))	C	FRS00290
C	IF(A(I).GT.WSQ) GO TO 30	C	FRS00300
C	GO TO 20	C	FRS00310
C	10 CONTINUE	C	FRS00320
C	START AT BOTTOM OF ARRAY	C	FRS00330
C	GO TO 80	C	FRS00340
C	FIND DISTANCE TO FREQUENCY BELOW	C	FRS00350
C	20 TST2=DABS(WSQ-A(I+1))	C	FRS00360
C	IF(TST1-TST2) 40,50,50	C	FRS00370
C	FIND DISTANCE TO FREQUENCY ABOVE	C	FRS00380
C	30 TST2=DABS(WSQ-A(I+1))	C	FRS00390
C	IF(TST2-TST1) 60,70,70	C	FRS00400
C	DEFINE INDEX AND SIGN	C	FRS00410
C	40 K=-1	C	FRS00420
C	RETURN	C	FRS00430
C	50 K=I-1	C	FRS00440
C	RETURN	C	FRS00450
C	60 K=-(I+1)	C	FRS00460
C	RETURN	C	FRS00470
C	70 K=I	C	FRS00480
C	RETURN	C	FRS00490
C	80 K=NSIZE	C	FRS00500
C	RETURN	C	FRS00510
C	END	C	FRS00520

( JUN 74 )

OS/360 FORTRAN H

JMPILER OPTIONS - NAME= MAIN,OPT=02,LINECNT=56,SIZE=0000K,  
SOURCE,EBODIC,NOCIST,NODECK,LCAD,PAF,NCE01T,IC,NCXREF  
FUNCTION GAMA (M,IP)

```
C
C *****
C
C   THIS FUNCTION CALCULATES THE ACCEPTANCE FUNCTION BETWEEN
C   STRUCTURAL MODE IP AND ACOUSTIC MODE M.
C *****
C
C   IMPLICIT REAL*8 (A-D,F-H,C-Z)
COMMON /CONST/PI
COMMON /TERMS/RATIO,SEGLTH,PICYL,Z0,PICYLZ,PILSC,PISEG
C
C   RATH=M*RATIO
C   CHECK FOR SPECIAL CASE OF INDEX COMBINATION
C   IF(DFLOAT(IP).EQ.RATH) GO TO 10
RATMPI=RATH*PI
F1=M*PICYL
F2=IP*PISEG
F1F2=F2-F1
FRONT=1.00/(2.00*F1F2)
FRNT=1.00/(2.00*(F1+F2))
ARG3=F1*Z0
ARG1=ARG3
F3=RATMPI+ARG3
ARG2=IP*PI-F3
ARG4=IP*PI+F3
TSTANG=DABS(ARG1-ARG2)
ANGUM=DMOD(TSTANG,PI*2.00)
IFTANGUM.LT.1.0-2.00*(2.00*PI-ANGUM).LT.1.0-2)GO TO 20
GAMA=FRONT*(DCOS(ARG1)-DCOS(ARG2))+FRNT*(DCCS(ARG3)-DCCS(ARG4))
RETURN
10 ARG1=IP*PISEG*Z0
SIND=DSIN(ARG1)
IF(DABS(SIND).LT.1.0-2)GO TO 20
GAMA=SEGLTH*SIND/2.00
RETURN
20 GAMA=C.00
RETURN
END
```

GAM00010  
GAM00020  
GAM00030  
GAM00040  
GAM00050  
GAM00060  
GAM00070  
GAM00080  
GAM00090  
GAM00100  
GAM00110  
GAM00120  
GAM00130  
GAM00140  
GAM00150  
GAM00160  
GAM00170  
GAM00180  
GAM00190  
GAM00200  
GAM00210  
GAM00220  
GAM00230  
GAM00240  
GAM00250  
GAM00260  
GAM00270  
GAM00280  
GAM00290  
GAM00300  
GAM00310  
GAM00320  
GAM00330  
GAM00340  
GAM00350  
GAM00360  
GAM00370  
GAM00380  
GAM00390  
GAM00400

JUN 74 1

OS/360 FORTRAN H

COMPILER OPTIONS - NAME= MAIN,OPT=02,LINECNT=56,SIZE=3000K,  
 SOURCE,ZBCDIC,NOLIST,NODECK,LCAD,MAP,NOEDIT,ID,NOXREF  
 SUBROUTINE HSQMNB (W2MNS,IWORD,M,N,HCTHR,H2MNS,\*)

```

C
C *****
C
C   THIS ROUTINE CALCULATES THE ACCLUSTICAL MODE AMPLIFICATION
C   FUNCTION SQUARED, INTEGRATED OVER A BANDWIDTH. THIS ROUTINE
C   IS USED BY MAIN PROGRAM 'ACOBAN'.
C *****
C
C   IMPLICIT REAL*8 (A-D,F-H,C-Z)
C   COMMON /ACDAMP/ACDAMA,ACDAMB
C   COMMON /BESQR/B2
C   COMMON /CONST/PI
C   COMMON /FREQ/WSQ
C   COMMON /NORMAL/DENOM
C   COMMON /RADII/RIN,ROUT
C   COMMON /VRBLS/PIOL4,RIN2,ACDACC
C   COMMON /SOLNS/SNK(400),KNS(400),NLNK
C   COMMON /OTHER/ROTHR(4),ZOTHR(4),CYLNTH
C   DIMENSION HOTH(4)
C
C   FIND MATCHING EIGENVALUE
C   NS=MOD(IWORD,1000000)
C   DO 10 I=1,NLNK
C     IF(KNS(I).EQ.NS) GO TO 20
C   10 CONTINUE
C   WRITE(6,2000)
C   2000 FORMAT(1X,'MATCHING EIGENVALUE INDICES NOT FOUND FOR REQUESTED COMBINATION',/)
C   RETURN 1
C   20 SQN=N*N
C   EM=1.
C   IF(IWORD.LT.1000000) EM=2.
C   EN=1.
C   IF(N.EQ.0) EN=2.
C   SQETA=(ACDAMA**2/(2.00*PI)**(2.00*ACDAMB))*W2MNS**((1.00+ACDAMB)
C   TERM=DSQRT(SQETA)/PI
C   SNKNOR=SNK(I)/DENOM
C   IF(SNK(I).EQ.0.00) GO TO 30
C   NORMALIZE EIGENVALUE FOR CUR USE
C   QB=QSQ(N,SNKNOR,ROUT)
C   DIV=SQN/(SNKNOR*SNKNOR)
C   NOTE THIS EXPRESSION TAKES CARE OF ITSELF FOR
C   THE HOLLOW CYLINDER CASE
C   AGEMO=EM*EN*PIOL4*((B2-DIV)*QB-(RIN2-DIV)*QSQ(N,SNKNOR,RIN))
C   H2MNS=QB/(AGEMO*TERM)
C   GO TO 50
C   30 AGEMO=EM*EN*PIOL4*(B2-RIN2)
C   NOTE CANCELLATION OF THE QSQ(0) TERM
C   H2MNS=1.00/(AGEMO*TERM)
C   50 DO 60 IDX=1,4

```

```

HSQ00010
HSQ00020
HSQ00030
HSQ00040
HSQ00050
HSQ00060
HSQ00070
HSQ00080
HSQ00090
HSQ00100
HSQ00110
HSQ00120
HSQ00130
HSQ00140
HSQ00150
HSQ00160
HSQ00170
HSQ00180
HSQ00190
HSQ00200
HSQ00210
HSQ00220
HSQ00230
HSQ00240
HSQ00250
HSQ00260
HSQ00270
HSQ00280
HSQ00290
HSQ00300
HSQ00310
HSQ00320
HSQ00330
HSQ00340
HSQ00350
HSQ00360
HSQ00370
HSQ00380
HSQ00390
HSQ00400
HSQ00410
HSQ00420
HSQ00430
HSQ00440
HSQ00450
HSQ00460
HSQ00470
HSQ00480
HSQ00490
HSQ00500
HSQ00510
HSQ00520

```

```

R=ROTHR(IDX)
Z=ZOTHR(IDX)
HOTHr(IDX)=H2MNS*(DCOS(PI*M*Z/CYLNTH))**2
1/AGEMO
IF(SNK(I).NE.3.00)HOTHr(IDX)=HCTHR(IDX)*QSQ(N,SAKOR,R)
60 CONTINUE
RETURN
END

```

```

HSQ00530
HSQ00540
HSQ00550
HSQ00560
HSQ00570
HSQ00580
HSQ00590
HSQ00600

```

JUN 74 )

QS/36J FORTRAN H

MPILER OPTIONS - NAME= MAIN,OPT=C2,LINECNT=56,SIZE=0C0CK,  
 SOURCE,EBCDIC,NOLIST,NODECK,LCAC,MAP,NCEDIT,IC,NCXREF  
 SUBROUTINE HSQMNS (W2MNS,IWCRD,M,N,HCTHR,H2MNS,\*)

C		HSQ00010
C	*****	HSQ00020
C		HSQ00030
C		HSQ00040
C	THIS ROUTINE CALCULATES THE ACOUSTICAL MODE AMPLIFICATION	HSQ00050
C	FUNCTION SQUARED. THIS ROUTINE IS USED BY MAIN PROGRAMS	HSQ00060
C	'PURTON' AND 'STRBAN'.	HSQ00070
C		HSQ00080
C	*****	HSQ00090
C		HSQ00100
	IMPLICIT REAL*8 (A-D,F-H,O-Z)	HSQ00110
	COMMON /ACDAMP/ACDAMA,ACDAMB	HSQ00120
	COMMON /BESQR/B2	HSQ00130
	COMMON /CONST/PI	HSQ00140
	COMMON /FREQ/WSQ	HSQ00150
	COMMON /NORMAL/DENOM	HSQ00160
	COMMON /RADII/RIN,ROUT	HSQ00170
	COMMON /VRBL5/PIOL4,RIN2,ACDACC	HSQ00180
	COMMON /SOLNS/SNK(400),KNS(400),NUMK	HSQ00190
	COMMON /OTHER/ROTHP(4),ZOTHR(4),CYLATH	HSQ00200
	DIMENSION MOTH(4)	HSQ00210
C		HSQ00220
C	FIND MATCHING EIGENVALUE	HSQ00230
	NS=MOD(IWORD,1000000)	HSQ00240
	DO 10 I=1,NUMK	HSQ00250
	IF(KNS(I).EQ.NS) GO TO 20	HSQ00260
	10 CONTINUE	HSQ00270
	WRITE(6,2000)	HSQ00280
	2000 FORMAT(1X,'MATCHING EIGENVALUE INDICES NOT FOUND FOR REQUESTED COM-	HSQ00290
	INATION',/)	HSQ00300
	RETURN 1	HSQ00310
	20 SQN=N*N	HSQ00320
	EM=1.	HSQ00330
	IF(IWORD.LT.1000000) EM=2.	HSQ00340
	EN=1.	HSQ00350
	IF(N.EQ.0) EN=2.	HSQ00360
	SQETA=0.00	HSQ00370
	IF(W2MNS.EQ.0.00) GO TO 40	HSQ00380
	SQETA=(ACDAMA**2/(2.0J*PI)**(2.0J*ACDAMB))*W2MNS**(1.0J+ACDAMB)	HSQ00390
	40 TERM=(W2MNS-WSQ)**2+SQETA*WSQ	HSQ00400
	SNKNOR=SNK(I)/DENOM	HSQ00410
	IF(SNK(I).EQ.0.00) GO TO 30	HSQ00420
C	NORMALIZE EIGENVALUE FOR OUR USE	HSQ00430
	QB=QSQ(N,SNKNOR,ROUT)	HSQ00440
	DIV=SQN/(SNKNOR*SNKNOR)	HSQ00450
C	NOTE THIS EXPRESSION TAKES CARE OF ITSELF FOR	HSQ00460
C	THE HOLLOW CYLINDER CASE	HSQ00470
	AGEMO=EM*EN*PIOL4*(B2-DIV)*QB*(RIN2-DIV)*QSQ(N,SNKNOR,RIN)	HSQ00480
	H2MNS=QB/(AGEMO*TERM)	HSQ00490
	GO TO 50	HSQ00500
	30 AGEMO=EM*EN*PIOL4*(B2-RIN2)	HSQ00510
C	NOTE CANCELLATION OF THE QSQ(0) TERM	HSQ00520

```

H2MNS=1.00/(AGEMO*TERM)
50 DO 60 IDX=1,4
   R=ROTHR(IDX)
   Z=ZOTHR(IDX)
   HOTHX(IDX)=H2MNS*(DCOS(P1*M*Z/CYLNTH))*2
   1/AGEMO
   IF(SNK(1).NE.0.00) HOTHX(IDX)=HOTHX(IDX)*QSG(N,SNKNCF,R)
60 CONTINUE
   RETURN
   END

```

```

HSQ00530
HSQ00540
HSQ00550
HSQ00560
HSQ00570
HSQ00580
HSQ00590
HSQ00600
HSQ00610
HSQ00620

```

JUN 74 )

OS/360 FORTRAN H

MPILER OPTIONS - NAME= MAIN,OPT=C2,LINECNT=56,SIZE=0000K,  
 SOURCE,EBCTIC,NOLIST,NODECK,LCAD,MAP,NCEDIT,IO,NCXREF  
 SUBROUTINE MCMAHN (N,NTH,XMN)

```

C*****
C THIS ROUTINE USES THE FIRST FOUR TERMS OF THE ASYMPTOTIC
C SERIES METHOD DEVELOPED BY MCMAHN TO FIND THE EIGENVALUES
C OF THE DERIVATIVES OF THE CROSS PRODUCT OF THE BESSEL AND
C NEUMANN FUNCTIONS. THE SECOND HALF OF THIS ROUTINE USES THE
C FIRST FOUR TERMS OF THE SERIES FOR THE DERIVATIVE OF J(X).
C*****
C
C IMPLICIT REAL*8 (A-D,F-H,C-Z)
C COMMON /CONST/PI
C COMMON /EIGEN/BETA,BETA3,BETA5
C COMMON /RADIO/RIN,ROUT
C
C IF(N.NE.C1) J=NTH+1
C RM=4.00*N*N
C RMSQ=RM**2
C RMCUB=RM**3
C CHECK FOR THE HOLLOW CYLINDER CASE.
C IF(RIN.EQ.0.00) GO TO 10
C RK=(NTH*PI)/(BETA-1.00)
C C1=(RM+3.00)/(3.00*BETA)
C C2=4.00*(RMSQ+46.00*RM-63.00)*(BETA3-1.00)/
C 1 (1536.00*BETA3*(BETA-1.00))
C C3=32.00*(RMCUB+185.00*RMSQ-2053.00*RM+1899.00)*(BETA5-1.00)/
C 1 (1.638405*BETA5*(BETA-1.00))
C C1SQ=C1*C1
C C1CUB=C1SQ*C1
C RKCUB=RK**3
C RKFIF=RKCUB*RK*RK
C TRM3=(C2-C1SQ)/RKCUB
C TRM4=(C3-4.00*C1*C2+2.00*C1CUB)/RKFIF
C XMN=RK+C1/RK+TRM3+TRM4
C RETURN
10 J=NTH
C ZERO IS THE ZEROth SOLUTION IN THE HOLLOW CYLINDER CASE
C ONLY FOR N=J. THEREFORE RE-ADJUST THE SOLUTION NUMBER.
C RK=PI*(2*N+4*J+1)/4.00
C RKCUB=RK**3
C RKFIF=RKCUB*RK*RK
C TRM3=4.00*(7.00*RMSQ+82.00*RM-9.00)/(1536.00*RKCUB)
C TRM4=32.00*(83.00*RMCUB+2075.00*RMSQ-3039.00*RM+3537.00)/
C 1 (4.915205*RK*FIF)
C XMN=RK-(RM+3.00)/(8.00*RK)-TRM3-TRM4
C RETURN
C END

```

MCM00010  
 MCM00020  
 MCM00030  
 MCM00040  
 MCM00050  
 MCM00060  
 MCM00070  
 MCM00080  
 MCM00090  
 MCM00100  
 MCM00110  
 MCM00120  
 MCM00130  
 MCM00140  
 MCM00150  
 MCM00160  
 MCM00170  
 MCM00180  
 MCM00190  
 MCM00200  
 MCM00210  
 MCM00220  
 MCM00230  
 MCM00240  
 MCM00250  
 MCM00260  
 MCM00270  
 MCM00280  
 MCM00290  
 MCM00300  
 MCM00310  
 MCM00320  
 MCM00330  
 MCM00340  
 MCM00350  
 MCM00360  
 MCM00370  
 MCM00380  
 MCM00390  
 MCM00400  
 MCM00410  
 MCM00420  
 MCM00430  
 MCM00440  
 MCM00450  
 MCM00460  
 MCM00470  
 MCM00480  
 MCM00490

JUN 74 1

OS/360 FORTRAN H

IMPIER OPTIONS - NAME= MAIN,OPT=02,LINECNT=56,SIZE=0000K,  
 SOURCE,EBCDIC,NOLIST,NODECK,LCAD,MAP,NOEDIT,IC,NCXREF  
 SUBROUTINE MNCALB (M,N)

C		MNC00010
C	*****	MNC00020
C		MNC00030
C		MNC00040
C	THIS IS THE SUBROUTINE THAT KEEPS TRACK OF THE CUMULATIVE	MNC00050
C	TOTAL IN THE SUM OVER THE M AND N MODAL INDICES.	MNC00060
C		MNC00070
C	*****	MNC00080
C		MNC00090
C	IMPLICIT REAL*8 (A-D,F-H,C-Z)	MNC00100
	COMMON /DIR/ISAME,IOPP	MNC00110
	COMMON /ERROR/LAST	MNC00120
	COMMON /FINAL/GRNOPP,GRNTOT,BIGSUM,BGSMT(4),SPGTCT(4)	MNC00130
	COMMON /FREQ/WSQ	MNC00140
	COMMON /STOP/VCRT	MNC00150
	COMMON /TABS/ISAVE,MNDIR,K	MNC00160
	COMMON /TOTALS/STOT,PTOT,SPTCT(4)	MNC00170
	COMMON /ACUSTK/ACMODS(8000),MNS(8000),NUMAC	MNC00180
	DIMENSION BSPRD(4),SPCOSS(4)	MNC00190
C		MNC00200
C	COMBINE 'P' AND 'Q' SUMS	MNC00210
	PTYMS=PTOT*STOT*WSQ	MNC00220
	DO 60 IDX=1,4	MNC00230
	60 BSPRD(IDX)=SPTOT(IDX)*PTOT*WSQ	MNC00240
C	CALCULATE THE CONTRIBUTION	MNC00250
	COSSUM=PTYMS	MNC00260
	DO 70 IDX=1,4	MNC00270
	70 SPCOSS(IDX)=BSPRD(IDX)	MNC00280
	GRNTOT=BIGSUM+COSSUM	MNC00290
	DO 80 IDX=1,4	MNC00300
	80 SPGTOT(IDX)=BGSMT(IDX)+SPCOSS(IDX)	MNC00310
	BIGSUM=GRNTOT	MNC00320
	DO 90 IDX=1,4	MNC00330
	90 BGSMT(IDX)=SPGTOT(IDX)	MNC00340
	RETURN	MNC00350
	END	MNC00360



JUN 74 1

OS/360 FCRTRAN M

COMPILER OPTIONS - NAME= MAIN,OPT=C2,LINECNT=56,SIZE=C300K,  
 SOURCE,EBCDIC,NOLIST,NODECK,LCAD,MAP,NGEDIT,ID,NOXREF  
 SUBROUTINE MNCALC (M,N,\*)

```

C *****
C
C   THIS IS THE SUBROUTINE THAT KEEPS TRACK OF THE CUPULATIVE
C   TOTAL IN THE SUM OVER THE M AND N MODAL INDICIES. THIS
C   ROUTINE IS USED BY MAIN PROGRAM 'PLRTCN'.
C *****
C
C   IMPLICIT REAL*8 (A-D,F-H,C-Z)
C   COMMON /DIR/ISAME,IOPP
C   COMMON /ERROR/LAST
C   COMMON /FINAL/GRNOPP,GRNTOT,BIGSUM,BGSMT(4),SPGTCT(4)
C   COMMON /STOP/VCRIT
C   COMMON /TABS/ISAVE,MNDIR,K
C   COMMON /TOTALS/STOT,PTOT,SPCTCT(4)
C   COMMON /ACUSTK/ACMODS(8000),MNS(8000),NUMAC
C   DIMENSION BSPRD(4),SPCOSS(4)
C
C   COMBINE 'P' AND 'Q' SUMS
C   PTYMS=PTOT*STOT
C   DO 60 IDX=1,4
C     60 BSPRD(IDX)=SPCTCT(IDX)*PTYMS
C   CALCULATE THE CONTRIBUTION
C   COSSUM=PTYMS
C   DO 70 IDX=1,4
C     70 SPCOSS(IDX)=BSPRD(IDX)
C   SUM TO GRAND TOTAL
C   IF TERM EQUALS ZERO IGNORE IT
C   IF(COSSUM.EQ.0.00) CALL NXTMN (ISAME,640,650)
C   GRNTOT=BIGSUM+COSSUM
C   DO 80 IDX=1,4
C     80 SPGTOT(IDX)=BGSMT(IDX)+SPCOSS(IDX)
C   CHECK CONVERGENCE OF MN SUM IN ONE DIRECTION
C   IF((BIGSUM/GRNTOT).GT.VCRIT) GO TO 20
C   BIGSUM=GRNTOT
C   DO 90 IDX=1,4
C     90 BGSMT(IDX)=SPGTOT(IDX)
C   FIND NEXT CLOSEST 'MN' FREQUENCY SAME DIRECTION AS LAST IF
C   THE CONTRIBUTION IS GREATER THEN THE CONTRIBUTION FROM THE
C   LAST TERM IN THE OPPOSITE DIRECTION
C   IF(COSSUM.GT.GRNOPP) CALL NXTMN(ISAME,640,650)
C   REDEFINE OPPOSITE TERM CONTRIBUTION VALUE
C   GRNOPP=COSSUM
C   GO TO 30
C   20 BIGSUM=GRNTOT
C   DO 100 IDX=1,4
C     100 BGSMT(IDX)=SPGTOT(IDX)
C   CHECK IF CONVERGENCE HAS OCCURRED IN BOTH DIRECTIONS
C   25 IF(GRNOPP.EQ.-1.00) RETURN
C   INSURE SUM WILL CONTINUE IN DIRECTION FOR WHICH

```

MNC00010  
 MNC00020  
 MNC00030  
 MNC00040  
 MNC00050  
 MNC00060  
 MNC00070  
 MNC00080  
 MNC00090  
 MNC00100  
 MNC00110  
 MNC00120  
 MNC00130  
 MNC00140  
 MNC00150  
 MNC00160  
 MNC00170  
 MNC00180  
 MNC00190  
 MNC00200  
 MNC00210  
 MNC00220  
 MNC00230  
 MNC00240  
 MNC00250  
 MNC00260  
 MNC00270  
 MNC00280  
 MNC00290  
 MNC00300  
 MNC00310  
 MNC00320  
 MNC00330  
 MNC00340  
 MNC00350  
 MNC00360  
 MNC00370  
 MNC00380  
 MNC00390  
 MNC00400  
 MNC00410  
 MNC00420  
 MNC00430  
 MNC00440  
 MNC00450  
 MNC00460  
 MNC00470  
 MNC00480  
 MNC00490  
 MNC00500  
 MNC00510  
 MNC00520

C CONVERGENCE HAS NOT YET OCCURRED

GRNOPP=-1.00

C FIND NEXT CLOSEST 'MN' FREQUENCY OPPOSITE DIRECTION FROM LAST

30 CALL NXTMN (IOPP,640,650)

40 RETURN 1

50 CONTINUE

GO TO 25

END

MNC00530

MNC00540

MNC00550

MNC00560

MNC00570

MNC00580

MNC00590

MNC00600

JUN 74 )

05/360 FGRTRAN H

COMPILER OPTIONS - NAME= MAIN,OPT=02,LINECNT=56,SIZE=0000K,  
 SOURCE,EBUDIC,NOLIST,NCDECK,LCAD,MAP,NGED17,10,NOXREF  
 SUBROUTINE MNSUM (M,N,IP,IQ,\*)

C		C	MNS00010
C	*****	C	MNS00020
C		C	MNS00030
C		C	MNS00040
C	THIS IS THE SUBROUTINE THAT KEEPS TRACK OF THE CUMULATIVE	C	MNS00050
C	TOTAL IN THE SUM OVER THE M AND N MODAL INDICES. THIS	C	MNS00060
C	ROUTINE IS USED BY MAIN PROGRAM 'STRBAN'.	C	MNS00070
C		C	MNS00080
C	*****	C	MNS00090
C		C	MNS00100
	IMPLICIT REAL*8 (A-D,F-H,C-Z)		MNS00110
	COMMON /DIR/ISAME,IOPP		MNS00120
	COMMON /ERROR/LAST		MNS00130
	COMMON /FINAL/GRNOPP,GRNTOT,BIGSUM,BGSMT(4),SPGTCT(4)		MNS00140
	COMMON /STOP/VCRIT		MNS00150
	COMMON /TABS/ISAVE,MNDIR,K		MNS00160
	COMMON /TOTALS/STOT,PTOT,SPTCT(4)		MNS00170
	COMMON /ACLSK/ACMODS(8000),MNS(8000),NUMAC		MNS00180
	DIMENSION BSPRD(4),SPCOSS(4)		MNS00190
C			MNS00200
C	GET ACCEPTANCES SQUARED - NOTE CAPGAM IS ALREADY SQUARED		MNS00210
	PTOT=(GAMA(M,IP)**2)*CAPGAM(N,IQ)		MNS00220
C	MULTIPLY 'S' SUM BY ACCEPTANCES SQUARED		MNS00230
	PTYMS=PTOT*STOT		MNS00240
	DO 60 IDX=1,4		MNS00250
	60 BSPRD(IDX)=SPTOT(IDX)*PTOT		MNS00260
C	CALCULATE THE CONTRIBUTION		MNS00270
	COSSUM=PTYMS		MNS00280
	DO 70 IDX=1,4		MNS00290
	70 SPCOSS(IDX)=BSPRD(IDX)		MNS00300
C	SUM TO GRAND TOTAL		MNS00310
C	IF TERM EQUALS ZERO IGNORE IT		MNS00320
	IF(COSSUM.EQ.0.00) CALL NXTMN (ISAME,840,850)		MNS00330
	GRNTOT=BIGSUM+COSSUM		MNS00340
	DO 80 IDX=1,4		MNS00350
	80 SPGTOT(IDX)=BGSMT(IDX)+SPCOSS(IDX)		MNS00360
C	CHECK CONVERGENCE OF MN SUM IN ONE DIRECTION		MNS00370
	IF((BIGSUM/GRNTOT).GT.VCRIT) GO TO 20		MNS00380
	BIGSUM=GRNTOT		MNS00390
	DO 90 IDX=1,4		MNS00400
	90 BGSMT(IDX)=SPGTOT(IDX)		MNS00410
C	FIND NEXT CLOSEST 'MN' FREQUENCY SAME DIRECTION AS LAST IF		MNS00420
C	THE CONTRIBUTION IS GREATER THEN THE CONTRIBUTION FROM THE		MNS00430
C	LAST TERM IN THE OPPOSITE DIRECTION		MNS00440
	IF(COSSUM.GT.GRNOPP) CALL NXTMN(ISAME,840,850)		MNS00450
C	REDEFINE OPPOSITE TERM CONTRIBUTION VALUE		MNS00460
	GRNOPP=COSSUM		MNS00470
	GO TO 30		MNS00480
	20 BIGSUM=GRNTOT		MNS00490
	DO 100 IDX=1,4		MNS00500
	100 BGSMT(IDX)=SPGTOT(IDX)		MNS00510
C	CHECK IF CONVERGENCE HAS OCCURRED IN BOTH DIRECTIONS		MNS00520

25 IF (GRNOPP.FQ.-1.00) RETURN

C INSURE SUM WILL CONTINUE IN DIRECTION FOR WHICH  
C CONVERGENCE HAS NOT YET OCCURRED

GRNOPP=-1.00

C FIND NEXT CLOSEST 'MN' FREQUENCY OPPOSITE DIRECTION FROM LAST

30 CALL NXTMN (IOPP, &4C, &5C)

40 RETURN 1

50 CONTINUE

GO TO 25

END

MNS00530

MNS00540

MNS00550

MNS00560

MNS00570

MNS00580

MNS00590

MNS00600

MNS00610

MNS00620

1 JUN 74 )

OS/360 FORTRAN H

COMPILER OPTIONS - NAME= MAIN,OPT=02,LINECNT=50,SIZE=0000K,  
SOURCE,EBCDIC,NOLIST,NODECK,LCAD,MAF,ACEDIT,IO,ACXREF  
SUBROUTINE NXTMN (L,\*,\*)

C		C	NXT00010
C	*****	C	NXT00020
C		C	NXT00030
C		C	NXT00040
C	THIS SUBROUTINE SEARCHES THE ACOUSTIC MODE INDICES ARRAY	C	NXT00050
C	FOR THE 'NEXT' CLOSEST VALUE TO THE EXTERIOR EXCITATION	C	NXT00060
C	FREQUENCY THAN WAS FOUND THE PREVIOUS TIME THIS SUBROUTINE	C	NXT00070
C	WAS CALLED. THE INPUT PARAMETER L IS NEGATIVE IF THE	C	NXT00080
C	SEARCH IS TO PROCEED IN A DIRECTION IN THE ARRAY OPPOSITE	C	NXT00090
C	FROM THE DIRECTION SEARCHED THE LAST TIME THE SUBROUTINE WAS	C	NXT00100
C	CALLED. L IS POSITIVE IF THE SAME DIRECTION SHOULD BE SEARCHED	C	NXT00110
C	*****	C	NXT00120
C		C	NXT00130
C		C	NXT00140
	IMPLICIT REAL*8 (A-D,F-H,C-Z)		NXT00150
	COMMON /ERRCR/LAST		NXT00160
	COMMON /TABS/ISAVE,MNDIR,K		NXT00170
	COMMON /ACUSTK/ACMODES(8000),MNS(8000),NUMAC		NXT00180
C			NXT00190
C	SAVE CURRENT INDEX		NXT00200
	LAST=IABS(MNDIR)		NXT00210
C	LESS THAN ZERO MEANS PROCEED IN THE DOWNWARDS DIRECTION		NXT00220
	IF(L*MNDIR) 30,30,5		NXT00230
C	OPPOSITE DIRECTION ?		NXT00240
	5 IF(L.EQ.-1) GO TO 10		NXT00250
C	SINCE ARRAY IS SORTED THE NEXT CLOSEST IS THE PREVIOUS		NXT00260
C	ELEMENT IN THE ARRAY		NXT00270
	K=MNDIR-1		NXT00280
	GO TO 20		NXT00290
	10 K=ISAVE-1		NXT00300
C	SAVE LAST INDEX BEFORE DIRECTION CHANGE		NXT00310
	ISAVE=LAST		NXT00320
C	K MUST BE POSITIVE HERE SINCE WE ARE PROCEEDING UPWARDS		NXT00330
	20 MNDIR=K		NXT00340
	IF(K.GT.0) RETURN 1		NXT00350
	RETURN 2		NXT00360
	30 IF(L.EQ.-1) GO TO 40		NXT00370
C	NEXT FREQUENCY IS NEXT ELEMENT IN THE ARRAY		NXT00380
	K=-(IABS(MNDIR)+1)		NXT00390
	GO TO 50		NXT00400
	40 K=-(ISAVE+1)		NXT00410
	ISAVE=LAST		NXT00420
C	SINCE K IS USED AGAIN AND MODIFIED, SAVE IT'S VALUE		NXT00430
	50 MNDIR=K		NXT00440
	IF(IABS(MNDIR).LE.NUMAC) RETURN 1		NXT00450
	RETURN 2		NXT00460
	END		NXT00470

( JUN 74 )

OS/360 FORTRAN H

COMPILER OPTIONS - NAME= MAIN,OPT=C2,LINECNT=56,SIZE=000CK,  
SOURCE=FBCDIC,NOLIST,NODECK,LCAD,MAP,NCEDIT,ID,ACXREF  
SUBROUTINE PCALB(KS,IP,IQ,TOTALL,POTALL)

```
C
C *****
C
C   THIS SUBROUTINE COMPUTES THE BANDWIDTH STRUCTURAL AMPLIFI-
C   CATION FUNCTION TIMES THE JOINT ACCEPTANCE.  IT IS USED BY
C   MAIN PROGRAM 'STRBAN'.
C *****
C
C   IMPLICIT REAL*8(A-D,F-H,O-Z)
C   COMMON /FINAL/ GRNOPP,GRNTOT,BIGSUM,BGSMT(4),SPGTCT(4)
C   COMMON /FREQ/WSQ
C   COMMON /LEAD/ HFTERM,BBB
C   DIMENSION POTALL(4)
C   CALL STAMFB(KS,H2PQ,62)
C   PROD=H2PQ*PQJ(IP,IQ,BBB)*WSQ
C   TOTALL=TOTALL+PROD*BIGSUM
C   DO 1 IDX=1,4
C 1  POTALL(IDX)=POTALL(IDX)+PROD*BGSMT(IDX)
C   RETURN
C 2  STOP 69
C   END
```

PCA00010  
PCA00020  
PCA00030  
PCA00040  
PCA00050  
PCA00060  
PCA00070  
PCA00080  
PCA00090  
PCA00100  
PCA00110  
PCA00120  
PCA00130  
PCA00140  
PCA00150  
PCA00160  
PCA00170  
PCA00180  
PCA00190  
PCA00200  
PCA00210  
PCA00220  
PCA00230

1 JUN 74 1

05/363 FCRTRAN H

COMPILER OPTIONS - NAME= MAIN,OPT=C2,LINECAT=56,SIZE=000CK,  
SOURCE,EBCDIC,NOLIST,NODECK,LCAD,MAP,NGEDIT,ID,NCXREF  
SUBROUTINE PCALCC (M,N,\*)

```

C *****
C
C THIS SUBROUTINE PERFORMS THE SLM OVER THE STRUCTURAL MCEES.
C THIS ROUTINE IS USED BY MAIN PROGRAMS 'PURTON' AND 'ACOBAN'.
C *****
      IMPLICIT REAL*8 (A-D,F-H,O-Z)
      COMMON /DIR/ISAME,IOPP
      COMMON /INFO/INDEX
      COMMON /STOP/VCRT,KCV
      COMMON /TOTALS/STOT,PTOT,SPTCT(4)
      COMMON /SAMPLE/TEMP(1200),LPQS(1200),NUMTMP
C
      PSUM=0.00
      PTOT=0.00
      KDN=0
      KUP=0
C
      CREATE MINI ARRAY OF SELECTED VALUES
      CALL COPYC (N)
      IF(NUMTMP.GT.0) GO TO 100
      WRITE(6,3000) N
3000 FORMAT('NO MODES FOR N = ',I5)
      RETURN
C
      FIND CLOSEST FREQUENCY TO THE INPUT FREQUENCY IN THIS ARRAY
100 CALL FRSFND (TEMP,NUMTMP,K)
C
      INSURE NEXT DIRECTION WILL BE CPFC SITE
      HSQOPP=1.070
C
      STRIP SIGN FROM K
      I=IABS(K)
      ISAVE=I
C
      CALCULATE STRUCTURAL AMPLIFICATION FUNCTION
10 CALL STAMFC (I,M,N,IQ,HGAMI,650)
      FGAMI=FGAMI*CAPGAM(N,IQ)
C
      IF HGAMI I.E. GAMA EQUALS ZERO IGNORE THAT TERM AND PROCEED
      IF(FGAMI.EQ.0.00)
1 CALL FNDNST(ISAME,K,I,ISAVE,N,LPGS,NUMTMP,610,640)
      PTOT=PSUM+HGAMI
C
      CHECK CONVERGENCE IN ONE DIRECTION
      IF((PSUM/PTOT).GT.VCRT) GO TO 60
      IF(K.GT.0) KUP=0
      IF(K.LT.0) KDN=0
15 PSUM=PTOT
C
      FIND NEXT FREQUENCY IN SAME DIRECTION IF THE CONTRIBUTION
C IS GREATER THEN THE CONTRIBUTION FROM THE LAST TERM IN
C THE OPPOSITE DIRECTION
      IF(FGAMI.GT.HSQOPP)
1 CALL FNDNST(ISAME,K,I,ISAVE,N,LPGS,NUMTMP,610,640)
C
      REDEFINE OPPOSITE TERM CONTRIBUTION VALUE
      HSQOPP=-FGAMI
      GO TO 30

```

PCAC0010  
PCAC0020  
PCAC0030  
PCAC0040  
PCAC0050  
PCAC0060  
PCAC0070  
PCAC0080  
PCAC0090  
PCAC0100  
PCAC0110  
PCAC0120  
PCAC0130  
PCAC0140  
PCAC0150  
PCAC0160  
PCAC0170  
PCAC0180  
PCAC0190  
PCAC0200  
PCAC0210  
PCAC0220  
PCAC0230  
PCAC0240  
PCAC0250  
PCAC0260  
PCAC0270  
PCAC0280  
PCAC0290  
PCAC0300  
PCAC0310  
PCAC0320  
PCAC0330  
PCAC0340  
PCAC0350  
PCAC0360  
PCAC0370  
PCAC0380  
PCAC0390  
PCAC0400  
PCAC0410  
PCAC0420  
PCAC0430  
PCAC0440  
PCAC0450  
PCAC0460  
PCAC0470  
PCAC0480  
PCAC0490  
PCAC0500  
PCAC0510  
PCAC0520  
PCAC0530

```

20 PSUM=PTOT
C CHECK CONVERGENCE IN BOTH DIRECTIONS
25 IF(HSQOPP.EQ.-1.00) RETURN
C INSURE PROGRESS WILL CONTINUE IN THE DIRECTION FOR WHICH
C CONVERGENCE HAS NOT OCCURRED
HSQOPP=-1.00
C FIND NEXT FREQUENCY IN OPPOSITE DIRECTION
30 CALL FNDNST(IOPP,K,I,ISAVE,N,LPQS,NUMTMP,610,635)
35 K=-K
40 CONTINUE
GO TO 25
50 WRITE(7,101)I,M,N,ISAVE,K
101 FORMAT('ERROR RET FROM STAMFC. I=',I5,' M,N=',2I5,' ISAVE=',
1I5,' K=',I5)
RETURN 1
60 IF(K.GT.0) GO TO 70
KCN=KDN+1
IF(KCN.GE.KCV) GO TO 20
GO TO 15
70 KUP=KUP+1
IF(KUP.GE.KCV) GO TO 20
GO TO 15
END

```

PCA00540  
 PCA00550  
 PCA00560  
 PCA00570  
 PCA00580  
 PCA00590  
 PCA00600  
 PCA00610  
 PCA00620  
 PCA00630  
 PCA00640  
 PCA00650  
 PCA00660  
 PCA00670  
 PCA00680  
 PCA00690  
 PCA00700  
 PCA00710  
 PCA00720  
 PCA00730  
 PCA00740  
 PCA00750  
 PCA00760



JUN 74 )

OS/360 FORTRAN H

COMPILER OPTIONS - NAME= MAIN,OPT=02,LINECNT=56,SIZE=CCOCK,  
 SOURCE,EBCDIC,NOLIST,NODECK,LCAD,MAP,NCEDIT,IO,ACXREF  
 FUNCTION PQJ(IP,IQ,88)

C		PQJ00010
C	*****	PQJ00020
C		PQJ00030
C		PQJ00040
C	THIS SUBROUTINE COMPUTES THE JCINT ACCEPTANCE FUNCTION FOR	PQJ00050
C	JET AND ROCKET NOISE.	PQJ00060
C		PQJ00070
C	*****	PQJ00080
C		PQJ00090
	IMPLICIT REAL*8 (A-D,F-H,C-Z)	PQJ00100
	COMMON /ACCEPT/ALFA	PQJ00110
	COMMON /CONST/PI	PQJ00120
	COMMON /LETTRS/A,B,C,CK,CRAT,DRAT	PQJ00130
	COMMON /MORE/WOLCPI,PICER	PQJ00140
	COMMON /EPRCOR/TVXR,AXCDF,TVYR,AYCDF	
	DIMENSION AI(3,2),DEL(2),GAM(2),ACPT(2)	PQJ00150
	DEL(1)=TVXR/AXCDF*WOLCPI	
	DEL(2)=TVYR/AYCDF*PICER*ALFA/PI	
	GAM(1)=TVXR*WOLCPI	
	GAM(2)=TVYR*PICER*ALFA/PI	
	DO 10 I=1,2	PQJ00200
	J = (2-I)*IP+(I-1)*IQ	PQJ00210
	FLJ = DFLUAT(J)	PQJ00220
	DNM1 = DEL(I)**2+(GAM(I)+FLJ)**2	PQJ00230
	DNM2 = DEL(I)**2+(GAM(I)-FLJ)**2	PQJ00240
	DELT = DEL(I)	PQJ00250
	GAMY = GAM(I)	PQJ00260
	FACT = DEXP(-DELT*PI)*(-1.00)**J	PQJ00270
	SNFT = FACT*DSIN(GAMY*PI)	PQJ00280
	CSFT = FACT*DCOS(GAMY*PI)	PQJ00290
	AI(1,I) = DELT*(1.00-CSFT)*(1.00/DNM1+1.00/DNM2)	PQJ00300
1	+SNFT*((GAMY+FLJ)/DNM1+(GAMY-FLJ)/DNM2)	PQJ00310
	AI(2,I) = SNFT*((GAMY+FLJ)*(PI+2.00*DELT/DNM1)/DNM1	PQJ00320
1	+(GAMY-FLJ)*(PI+2.00*DELT/DNM2)/DNM2)	PQJ00330
2	-CSFT*((PI*DELT+(DELT**2-(GAMY+FLJ)**2)/DNM1)/DNM1	PQJ00340
3	+(PI*DELT+(DELT**2-(GAMY-FLJ)**2)/DNM2)/DNM2)	PQJ00350
4	+(DELT**2-(GAMY+FLJ)**2)/(DNM1**2)	PQJ00360
5	+(DELT**2-(GAMY-FLJ)**2)/(DNM2**2)	PQJ00370
	AI(3,I) = DELT*SNFT*(1.00/DNM2-1.00/DNM1)	PQJ00380
1	+CSFT*((GAMY-FLJ)/DNM2-(GAMY+FLJ)/DNM1)	PQJ00390
2	+(GAMY+FLJ)/DNM1-(GAMY-FLJ)/DNM2	PQJ00400
	ACPT(I) = (PI*AI(1,I)-AI(2,I)+AI(3,I)/FLJ)/2.00	PQJ00410
10	CONTINUE	PQJ00420
	PQJ = 4.*ACPT(1)*ACPT(2)/B	PQJ00430
	PQJ = (ALFA/PI)**2*ACPT(1)*ACPT(2)/B	PQJ00430
	RETURN	PQJ00440
	END	PQJ00450

ORIGINAL PAGE IS  
 OF POOR QUALITY

( JUN 74 )

OS/360 FORTRAN H

COMPILER OPTIONS - NAME= MAIN,OPT=02,LINECNT=56,SIZE=0000K,  
SOURCE,FBCDIC,NOLIST,NODECK,LCAD,MAP,NCEDIT,IC,ACXREF  
SUBROUTINE PSQS (N,X,TOTP,TCTQ,ARG)

```
C
C*****
C
C THIS ROUTINE CALCULATES THE P AND Q SERIES WHEN USING THE
C ASYMPTOTIC SERIES METHOD FOR BESSEL AND NEUMANN FUNCTIONS.
C NOTE: THIS P AND Q SERIES IS NOT THE SAME AS THE MODAL
C P AND Q INDICES.
C*****
C
C IMPLICIT REAL*8 (A-D,F-H,C-Z)
C COMMON /CONST/PI
C COMMON /CONV/UP,DN
C COMMON /CTRL/FAC(57),PSI(60)
C
C U=4.00*N*N
C ATEX=8.00*X
C EJ=-1.0
C TRMP=1.00
C SUMP=1.00
C SUMQ=0.00
C RJ=1.00
C
C CALCULATE 'P' AND 'Q' SERIES SIMULTANEOUSLY
C DO 10 M=2,56,2
C RK=RJ+2.00
C TRMQ=TRMP*(U-RJ*RJ)/ATEX
C TRMP=TRMQ*(U-RK*RK)/ATEX
C TOTP=SUMP+EJ*TRMP/FAC(M+1)
C EJ=-EJ
C TOTQ=SUMQ+EJ*TRMQ/FAC(M)
C IF(TOTQ.EQ.0.00) GO TO 5
C IF 'Q' SERIES HAS CONVERGED THEN THE 'P' SERIES HAS
C ALSO CONVERGED SINCE ONE MORE 'P' TERM HAS BEEN CALCULATED
C VAL=SUMQ/TOTQ
C IF(VAL.GT.DN.AND.VAL.LT.UP) GO TO 20
C 5 SUMQ=TOTQ
C SUMP=TOTP
C RJ=RK+2.00
C 10 CONTINUE
C
C TERM USED IN ASYMPTOTIC SERIES EXPRESSION FOR BESSEL FUNCTIONS
C 20 ARG=X-PI*(N/2.00+0.2500)
C RETURN
C END
```

PSQ00010  
PSQ00020  
PSQ00030  
PSQ00040  
PSQ00050  
PSQ00060  
PSQ00070  
PSQ00080  
PSQ00090  
PSQ00100  
PSQ00110  
PSQ00120  
PSQ00130  
PSQ00140  
PSQ00150  
PSQ00160  
PSQ00170  
PSQ00180  
PSQ00190  
PSQ00200  
PSQ00210  
PSQ00220  
PSQ00230  
PSQ00240  
PSQ00250  
PSQ00260  
PSQ00270  
PSQ00280  
PSQ00290  
PSQ00300  
PSQ00310  
PSQ00320  
PSQ00330  
PSQ00340  
PSQ00350  
PSQ00360  
PSQ00370  
PSQ00380  
PSQ00390  
PSQ00400  
PSQ00410  
PSQ00420  
PSQ00430  
PSQ00440

JUN 74 )

QS/360 FCRTAN H

COMPILER OPTIONS - NAME= MAIN,OPT=02,LINECNT=56,SIZE=0007K,  
 SOURCE,EBCDIC,NOLIST,NODECK,LCAD,MAP,NCEDIT,IC,NOXREF  
 FUNCTION QSQ(N,XNS,R)

C		QSQC0010
C	*****	QSQC0020
C		QSQC0030
C		QSQC0040
C	THIS FUNCTION CALCULATES THE 'Q' FUNCTION SQUARED. THE	QSQC0050
C	FUNCTION IS A TERM IS THE ACOUSTIC AMPLIFICATION FUNCTION	QSQC0060
C	*****	QSQC0070
C		QSQC0080
C		QSQC0090
	IMPLICIT REAL*8 (A-D,F-H,O-Z)	QSQC0100
	COMMON /RADII/RIN,ROUT	QSQC0110
C		QSQC0120
	RKNS=R*XNS	QSQC0130
C	CALCULATE DERIVATIVE USING RECURRENCE RELATION	QSQC0140
	CALL BESSEL (N,RKNS,BJRN,BYRN)	QSQC0150
C	TAKE CARE OF THE HOLLOW CYLINDER CASE	QSQC0160
	IF(RIN.EQ.C.D0) GO TO 10	QSQC0170
	BKNS=ROUT*XNS	QSQC0180
	DIVN=N/BKNS	QSQC0190
	CALL BESSEL (N,BKNS,BJBN,BYBN)	QSQC0200
	CALL BESSEL (N+1,BKNS,BJBNP1,BYBNP1)	QSQC0210
	Q=BJRN-(DIVN*BJBN-BJBNP1)*BYRN/(DIVN*BYBN-BYBNP1)	QSQC0220
	QSQ=Q*Q	QSQC0230
	RETURN	QSQC0240
	10 QSQ=BJRN**2	QSQC0250
	RETURN	QSQC0260
	END	QSQC0270

( JUN 74 )

OS/360 FORTRAN H

COMPILER OPTIONS - NAME= MAIN,OPT=J2,LINECNT=56,SIZE=000K,  
SOURCE,ZBCDIC,NOLIST,NODECK,LCAD,MAP,ACEDIT,IC,ACXREF  
SUBROUTINE RECUR (N,X,BSLN,BSLNM1,BSL)

```
C
C*****
C
C THIS ROUTINE USES THE RECURSION RELATION FOR BESSEL AND
C NEUMANN FUNCTIONS TO FIND VALUES OF HIGH ORDER.
C*****
C
C IMPLICIT REAL*8 (A-D,F-H,C-Z)
C
C QNT=2.00/X
C K=N-1
C START RECURRENCE TO FIND ORDER 9 SINCE 8 AND 7 ARE KNOWN
DO 10 I=8,K
BSLNP1=QNT*I*BSLN-BSLNM1
BSLNM1=BSLN
BSLN=BSLNP1
10 CONTINUE
BSL=BSLN
RETURN
END
```

```
REC00010
REC00020
REC00030
REC00040
REC00050
REC00060
REC00070
REC00080
REC00090
REC00100
REC00110
REC00120
REC00130
REC00140
REC00150
REC00160
REC00170
REC00180
REC00190
REC00200
REC00210
REC00220
```

JUN 74 1

05/363 FCRTRAN H

MPILER OPTIONS - NAME= MAIN,OPT=02,LINECNT=56,SIZE=0000K,  
 SOURCE,EBCDIC,NOLIST,ACDECK,LCAC,MAP,NCEDIT,IO,NCXREF  
 SUBROUTINE REGFAL (N,XL,\*)

C		C	REG00010
C	*****	C	REG00020
C		C	REG00030
C		C	REG00040
C	THIS SUBROUTINE USES THE REGULA FALSI (FALSE POSITION)	C	REG00050
C	TECHNIQUE TO FIND THE EIGENVALUES OF THE CROSS PRODUCT OF	C	REG00060
C	THE DERIVATIVES OF THE BESSEL AND NEUMANN FUNCTIONS. IN THE	C	REG00070
C	FOLLOW CYLINDER CASE FUNCTION DOB IS THE DERIVATIVE OF J(X)	C	REG00080
C	*****	C	REG00090
C		C	REG00100
C		C	REG00110
	IMPLICIT REAL*8 (A-D,F-H,G-Z)		REG00120
	COMMON /HALT/QUIT		REG00130
	DATA I/3/		REG00140
	IF(I.EQ.3) GO TO 5		REG00150
C	START OVER AGAIN FOR NEW ORDER OF FUNCTION		REG00160
	I=N		REG00170
	XL=J.DO		REG00180
C	STEPSIZE IS 0.1		REG00190
5	XL=XL+0.100		REG00200
	VLFT=DOB(N,XL)		REG00210
10	XR=XL+0.100		REG00220
	VRT=DOB(N,XR)		REG00230
	IF(VLFT*VRT) 40,30,20		REG00240
20	VLFT=VRT		REG00250
	XL=XR		REG00260
	GO TO 10		REG00270
30	IF(DABS(VLFT).LE.QUIT) RETURN		REG00280
	XL=XR		REG00290
	RETURN		REG00300
C	CLOSE IN ON ZERO VALUE		REG00310
40	DO 60 J=1,2		REG00320
	XTST=(XL*VRT-XR*VLFT)/(VRT-VLFT)		REG00330
	VLTST=DOB(N,XTST)		REG00340
	IF(DABS(VLTST).LE.QUIT) GO TO 60		REG00350
	IF((VLTST*VLFT).LT.0.DO) GO TO 70		REG00360
	XL=XTST		REG00370
	VLFT=VLTST		REG00380
	GO TO 80		REG00390
60	XL=XTST		REG00400
	RETURN		REG00410
70	XR=XTST		REG00420
	VRT=VLTST		REG00430
80	CONTINUE		REG00440
	RETURN 1		REG00450
	END		REG00460
			REG00470

JUN 74 )

DS/360 FORTRAN H

MPILER OPTIONS - NAME= MAIN,OPT=02,LINECNT=56,SIZE=0000K,  
 SOURCE,EBCTIC,NOLIST,NODECK,LCAD,MAP,NCEDIT,IO,NCXREF  
 SUBROUTINE ROOT (N,NTH,XNS,\*)

```

C *****
C THIS SUBROUTINE TESTS AND DECIDES WHICH METHOD (REGULA FALSI
C OR ASYMPTOTIC SERIES) WILL BE USED TO FIND THE NEXT EIGENVALUE
C FOR THE DERIVATIVES OF THE CROSS PRODUCT OF THE BESSEL
C AND NEUMANN FUNCTIONS. THE DERIVATIVE OF J(X) IS ALSO HANDLED
C IN THE HOLLOW CYLINDER CASE.
C *****
C
C IMPLICIT REAL*8 (A-D,F-H,C-Z)
C LOGICAL L/.FALSE./
C COMMON /RADII/RIN,ROUT
C COMMON /STOP/VCRIT
C DATA BIG/1.0007500/,I/O/
C
C IF(I.EQ.N) GO TO 5
C I=N
C L=.FALSE.
C 5 IF(NTH.EQ.0) GO TO 25
C IF (L) GO TO 10
C 7 CALL REGFAL (N,XNS,830)
C MAKE SURE MCMAHN DOES NOT GET A VALUE OF 'NTH' EQUAL TO ZERO
C 10 IF(NTH.LE.1) RETURN
C J=NTH
C SINCE ZERO IS THE ZEROETH SOLUTION ADJUST SOLUTION NUMBER FOR
C N NOT EQUAL TO ZERO. N=0 BEHAVES DIFFERENTLY
C CALL MCMAHN (N,J,XMN)
C IF (L) GO TO 21
C USE REGULA FALSI UNTIL THE MCMAHN SERIES PROVIDES GOOD
C AGREEMENT, THEN USE THE SERIES ALONE FOR THE REMAINING ROOTS
C FOR THIS ORDER OF THE FUNCTION
C DIV=XNS/XMN
C IF(DIV.GT.VCRIT.AND.DIV.LT.BIG) GO TO 20
C RETURN EIGENVALUES
C RETURN
C 20 L=.TRUE.
C 21 XNS=XMN
C RETURN
C CHECK FOR HOLLOW CYLINDER CASE
C 25 IF(N.NE.0) GO TO 7
C XNS=J.D0
C RETURN
C 30 WRITE(6,2000)
C 2000 FORMAT(1X,'NO CONVERGENCE WHILE USING REGULA FALSI PROCEDURE',/)
C RETURN I
C END

```

R0000010  
 R0000020  
 R0000030  
 R0000040  
 R0000050  
 R0000060  
 R0000070  
 R0000080  
 R0000090  
 R0000100  
 R0000110  
 R0000120  
 R0000130  
 R0000140  
 R0000150  
 R0000160  
 R0000170  
 R0000180  
 R0000190  
 R0000200  
 R0000210  
 R0000220  
 R0000230  
 R0000240  
 R0000250  
 R0000260  
 R0000270  
 R0000280  
 R0000290  
 R0000300  
 R0000310  
 R0000320  
 R0000330  
 R0000340  
 R0000350  
 R0000360  
 R0000370  
 R0000380  
 R0000390  
 R0000400  
 R0000410  
 R0000420  
 R0000430  
 R0000440  
 R0000450  
 R0000460  
 R0000470  
 R0000480  
 R0000490

JUN 74 )

05/360 FCRTRAN H

MPILER OPTIONS - NAME= MAIN,OPT=02,LINECNT=56,SIZE=0000K,

SOURCE,EBCDIC,NOLIST,NODECK,LCAD,MAP,ACEDIT,ID,ACXREF

SUBROUTINE SCALC (K,M,N,\*)

C		SCA0001C
C	*****	SCA0002C
C		SCA0003C
C		SCA0004C
C	THIS ROUTINE PERFORMS THE SUM OVER THE IS ACUSTIC MODE INDEX.	SCA0005C
C	IT IS USED BY MAIN PROGRAMS 'PLUTCN' AND 'STRBAN'.	SCA0006C
C		SCA0007C
C	*****	SCA0008C
C		SCA0009C
	IMPLICIT REAL*8 (A-D,F-H,G-Z)	SCA0010C
	COMMON /DIR/ISAME,IOPP	SCA0011C
	COMMON /ERROR/LAST	SCA0012C
	COMMON /STOP/VCRIT	SCA0013C
	COMMON /TOTALS/STOT,PTOT,SPTCT(4)	SCA0014C
	COMMON /ACUSTK/ACMODS(8000),MNS(8000),NUMAC	SCA0015C
	DIMENSION HOTH(4),SPSUM(4)	SCA0016C
C		SCA0017C
C	INSURE NEXT TERM WILL BE FROM OPPOSITE DIRECTION	SCA0018C
	HSQOPP=1.07C	SCA0019C
	SSUM=0.00	SCA0020C
	STOT=0.00	SCA0021C
	DO 100 IDX=1,4	SCA0022C
	SPSUM(IDX) = 0.00	SCA0023C
	100 SPTOT(IDX)=0.00	SCA0024C
C	STRIP SIGN OF K	SCA0025C
	I=IABS(K)	SCA0026C
	ISAVE=I	SCA0027C
C	UNPACK ACOUSTIC MODAL INDICES AND COMBINATIONS	SCA0028C
	NS=MOD(MNS(I),1000000)	SCA0029C
	N=NS/1000	SCA0030C
	MN=MNS(I)/1000	SCA0031C
	M=MN/100	SCA0032C
C	CALCULATE ACOUSTIC AMPLIFICATION FUNCTION	SCA0033C
	10 CALL HSQMNS (ACMODS(I),MNS(I),M,N,HOTH,H2MNS,&50)	SCA0034C
C	CHECK FOR ZERO CASE	SCA0035C
	IF(H2MNS.EQ.0.00)	SCA0036C
	1 CALL FNDNXT(ISAME,K,I,ISAVE,MN,MNS,NUMAC,&10,&40)	SCA0037C
	STOT=SSUM+H2MNS	SCA0038C
	DO 200 IDX=1,4	SCA0039C
	200 SPTOT(IDX)=SPSUM(IDX)+HOTH(IDX)	SCA0040C
C	CHECK CONVERGENCE IN ONE DIRECTION	SCA0041C
	IF((SSUM/STOT).GT.VCRIT) GO TO 20	SCA0042C
	SSUM=STOT	SCA0043C
	DO 300 IDX=1,4	SCA0044C
	300 SPSPSUM(IDX)=SPTOT(IDX)	SCA0045C
C	FIND NEXT FREQUENCY IN SAME DIRECTION IF THE LAST CONTRIBUTION	SCA0046C
C	FROM THIS DIRECTION IS GREATER THEN THE CONTRIBUTION FROM	SCA0047C
C	THE PREVIOUS TERM IN THE OPPOSITE DIRECTION	SCA0048C
	IF(H2MNS.GT.HSQOPP)	SCA0049C
	1 CALL FNDNXT(ISAME,K,I,ISAVE,MN,MNS,NUMAC,&10,&40)	SCA0050C
C	REDEFINE OPPOSITE TERM VALUE	SCA0051C
	HSQOPP=H2MNS	SCA0052C

```

      GO TO 30
20  SSUM=STOT
      CO 400 IDX=1,4
400  SPSUM(IDX)=SPTOT(IDX)
C    CHECK CONVERGENCE IN BOTH DIRECTIONS
25  IF(HSQOPP.EQ.-1.00) RETURN
C    INCURE CONTINUED PROGRESS IN THE OPPOSITE DIRECTION
      HSQOPP=-1.00
C    FIND NEXT FREQUENCY IN OPPOSITE DIRECTION
30  CALL FN0NXT (IOPP,K,I,ISAVE,MN,MNS,NUMAC,010,635)
35  K=-K
40  CONTINUE
      GO TO 25
50  RETURN 1
      END

```

SCA00530  
 SCA00540  
 SCA00550  
 SCA00560  
 SCA00570  
 SCA00580  
 SCA00590  
 SCA00600  
 SCA00610  
 SCA00620  
 SCA00630  
 SCA00640  
 SCA00650  
 SCA00660  
 SCA00670



JUN 74 )

05/360 FORTRAN H

IMPIER OPTIONS - NAME= MAIN,OPT=02,LINECNT=56,SIZE=0000K,  
 SOURCE,EBCDIC,NOLIST,NODECK,LCAD,MAP,ACEDIT,ID,NOXREF  
 SUBROUTINE SCALCB (K,M,N,\*)

C		C	SCA00010
C	*****	C	SCA00020
C		C	SCA00030
C		C	SCA00040
C	THIS ROUTINE OBTAINS THE BANDWIDTH ACOUSTICAL AMPLIFICATION	C	SCA00050
C	FUNCTION. IT IS USED BY MAIN PROGRAM 'ACOBAN'	C	SCA00060
C		C	SCA00070
C	*****	C	SCA00080
C		C	SCA00090
	IMPLICIT REAL*8 (A-D,F-H,G-Z)		SCA00100
	COMMON /ERROR/LAST		SCA00110
	COMMON /STOP/VCRT		SCA00120
	COMMON /TOTALS/STOT,PTOT,SPTCT(4)		SCA00130
	COMMON /ACLSYK/ACMODS(8000),MNS(8000),NUMAC		SCA00140
	DIMENSION HOTH(4),SPSUM(4)		SCA00150
C			SCA00160
	I=K		SCA00170
	STOT=0.00		SCA00180
	DO 100 IDX=1,4		SCA00190
100	SPTOT(IDX)=0.00		SCA00200
C	UNPACK ACOUSTIC MODAL INDICES AND COMBINATIONS		SCA00210
	NS=MOD(MNS(I),1000*2)		SCA00220
	N=NS/1000		SCA00230
	MN=MNS(I)/1000		SCA00240
	M=MN/1000		SCA00250
C	CALCULATE ACOUSTIC AMPLIFICATION FUNCTION		SCA00260
10	CALL HSQMN(ACMODS(I),MNS(I),M,N,HOTH,H2MNS,&50)		SCA00270
C	CHECK FOR ZERO CASE		SCA00280
	STOT=H2MNS		SCA00290
	DO 200 IDX=1,4		SCA00300
200	SPTOT(IDX)=HOTH(IDX)		SCA00310
	RETURN		SCA00320
50	RETURN 1		SCA00330
	END		SCA00340

JUN. 74 )

OS/360 FORTRAN H

MPILER OPTIONS - NAME= MAIN,OPT=C2,LINECNT=56,SIZE=CCCC K,  
 SOURCE,EBCDIC,NOLIST,NODECK,LCAC,MAP,NCEDIT,IC,NOXREF  
 SUBROUTINE SMODSC (IPST,IPEND,IGST,IGEND,ICN)

```

C *****
C
C THIS SUBROUTINE CALCULATES THE STRUCTURAL MODAL FREQUENCIES
C FOR AN ORTHOTROPIC SHELL SEGMENT STIFFENED BY RINGS. THE
C CALCULATION IS PERFORMED OVER TWO MODAL INDICIES, IP AND IG.
C EACH COMBINATION OF IP AND IG HAS THREE ASSOCIATED MODAL
C FREQUENCIES. THE INDICIES ARE PACKED INTO ARRAY MPQ IN THE
C ORDER IG AND IP. THE FREQUENCIES SQUARED ARE STORED IN
C ARRAY STMDS. IN ADDITION, THE THREE ASSOCIATED CONSTANTS
C NEEDED FOR THE AMPLITUDE FUNCTION FOR EACH MODE ARE CALCULATED
C AND THE SQUARES STORED IN ARRAY STMCD3, THE INDICIES (SAME
C AS FOR THE THREE FREQUENCIES) ARE STORED IN ARRAY MPC3.
C *****
C
      IMPLICIT REAL*8 (A-D,F-H,C-Z)
      DIMENSION BUF(3),IBUF(3),X(3)
      COMMON/ACCEPT/ALFA
      COMMON /CONST/PI
      COMMON /LETTRS/A,B,C,CK,CRAT,DRAT
      COMMON /STRUCT/STMDS(1200),MPQ(1200),STMCD3(400,3),MPC3(400),
      1      NUMST,NUM3
      PNU=1.00-2.00*A
C
      GO TO (100,200,100,200),ICN
100 J=1
      K=1
      FLAST = 1.000
      FLAST1=FLAST
C      LOOP OVER P AND Q STRUCTURAL MODES
      DO 20 IP=IPST,IPEND
      RP2=IP*IP
      P2B=8*RP2
10 IQ=IGST
11 RQ2=(IQ*PI/ALFA)**2
      TER1=P2B*P2B+2.00*P2B*RQ2+DRAT*RQ2*RQ2
      TER2=(1.00+A)*P2B+(CRAT+A)*RQ2
      TER3=P2B*P2B+(CRAT-PNU)*RQ2+P2B/A+CRAT*RQ2*RQ2
      COF2=CRAT+CK*TER1+TER2
      COF1=CRAT*(11.00+A-PNU*PNU/CRAT)*P2B+A*RQ21+CK*TER2*TER1+A*TER3
      COF0=A*(CK*TER3*TER1+(CRAT-PNU*PNU)*P2B*P2B)
      COF2=(1-1.00)*COF2
      COF0=(1-1.00)*COF0
      CALL CUBIC(X,COF2,COF1,COF0,.65001
      STMDS(J)=X(1)/C
      IWORD = IQ*1000+IP
      MPQ(J)=IWORD
      J=J+1
      STMDS(J)=X(2)/C
      MPQ(J)= IWORD

```

SM000010  
 SM000020  
 SM000030  
 SM000040  
 SM000050  
 SM000060  
 SM000070  
 SM000080  
 SM000090  
 SM000100  
 SM000110  
 SM000120  
 SM000130  
 SM000140  
 SM000150  
 SM000160  
 SM000170  
 SM000180  
 SM000190  
 SM000200  
 SM000210  
 SM000220  
 SM000230  
 SM000240  
 SM000250  
 SM000260  
 SM000270  
 SM000280  
 SM000290  
 SM000300  
 SM000310  
 SM000320  
 SM000330  
 SM000340  
 SM000350  
 SM000360  
 SM000370  
 SM000380  
 SM000390  
 SM000400  
 SM000410  
 SM000420  
 SM000430  
 SM000440  
 SM000450  
 SM000460  
 SM000470  
 SM000480  
 SM000490  
 SM000500  
 SM000510  
 SM000520

```

J=J+1
STMDS(J)=X(3)/C
MPQ(J)=IWORD
J=J+1
STMDS(K,1)=(P2B+A*RQ2)/C
STMDS(K,2)=(A*P2B+RQ2*CRAT)/C
STMDS(K,3)=(P2B+RQ2)*(1.0J-A)**2)/C
MPQ(K)=IWORD
K=K+1
FLAST2=FLAST1
FLAST1=DMIN1(STMDS(J-3),STPCDS(J-2),STPCDS(J-1))
IF(IQ.EQ.IQST)FLAST2=FLAST1
IF((FLAST1.GE.FLAST1).AND.(FLAST1.GT.FLAST2)) GO TO 16
15 IQ=IQ+1
IF(IQ.GT.IQEND) GO TO 16
GO TO 11
16 IF(IP.EQ.IPST)FLAST=FLAST1
20 CONTINUE
C      NUMBER OF STRUCTURAL MODES
NUMST=J-1
NUM3=K-1
CALL SORT(STMDS,MPQ,NUMST)
WRITE(2,250)IPST,IPEND,IQST,IQEND,NUMST,NUM3
250 FORMAT(8I10)
NREC=NUMST/5
IF(NREC*5.LT.NUMST)NREC=NREC+1
DO 60 III=1,NREC
IND1=5*(III-1)+1
IND2=IND1+4
IF(IND2.GT.NUMST)IND2=NUMST
WRITE(2,250)(MPQ(JJJ),JJJ=IND1,IND2)
WRITE(2,250)(STMDS(JJJ),JJJ=IND1,IND2)
60 CONTINUE
NREC=NUM3/5
IF(NREC*5.LT.NUM3)NREC=NREC+1
DO 61 III=1,NREC
IND1=5*(III-1)+1
IND2=IND1+4
IF(IND2.GT.NUM3)IND2=NUM3
WRITE(2,250)(MPQ(JJJ),JJJ=IND1,IND2)
DO 611 KKK=1,3
WRITE(2,250)(STMDS(JJJ,KKK),JJJ=IND1,IND2)
611 CONTINUE
61 CONTINUE
350 FORMAT(5D16.10)
TWOPI=2.0C*PI
WRITE(6,2003)
2000 FORMAT(1H1,T16,'STRUCTURAL MODAL FREQUENCIES AND INDICES',
1 ///, 3('INDICES',3X,'FREQUENCIES',3X),//)
KOUNT=0
DO 30 I=1,NUMST,3
K=I+2
C      WRITE FREQUENCIES IN HERTZ
L=1

```

```

SM000530
SM000540
SM000550
SM000560
SM000570
SM000580
SM000590
SM000600
SM000610
SM000620
SM000630
SM000640
SM000650
SM000660
SM000670
SM000680
SM000690
SM000700
SM000710
SM000720
SM000730
SM000740
SM000750
SM000760
SM000770
SM000780
SM000790
SM000800
SM000810
SM000820
SM000830
SM000840
SM000850
SM000860
SM000870
SM000880
SM000890
SM000900
SM000910
SM000920
SM000930
SM000940
SM000950
SM000960
SM000970
SM000980
SM000990
SM001000
SM001010
SM001020
SM001030
SM001040
SM001050
SM001060

```

```

DO 25 J=1,K
BUF(L)=DSQRT(STMODS(J))/THOP1
IBUF(L)=MPQ(J)
25 L=L+1
WRITE(6,2001) (IBUF(J),BUF(J),J=1,3)
2001 FORMAT(1H,3(I9,3X,F8.1,4X))
KOUNT=KOUNT+1
IF(MOD(KOUNT,50).EQ.0) WRITE(6,2000)
30 CONTINUE
DO 6111 KKK=1,3
WRITE(6,2002)KKK
2002 FORMAT(1H1,T11,' STRUCTURAL CONSTANTS C',I1,' AND INCICIES'
1,///, 3('INDICES',3X,'CONSTANTS', 3X),//)
KOUNT=0
DO 40 I=1,NUM3,3
K=I+2
L=1
DO 35 J=1,K
BUF(L)=DSQRT(STMOD3(J,KKK))/THOP1
IBUF(L)=MPQ3(J)
35 L=L+1
WRITE(6,2001) (IBUF(J),BUF(J),J=1,3)
KOUNT=KOUNT+1
IF(MOD(KOUNT,50).EQ.0) WRITE(6,2002)
40 CONTINUE
6111 CONTINUE
WRITE(6,2003)
2003 FORMAT(1H1)
RETURN
200 READ(2,250)IPST,IPEND,IQST,IGEND,NUMST,NUM3
NREC=NUMST/5
IF(NREC*5.LT.NUMST)NREC=NREC+1
DO 70 III=1,NREC
IND1=5*(III-1)+1
IND2=IND1+4
IF(IND2.GT.NUMST)IND2=NUMST
READ(2,250)(MPQ(JJJ),JJJ=IND1,IND2)
READ(2,350)(STMODS(JJJ),JJJ=IND1,IND2)
70 CONTINUE
NREC=NUM3/5
IF(5*NREC.LT.NUM3)NREC=NREC+1
DO 71 III=1,NREC
IND1=5*(III-1)+1
IND2=IND1+4
IF(IND2.GT.NUM3)IND2=NUM3
READ(2,250)(MPQ3(JJJ),JJJ=IND1,IND2)
DO 711 KKK=1,3
READ(2,350)(STMOD3(JJJ,KKK),JJJ=IND1,IND2)
711 CONTINUE
71 CONTINUE
RETURN
500 STOP 699
END

```

SM001070  
SM001080  
SM001090  
SM001100  
SM001110  
SM001120  
SM001130  
SM001140  
SM001150  
SM001160  
SM001170  
SM001180  
SM001190  
SM001200  
SM001210  
SM001220  
SM001230  
SM001240  
SM001250  
SM001260  
SM001270  
SM001280  
SM001290  
SM001300  
SM001310  
SM001320  
SM001330  
SM001340  
SM001350  
SM001360  
SM001370  
SM001380  
SM001390  
SM001400  
SM001410  
SM001420  
SM001430  
SM001440  
SM001450  
SM001460  
SM001470  
SM001480  
SM001490  
SM001500  
SM001510  
SM001520  
SM001530  
SM001540  
SM001550  
SM001560  
SM001570  
SM001580  
SM001590

( JUN 74 )

OS/360 FCHTRAN H

COMPILER OPTIONS - NAME= MAIN,OPT=02,LINECNT=56,SIZE=C000K,  
SOURCE,EBCDIC,NOLIST,NCDECK,LCAD,MAP,NCEDIT,IO,NCXREF  
SUBROUTINE SORT (RA,IA,NUM)

C		C	SOR00010
C	*****	C	SOR00020
C		C	SOR00030
C		C	SOR00040
C	THIS ROUTINE PERFORMS A NUMERICAL SORT ON INPUT ARRAY RA AND	C	SOR00050
C	SORTS THE CONTENTS OF ARRAY IA IN THE SAME ORDER.	C	SOR00060
C		C	SOR00070
C	*****	C	SOR00080
C		C	SOR00090
	IMPLICIT REAL*8 (A-D,F-H,C-Z)		SOR00100
	DIMENSION IA(1),RA(1)		SOR00110
C			SOR00120
	IF(NUM.EQ.1) RETURN		SOR00130
	JK=NUM-1		SOR00140
	DO 10 I=1,JK		SOR00150
	KK=I+1		SOR00160
	DO 10 J=KK,NUM		SOR00170
	IF(RA(I).GT.RA(J)) GO TO 15		SOR00180
	XX=RA(I)		SOR00190
	RA(I)=RA(J)		SOR00200
	RA(J)=XX		SOR00210
	II=IA(I)		SOR00220
	IA(I)=IA(J)		SOR00230
	IA(J)=II		SOR00240
10	CONTINUE		SOR00250
	RETURN		SOR00260
	END		SOR00270

JUN 74 )

OS/360 FCRTRAN H

COMPILER OPTIONS - NAME= MAIN,OPT=02,LINECNT=56,SIZE=0000K,  
 SOURCE,EBCDIC,NOLIST,NODECK,LCAD,MAP,NOEDIT,IC,ACXREF  
 SUBROUTINE STAMFB (I,H2PQ,\*)

```

C *****
C THIS ROUTINE CALCULATES THE STRUCTURAL AMPLIFICATION FUNCTION
C INTEGRATED OVER A BAND. THIS IS USED BY MAIN PROGRAM 'STRBAN'.
C *****
C
  IMPLICIT REAL*8 (A-D,F-H,C-Z)
  COMMON /STDAMP/STDAMA,STDAMB
  COMMON/CONST/PI
  COMMON /FREQ/WSQ
  COMMON /INFO/INDEX
  COMMON /LEAD/HFTERM,BBB
  COMMON /STRUCT/STMODS(120),MPQ(120),STMCD3(400,3),MPC3(400),
  1      NUMST,NUM3
C
C      FIND INDEX FOR CONSTANTS
  DO 10 J=1,NUM3
    IF(MPQ3(J).EQ.MPQ(1)) GO TO 20
  10 CONTINUE
  WRITE(7,2000) I
  2000 FORMAT(IX,'CONSTANTS NOT FOUND FOR MODAL INDEX ',I9,/)
  WRITE(6,2002)
  2002 FORMAT(1H0,'INDEX',5X,' MPQ ',5X,'STMODS',/)
  DO 3000 JJJ=1,NUMST
    WRITE(6,2003)JJJ,MPQ(JJJ),STMODS(JJJ)
  2003 FORMAT(1H ,I5,5X,I9,5X,D10.4)
  3000 CONTINUE
  RETURN 1
C
C      FIND SECOND FREQUENCY AND DESTROY ITS INDICES SO THAT IT WILL
C      NOT BE USED AGAIN AS A FIRST FREQUENCY BY MISTAKE
  20 ITST=MPQ(I)
  W2PQ1=STMODS(I)
  DO 30 JK=1,NUMST
    IF(MPQ(JK).EQ.ITST.AND.I.NE.JK) GO TO 40
  30 CONTINUE
  WRITE(7,2001)
  2001 FORMAT(IX,'SECOND FREQUENCY NOT FOUND')
  RETURN 1
  40 W2PQ2=STMODS(JK)
C      INDEX IS USED IN THE ERROR MESSAGE INDICATING MODE EXHAUSTION
  JKKK=JK+1
  DO 70 JKK=JKKK,NUMST
    IF(MPQ(JKK).EQ.ITST.AND.I.NE.JKK) GO TO 80
  70 CONTINUE
  WRITE(7,2004)
  2004 FORMAT(IX,'THIRD FREQUENCY NOT FOUND')
  RETURN 1
  80 W2PQ3 = STMODS(JKK)
  INDEX = MPQ(JKK)

```

STA00010  
 STA00020  
 STA00030  
 STA00040  
 STA00050  
 STA00060  
 STA00070  
 STA00080  
 STA00090  
 STA00100  
 STA00110  
 STA00120  
 STA00130  
 STA00140  
 STA00150  
 STA00160  
 STA00170  
 STA00180  
 STA00190  
 STA00200  
 STA00210  
 STA00220  
 STA00230  
 STA00240  
 STA00250  
 STA00260  
 STA00270  
 STA00280  
 STA00290  
 STA00300  
 STA00310  
 STA00320  
 STA00330  
 STA00340  
 STA00350  
 STA00360  
 STA00370  
 STA00380  
 STA00390  
 STA00400  
 STA00410  
 STA00420  
 STA00430  
 STA00440  
 STA00450  
 STA00460  
 STA00470  
 STA00480  
 STA00490  
 STA00500  
 STA00510  
 STA00520

ORIGINAL PAGE IS  
 OF POOR QUALITY

```

C      STRUCTURAL AMPLIFICATION FUNCTION
      AFACT=STDAMA/((2.00*PI)**STDAMB)
      AFACT=AFACT*AFACT
      BFACT=1.00+STDAMB
      SQETA1=AFACT*W2PQ1**BFACT
      SQETA2=AFACT*W2PQ2**BFACT
      SQETA3=AFACT*W2PQ3**BFACT
      H2PQ = HFTERM*((WSQ-STMOD3(J,1))*(WSQ-STMOD3(J,2))
1      -STMOD3(J,3))**2
      H2PQ = H2PQ/((DSQRT(SQETA1)/PI)
1      *((W2PQ2-WSQ)**2+SQETA2*WSQ)
2      *((W2PQ3-WSQ)**2+SQETA3*WSQ))
      RETURN
      END

```

```

STA00530
STA00540
STA00550
STA00560
STA00570
STA00580
STA00590
STA00600
STA00610
STA00620
STA00630
STA00640
STA00650
STA00660

```

( JUN 74 )

CS/360 FORTRAN H

COMPILER OPTIONS - NAME= MAIN,OPT=02,LINECNT=56,SIZE=0000K,  
SOURCE,EBCDIC,NOLIST,NCDECK,LCAD,MAP,ACEDIT,ID,NCXREF  
SUBROUTINE STAMFC (I,M,N,IQ,HGAMI,\*)

```
C
C*****
C
C THIS ROUTINE CALCULATES THE STRUCTURAL AMPLIFICATION FUNCTION
C SQUARED TIMES THE ACCEPTANCE FUNCTION FOR STRUCTURAL MODES
C SQUARED TIMES THE ACCEPTANCE FUNCTION BETWEEN THE EXTERNAL
C PRESSURE FIELD AND STRUCTURAL MODES. THIS IS THE TERM WHICH
C COMPRISES THE SUM OVER THE IP STRUCTURAL MODE INDICES. THIS
C ROUTINE IS USED BY MAIN PROGRAMS 'PURTCN' AND 'ACCBAN'.
C*****
C
C IMPLICIT REAL*8 (A-D,F-H,C-Z)
C COMMON /STDAMP/STDAMA,STDAMB
C COMMON/CONST/PI
C COMMON /FREQ/WSQ
C COMMON /INFO/INDEX
C COMMON /LEAD/HFTERM,BBB
C COMMON /SAMPLE/TEMP(1200),LPQS(1200),NUMTMP
C COMMON /STRUCT/STMODS(1200),MPC(1200),STMOD3(400,3),MPC3(400),
C 1 NUMST,NUM3
C
C FIND ASSOCIATED THIRD FREQUENCY
C DO 10 J=1,NUM3
C IF(MPC3(J).EQ.LPQS(I)) GO TO 23
10 CONTINUE
C WRITE(7,2000) I
2000 FORMAT(1X,'CONSTANTS NOT FOUND FOR MODAL INDEX ',I9,/)
C WRITE(6,2002)
2002 FORMAT(1H,'INDEX',5X,' LPQS ',5X,'TEMP',/)
C DO 3000 JJJ=1,NUMTMP
C WRITE(6,2003)JJJ,LPQS(JJJ),TEMP(JJJ)
2003 FORMAT(1H,'I5,5X,I9,5X,D10.4)
3000 CONTINUE
C RETURN I
C FIND SECOND FREQUENCY AND DESTROY ITS INDICES SO THAT IT WILL
C NOT BE USED AGAIN AS A FIRST FREQUENCY BY MISTAKE
20 ITST=LPQS(I)
C UNPACK THE IP INDEX
C IQ = LPQS(I)/1000
C IP=MOD(LPQS(I),1000)
C LPQS(I)=999999
C W2PQ1=TEMP(I)
C DO 30 JK=1,NUMTMP
C IF(LPQS(JK).EQ.ITST) GO TO 40
30 CONTINUE
C WRITE(7,2001)
2001 FORMAT(1X,'SECOND FREQUENCY NOT FOUND')
C RETURN I
40 W2PQ2=TEMP(JK)
C INDEX IS USED IN THE ERROR MESSAGE INDICATING MODE EXHAUSTION
```

STAC0010  
STAC0020  
STAC0030  
STAC0040  
STAC0050  
STAC0060  
STAC0070  
STAC0080  
STAC0090  
STAC0100  
STAC0110  
STAC0120  
STAC0130  
STAC0140  
STAC0150  
STAC0160  
STAC0170  
STAC0180  
STAC0190  
STAC0200  
STAC0210  
STAC0220  
STAC0230  
STAC0240  
STAC0250  
STAC0260  
STAC0270  
STAC0280  
STAC0290  
STAC0300  
STAC0310  
STAC0320  
STAC0330  
STAC0340  
STAC0350  
STAC0360  
STAC0370  
STAC0380  
STAC0390  
STAC0400  
STAC0410  
STAC0420  
STAC0430  
STAC0440  
STAC0450  
STAC0460  
STAC0470  
STAC0480  
STAC0490  
STAC0500  
STAC0510  
STAC0520



```

      LPQS(JK)=999999
      GO TO JKK=JK,NUMTMP
      IF(LPQS(JKK).EQ.ITST) GO TO 80
70  CONTINUE
      WRITE(7,2004)
2004  FORMAT(1X,'THIRD FREQUENCY NOT FOUND')
      RETURN 1
80  W2PQ3 = TEMP(JKK)
      INDEX = LPQS(JKK)
      LPQS(JKK) = 999999
C      CHECK FOR ZERO CASE
      AMAG=GAMA(M,IP)
      IF(AMAG.EQ.0.00) GO TO 50
C      STRUCTURAL AMPLIFICATION FUNCTION
      AFACT=STDAMA/((2.00*PI)**STDAMB)
      AFACT=AFACT*AFACT
      BFACT=1.00+STDAMB
      SQETA1=AFACT*W2PQ1**BFACT
      SQETA2=AFACT*W2PQ2**BFACT
      SQETA3=AFACT*W2PQ3**BFACT
      H2PQ = HFTERM*((WSQ-STMOD3(J,1))*(WSQ-STMOD3(J,2))
1      -STMOD3(J,3))**2
      H2PQ = H2PQ/(((W2PQ1-WSQ)**2+SQETA1*WSQ)
1      *((W2PQ2-WSQ)**2+SQETA2*WSQ)
2      *((W2PQ3-WSQ)**2+SQETA3*WSQ))
      DUMMY=PQJ(IP,IQ,BBB)
      HGAMI=H2PQ*AMAG**2*DUMMY
      RETURN
50  HGAMI=0.00
      RETURN
      END

```

```

STA00530
STA00540
STA00550
STA00560
STA00570
STA00580
STA00590
STA00600
STA00610
STA00620
STA00630
STA00640
STA00650
STA00660
STA00670
STA00680
STA00690
STA00700
STA00710
STA00720
STA00730
STA00740
STA00750
STA00760
STA00770
STA00780
STA00790
STA00800
STA00810
STA00820
STA00830

```

ORIGINAL PAGE IS  
UNCLASSIFIED

( JUN 74 )

05/360 FORTRAN H

JMPILER OPTIONS - NAME= MAIN,OPT=02,LINECNT=56,SIZE=CCOCK,  
SOURCE,EBCDIC,NOLIST,NODECK,LCAD,MAP,NOEDIT,IC,ACXREF  
FUNCTION PPN (N,IP)

```
C *****  
C THIS FUNCTION CALCULATES THE ACCEPTANCE BETWEEN THE EXTERNAL  
C PRESSURE FIELD AND THE STRUCTURAL MODES.  
C *****  
C  
C IMPLICIT REAL*8 (A-D,F-H,C-Z)  
C COMMON /CONST/PI  
C COMMON /FREQ/WSQ  
C COMMON /MORE/PFRONT,WOLC,WOLCPI,RECIP,CBW,PICER,PICEPI,  
1 WOLCOS,PICCOS,QTERM  
C  
C PPI=IP*PI  
C ZONE=WOLC+PPI  
C ZTWO=WOLC-PPI  
C EVALUATE THE SI AND CIN FUNCTIONS FOR THE 'P' TERM  
C CALL SINCOS(ZONE,SINONE,COSCNE)  
C CALL SINCOS(ZTWO,SINTWO,CCSTWO)  
C DJ=1.00  
C IIP=IP  
C CHECK IF IIP IS EVEN OR ODD  
C IF(MOD(IIP,2).NE.0) DJ=-1.00  
C PTERM=PFRONT*((PI/2.00)*(SINCNE+SINTWC)+(COSCNE-CCSTWO)/(2.00*IP))  
C CHECK FOR SPECIAL CASE  
C IF((WOLCPI-IP*IP*RECIP).NE.0.00) PTERM=PTERM-PFRONT*  
1 ((1.00-DJ*WOLCOS)/(WOLCPI-IP*IP*RECIP))  
C IF(N.EQ.0) GO TO 10  
C PPI=2.00*PI*N  
C ZONE=PICEPI+PPI  
C ZTWO=PICEPI-PPI  
C EVALUATE THE SI AND CIN FUNCTIONS FOR THE 'Q' TERM  
C CALL SINCOS(ZONE,SINONE,COSCNE)  
C CALL SINCOS(ZTWO,SINTWO,CCSTWO)  
C QTERM=CBW*(PI*(SINONE+SINTWC)-(COSCNE-CCSTWO)/(2.00*N))  
C IF((PICER-N*N*CBW).NE.0.00) QTERM=QTERM-CBW*(1.00-PICCOS)/  
1 (PICER-N*N*CBW)  
C PPN=PTERM*QTERM  
C RETURN  
C USE LIMITING FORM OF 'Q' TERM  
10 PPN=PTERM*QTERM  
C RETURN  
C END
```

PPN00010  
PPN00020  
PPN00030  
PPN00040  
PPN00050  
PPN00060  
PPN00070  
PPN00080  
PPN00090  
PPN00100  
PPN00110  
PPN00120  
PPN00130  
PPN00140  
PPN00150  
PPN00160  
PPN00170  
PPN00180  
PPN00190  
PPN00200  
PPN00210  
PPN00220  
PPN00230  
PPN00240  
PPN00250  
PPN00260  
PPN00270  
PPN00280  
PPN00290  
PPN00300  
PPN00310  
PPN00320  
PPN00330  
PPN00340  
PPN00350  
PPN00360  
PPN00370  
PPN00380  
PPN00390  
PPN00400  
PPN00410  
PPN00420  
PPN00430  
PPN00440  
PPN00450

( JUN 74 )

OS/360 FORTRAN H

COMPILER OPTIONS - NAME= MAIN,OPT=02,LINECNT=56,SIZE=C000K,  
SOURCE,EBCDIC,NOLIST,NODECK,LCAD,MAP,ACEDIT,IC,NCXREF  
SUBROUTINE SINCOS (Z,SININT,COSINT)

```
C
C*****C
C THIS ROUTINE CALCULATES THE VALUE OF THE SINE AND COSINE C
C INTEGRAL FUNCTIONS. THE COSINE FUNCTION EVALUATED IS ACTUALLY C
C THE CIN FUNCTION. SERIES TECHNIQUES ARE USED FOR ARGUMENTS C
C LESS THAN ONE. RATIONAL APPROXIMATIONS ARE OTHERWISE USED. C
C*****C
C
C IMPLICIT REAL*8 (A-D,F-H,C-Z)
C DIMENSION FAX(4),FBX(4),GAX(4),GBX(4)
C COMMON /CONST/PI
C COMMON /CONV/UP,DN
C COMMON /CTRL/FAC(57),PSI(60)
C DATA FAX/38.027264,265.187033,335.67732,38.102495/
C DATA FBX/43.721433,322.624911,575.236280,157.105423/
C DATA GAX/42.242855,332.757865,352.318498,21.821899/
C DATA GBX/48.156527,482.485984,1114.978885,449.690326/
C
C IF(Z.EQ.C.D0) GO TO 40
C IF(DABS(Z).GE.1.D0) GO TO 30
C XX=Z
C EJ=1.
C SUMSIN=0.00
C SUMCOS=0.00
C DO 10 I=1,57
C K=2*I-1
C L=K+1
C TOT SIN=SUMSIN+(EJ*XX)/(K*FAC(L))
C EJ=-EJ
C XX=XX*Z
C K=2*I
C L=K+1
C TOT COS=SUMCOS+(EJ*XX)/(K*FAC(L))
C IF(TOT SIN.EQ.0.D0) GO TO 5
C IF THE SIN SERIES HAS CONVERGED THEN THE CIN SERIES
C HAS ALSO CONVERGED
C VAL=SUMSIN/TOT SIN
C IF(VAL.GT.DN.AND.VAL.LT.UP) GO TO 20
C 5 XX=XX*Z
C SUMCOS=TOT COS
C SUMSIN=TOT SIN
C 10 CONTINUE
C 20 SININT=TOT SIN
C COSINT=-TOT COS
C RETURN
C 30 Z2=Z*Z
C Z4=Z2*Z2
C Z6=Z4*Z2
C Z8=Z6*Z2
```

SIN00010  
SIN00020  
SIN00030  
SIN00040  
SIN00050  
SIN00060  
SIN00070  
SIN00080  
SIN00090  
SIN00100  
SIN00110  
SIN00120  
SIN00130  
SIN00140  
SIN00150  
SIN00160  
SIN00170  
SIN00180  
SIN00190  
SIN00200  
SIN00210  
SIN00220  
SIN00230  
SIN00240  
SIN00250  
SIN00260  
SIN00270  
SIN00280  
SIN00290  
SIN00300  
SIN00310  
SIN00320  
SIN00330  
SIN00340  
SIN00350  
SIN00360  
SIN00370  
SIN00380  
SIN00390  
SIN00400  
SIN00410  
SIN00420  
SIN00430  
SIN00440  
SIN00450  
SIN00460  
SIN00470  
SIN00480  
SIN00490  
SIN00500  
SIN00510  
SIN00520

C

## RATIONAL APPROXIMATION

$$FOFZ = (1.00/Z) * ((Z^8 + FAX(1)*Z^6 + FAX(2)*Z^4 + FAX(3)*Z^2 + FAX(4)) /$$

$$1 \quad (Z^8 + FBX(1)*Z^6 + FBX(2)*Z^4 + FBX(3)*Z^2 + FBX(4)))$$

$$GOFZ = (1.00/Z^2) * ((Z^8 + GAX(1)*Z^6 + GAX(2)*Z^4 + GAX(3)*Z^2 + GAX(4)) /$$

$$1 \quad (Z^8 + GBX(1)*Z^6 + GBX(2)*Z^4 + GBX(3)*Z^2 + GBX(4)))$$

$$SININT = \pi/2.00 - FOFZ * DCOS(Z) - GCFZ * DSIN(Z)$$

$$CIOFZ = FOFZ * DSIN(Z) - GOFZ * DCOS(Z)$$

C

PSI(1) IS NEGATIVE EULER'S CONSTANT

$$COSINT = -CIOFZ + DLOG(DABS(Z)) - PSI(1)$$

RETURN

40 SININT=0.00

COSINT=0.00

RETURN

END

SIN00530

SIN00540

SIN00550

SIN00560

SIN00570

SIN00580

SIN00590

SIN00600

SIN00610

SIN00620

SIN00630

SIN00640

SIN00650

SIN00660

F88-LEVEL LINKAGE EDITOR OPTIONS SPECIFIED MAP,LET,LIST  
 DEFAULT OPTION(S) USED - SIZE=(131072,32768)

MODULE MAP

CONTROL SECTION

ENTRY

NAME	ORIGIN	LENGTH	NAME	LOCATION	NAME	LOCATION
MAIN	00	167A				
AMCDES	1680	82C				
BESSEL	2180	508				
BLJDEF	2788	2A6				
BLYDEF	2A30	396				
CAPGAM	2DC8	3A0				
COPYC	3168	13E				
CUBIC	32A8	364				
CONST	361C	8				
CCNV	3618	10				
DIR	3628	8				
FCTRL	363C	3A8				
DOB	39C8	2D0				
FNDNST	3CA8	2D8				
FNDNXT	3F80	3CE				
FRSFND	4290	236				
GAMA	44C8	3AC				
HSQMNB	4878	5FA				
HSQMNS	4E78	60A				
MCAHNN	5488	4A0				
MNCALB	5928	1EA				
MNCALC	5B18	2F8				
MNSUM	5E1C	3AE				
NXTMN	61C0	19C				
PCALB	636C	21C				
PCALCC	6580	48C				
PQJ	6A00	56C				
PSQS	6F70	314				
CSQ	7288	262				
RECUR	74FC	1BE				
REGFAL	768C	29A				
ROCT	7950	276				
SCALC	7BC8	432				
SCALCB	800C	254				
SMOOSC	8258	F74				
SORT	91C0	2C6				
STAMFB	93C8	5EC				
STAMFC	99C8	71E				
PPN	A0E8	3AE				
SINCCS	A499	55E				
IHCLSCN *	A9F8	26C	DCOS	A9F8	DSIN	AA12
IHCLLOG *	AC68	2C0	DLOG10	AC68	DLOG	AC80

ORIGINAL PAGE IS  
 OF POOR QUALITY

NAME	ORIGIN	LENGTH	NAME	LOCATION	NAME	LOCATION
IHCLSQRT*	AE68	15B	DSQRT	AE68		
IHCFCPT *	AFC8	3C4	ERRSET	AFC8	ERRSAV	91C2
IHCFCXPD*	B2C3	1A3	FDXPD#	B2D0		
IHCFCXPI*	B470	14D	FDXPI#	B470		
IHCFCOMH*	B5C3	F61	IBCOM#	B5C0	FDICLS#	B67C
IHCFCOMH2*	C528	65D	SEQDASD	C8A3		
SDUMP *	C888	1E	ADCON#	C8A8	FCVACUTP	CC52
IHCFCVTH*	C8A8	11B5	FCVIDUTP	D1E5	FCVECLTP	D6F0
IHCFCNTH*	DD60	542	ARITH#	DD60	ACJSWTH	E0FC
IHCLASCN*	E2A8	24F	DARCOS	E2A8	DARSIN	E2C3
IHCLEXP *	E4F8	288	DEXP	E4F8		
IHCFCIOS*	E78C	F28	FIOCS#	E78C	FICCSBEP	E786
IHCFCIOS2*	F6A8	52E				
IHCERRM *	F8D8	5CC	ERRMON	F8D8	IHCERRE	F8F3
IHCLOPT *	10188	3A3				
IHCETRCH*	10558	26E	IHCTRCH	10556	ERRTRA	10560
IHCUTBL*	107E8	628				
ACCEPT	10E20	8				
BESQR	10E28	8				
EIGEN	10E3C	18				
FINAL	10E48	58				
FREQ	10EA0	8				
HALT	10EA8	8				
LEAD	10E80	10				
LEFTRS	10ECC	30				
MORE	10EF0	50				
NORMAL	10F40	8				
RADII	10F48	10				
CTHER	10F58	48				
STCAMP	10FA0	10				
ACCAMP	10F80	10				
STOP	10FC0	C				
TABS	10FD0	C				
TERMS	10FE0	38				
VARSG	11018	10				
VRBLS	11028	18				
ACUSTK	11040	17704				
SCLNS	28748	12C4				

NAME	ORIGIN	LENGTH	NAME	LOCATION	NAME	LOCATION
STRUCT	29A10	6408				
EPRCOR	2FE18	23				
SAMPLE	2FE38	3844				
ERROR	33680	4				
TOTALS	33688	30				
INFC	33688	4				

ENTRY ADDRESS 00  
TCTAL LENGTH 336C0

\*\*\*MAIN DOES NOT EXIST BUT HAS BEEN ADDED TO DATA SET

JCB TITLE:

BBN TEST NO. 2 AND 3

INPUT DATA:

LENGTH OF CYLINDER =	60.00000	FEET
LENGTH OF SEGMENT =	60.00000	FEET
SEGMENT DISTANCE FROM END OF CYLINDER =	0.0	FEET
RADIUS OF INNER CYLINDER =	0.0	FEET
RADIUS OF OUTER CYLINDER =	8.00000	FEET
SHELL STRUCTURAL THICKNESS =	0.00400	FEET
SHELL FILLER THICKNESS =	0.05000	FEET
SHELL DENSITY =	0.09890	SLUGS/FOOT**2
LONGITUDINAL YOUNGS MODULUS =	.18432E 10	LBS/FT**2
CIRCUMFERENTIAL YOUNGS MODULUS =	.50400E 09	LBS/FT**2
POISSON'S RATIO =	0.30000	
SPEED OF SOUND =	1116.00000	FEET/SECCAD
FRAME AREA =	.586100-C2	FEET**2
FRAME MOMENT OF INERTIA =	.183000-C3	FEET**4
FRAME-SKIN CENTROID DIST =	.109000 C0	FEET
FRAME SPACING =	.158000 01	FEET
FRAME YOUNGS MODULUS =	.18432E 10	LBS/FT**2

ADJUST CIRCUMFERENTIAL BENDING STIFFNESS BY 0.0500



# ACOUSTIC MODAL FREQUENCIES AND INDICES

INDICES	FREQUENCIES	INDICES	FREQUENCIES	INDICES	FREQUENCIES
20000000	279.0	22001002	278.9	24006000	278.5
23003001	278.2	29002000	278.1	19008000	277.7
20004001	277.6	27001001	277.6	18002002	277.5
27004000	277.5	10001000	277.4	16005001	276.9
10006001	276.6	28003000	276.6	25002001	276.1
10001003	276.0	15009000	275.7	17000003	275.7
12003002	275.5	9010000	274.4	28000001	273.9
9006001	273.7	9501003	273.0	29001000	272.8
21007000	272.6	25005000	272.7	24000002	272.2
21001002	272.1	18005001	272.1	17002002	272.0
11003002	271.9	18008000	271.8	8010000	271.7
19004001	271.5	22003001	271.2	14009000	271.1
23006000	271.1	8706001	271.0	16000003	270.5
8001003	270.3	29000000	269.7	7010000	269.3
26001001	269.2	28002000	269.1	26004000	269.1
7006001	268.6	10003002	268.5	24002001	268.3
7001003	267.9	27003000	267.9	14005001	267.4
6010000	267.2	13009000	266.8	16002002	266.7
6006001	266.4	17008000	266.2	20007000	266.2
6001003	265.6	20001002	265.5	18004001	265.5
15000003	265.5	9002002	265.5	5010000	265.4
27000001	265.1	24005000	264.8	5006001	264.7
23000002	264.6	21003001	264.2	5001003	264.0
4010000	264.0	22006000	263.8	28001000	263.6
4006001	263.2	13005001	263.0	3010000	262.8
12009000	262.7	8002002	262.7	4001003	262.5
3006001	262.0	2010000	262.0	15002002	261.6
1510000	261.5	3001003	261.4	10000	261.3
2006001	261.2	25001001	260.9	16008000	260.8
25004000	260.8	14000003	260.7	1006001	260.7
23002001	260.6	2001003	260.6	6001	260.5
28000000	260.4	7003002	260.2	27002000	260.1
1001003	260.1	1003	259.9	19007000	259.8
17004001	259.7	26003000	259.2	19001002	259.1
11009000	258.9	12005001	258.9	6003002	258.0
20003001	257.4	22000002	257.1	23005000	257.0
14002002	256.8	21006000	256.7	26000001	256.3
13000003	256.2	5002002	256.2	15008000	255.6
10009000	255.4	11005001	255.0	4003002	254.6
27001000	254.4	16004001	254.2	18007000	253.6
3003002	253.4	22002001	253.0	18001002	252.9
24001001	252.6	2003002	252.6	24004000	252.5
13002002	252.2	9009000	252.1	1003002	252.1
12000003	251.9	3002	251.9	10005001	251.4
26002000	251.1	27000000	251.1	19003001	250.8
14008000	250.7	25003000	250.5	21000002	249.8
20006000	249.7	22005000	249.3	8009000	249.2
15004001	248.9	9005001	248.1	11000003	248.0
12002002	247.9	25000001	247.6	17007000	247.5
17001002	246.6	7009000	246.6	13008000	245.9

# ACQUSTIC MODAL FREQUENCIES AND INDICES

INDICES	FREQUENCIES	INDICES	FREQUENCIES	INDICES	FREQUENCIES
21002001	245.6	26001000	245.2	8005001	245.1
23001001	244.5	18003001	244.3	23004000	244.3
6009000	244.3	10006003	244.3	11002002	243.8
14004001	243.8	19006000	242.8	20000012	242.6
7005001	242.5	5009000	242.3	25002000	242.2
24003000	241.9	26000000	241.8	21005000	241.7
16007000	241.7	12008000	241.5	16001002	241.0
9000003	240.9	4009000	240.7	6005001	240.1
10002002	240.1	3009000	239.4	13004001	238.9
24001001	238.9	2009000	238.5	20002001	238.3
5005001	238.1	17003001	238.0	1009000	238.0
9000	237.8	8000003	237.8	11008000	237.4
9002002	236.6	4005001	236.5	22001001	236.4
22004000	236.2	18006000	236.1	25001000	236.1
15007000	236.1	19000002	235.6	15001002	235.3
3005001	235.2	7000003	235.1	12004001	234.4
2005001	234.3	20005000	234.3	1005001	233.7
5001	233.6	8002002	233.5	10008000	233.5
23003000	233.4	24002000	233.3	6000003	232.7
25000000	232.5	16003001	232.0	19002001	231.1
7002002	230.7	14007000	230.7	5000003	230.6
23005001	230.2	11004001	230.1	9008000	230.0
14001002	229.9	17006000	229.6	4000003	228.9
18000002	228.7	21001001	228.4	6002002	228.3
21004000	228.2	3000003	227.6	19005000	227.0
24001000	226.9	8008000	226.7	2000003	226.6
5002002	226.2	15003001	226.1	10004001	226.1
1000003	226.1	3	225.9	13007000	225.6
22003000	224.9	13001002	224.8	4002002	224.4
23002000	224.4	18002001	224.0	7008000	223.9
16006000	223.3	24000000	223.2	3002002	223.1
9004001	222.4	2002002	222.1	17000002	221.9
22000001	221.6	1002002	221.5	2002	221.3
6008000	221.3	12007000	220.7	14003001	220.5
20001001	220.5	20004000	220.3	12001002	219.9
18005000	219.8	5008000	219.2	8004001	219.1
23001000	217.8	4008000	217.4	15006000	217.2
17002001	217.2	21003000	216.4	11007000	216.2
7004001	216.1	3008000	216.0	22002000	215.5
16000002	215.4	11001002	215.4	13003001	215.1
2008000	215.0	1308000	214.4	8000	214.2
23000000	213.9	6004001	213.5	21000001	213.0
17005000	212.8	19001001	212.7	19004000	212.5
10007000	211.9	14006000	211.4	5004001	211.3
10001002	211.1	16002001	210.5	12003001	210.1
4004001	209.4	15000002	209.1	22001000	208.6
20003000	208.1	9007000	208.0	3004001	208.0
9001002	207.2	2004001	206.9	21002000	206.7
1004001	206.3	4001	206.1	16005000	206.0
13006000	205.8	11003001	205.3	18001001	205.0

# ACOUSTIC MODAL FREQUENCIES AND INDICES

INDICES	FREQUENCIES	INDICES	FREQUENCIES	INDICES	FREQUENCIES
18004000	204.8	22000000	204.6	20000001	204.5
8007000	204.5	15002001	204.0	8001002	203.6
14000002	203.6	7007000	201.3	10003001	200.8
12006000	200.5	7001002	200.4	15003000	199.8
21001000	199.5	15005000	199.4	6007000	198.4
20002000	198.6	14002001	197.8	6001002	197.6
17001001	197.5	17004000	197.3	13000002	197.2
9003001	196.7	19000001	196.1	5007000	196.0
11006000	195.5	21000000	195.3	5001002	195.1
4007000	194.5	4001002	193.1	14005000	193.0
8003001	192.9	3007000	192.5	13002001	191.8
18003000	191.6	12000002	191.6	3001002	191.6
2007000	191.3	13006000	190.8	1007000	190.7
20001000	190.4	7000	190.4	2001002	190.4
16001001	190.1	16004000	189.9	1001002	189.8
1002	189.5	7003001	189.5	15002000	189.3
18000001	187.8	13005000	186.8	6003001	186.5
9006000	186.4	11000002	186.4	12002001	186.1
20000000	186.0	5003001	183.9	17003000	183.6
15001001	183.0	15004000	182.7	8006000	182.4
4003001	181.8	10000002	181.4	15001000	181.4
12005000	180.5	11002001	180.7	18002000	180.6
3003001	180.1	17000001	179.5	2003001	178.9
7006000	178.8	1003001	178.2	3001	178.0
9000002	176.8	19000000	176.7	14001001	176.0
14004000	175.8	6006000	175.6	16003000	175.6
10002001	175.6	11005000	175.4	5006000	172.9
8000002	172.6	18001000	172.3	17002000	172.0
16000001	171.4	9002001	170.8	4006000	170.6
10005000	170.1	13001001	169.2	13004000	169.0
3006000	168.9	7000002	168.8	15003000	167.8
2006000	167.6	18000000	167.4	1006000	166.8
6000	166.5	8002001	166.4	6000002	165.5
9005000	165.2	16002000	163.5	15000001	163.4
17001000	163.3	12001001	162.7	5000002	162.6
7002001	162.5	12004000	162.5	8005000	160.7
14003000	160.2	4000002	160.1	6002001	159.0
3000002	158.2	17000000	158.1	2000002	156.9
7005000	156.6	11001001	156.5	11004000	156.2
1000002	156.0	5002001	156.0	2	155.8
14000001	155.5	15002000	155.1	16001000	154.3
4002001	153.5	6003000	153.0	13003000	152.7
3002001	151.5	10001001	150.5	10004000	150.3
2002001	150.1	5005000	149.8	1002001	149.2
2001	148.9	16000000	148.8	13000001	147.8
4005000	147.2	14002000	146.8	12003000	145.4
15001000	145.4	3005000	145.1	5001001	145.0
9004000	144.7	2005000	143.6	1005000	142.7
5000	142.4	12000001	140.3	8001001	139.8
8004000	139.5	15000000	139.5	13002000	138.6

# ACOUSTIC MODAL FREQUENCIES AND INDICES

NOICES	FREQUENCIES	INDICES	FREQUENCIES	INDICES	FREQUENCIES
11003000	138.4	14001000	136.5	7001001	135.1
7004000	134.8	11000001	133.1	10003000	131.7
6001001	130.9	12002000	130.6	6004000	130.6
14000000	130.2	13001000	127.6	5001001	127.2
5004000	126.9	10000001	126.0	9003000	125.3
4001001	124.1	4004000	123.8	11002000	122.7
3001001	121.6	3004000	121.3	13000000	120.9
2001001	119.8	2004000	119.5	9000001	119.3
8003000	119.2	12001000	118.9	1001001	118.7
1004000	118.4	1001	118.4	4000	118.1
10002000	115.1	7003000	113.7	8000001	113.0
12000000	111.6	11001000	110.2	6003000	108.7
9002000	107.7	7000001	107.1	5003000	104.2
11000000	102.3	6000001	101.7	10001000	101.6
8002000	100.7	4003000	100.4	3003000	97.4
5000001	97.0	2003000	95.1	7002000	94.0
1003000	93.7	3000	93.3	9001000	93.1
10000000	93.0	4000001	92.8	3000001	89.5
6002000	87.8	2000001	87.1	1000001	85.6
1	85.1	8001000	84.9	9000000	83.7
5002000	82.2	4002000	77.3	7001000	76.9
8000000	74.4	3002000	73.3	2002000	70.3
6001000	69.2	1002000	68.4	2000	67.8
7000000	65.1	5001000	61.9	6000000	55.8
4001000	55.3	3001000	49.5	5000000	46.5
2001000	44.9	1001000	41.9	1000	40.9
4000000	37.2	3000000	27.9	2000000	18.6
1000000	9.3	0	0.0	*****	*****

ORIGINAL PAGE IS  
OF POOR QUALITY

# EIGENVALUE RESULTS

INDICES	EIGENVALUES	INDICES	EIGENVALUES	INDICES	EIGENVALUES
0	0.0	1	0.28320 01	2	0.70160 01
3	0.10170 02	1000	0.18410 01	1001	0.52320 01
1002	0.85360 01	1003	0.11710 02	2000	0.30540 01
2001	0.67060 01	2002	0.99700 01	3000	0.42010 01
3001	0.80150 01	3002	0.11350 02	4000	0.53170 01
4001	0.92820 01	5000	0.64150 01	5001	0.10520 02
6000	0.75010 01	6001	0.11730 02	7000	0.85780 01
8000	0.96470 01	9000	0.10710 02	10000	0.11770 02

# STRUCTURAL MODAL FREQUENCIES AND INDICES

INDICES	FREQUENCIES	INDICES	FREQUENCIES	INDICES	FREQUENCIES
20020	5231.0	20019	5016.5	20018	5002.7
20017	4989.7	20016	4977.5	20015	4966.0
20014	4955.2	20013	4945.2	20012	4936.0
20011	4927.5	20010	4919.7	20009	4912.7
20008	4906.4	20007	4900.9	20006	4896.1
20005	4892.0	20004	4888.7	20003	4886.1
20002	4884.3	20001	4883.2	19020	4795.2
19019	4780.0	19018	4765.5	19017	4751.8
19016	4738.9	19015	4726.8	19014	4715.5
19013	4705.0	19012	4695.3	19011	4686.3
19010	4678.1	19009	4670.8	19008	4664.1
19007	4658.3	19006	4653.3	19005	4649.0
19004	4645.5	19003	4642.8	19002	4640.9
19001	4639.7	18020	4560.4	18019	4544.3
18018	4529.0	18017	4514.6	18016	4501.0
18015	4488.2	18014	4476.3	18013	4465.2
18012	4454.9	18011	4445.4	18010	4436.8
18009	4429.0	18008	4422.0	18007	4415.9
18006	4410.6	18005	4406.1	18004	4402.4
18003	4399.5	18002	4397.5	18001	4396.2
17020	4326.7	17019	4309.6	17018	4293.4
17017	4278.1	17016	4263.7	17015	4250.2
17014	4237.5	17013	4225.8	17012	4214.9
17011	4204.9	17010	4195.8	17009	4187.5
17008	4180.1	17007	4173.6	17006	4168.0
17005	4163.2	17004	4159.3	17003	4156.3
17002	4154.1	17001	4152.8	16020	4094.2
16019	4076.1	16018	4058.8	16017	4042.6
16016	4027.2	16015	4012.9	16014	3999.4
16013	3986.9	16012	3975.4	16011	3964.8
16010	3955.1	16009	3946.3	16008	3938.5
16007	3931.5	16006	3925.6	16005	3920.5
16004	3916.4	16003	3913.1	16002	3910.8
16001	3909.5	15020	3863.3	15019	3843.9
15018	3825.5	15017	3808.1	15016	3791.8
15015	3776.4	15014	3762.1	15013	3748.8
15012	3736.4	15011	3725.1	15010	3714.8
15009	3705.4	15008	3697.1	15007	3689.7
15006	3683.3	15005	3677.9	15004	3673.5
15003	3670.1	15002	3667.6	15001	3666.2
14020	3634.2	14019	3613.4	14018	3593.6
14017	3575.0	14016	3557.5	14015	3541.0
14014	3525.7	14013	3511.4	14012	3498.2
14011	3486.1	14010	3475.0	14009	3465.0
14008	3456.0	14007	3448.1	14006	3441.3
14005	3435.5	14004	3430.8	14003	3427.1
14002	3424.5	14001	3422.9	13020	3407.4
13019	3384.9	13018	3363.6	13017	3343.6
13016	3324.7	13015	3307.0	13014	3290.4
13013	3275.0	13012	3260.8	13011	3247.7

# STRUCTURAL MODAL FREQUENCIES AND INDICES

INDICES	FREQUENCIES	INDICES	FREQUENCIES	INDICES	FREQUENCIES
13010	3235.6	13009	3225.0	13008	3215.4
13007	3206.9	13006	3199.6	13005	3193.3
13004	3188.2	13003	3184.3	12020	3183.4
13002	3181.5	13001	3179.8	12019	3159.0
12018	3135.9	12017	3114.2	12016	3093.7
12015	3074.5	12014	3056.5	12013	3039.9
12012	3024.5	12011	3010.3	12010	2997.4
12009	2985.7	12008	2975.3	12007	2966.1
11020	2963.0	12006	2958.2	12005	2951.4
12004	2945.5	12003	2941.7	12002	2938.6
12001	2936.8	11019	2936.4	11018	2911.2
11017	2887.4	11016	2865.0	11015	2844.0
11014	2824.5	11013	2806.3	11012	2789.4
11011	2774.0	11010	2759.9	10020	2747.4
11009	2747.2	11008	2735.9	11007	2725.9
10019	2718.0	11006	2717.2	11005	2709.9
11004	2703.9	11003	2699.2	11002	2695.9
11001	2693.9	10018	2690.3	10017	2664.0
10016	2639.4	10015	2616.3	10014	2594.7
10013	2574.7	10012	2556.2	10011	2539.2
9020	2538.1	10010	2523.7	10009	2509.8
9019	2505.4	10008	2497.3	10007	2486.3
20020	2478.3	10006	2476.8	9018	2474.4
10005	2468.8	10004	2462.2	10003	2457.1
10002	2453.4	10001	2451.3	20019	2447.1
9017	2445.2	9016	2417.7	20018	2417.0
9015	2392.0	20017	2388.1	19020	2386.8
9014	2368.0	20016	2360.5	19019	2354.5
9013	2345.6	8020	2337.3	20015	2334.1
9012	2325.2	19018	2323.3	20014	2309.1
9011	2306.4	8019	2300.4	18020	2296.4
19017	2293.3	9010	2289.2	20013	2285.5
9009	2273.7	8018	2265.5	19016	2264.5
20012	2263.4	18019	2263.0	9008	2259.8
9007	2247.7	20011	2242.8	9006	2237.1
19015	2237.1	8017	2232.6	18018	2230.6
9005	2228.2	20010	2223.8	9004	2220.9
9003	2215.3	9002	2211.3	19014	2211.0
9001	2208.8	17020	2207.4	20009	2206.5
8016	2201.6	18017	2195.5	20008	2190.8
19013	2186.4	20007	2176.9	17019	2172.7
8015	2172.6	18016	2169.6	20006	2164.7
19012	2163.4	20005	2154.3	7020	2148.3
20004	2145.6	8014	2145.6	19011	2141.8
18015	2141.0	17018	2139.2	20003	2139.1
20002	2134.4	20001	2131.5	19010	2122.0
8013	2120.5	16020	2119.3	18014	2113.8
17017	2106.8	7019	2106.3	19009	2103.8
8012	2097.4	18013	2088.1	19008	2087.3
16019	2083.9	6011	2076.2	17016	2075.7

# STRUCTURAL MODAL FREQUENCIES AND INDICES

INDICES	FREQUENCIES	INDICES	FREQUENCIES	INDICES	FREQUENCIES
19007	2072.7	7018	2066.4	18012	2064.0
19006	2059.9	8013	2056.9	16018	2049.1
19005	2049.0	17015	2045.9	18011	2041.4
19004	2040.1	8009	2039.5	15020	2033.7
19003	2033.1	7017	2028.7	19002	2028.0
19001	2025.0	8008	2023.9	18010	2020.6
17014	2017.5	16017	2015.4	8007	2010.3
18009	2001.5	8006	1998.5	15019	1996.6
7016	1993.3	17013	1990.6	8005	1988.5
18008	1984.2	16016	1982.0	8004	1980.3
6020	1975.9	8003	1974.0	8002	1969.5
18007	1968.8	8001	1966.8	17012	1965.3
15018	1960.4	7015	1960.1	18006	1955.4
16015	1951.9	14020	1949.3	18005	1943.9
17011	1941.6	18004	1934.4	7014	1929.1
6019	1927.6	18003	1927.0	15017	1925.4
16014	1922.2	18002	1921.7	17010	1919.7
18001	1918.6	14019	1910.9	7013	1900.4
17009	1899.7	16013	1894.0	15016	1891.6
17008	1881.5	6018	1891.5	7012	1874.0
14018	1873.4	16012	1867.5	13020	1866.8
17007	1865.2	15015	1859.1	17006	1851.0
7011	1849.7	16011	1842.6	17005	1838.9
6017	1837.7	14017	1837.0	17004	1829.9
15014	1828.1	7010	1827.7	13019	1827.1
5020	1826.1	17003	1821.1	16010	1819.6
17002	1815.5	17001	1812.1	7009	1807.9
14016	1801.8	15013	1798.5	16009	1798.4
6016	1796.5	7008	1790.2	13018	1788.3
12020	1786.1	16008	1779.2	7007	1774.6
15012	1770.6	5019	1773.4	14015	1767.9
16007	1762.0	7006	1761.2	6015	1757.7
13017	1750.4	7005	1749.8	16006	1746.9
12019	1745.2	15011	1744.4	7004	1740.6
14014	1735.2	16005	1734.1	7003	1733.4
7002	1728.3	7001	1725.2	16004	1723.5
6014	1721.6	15010	1720.1	5018	1716.9
16003	1715.2	13016	1713.7	16002	1709.2
11020	1707.4	16001	1705.6	12018	1705.0
4020	1704.7	14013	1704.3	15009	1697.7
6013	1688.1	13015	1678.2	15008	1677.4
14012	1674.9	12017	1665.8	5017	1665.7
11019	1665.4	15007	1659.2	6012	1657.2
14011	1647.3	13014	1644.1	15006	1643.2
4019	1641.8	10020	1631.5	15005	1629.5
6011	1628.9	12016	1627.5	11018	1623.9
14010	1621.6	15004	1618.2	5016	1617.0
3020	1614.7	13013	1611.5	15003	1609.4
6010	1603.2	15002	1603.0	15001	1599.2
14009	1597.8	12015	1590.5	10019	1587.5



# STRUCTURAL MODAL FREQUENCIES AND INDICES

INDICES	FREQUENCIES	INDICES	FREQUENCIES	INDICES	FREQUENCIES
11017	1582.3	13012	1580.5	4018	1580.4
6009	1580.1	14008	1576.2	5015	1571.0
6008	1559.6	14007	1556.8	9020	1555.1
12014	1554.7	2520	1554.5	13011	1551.3
3019	1545.8	10018	1545.3	11016	1543.5
6007	1541.5	14006	1539.8	5014	1527.8
6006	1525.9	14005	1525.2	13010	1524.0
4017	1520.8	1020	1520.5	12013	1520.4
14004	1513.1	6005	1512.8	9019	1511.5
11015	1504.6	14003	1503.7	10017	1503.0
6004	1502.1	13009	1498.8	14002	1496.9
6003	1493.8	14001	1492.8	6002	1487.9
12012	1487.7	5013	1487.7	6001	1484.4
2019	1481.8	8020	1480.4	3018	1477.8
13008	1475.8	9018	1468.1	11014	1467.4
4016	1463.4	10016	1461.8	12011	1456.8
13007	1455.1	5012	1450.7	1019	1445.7
13006	1436.9	8019	1436.0	11013	1431.3
12010	1427.8	9017	1425.1	10015	1421.5
13005	1421.2	5011	1416.7	3017	1410.8
2018	1409.3	4015	1408.4	13004	1408.3
7020	1403.1	12009	1400.9	13003	1398.1
11012	1396.7	8018	1392.9	13002	1390.8
13001	1386.3	5010	1386.0	9016	1382.6
10014	1382.3	12008	1376.3	1018	1371.0
11011	1363.9	7019	1361.9	5009	1358.3
4014	1356.2	12007	1354.1	8017	1349.2
3016	1345.1	10013	1344.4	9015	1340.8
2017	1337.3	12006	1334.5	5008	1333.8
11010	1333.1	6020	1327.2	7018	1318.4
12005	1317.7	5007	1312.3	10012	1307.9
4013	1307.1	8016	1305.7	11009	1304.3
12004	1303.7	9014	1299.9	1017	1290.4
5006	1293.8	12003	1292.7	6019	1285.3
12002	1284.7	3015	1280.9	12001	1279.9
5005	1278.3	11008	1277.9	7017	1274.6
10011	1273.1	2016	1265.8	5004	1265.7
8015	1262.7	4012	1261.4	9013	1260.1
5003	1255.9	11007	1254.0	5002	1246.9
5001	1244.7	5020	1243.9	6018	1242.8
10010	1240.2	11006	1232.9	7016	1230.8
1016	1227.0	9012	1221.6	8014	1220.3
4011	1219.3	3014	1218.7	11005	1214.6
10009	1209.4	5019	1203.9	6017	1199.9
11004	1199.4	2015	1194.9	11003	1187.4
7015	1187.0	9011	1184.6	4010	1181.0
10008	1180.9	11002	1178.8	8013	1178.7
11001	1173.6	5018	1163.4	3013	1158.8
6016	1156.5	10007	1155.1	4020	1154.1
9013	1149.5	1015	1147.6	4009	1146.6

# STRUCTURAL MODAL FREQUENCIES AND INDICES

INDICES	FREQUENCIES	INDICES	FREQUENCIES	INDICES	FREQUENCIES
7014	1143.5	8012	1138.2	10006	1132.1
2014	1124.9	5017	1122.2	9009	1116.4
4008	1116.2	4019	1115.6	6015	1112.8
13005	1112.2	3012	1101.8	7013	1100.4
8011	1099.1	10024	1095.6	4007	1089.6
9008	1085.7	15003	1082.5	5016	1080.5
4018	1077.0	1014	1073.5	10002	1073.0
6014	1068.9	13001	1067.2	4006	1066.9
8010	1061.6	3020	1061.4	7012	1058.1
9007	1057.7	2013	1055.8	3011	1048.2
4005	1047.8	4017	1038.0	5015	1038.0
9006	1032.6	4004	1022.4	8009	1026.0
6013	1025.3	3019	1022.9	4003	1020.5
7011	1016.8	4002	1012.1	9005	1010.7
4001	1007.0	1013	999.5	4016	998.6
3015	998.6	5014	995.0	8008	992.7
9004	992.4	2012	988.1	3018	984.7
6012	981.4	5003	977.8	7010	976.9
2020	976.6	9002	967.3	8007	962.1
9001	960.9	4015	958.6	3009	953.6
5013	951.4	3017	946.6	7009	938.7
6011	938.2	2019	936.1	8006	934.5
1012	925.9	2011	922.2	4014	917.9
1020	915.2	3008	913.6	8005	910.4
3016	908.6	5012	907.4	7008	902.6
6010	896.1	2018	895.9	8004	890.0
3007	878.8	4013	876.3	8003	873.7
1019	871.9	3015	870.6	7007	869.1
5011	863.4	8002	861.9	2010	858.7
2017	856.2	6009	855.2	8001	854.6
1011	852.6	3006	849.2	7006	838.6
4012	833.8	3014	832.4	1018	828.8
3005	824.7	5010	819.6	2016	816.9
6008	816.1	7005	811.6	3004	805.0
2009	798.6	3013	793.9	4011	790.5
3003	790.0	7004	788.7	1017	785.8
1010	779.9	3002	779.4	6007	779.4
2015	778.0	5009	776.4	3001	773.2
7003	770.2	7002	756.7	3012	754.7
7001	748.5	4010	748.6	6006	745.5
1016	743.2	2008	743.1	2014	739.7
5008	734.4	6005	715.1	3011	714.6
1009	708.0	4009	702.3	2013	701.8
1015	700.8	5007	694.1	2007	693.5
6004	689.0	3010	673.3	6003	667.8
2012	664.4	1014	658.8	4008	658.1
5006	656.4	6002	652.1	2006	651.0
6001	642.4	1008	637.4	3009	630.7
2011	627.3	5005	622.0	1013	617.3
2005	616.3	4007	614.8	5004	591.8

# STRUCTURAL MODAL FREQUENCIES AND INDICES

INDICES	FREQUENCIES	INDICES	FREQUENCIES	INDICES	FREQUENCIES
2010	590.2	2004	589.3	3008	586.9
1012	576.5	4006	573.0	2003	569.4
1007	568.8	5003	566.9	2002	555.8
2009	552.6	5052	548.2	2001	547.8
3007	542.2	5001	536.6	1011	536.4
4015	533.9	2008	513.8	1006	504.1
4004	498.7	1010	497.4	3006	497.4
2007	473.1	4003	468.8	1009	459.8
3005	453.6	1005	446.6	4002	445.7
20020	441.6	20019	438.2	20018	434.9
20017	431.9	4001	431.1	2006	429.9
20016	429.1	20013	426.4	20014	424.0
1008	423.7	20013	421.7	20012	419.6
20011	417.8	20010	416.0	20009	414.5
20008	413.1	3004	412.3	20007	411.9
20006	410.9	20005	410.0	20004	409.3
20003	408.7	20002	408.3	20001	408.1
19020	402.2	1004	401.9	19019	398.7
19018	395.4	19017	392.3	1007	389.5
19016	389.4	19015	386.7	2005	384.3
19014	384.3	19013	382.7	19012	379.9
19011	378.0	19010	376.2	3003	375.6
19009	374.7	19008	373.3	1003	372.7
19007	372.1	19006	371.0	19005	370.2
19004	369.5	19003	368.9	19002	368.5
19001	368.3	18020	364.8	18019	361.3
18018	357.9	1006	356.3	1002	356.0
18017	354.8	18016	351.9	18015	349.1
1701	347.5	18014	346.6	3002	346.0
18013	344.3	18012	342.2	18011	340.2
18010	338.5	2004	337.8	18009	336.9
18008	335.5	18007	334.3	18006	333.3
18005	332.4	18004	331.7	18003	331.1
18002	330.7	18001	330.5	17020	329.7
3001	326.5	17019	326.0	17018	322.6
1005	321.6	17017	319.4	17016	316.4
17015	313.6	17014	311.1	17013	308.7
17012	306.5	17011	304.6	17010	302.8
17009	301.2	17008	299.8	17007	298.6
17006	297.5	16020	296.8	17005	296.6
17004	295.9	17003	295.4	17002	295.0
17001	294.7	16019	293.0	2003	292.8
16018	289.5	16017	286.2	16016	283.1
1004	285.6	16015	283.3	16014	277.6
16013	275.2	16012	273.0	16011	271.0
16010	269.2	16009	267.5	15020	266.2
16008	266.1	16007	264.9	16006	263.8
16005	262.9	15019	262.3	16004	262.2
16003	261.7	16002	261.3	16001	261.0
15018	258.6	15017	255.2	2002	253.0

# STRUCTURAL MODAL FREQUENCIES AND INDICES

INDICES	FREQUENCIES	INDICES	FREQUENCIES	INDICES	FREQUENCIES
15016	252.0	15015	249.1	15014	246.3
15013	243.8	15012	241.5	15011	239.5
14020	238.1	15010	237.6	15009	236.0
1020	235.0	15008	234.5	14019	234.0
1019	233.3	15007	233.3	15006	232.2
1018	231.5	15005	231.3	15003	231.3
15004	230.6	14018	230.1	15002	229.4
1017	229.7	15002	229.6	1015	225.5
1016	227.7	14017	226.6	1014	223.1
2001	224.0	14016	223.2	14014	217.2
1013	220.1	14015	220.1	14013	214.6
2020	216.7	1012	216.6	14012	212.2
2019	213.2	13020	212.6	2018	209.4
1011	212.2	14011	210.1	1010	206.6
13019	208.3	14010	209.2	14008	205.0
14009	206.5	2017	205.3	14006	202.6
13018	204.2	14007	203.7	2016	200.8
14005	201.7	14004	201.9	14002	200.0
14003	200.4	13017	200.4	13016	196.8
14001	199.8	1009	199.4	13015	193.5
2015	195.9	3020	194.3	12020	190.0
13014	190.5	2014	190.3	13013	187.7
1008	189.8	3019	189.1	2013	183.9
12019	185.2	13012	185.2	12018	181.0
3018	183.7	13011	182.9	1002	178.1
13010	180.9	13009	179.1	1007	177.1
3017	177.9	13008	177.5	13007	176.2
12017	176.8	2012	176.6	13004	173.4
12006	175.0	13005	174.1	13003	172.8
4020	173.1	12016	173.0	3016	171.6
13002	172.4	13011	172.2	2011	168.2
11020	170.6	12015	169.4	11019	165.6
4019	166.9	12014	166.1	11018	160.8
3015	164.8	12013	163.1	12012	160.4
1006	160.5	4018	160.4	3014	157.4
2010	158.5	12011	157.9	12010	155.7
11017	156.4	5020	155.9	4017	153.6
10020	155.1	12009	153.8	12007	150.8
12008	152.2	11016	152.1	3013	149.4
10019	149.6	12016	149.6	11013	148.2
5019	149.1	12005	148.6	12003	147.3
12004	147.9	2009	147.4	4016	146.5
12002	146.9	12001	146.6	9020	144.0
11014	144.5	10018	144.4	11013	141.2
6020	144.0	5018	142.2	1005	139.3
3012	140.6	10017	139.4	8020	138.1
4015	138.9	11012	138.1	6019	137.1
9019	138.0	7020	138.0	10016	134.7
11011	135.4	5017	135.0	9018	132.3
2003	134.5	11010	133.0		

# STRUCTURAL MODAL FREQUENCIES AND INDICES

NOTICES	FREQUENCIES	INDICES	FREQUENCIES	INDICES	FREQUENCIES
8019	131.7	7019	131.2	3011	131.0
4014	130.9	11009	130.8	10015	130.2
6018	130.1	1001	130.0	11008	129.0
5016	127.6	11007	127.5	9017	126.7
11006	126.2	10014	126.1	8018	125.4
11005	125.2	7018	124.5	11004	124.4
11003	123.8	11002	123.4	11001	123.2
6017	123.0	4013	122.5	10013	122.2
9016	121.2	3010	120.5	5015	120.0
2007	119.8	8017	119.2	10012	118.7
7017	117.7	9015	116.2	6016	115.8
10011	115.5	4012	113.6	1004	113.6
8016	113.1	10010	112.7	5014	112.1
9014	111.4	7016	111.0	10009	110.3
3009	109.0	6015	108.5	10008	108.2
8015	107.2	5013	106.9	10007	106.4
10006	105.0	7015	104.4	4011	104.1
5013	104.0	10005	103.8	2006	103.2
10004	103.0	9012	102.7	10003	102.4
10002	101.9	10001	101.7	8014	101.6
6014	101.1	9011	98.8	7014	97.8
3008	96.6	8013	96.1	5012	95.6
9010	95.4	4010	94.2	6013	93.7
9009	92.4	7013	91.3	8012	91.0
9008	89.8	9007	87.7	5011	87.0
6012	86.2	8011	86.2	9006	86.0
7012	85.0	2005	84.7	9005	84.6
4009	83.8	9004	83.7	1003	83.6
3007	83.2	9003	83.0	9002	82.5
9001	82.2	8010	81.8	7011	79.0
6011	78.8	5010	78.2	8009	77.9
8008	74.5	7010	73.3	4008	73.0
8007	71.7	6010	71.5	8006	69.4
5009	69.2	3006	69.2	7009	68.0
8005	67.7	8004	66.5	8003	65.7
8002	65.2	8001	64.9	2004	64.5
6009	64.5	7008	63.3	4007	61.9
5008	60.5	7007	59.2	6008	57.9
7006	55.9	3005	54.6	7005	53.4
5007	52.0	6007	51.8	7004	51.6
4006	50.7	7003	50.5	1002	50.5
7002	49.9	7001	49.6	6006	46.6
5006	43.9	2003	43.4	6005	42.5
4005	42.0	3004	39.8	6004	39.5
6003	37.7	5005	36.9	6002	36.7
6001	36.4	5004	31.3	4004	30.2
5003	27.6	3003	26.0	5002	25.8
5001	25.1	2002	23.1	4003	22.4
1001	17.7	4002	17.6	4001	16.0
3002	14.9	3001	9.3	2001	7.5

# STRUCTURAL CONSTANTS C1 AND INDICIES

INDICES	CONSTANTS	INDICES	CONSTANTS	INDICES	CONSTANTS
1001	130.5	2001	226.0	3001	328.4
4001	452.7	5001	538.0	6001	643.6
7001	749.5	8001	855.6	9001	961.7
10001	1067.9	11001	1174.2	12001	1280.6
13001	1386.9	14001	1493.3	15001	1599.7
16001	1706.1	17001	1812.5	18001	1919.0
19001	2025.4	20001	2131.9	1002	184.7
2002	261.1	3002	353.4	4002	452.0
5002	553.6	6002	656.7	7002	760.8
8002	865.5	9002	970.5	10002	1075.9
11002	1181.5	12002	1287.2	13002	1393.0
14002	1499.0	15002	1605.0	16002	1711.1
17002	1817.2	18002	1923.4	19002	2029.6
20002	2135.9	1003	250.1	2003	310.8
3003	391.6	4003	482.5	5003	578.7
6003	678.0	7003	779.3	8003	881.7
9003	985.1	10003	1089.0	11003	1193.4
12003	1298.2	13003	1403.2	14003	1508.5
15003	1613.9	16003	1719.4	17003	1825.0
18003	1930.8	19003	2036.6	20003	2142.5
1004	320.0	2004	369.3	3004	439.5
4004	522.1	5004	612.1	6004	706.8
7004	804.4	8004	904.0	9004	1005.1
10004	1107.2	11004	1210.0	12004	1313.4
13004	1417.3	14004	1521.6	15004	1626.1
16004	1730.9	17004	1835.9	18004	1941.1
19004	2046.4	20004	2151.8	1005	391.9
2005	433.1	3005	494.3	4005	569.0
5005	652.6	6005	742.1	7005	835.6
9005	931.9	9005	1030.3	10005	1130.1
11005	1231.0	12005	1332.8	13005	1435.3
14005	1538.3	15005	1641.8	16005	1745.7
17005	1849.8	18005	1954.2	19005	2058.9
20005	2163.7	1006	464.9	2006	500.2
3006	554.0	4006	621.6	5006	698.9
6006	783.2	7006	872.3	8006	964.9
9006	1060.2	10006	1157.4	11006	1256.2
12006	1356.1	13006	1456.9	14006	1553.5
15006	1660.8	16006	1763.5	17006	1866.7
18006	1970.2	19006	2074.2	20006	2178.1
1007	538.6	2007	569.3	3007	617.2
4007	676.5	5007	750.0	6007	829.0
7007	913.7	8007	1002.5	9007	1094.5
10007	1188.9	11007	1285.3	12007	1383.1
13007	1482.1	14007	1582.1	15007	1682.9
16007	1784.3	17007	1886.4	18007	1983.9
19007	2091.8	20007	2195.0	1008	612.7
2008	639.9	3008	682.8	4008	738.7
5008	804.9	6008	879.0	7008	959.2
8008	1044.2	9008	1132.3	10008	1224.3

ORIGINAL PAGE IS  
OF POOR QUALITY

# STRUCTURAL CONSTANTS C

11008	1318.0	12008	1413.6	13008	1510.6
14008	1608.8	15008	1708.0	16008	1808.1
17008	1908.8	18008	2010.2	19008	2112.1
20008	2214.3	10009	687.1	20009	711.5
3009	750.3	4009	801.5	5009	862.8
6009	932.4	7009	1008.4	8009	1089.5
9009	1174.7	10009	1263.2	11009	1354.2
12009	1447.4	13009	1542.3	14009	1638.6
15009	1736.1	16009	1834.6	17009	1934.0
18009	2034.1	19009	2134.8	20009	2236.1
1010	761.7	2010	783.8	3010	819.2
4010	866.3	5010	923.4	6010	988.6
7010	1060.6	8010	1138.1	9010	1219.9
10010	1305.3	11010	1353.6	12010	1484.3
13010	1576.9	14010	1671.3	15010	1767.0
16010	1863.9	17010	1961.8	18010	2060.5
19010	2160.0	20010	2260.1	1011	836.5
2011	856.6	3011	889.1	4011	932.7
5011	985.9	6011	1047.3	7011	1115.5
8011	1189.4	9011	1267.9	10011	1350.2
11011	1435.8	12011	1524.0	13011	1614.4
14011	1736.6	15011	1800.5	16011	1895.6
17011	1992.0	18011	2089.3	19011	2187.5
20011	2286.4	1012	911.3	2012	929.8
3012	959.9	4012	1000.4	5012	1050.2
6012	1108.0	7012	1172.7	8012	1243.2
9012	1318.5	10012	1397.9	11012	1480.7
12012	1566.3	13012	1654.4	14012	1744.5
15012	1836.4	16012	1929.9	17012	2024.6
18012	2120.4	19012	2217.2	20012	2314.8
1013	986.3	2013	1003.4	3013	1031.3
4013	1069.1	5013	1115.9	6013	1170.5
7013	1231.9	8013	1299.1	9013	1371.4
10013	1447.8	11013	1527.9	12013	1611.1
13013	1696.8	14013	1784.8	15013	1874.8
16013	1966.4	17013	2059.4	18013	2153.7
19013	2249.0	20013	2345.4	1014	1061.3
2014	1077.2	3014	1103.3	4014	1138.7
5014	1182.7	6014	1234.3	7014	1292.7
8014	1356.9	9014	1426.3	10014	1499.9
11014	1577.4	12014	1658.1	13014	1741.5
14014	1827.4	15014	1915.3	16014	2005.0
17014	2096.3	18014	2189.0	19014	2282.9
20014	2377.9	1015	1136.4	2015	1151.3
3015	1175.6	4015	1209.0	5015	1250.5
6015	1299.4	7015	1355.0	8015	1416.4
9015	1483.0	10015	1554.0	11015	1628.8
12015	1707.1	13015	1788.3	14015	1872.0
15015	1957.9	16015	2045.8	17015	2135.3
18015	2226.4	19015	2318.8	20015	2412.3

ORIGINAL PAGE IS  
OF POOR QUALITY

# STRUCTURAL CONSTANTS C

1016	1211.5	2016	1225.5	3016	1248.4
4016	1279.8	5016	1319.1	6016	1365.6
7516	1418.6	8016	1477.4	9016	1541.3
10016	1609.7	11016	1682.1	12016	1758.0
13016	1836.9	14016	1918.5	15016	2002.4
16016	2088.4	17016	2176.2	18016	2265.6
19016	2356.5	20016	2448.6	1017	1286.6
2017	1299.8	3017	1321.5	4017	1351.2
5017	1388.5	6017	1432.7	7017	1483.3
8017	1539.6	9017	1601.0	10017	1667.0
11017	1737.0	12017	1810.6	13017	1887.3
14017	1966.8	15017	2048.8	16017	2132.9
17017	2218.9	18017	2306.7	19017	2396.0
20017	2486.6	1018	1361.8	2018	1374.3
3018	1394.6	4018	1423.0	5018	1458.4
6018	1500.6	7018	1549.0	8018	1603.0
9018	1662.1	10018	1725.7	11018	1793.4
12018	1864.8	13018	1939.3	14018	2016.8
15018	2096.8	16018	2179.1	17018	2263.4
18018	2349.5	19018	2437.2	20018	2526.4
1019	1437.0	2019	1448.8	3019	1468.3
4019	1495.1	5019	1528.9	6019	1569.2
7019	1615.5	8019	1667.3	9019	1724.2
10019	1785.6	11019	1851.2	12019	1920.4
13019	1992.9	14019	2068.3	15019	2146.4
16019	2226.8	17019	2309.4	18019	2393.8
19019	2480.0	20019	2567.7	1020	1512.3
2020	1523.5	3020	1542.0	4020	1567.5
5020	1599.8	6020	1638.3	7020	1682.7
8020	1732.6	9020	1787.4	10020	1846.7
11020	1915.2	12020	1977.3	13020	2047.8
14020	2121.3	15020	2197.5	16020	2276.1
17020	2356.9	18020	2439.7	19020	2524.3
20020	2610.5	1200	247.9	400	489.7

C-3



# STRUCTURAL CONSTANTS C2 AND INDICIES

INDICES	CONSTANTS	INDICES	CONSTANTS	INDICES	CONSTANTS
1001	247.9	2001	489.7	3001	732.9
4001	976.4	5001	1220.0	6001	1463.7
7001	1737.4	8001	1951.2	9001	2195.0
10001	2438.7	11001	2662.5	12001	2926.3
13001	3170.2	14001	3414.0	15001	3657.8
16001	3901.6	17001	4145.4	18001	4389.2
19001	4633.1	20001	4876.9	1002	259.7
2002	495.8	3002	736.9	4002	979.4
5002	1222.4	6002	1465.7	7002	1709.2
8002	1952.7	9002	2196.3	10002	2440.0
11002	2683.7	12002	2927.4	13002	3171.1
14002	3414.8	15002	3658.6	16002	3902.4
17002	4146.1	18002	4389.9	19002	4633.7
20002	4877.5	1003	278.2	2003	505.7
3003	743.7	4003	984.5	5003	1226.5
6003	1469.1	7003	1712.1	8003	1955.3
9003	2198.6	10003	2442.0	11003	2685.5
12003	2929.1	13003	3172.7	14003	3416.3
15003	3660.0	16003	3903.6	17003	4147.3
18003	4391.1	19003	4634.8	20003	4878.5
1004	302.2	2004	519.3	3004	753.0
4004	991.5	5004	1232.2	6004	1473.9
7004	1716.1	8004	1958.8	9004	2201.8
10004	2444.9	11004	2688.1	12004	2931.4
13004	3174.9	14004	3418.3	15004	3661.9
16004	3905.4	17004	4149.0	18004	4392.6
19004	4636.3	20004	4879.9	1005	330.5
2005	536.3	3005	764.8	4005	1000.5
5005	1239.4	6005	1479.9	7005	1721.4
8005	1963.4	9005	2205.8	10005	2448.5
11005	2691.4	12005	2934.5	13005	3177.7
14005	3421.0	15005	3664.3	16005	3907.7
17005	4151.2	18005	4394.7	19005	4638.2
20005	4881.8	1006	362.1	2006	556.3
3006	779.0	4006	1011.4	5006	1248.2
6006	1487.3	7006	1727.7	8006	1969.0
9006	2210.8	10006	2453.0	11006	2695.5
12006	2938.2	13006	3181.1	14006	3424.2
15006	3667.3	16006	3911.5	17006	4153.8
18006	4397.2	19006	4645.6	20006	4884.0
1007	396.3	2007	579.1	3007	795.4
4007	1024.1	5007	1258.5	6007	1496.0
7007	1735.2	8007	1975.5	9007	2216.6
10007	2458.3	11007	2700.3	12007	2942.6
13007	3185.2	14007	3427.9	15007	3671.8
16007	3913.8	17007	4156.9	18007	4400.1
19007	4643.4	20007	4886.7	1008	432.3
2008	604.4	3008	814.0	4008	1038.6
5008	1270.4	6008	1505.9	7008	1743.8
8008	1983.1	9008	2223.4	10008	2464.3

# STRUCTURAL CONSTANTS C

11008	2705.8	12008	2947.7	13008	3189.9
14008	3432.2	15008	3674.9	16008	3917.6
17008	4160.5	18008	4403.5	19008	4646.6
20008	4689.7	1009	469.8	2009	631.7
3009	834.5	4009	1054.8	5009	1283.6
6009	1517.1	7009	1753.4	8009	1991.6
9009	2231.0	10009	2471.2	11009	2712.1
12009	2953.4	13009	3195.2	14009	3437.2
15009	3679.5	16009	3922.7	17009	4164.6
18009	4407.3	19009	4650.2	20009	4893.2
1010	508.5	2010	661.0	3010	850.9
4010	1072.6	5010	1298.3	6010	1529.5
7010	1764.2	8010	2001.1	9010	2239.4
10010	2478.8	11010	2719.0	12010	2959.8
13010	3251.1	14010	3442.7	15010	3684.6
16010	3926.8	17010	4169.1	18010	4411.6
19010	4654.3	20010	4897.1	1011	548.1
2011	691.9	3011	880.9	4011	1091.9
5011	1314.3	6011	1543.1	7011	1776.0
8011	2011.5	9011	2248.7	10011	2487.3
11011	2726.7	12011	2966.9	13011	3207.6
14011	3448.8	15011	3690.3	16011	3932.1
17011	4174.1	18011	4416.4	19011	4658.8
20011	4901.3	1012	588.4	2012	724.3
3012	906.5	4012	1112.7	5012	1331.6
6012	1557.9	7012	1788.9	8012	2022.8
9012	2258.5	10012	2496.4	11012	2735.1
12012	2974.6	13012	3214.8	14012	3455.4
15012	3696.5	16012	3937.9	17012	4179.6
18012	4421.6	19012	4663.7	20012	4906.0
1013	629.3	2013	757.8	3013	933.6
4013	1134.8	5013	1350.1	6013	1573.8
7013	1802.7	8013	2035.1	9013	2269.9
10013	2506.4	11013	2744.2	12013	2983.0
13013	3221.5	14013	3462.6	15013	3703.2
16013	3944.2	17013	4185.6	18013	4427.2
19013	4669.0	20013	4911.1	1014	670.6
2014	792.5	3014	962.0	4014	1158.2
5014	1369.9	6014	1590.8	7014	1817.6
8014	2048.3	9014	2281.7	10014	2517.1
11014	2754.0	12014	2992.0	13014	3230.8
14014	3470.4	15014	3710.5	16014	3951.0
17014	4192.0	18014	4433.2	19014	4674.8
20014	4916.5	1015	712.4	2015	828.1
3015	991.5	4015	1182.9	5015	1390.8
6015	1608.8	7015	1833.4	8015	2062.3
9015	2294.3	10015	2528.5	11015	2764.4
12015	3001.6	13015	3239.7	14015	3478.7
15015	3718.3	16015	3958.3	17015	4198.9
18015	4439.8	19015	4680.9	20015	4922.4

ORIGINAL PAGE IS  
OF POOR QUALITY

# STRUCTURAL CONSTANTS C

1016	754.4	2016	864.6	3016	1022.2
4016	1208.7	5016	1412.8	6016	1627.9
7016	1850.1	8016	2077.2	9016	2307.7
10016	2540.7	11016	2775.6	12016	3011.9
13016	3249.3	14016	3487.5	15016	3726.5
16016	3966.1	17016	4206.2	18016	4446.7
19016	4687.5	20016	4928.7	1017	796.8
2017	901.8	3017	1053.8	4017	1235.6
5017	1435.9	6017	1648.0	7017	1867.8
8017	2093.0	9017	2321.9	10017	2553.6
11017	2787.4	12017	3022.7	13017	3259.3
14017	3496.9	15017	3735.3	16017	3974.4
17017	4214.0	18017	4454.1	19017	4694.5
20017	4935.3	1018	839.4	2018	939.7
3018	1086.4	4018	1263.5	5018	1460.0
6018	1669.0	7018	1886.4	8018	2109.6
9018	2336.9	10018	2567.2	11018	2799.9
12018	3034.2	13018	3270.0	14018	3506.9
15018	3744.7	16018	3983.2	17018	4222.3
18018	4461.9	19018	4702.0	20018	4942.4
1019	882.2	2019	578.1	3019	1119.8
4019	1292.3	5019	1485.0	6019	1690.9
7019	1905.8	8019	2127.0	9019	2352.6
10019	2581.5	11019	2813.0	12019	3046.4
13019	3281.3	14019	3517.4	15019	3754.5
16019	3992.4	17019	4231.0	18019	4470.1
19019	4709.8	20019	4945.8	1020	925.2
2020	1017.0	3020	1153.9	4020	1322.0
5020	1512.9	6020	1713.7	7020	1926.1
8020	2145.1	9020	2369.0	10020	2596.5
11020	2826.7	12020	3059.1	13020	3293.1
14020	3528.4	15020	3764.8	16020	4002.1
17020	4240.2	18020	4478.8	19020	4718.0
20020	4957.7	1200	49.0	400	98.1

# STRUCTURAL CONSTANTS C3 AND INDICIES

INDICES	CONSTANTS	INDICES	CONSTANTS	INDICES	CONSTANTS
1001	49.0	2001	58.1	3001	147.1
4001	196.1	5001	245.1	6001	294.2
7001	343.2	8001	392.2	9001	441.2
10001	490.3	11001	539.3	12001	588.3
13001	637.3	14001	686.4	15001	735.4
16001	784.4	17001	833.4	18001	882.5
19001	931.5	20001	980.5	10002	98.1
20002	196.1	30002	254.2	40002	392.2
50002	490.3	60002	588.3	70002	686.4
80002	784.4	90002	882.5	100002	980.5
110002	1078.6	120002	1176.6	130002	1274.7
140002	1372.7	150002	1470.8	160002	1568.8
170002	1666.9	180002	1764.9	190002	1863.0
200002	1961.1	10003	147.1	20003	294.2
30003	441.2	40003	588.3	50003	735.4
60003	882.5	70003	1029.6	80003	1176.6
90003	1323.7	100003	1470.8	110003	1617.9
120003	1764.9	130003	1912.0	140003	2059.1
150003	2206.2	160003	2353.3	170003	2500.3
180003	2647.4	190003	2794.5	200003	2941.6
10004	196.1	20004	392.2	30004	588.3
40004	784.4	50004	588.5	60004	1176.6
70004	1372.7	80004	1568.8	90004	1764.9
100004	1961.1	110004	2157.2	120004	2353.3
130004	2549.4	140004	2745.5	150004	2941.6
160004	3137.7	170004	3333.8	180004	3529.9
190004	3726.0	200004	3922.1	10005	245.1
20005	490.3	30005	735.4	40005	980.5
50005	1225.7	60005	1470.8	70005	1715.9
80005	1961.1	90005	2206.2	100005	2451.3
110005	2696.4	120005	2941.6	130005	3186.7
140005	3431.8	150005	3677.0	160005	3922.1
170005	4167.2	180005	4412.4	190005	4657.5
200005	4902.6	10006	294.2	20006	588.3
30006	882.5	40006	1176.6	50006	1470.8
60006	1764.9	70006	2059.1	80006	2353.3
90006	2647.4	100006	2941.6	110006	3235.7
120006	3529.9	130006	3824.1	140006	4118.2
150006	4412.4	160006	4706.5	170006	5000.7
180006	5294.8	190006	5589.0	200006	5883.2
10007	343.2	20007	686.4	30007	1029.6
40007	1372.7	50007	1715.9	60007	2059.1
70007	2402.3	80007	2745.5	90007	3068.7
100007	3431.8	110007	3775.0	120007	4118.2
130007	4461.4	140007	4804.6	150007	5147.8
160007	5491.0	170007	5834.1	180007	6177.3
190007	6520.5	200007	6863.7	10008	392.2
20008	784.4	30008	1176.6	40008	1568.8
50008	1961.1	60008	2353.3	70008	2745.5
80008	3137.7	90008	3529.9	100008	3922.1

# STRUCTURAL CONSTANTS C

11008	4314.3	12008	4706.5	13008	5098.7
14008	5491.0	15008	5883.2	16008	6275.4
17008	6667.6	18008	7059.8	19008	7452.0
20008	7844.2	1009	441.2	2009	882.5
3009	1323.7	4009	1764.9	5009	2206.2
6009	2647.4	7009	3088.7	8009	3529.9
9009	3971.1	10009	4412.4	11009	4853.6
12009	5294.8	13009	5736.1	14009	6177.3
15009	6618.6	16009	7059.8	17009	7501.0
18009	7942.3	19009	8383.5	20009	8824.7
1010	490.3	2010	983.5	3010	1470.8
4010	1961.1	5010	2451.3	6010	2941.6
7010	3431.8	8010	3922.1	9010	4412.4
10010	4902.6	11010	5392.9	12010	5883.2
13010	6373.4	14010	6863.7	15010	7354.0
16010	7844.2	17010	8334.5	18010	8824.7
19010	9315.0	20010	9805.3	1011	539.3
2011	1178.6	3011	1617.9	4011	2157.2
5011	2696.4	6011	3235.7	7011	3775.0
8011	4314.3	9011	4853.6	10011	5392.9
11011	5932.2	12011	6471.5	13011	7010.8
14011	7550.1	15011	8089.3	16011	8628.6
17011	9167.9	18011	9707.2	19011	10246.5
20011	10785.8	1012	588.3	2012	1176.6
3012	1764.9	4012	2353.3	5012	2941.6
6012	3529.9	7012	4118.2	8012	4706.5
9012	5294.8	10012	5883.2	11012	6471.5
12012	7059.8	13012	7648.1	14012	8236.4
15012	8824.7	16012	9413.1	17012	10001.4
18012	10589.7	19012	11178.0	20012	11766.3
1013	637.2	2013	1274.7	3013	1912.0
4013	2549.4	5013	3186.7	6013	3824.1
7013	4461.4	8013	5098.7	9013	5736.1
10013	6373.4	11013	7010.8	12013	7648.1
13013	8285.5	14013	8922.8	15013	9560.1
16013	10197.5	17013	10834.8	18013	11472.2
19013	12109.5	20013	12746.8	1014	686.4
2014	1372.7	3014	2059.1	4014	2745.5
5014	3431.8	6014	4118.2	7014	4804.6
8014	5491.0	9014	6177.3	10014	6863.7
11014	7550.1	12014	8236.4	13014	8922.8
14014	9609.2	15014	10295.5	16014	10981.9
17014	11668.3	18014	12354.6	19014	13041.0
20014	13727.4	1015	735.4	2015	1470.8
3015	2206.2	4015	2941.6	5015	3677.0
6015	4412.4	7015	5147.8	8015	5883.2
9015	6618.6	10015	7354.0	11015	8089.3
12015	8824.7	13015	9560.1	14015	10295.5
15015	11030.9	16015	11766.3	17015	12501.7
18015	13237.1	19015	13972.5	20015	14707.9

# STRUCTURAL CONSTANTS C

1016	784.4	2016	1568.8	1016	2353.3
4016	3137.7	5016	3922.1	6016	4776.5
7016	5491.0	8016	6275.4	9016	7059.8
10016	7844.2	11016	8628.6	12016	9413.1
13016	10197.5	14016	10981.9	15016	11766.3
16016	12550.7	17016	13335.2	18016	14119.6
19016	14904.0	20016	15688.4	1017	833.4
2017	1666.9	3017	2500.3	4017	3333.8
5017	4167.2	6017	5000.7	7017	5834.1
8017	6667.6	9017	7501.0	10017	8334.5
11017	9167.9	12017	10001.4	13017	10834.8
14017	11668.2	15017	12501.7	16017	13335.2
17017	14168.6	18017	15002.1	19017	15835.5
20017	16669.0	1018	882.5	2018	1764.9
3018	2847.4	4018	3525.9	5018	4412.4
6018	5294.8	7018	6177.3	8018	7059.8
9018	7942.2	10018	8824.7	11018	9707.2
12018	10589.7	13018	11472.2	14018	12354.6
15018	13237.1	16018	14119.6	17018	15002.1
18018	15884.5	19018	16767.0	20018	17649.5
1019	931.5	2019	1863.7	3019	2794.5
4019	3726.0	5019	4657.5	6019	5589.0
7019	6520.5	8019	7452.0	9019	8383.5
10019	9315.0	11019	10246.5	12019	11178.0
13019	12109.5	14019	13041.0	15019	13972.5
16019	14904.0	17019	15835.5	18019	16767.0
19019	17698.5	20019	18630.0	1020	980.5
2020	1961.1	3020	2941.6	4020	3922.1
5020	4902.6	6020	5883.2	7020	6863.7
8020	7844.2	9020	8824.7	10020	9805.3
11020	10785.8	12020	11766.3	13020	12746.8
14020	13727.4	15020	14707.9	16020	15688.4
17020	16669.0	18020	17649.5	19020	18630.0
20020	19610.5	1200	0.0	400	0.0

\*\*\*VCL AVE AMPLIFICATION = -.7967D J1 DBS FOR 10.0 HERTZ BAND  
VCL AVE AMP W/INTERNAL PRESSURE EFFECT = -10.89

RADIUS(FT)	LNTH COORD(FT)	PNT AMPL(DBS)
0.0	15.00	-.8071D 01
0.0	30.00	-.7855D 01
7.000	15.00	-.8075D 01
7.000	30.00	-.7861D 01

\*\*\*VCL AVE AMPLIFICATION = 0.8231D 01 DBS FOR 16.0 HERTZ BAND  
VCL AVE AMP W/INTERNAL PRESSURE EFFECT = -2.85

RADIUS(FT)	LNTH COORD(FT)	PNT AMPL(DBS)
0.0	15.00	-.3770D 01
0.0	30.00	0.1107D 02
7.000	15.00	-.3812D 01
7.000	30.00	0.1107D 02

\*\*\*VCL AVE AMPLIFICATION = -.3715D 02 DBS FOR 20.0 HERTZ BAND  
VCL AVE AMP W/INTERNAL PRESSURE EFFECT = -37.31

RADIUS(FT)	LNTH COORD(FT)	PNT AMPL(DBS)
0.0	15.00	-.7700D 03
0.0	30.00	-.7000D 03
7.000	15.00	-.3588D 02
7.000	30.00	-.3700D 02

\*\*\*VCL AVE AMPLIFICATION = -.1297D 02 DBS FOR 25.0 HERTZ BAND  
VCL AVE AMP W/INTERNAL PRESSURE EFFECT = -14.73

RADIUS(FT)	LNTH COORD(FT)	PNT AMPL(DBS)
0.0	15.00	-.1746D 02
0.0	30.00	-.1177D 02
7.000	15.00	-.1438D 02
7.000	30.00	-.1105D 02

\*\*\*VCL AVE AMPLIFICATION = -.2164D 02 DBS FOR 31.5 HERTZ BAND  
VCL AVE AMP W/INTERNAL PRESSURE EFFECT = -22.33

RADIUS(FT)	LNTH COORD(FT)	PNT AMPL(DBS)
0.0	15.00	-.2194D 02
0.0	30.00	-.3172D 03
7.000	15.00	-.2102D 02
7.000	30.00	-.3165D 03

\*\*\*VCL AVE AMPLIFICATION = -.3062D 00 DBS FOR 40.0 HERTZ BAND  
VCL AVE AMP W/INTERNAL PRESSURE EFFECT = -6.18

RADIUS(FT)	LNTH COORD(FT)	PNT AMPL(DBS)
0.0	15.00	-.3409D 01
0.0	30.00	-.3684D 01
7.000	15.00	-.1989D 01
7.000	30.00	0.6068D 01

\*\*\*VCL AVE AMPLIFICATION = -.3375D 01 DBS FOR 50.0 HERTZ BAND  
VCL AVE AMP W/INTERNAL PRESSURE EFFECT = -7.87

RADIUS(FT)	LNTH COORD(FT)	PNT AMPL(DBS)
0.0	15.00	-.1673D 02
0.0	30.00	-.4391D 01
7.000	15.00	-.1052D 01
7.000	30.00	-.3654D 01

\*\*\*VCL AVE AMPLIFICATION = -.2317D 01 DBS FOR 63.0 HERTZ BAND  
VCL AVE AMP W/INTERNAL PRESSURE EFFECT = -7.26

RADIUS(FT)	LNTH COORD(FT)	PNT AMPL(DBS)
------------	----------------	---------------

0.0	15.00	-0.15510 02
0.0	30.00	-0.24380 02
7.000	15.00	0.26040 01
7.000	30.00	-0.13080 02

\*\*\*VOL AVE AMPLIFICATION = -0.43000 01 DBS FOR 80.0 HERTZ BAND  
VOL AVE AMP W/INTERNAL PRESSURE EFFECT = -8.43

RADIUS(FT)	LNTH COORD(FT)	PNT AMPL(DBS)
0.0	15.00	-0.82040 01
0.0	30.00	-0.19130 01
7.000	15.00	-0.63880 00
7.000	30.00	0.25260 01

\*\*\*VCL AVE AMPLIFICATION = 0.32310 01 DBS FOR 100.0 HERTZ BAND  
VCL AVE AMP W/INTERNAL PRESSURE EFFECT = -4.55

RADIUS(FT)	LNTH COORD(FT)	PNT AMPL(DBS)
0.0	15.00	-0.44850 01
0.0	30.00	-0.73320 01
7.000	15.00	0.20110 01
7.000	30.00	0.10760 02

\*\*\*VOL AVE AMPLIFICATION = 0.61280 01 DBS FOR 125.0 HERTZ BAND  
VOL AVE AMP W/INTERNAL PRESSURE EFFECT = -3.49

RADIUS(FT)	LNTH COORD(FT)	PNT AMPL(DBS)
0.0	15.00	-0.10590 02
0.0	30.00	-0.13080 02
7.000	15.00	0.11320 02
7.000	30.00	0.13570 02

\*\*\*VCL AVE AMPLIFICATION = 0.67780 01 DBS FOR 160.0 HERTZ BAND  
VCL AVE AMP W/INTERNAL PRESSURE EFFECT = -3.28

RADIUS(FT)	LNTH COORD(FT)	PNT AMPL(DBS)
0.0	15.00	-0.70260 01
0.0	30.00	-0.73010 01
7.000	15.00	0.12230 02
7.000	30.00	0.79560 01

\*\*\*VOL AVE AMPLIFICATION = 0.11510 02 DBS FOR 200.0 HERTZ BAND  
VOL AVE AMP W/INTERNAL PRESSURE EFFECT = -2.05

RADIUS(FT)	LNTH COORD(FT)	PNT AMPL(DBS)
0.0	15.00	-0.35220 01
0.0	30.00	-0.42670 01
7.000	15.00	0.15920 02
7.000	30.00	0.77240 01

\*\*\*VOL AVE AMPLIFICATION = -0.32800 01 DBS FOR 250.0 HERTZ BAND  
VOL AVE AMP W/INTERNAL PRESSURE EFFECT = -7.81

RADIUS(FT)	LNTH COORD(FT)	PNT AMPL(DBS)
0.0	15.00	0.52220 01
0.0	30.00	-0.69700 00
7.000	15.00	-0.60610 01
7.000	30.00	-0.89580 01

ORIGINAL PAGE IS  
OF POOR QUALITY